UNIVERSIDADE DE LISBOA
FACULDADE DE CIÊNCIAS

Crosstalk between the myotome and muscle stem cells during the development of the skeletal muscles of the back

"Documento Definitivo"

Doutoramento em Biologia

Especialidade de Biologia do Desenvolvimento

André Brás Gonçalves

Tese orientada por:

Professora Doutora Sólveig Thorsteinsdóttir
Doutora Marianne Deries

Documento especialmente elaborado para a obtenção do grau de doutor

2019

UNIVERSIDADE DE LISBOA
FACULDADE DE CIÊNCIAS

Crosstalk between the myotome and muscle stem cells during the development of the skeletal muscles of the back

Doutoramento em Biologia

Especialidade de Biologia do Desenvolvimento

André Brás Gonçalves

Tese orientada por:

Professora Doutora Sólveig Thorsteinsdóttir, Doutora Marianne Deries

Júri:

Presidente:

- Doutora Maria Manuela Gomes Coelho de Noronha Trancoso, Professora Catedrática e Presidente do Departamento de Biologia Animal da Faculdade de Ciências da Universidade de Lisboa.

Vogais:

- Doutora Perpétua da Conceição Pinto do Ó, Investigadora Principal, Instituto de Engenharia Biomédica da Universidade do Porto;
- Doutor Moisés Mallo Perez, Investigador Principal, Instituto Gulbenkian de Ciência;
- Doutora Ruth Cecilia Diez del Corral Baubry, Investigadora Associada, Champalimaud *Centre for the Unknown* da Fundação Champalimaud;
- Doutora Maria Leonor Tavares Saúde, Professora Auxiliar Convidada, Faculdade de Medicina da Universidade de Lisboa;
- Doutor Domingos Manuel Pinto Henrique, Investigador Auxiliar, Faculdade de Medicina da Universidade de Lisboa;
- Doutora Sólveig Thorsteinsdóttir, Professora Associada com Agregação, Faculdade de Ciências da Universidade de Lisboa (orientadora).

Documento especialmente elaborado para a obtenção do grau de doutor

Fundação para a Ciência e Tecnologia – SFRH/BD/90827/2012

2019

The work presented in this dissertation was developed with the support from the Fundação para a Ciência e Tecnologia, through a PhD Fellowship (SFRH/BD/90827/2012) and the Project Grant PTDC/SAU-BID/120130/2010).

Notas Prévias

1) Para a elaboração da presente tese de doutoramento foi usado integralmente como capítulo um artigo científico publicado numa revista internacional indexada. Uma vez que os trabalhos referidos na presente tese foram realizados em colaboração com outros investigadores, e de acordo com o disposto do nº1 do Artigo 45º do Regulamentos dos Estudos Pós-Graduados da Universidade de Lisboa, publicado no *Diário da República*, 2ª série, nº 65 de 30 de março de 2012, esclareço que participei integralmente na conceção e execução do trabalho experimental, na interpretação e discussão dos resultados, bem como na redação dos manuscritos.

2) O facto desta tese integrar um artigo científico levou a que o capítulo, cujo artigo está exposto, fosse escrito seguindo as normas da revista em que foi publicado, variando, portanto, das normas de escrita estabelecidas pela Universidade de Lisboa. O capítulo 5 consiste numa compilação de resultados considerados relevantes para esta tese, parte dos quais não foram publicados, enquanto que uma parte foi incluída num artigo já publicado (**Gomes de Almeida, P. G., Pinheiro, G. G., Nunes, A. M., Gonçalves, A. B. and Thorsteinsdóttir, S.** (2016). Fibronectin assembly during early embryo development: A versatile communication system between cells and tissues. *Developmental Dynamics* **245**, 520-535.).

Para a minha famíla,

especialmente para os meus pais

Acknowledgements

Dizem que na vida devemos fazer três coisas: plantar uma árvore, ter filhos e escrever um livro. Fazendo uma introspeção ao meu trajeto penso que comecei pelo fim (e talvez pela parte mais difícil). Não que uma tese de doutoramento seja considerada um livro, mas do meu ponto de vista, todo o processo alheio à mesma, desde a escrita ao trabalho no laboratório, tem algumas parecenças relativamente. E curiosamente, em alguns casos, uma tese chega mesmo a ser considerada como um filho próprio. Naturalmente, existem imensas pessoas por trás de todo este trabalho e que contribuíram, de forma direta ou indireta, para ter eu chegado a este ponto e estar a escrever estas palavras sentidas de apreciação.

Em primeiro lugar, os meus maiores agradecimentos vão para a Sólveig e Marianne. Pela sua enorme sapiência científica e pela maneira como me orientaram ao longo destes longos anos de forma precisa, tranquila e sempre em boa disposição e em ambiente amigável. São de facto, fontes infindáveis de conhecimento e sem elas não seria capaz de dar conta do recado sozinho. Irei recordar-me das infindáveis horas de reuniões, discussões de resultados e esquemas que desenhámos para tentar perceber os meus resultados. Resumindo, aprendi muito com vocês e espero levar alguma dessa bagagem nas minhas próximas aventuras científicas. Quero também agradecer à Gabriela Rodrigues e à Rita Zilhão pela enorme camaradagem, discussões científicas e amizade destes anos. Sempre em boa disposição, aprendi também muito com vocês, desde culturas de células, boas práticas no laboratório a biologia molecular. Obrigado por puxarem pelo meu espírito crítico científico!

O meu segundo grande agradecimento vai para os meus pais e familiares. Por todo o apoio dado ao longo destes anos, mesmo não compreendendo a totalidade do meu trabalho, nunca me deixaram de me perguntar se tinha resultados novos, como iam os" meus ratos", encorajando-me constante e diariamente, mesmo quando tenha implicado ir trabalhar em horários "alternativos" pouco convencionais, nunca hesitaram em me apoiar. Muito obrigado pela educação que me deram e por me terem mostrado que o mais importante é fazermos aquilo que gostamos, mesmo por vezes quando o retorno possa parecer frustrante. Esta tese é dedicada a vocês!

De seguida não podia deixar de agradecer aos meus colegas de laboratório: Ao Pedro Rifes e à Raquel Vaz, os meus sinceros agradecimentos por ter trabalhado com vocês e aprendido imensa coisa, desde organização no trabalho, espírito crítico científico e mesmo por

ter partilhado comigo um ambiente mais relaxado e corriqueiro em que senão gozássemos uns com os outros no dia a dia, nem valia a pena vir trabalhar.

Ao Luís Marques, incansável no auxílio informático e microscópico. Um *sensei* que sabe o que faz, desde as coisas mais fúteis às imprescindíveis no laboratório. Um grande obrigado por todas as horas de laboratório que partilhámos. Vou-me recordar dos podcasts, músicas, piadas e de nos rirmos que nem uns perdidos sobre as mais variadas temáticas discutidas, quando tínhamos o laboratório por conta própria. Como o próprio se intitula, és repositório inesgotável de informação inútil, mas muito valioso, porque assim dá para falar um pouco de tudo e parafraseando Rui Veloso sobre Carlos Tê "*Quem fala assim não é gago*".

À Marta Palma, grande companheira de aventuras extra laboratoriais, nas casas assombradas, idas a jogos de futebol e entre outras. Um grande obrigado por muitas das vezes teres sido tu a organizar a maior parte delas que tanta dinâmica deram ao grupo. Não me vou esquecer daquele dia de canoagem. Obrigado, porque sem ti o trabalho no laboratório não corria de forma eficaz, nem era tão aprazível, pois a tua ajuda no laboratório foi imprescindível. Obrigado por me teres ouvido e ajudados muitas vezes sobre os mais variados temas. O teu gabinete servia como uma espécie de consultório terapêutico que me fazia bem.

Às minhas companheiras de doutoramento, Patrícia Almeida e Andreia Nunes, por todos os momentos vividos dentro e fora do laboratório. Pelas sessões musicais neste, pelos dramas científicos diários, mas também por toda a amizade destes anos vindouros que remontam ao tempo em que ainda éramos alunos de mestrado e mal sabíamos por onde iam dar os nossos caminhos. It was a hell of a ride! Entre os altos e baixos de cada um, começámos juntos isto e sendo eu o último a encerrar o departamento dos doutorados do nosso ano no laboratório penso que fizemos todos um bom trabalho. Obrigado pelo apoio e, por certas vezes, me terem compensado nalgumas tarefas que me fizeram toda a diferença na minha logística diária.

À Inês Antunes e Ana Neto um enorme obrigado pela vossa boa disposição e constante disponibilidade para ajudar.

Ao Telmo Monteiro, pela ajuda prestada na micróscopia e análise de imagens, que muitas vezes me safaram quando ninguém estava por perto.

À D. Elvira pela sua alegria e bem-estar contagiantes. É de pessoas destas que precisamos nas nossas vidas, porque nos trazem sol em dias de chuva.

Em suma, à turma da FCUL, um enorme e sentido obrigado por todas estas aventuras, desde aos almoços rotineiros sempre em ambiente (demasiado) descontraído, aos jantares, cinemas, acampamentos e noites de copos. Tudo sempre num ambiente entre amigos, cheio de estupidez natural, mas altamente gratificante. Tive muita sorte em vos ter conhecido e em ter feito parte desta equipa muito boa!

Agradeço ao Moisés Mallo, Hélia Neves e Ruth Diez del Corral pelo empréstimo dos plasmídeos para as *in situs* emprestadas e também à Leonor Saúde, Ana Cristovão e Domingos Henrique, não só pelo empréstimo de outros tantos, mas também por me terem deixado usufruir das suas instalações para produzir as sondas. Sem elas, não teria muitos dos resultados aqui descritos. Obrigado pela vossa simpatia e amizade!

Quero ainda agradecer à Patricia Ybot-Gonzalez e à Beatriz Lopez-Escobar por todos os ensinamentos transmitidos sobre cultura de embriões e a todos os membros do laboratório do João Relvas por me terem feito sentir como em casa durante os meus períodos de rotação laboratorial. Em especial à Joana Faria, à Ana Seixas, Nuno Dias e ao Fábio Prata, tive muita sorte por a vida me ter posto de encontro com os vossos caminhos, pois vocês são pessoas incríveis. Fábio, continuo a aguardar as mensagens quinzenais de picardia sobre quem é o melhor piloto e equipa na fórmula 1!

Ao João Brazão e à Ana Sobral, pela vindoura amizade destes longos anos. Pelas noitadas, festas académicas, almoços e jantares sempre acompanhados de grande espírito de partilha.

E finalmente aos meus amigos e treinador "da minha outra vida", onde destaco o Francisco Quintas, Diogo Correia, Fábio Figueira, Ritinha, Jessica Vieira, Nuno Rola, João Gigante, Ricardo Lopes, Bruno e Filipa Silva, Marta Ferreira, Duarte Mourão, Daniel Viegas, Rosinhas, Simão Morgado e Fernando Couto. Para vocês não é preciso dizer muito, pois sabem o quão importante foram e são no meu dia a dia. Vivemos muito e partilhámos muito! Um grande obrigado por todo este tempo de amizade, loucura e momentos extraordinários que vivenciei convosco dentro e fora das piscinas. E espero que ainda tenhamos muitos mais pela frente. Sem dúvida contribuíram, mesmo sem se aperceberem, para a minha motivação diária e bem-estar pessoal.

Por fim, e não menos importante, um grande obrigado ao Florent Lenoir e à tia Micá, pelo incansável e preciosíssimo trabalho que tiveram em me ajudar na formatação desta tese. De longe que senão fossem vocês, eu ainda estaria aqui a desesperar para toda a eternidade.

Abstract

The deep back (or epaxial) muscles of amniotes derive from the transient myotomes, segmented embryonic muscles that develop from the delamination and differentiation of muscle stem cells (MuSCs) from the overlying dermomyotome. During embryonic development, myogenesis is ensured by the activation of key transcription factors: Myf5, Mrf4, MyoD and Myogenin.

The main goal of this thesis was to investigate the role of the myotome in epaxial muscle development. In **Chapter 2,** a technique of culturing mouse embryo explants was developed, which allowed us to study the *in vivo ex utero* development of the epaxial myotome and its extracellular matrix (ECM). In **Chapter 3**, we analysed to what extent the myotome is necessary for later epaxial muscle development using the *Myf5*$^{nlacZ/nlacZ}$ mouse line, in which the absence of *Myf5* and *Mrf4* results in the lack of an early myotome. We show that one specific epaxial muscle group (the transversospinalis) is able to differentiate through MyoD, while the other three epaxial muscle groups fail to form. Moreover, we show that due to the lack of myotomal factors, the maintenance of the identity of delaminating dermomyotomal MuSCs fails. In **Chapter 4**, we described the organisation of laminins, fibronectin and tenascin-C ECMs during myotome development showing that each one of these ECMs potentially has a specific spatial relationship with MuSCs. Finally, **Chapter 5** focuses on the role of the myotome in the organisation of these same ECMs and its role in tendon development, using *Myf5*$^{nlacZ/nlacZ}$ mouse embryos. We show that the myotome is necessary to assemble its own matrices, but these are not required for the development of the transversospinalis muscles.

The results of this thesis suggest that the transversospinalis muscles have a distinct developmental mechanism from that of the remaining epaxial muscles and we propose that they are evolutionary more recent.

Keywords: Epaxial myogenesis; Myotome; Muscle stem cell; Extracellular matrix; Mouse embryo.

Resumo

Os músculos profundos das costas (ou epaxiais) dos amniotas derivam dos miótomos transientes, músculos embrionários segmentados que se desenvolvem a partir da delaminação e diferenciação das células estaminais musculares (CEMs) do dermomiótomo sobreposto. Durante o desenvolvimento embrionário, a miogénese é assegurada pela ativação de fatores de transcrição-chave miogénicos: Myf5, Mrf4, MyoD e Miogenina.

Esta tese tem como principal objetivo perceber o papel do miótomo no desenvolvimento dos músculos epaxiais. No **capítulo 2**, descrevemos uma técnica de cultura de explantes de embrião de ratinho que nos permitiu estudar o desenvolvimento *in vivo ex utero* do miótomo epaxial e da sua matriz extracelular (MEC). No **capítulo 3**, analisamos até que ponto o miótomo é necessário para o desenvolvimento muscular epaxial que ocorre em fases mais tardias, recorrendo ao uso de embriões de ratinho *Myf5*$^{nlacZ/nlacZ}$, cuja incapacidade de expressar *Myf5* e *Mrf4*, leva a que não formem o miótomo embrionário. Aqui, demonstramos que um grupo muscular epaxial específico, nomeadamente o músculo transversospinalis é capaz de se diferenciar através da ativação de MyoD, ao passo que os restantes grupos musculares epaxiais não se formam. Mais ainda, demonstramos que a manutenção da identidade das CEMs do dermomiótomo que delaminam deste é comprometida devido à ausência de fatores parácrinos do miótomo. No **capítulo 4**, descrevemos a organização das matrizes de laminina, fibronectina e tenascina-C durante o desenvolvimento do miótomo, evidenciando que cada uma destas MECs tem uma potencial relação espacial com as CEMs. Por fim, o **capítulo 5** atenta para a contribuição do miótomo na organização destas mesmas MECs e para desenvolvimento dos tendões recorrendo novamente aos embriões de ratinho *Myf5*$^{nlacZ/nlacZ}$. Aqui, evidenciamos que o miótomo é apenas necessário para a montagem das suas próprias MECs, não sendo requerido para o desenvolvimento do músculo transversospinalis.

Os resultados desta tese sugerem que o músculo transversospinalis tenha um mecanismo de desenvolvimento distinto dos restantes músculos epaxiais, e como tal, propomos que este músculo em particular seja evolutivamente mais recente.

Palavras-chave: Miogénese epaxial; Miótomo; Célula estaminal muscular; Matriz extracelular; Embrião de ratinho.

Resumo alargado

A formação dos músculos esqueléticos, designada por miogénese, é um processo complexo que depende da combinação de uma variedade de fatores celulares autónomos e de sinais extrínsecos. Todos os músculos esqueléticos do tronco e dos membros derivam de estruturas embrionárias designadas por dermomiótomos. Estes são compostos pelas células dorsais dos sómitos epiteliais, segmentos mesodérmicos localizados de cada lado do tubo neural. Após a dispersão da parte ventral dos sómitos, que origina o esqueleto axial, as células dos dermomiótomos, adotam uma organização em camada epitelial, formando uma borda nas suas extremidades.

Os primeiros músculos esqueléticos a formar no embrião são os miótomos que se desenvolvem através da delaminação de células estaminais musculares (CEMs) das bordas dos dermomiótomos. Estas células diferenciam-se em miócitos que se dispõem paralelamente ao tubo neural, no lado ventral dos dermomiótomos, e formam assim músculos segmentados repetidos ao longo do eixo anterior-posterior do embrião. Ao entrar no miótomo, as CEMs, que se caracterizam pela expressão de Pax3 e/ou Pax7, ativam fatores de transcrição que induzem a diferenciação miogénica, nomeadamente Myf5, Mrf4, MyoD e Miogenina. A expressão destes fatores ocorre numa maneira hierárquica e específica ao longo do desenvolvimento embrionário. Myf5 é o primeiro fator de determinação a ser expresso, tanto na parte epaxial como na região hipaxial do miótomo. Seguem-se Mrf4 e MyoD que marcam os mioblastos em diferenciação no miótomo e por fim, a expressão de Miogenina que induz a diferenciação dos mioblastos em miócitos mononucleados, alongados e pós-mitóticos.

Tanto os dermomiótomos como os miótomos são estruturas transientes. Numa dada altura do desenvolvimento, as células do dermomiótomo de-epitelizam e entram nos miótomos como CEMs proliferativas que expressam Pax3 e/ou Pax7. Algumas delas diferenciam-se e fundem com os miócitos do miótomo enquanto outras mantém o estado estaminal. Simultaneamente, os miótomos transformam-se, perdendo a sua conformação segmentada embrionária e reorganizam-se na musculatura definitiva pré-adulta do tronco. Estas incluem os músculos epaxiais (ou músculos profundos das costas), que se associam à coluna vertebral contribuindo para o seu alinhamento e estabilização, e a musculatura hipaxial do tronco, onde fazem parte os músculos intercostais e abdominais que controlam os movimentos do tronco e protegem os órgãos internos.

Apesar de todo o conhecimento em torno da regulação miogénica durante o desenvolvimento do miótomo, muito pouco se sabe sobre a forma como este afeta as CEMs, aquando a sua entrada para o miótomo e também como o próprio influencia o desenvolvimento da musculatura epaxial. Assim, o principal objetivo desta tese foi estudar como o miótomo embrionário influencia o comportamento das CEMs e a morfogénese dos músculos epaxiais. Usámos embriões de ratinho selvagens e embriões knock-out *Myf5*$^{nlacZ/nlacZ}$, que não expressam nem *Myf5* nem *Mrf4* e consequentemente não formam os miótomos embrionários. No entanto os embriões *Myf5*$^{nlacZ/nlacZ}$ desenvolvem musculatura esquelética mais tardiamente.

O **capítulo 2** atenta para o desenvolvimento de uma técnica de cultura que permite o desenvolvimento *in vivo ex utero* de explantes preparados a partir de embriões de ratinho de estirpe selvagem. Esta técnica foi desenvolvida e otimizada para o estudo do desenvolvimento do miótomo e do seu ambiente extracelular. Foram realizados ensaios para detetar a proliferação celular e apoptose e também foi estudada a morfologia tridimensional da musculatura esquelética epaxial, assim como a organização da matriz extracelular (MEC) dentro e à volta do miótomo. Estas características foram depois comparadas com as dos embriões que se desenvolveram no interior do útero materno. Aqui, demonstramos que dentro de uma janela temporal de 12 horas e em condições de cultura de explantes em meio desprovido de soro, a morfogénese do miótomo procede de forma semelhante em comparação com a dos embriões desenvolvidos *in utero*. Ao mesmo tempo verificámos também que a MEC aumentava de complexidade ao longo do tempo, acompanhado o desenvolvimento do miótomo epaxial. Apesar de um ligeiro atraso no desenvolvimento, este fenótipo foi acompanhado pela ausência de diferenças na proliferação e morte celular, atestando a validade desta técnica. Ainda neste capítulo, são discutidas as vantagens e limitações desta técnica, a qual oferece uma forma rápida, acessível em termos de equipamento e manipulação, sendo assim económica e com potencial para múltiplas aplicabilidades, uma vez que permite o uso simultâneo de uma certa quantidade de embriões e aplica-se a vários estádios de desenvolvimento. Pode também ser acrescido o uso de diferentes inibidores para o estudo de vias de sinalização num determinado contexto biológico. Não menos importante, a aplicação desta técnica não é apenas útil para o estudo do desenvolvimento do miótomo, mas poderá ser transversal à análise de outras estruturas em desenvolvimento em fases de desenvolvimento semelhantes. O trabalho inserido neste capítulo foi publicado na revista *Differentiation* (2016) 91, 57-67.

No **capítulo 3** analisamos até que ponto o miótomo é necessário para o desenvolvimento e morfogénese dos músculos epaxiais. Para tal, usámos a linha de ratinho *Myf5*$^{nlacZ/nlacZ}$ que não

forma o miótomo e em que a miogénese se encontra atrasada por ser apenas induzida pelo fator de transcrição MyoD, uma vez que estes embriões mutantes não expressam *Myf5* nem *Mrf4*. Neste capítulo demonstramos que apenas um grupo muscular epaxial (designado por transversospinalis) é capaz de se diferenciar através da expressão de MyoD e que se desenvolve independentemente do miótomo, enquanto que os restantes três grupos epaxiais musculares não se desenvolvem. Verificámos também que a ausência do miótomo compromete a manutenção da identidade das CEMs derivadas do dermomiótomo, aquando a sua de-epitelização e entrada no espaço onde o miótomo deveria existir, sugerindo que o miótomo emite sinais para manter estas células. Sabe-se que o miótomo normalmente expressa vários fatores parácrinos, como fatores de crescimento dos fibroblastos (Fgfs) e o fator de crescimento A derivado das plaquetas (Pdgfa), que, na ausência do miótomo, não são expressos. Colocamos assim a hipótese que a perda de identidade estaminal das CEMs poderia dever-se à ausência destes fatores parácrinos. Quando se bloqueou a via de sinalização Fgf em embriões de ratinho de estirpe selvagem (isto é, embriões que formam um miótomo normal) verificou-se uma diminuição significativa no número de CEMs. No entanto, a inibição da via de sinalização Pdgf, não teve efeitos significativos na totalidade do número destas células. Estes dados sugerem que os Fgfs do miótomo mantêm a identidade das CEMs do dermomiótomo durante e após a sua de-epitelização. Estes resultados levam ainda à hipótese de que poderão existir mecanismos de desenvolvimento divergentes entre o transversospinalis e os restantes músculos epaxiais. Este capítulo consiste num manuscrito em preparação para publicação.

No **capítulo 4** descrevemos a organização dos componentes da MEC, incluindo a laminina, a fibronectina e a tenascina-C, em relação às CEMs durante o desenvolvimento do miótomo demonstrando que cada uma destas matrizes possui uma relação espacial específica relativamente às CEMs do dermomiótomo e do miótomo. Através de uma perspetiva tridimensional analisamos como as matrizes de laminina, fibronectina e tenascina-C se organizam durante a de-epitelização das CEMs do dermomiótomo central e a sua entrada no miótomo em embriões de ratinho da estirpe selvagem. Verificamos que a laminina é depositada na membrana basal do dermomiótomo e do miótomo e que as CEMs dentro do miótomo se localizam na proximidade da membrana basal deste. Verificámos ainda que as matrizes de fibronectina e tenascina-C também se encontram associadas as membranas basais do dermomiótomo e do miótomo e que são ambas depositadas no espaço entre estes dois territórios, antes de ocorrer a delaminação das CEMs do dermiótomo, levantando à hipótese de que possam ser usadas por estas células para colonizar o miótomo.

No capítulo 5, analisamos de que modo os padrões de expressão das MECs analisadas no capítulo 4 se encontram alterados nos embriões *Myf5*$^{nlacZ/nlacZ}$. Nestes embriões, evidenciamos que o miótomo é crucial para a formação da sua própria membrana basal composta por lamininas, uma vez que esta não se forma. Mais ainda, verificámos que o padrão típico das matrizes de fibronectina e tenascina-C do miótomo não se forma na ausência do miótomo. Contudo, quando as massas musculares do transversospinalis se desenvolvem, nos embriões *Myf5*$^{nlacZ/nlacZ}$, estas não só conseguem produzir as suas próprias MECs, como também induzem a expressão de *Scleraxis*, um marcador das células precursoras de tendinócitos, no mesênquima circundante. Estes dados demonstram que a MEC do miótomo não é necessária para o desenvolvimento do transversospinalis e que o mesmo é capaz de induzir a expressão de *Scleraxis* em seu redor na ausência do miótomo. Parte dos resultados deste capítulo foram incluídos no artigo Gomes de Almeida et al. *Developmental Dynamics* (2016) 235, 520-535.

Finalmente no **capítulo 6,** são discutidos os principais resultados de todos os capítulos de acordo com a bibliografia existente, destacando o papel do miótomo durante o desenvolvimento da musculatura epaxial e as particularidades do mecanismo de desenvolvimento do transversospinalis.

Palavras-chave: Miogénese epaxial; Miótomo; Célula estaminal muscular; Matriz extracelular; Embrião de ratinho.

Contents

List of Figures

List of Tables

List of Abbreviations and Acronyms

ACT - Activin

ADAM/TACE - A Disintegrin and Metalloproteinase

AKT - RAC-Alpha Serine/Threonine-Protein Kinase

AMH - Anti-Müllerian Hormone

APC - Adenomatosis Polyposis Coli

bHLH - Basic Helix-Loop-Helix

BMP - Bone Morphogenetic Protein

BMPRI/II - Bone Morphogenetic Protein Receptor Type I/II

Boc - Brother of Cdo

CAM - Cell Adhesion Molecule

CDK1 - Cyclin Dependent Kinase 1

Cdo - Cysteine Dioxygenase

CK1α- Casein Kinase I Alpha

CL - Caudal Lip of the Dermomyotome

CSL - DNA Binding Domain Protein CSL

CXCL12 - C-X-C Chemokine Ligand 12

CXCR4 - C-X-C Chemokine Receptor 4

Dhh - Desert Hedgehog

Dll - Delta-Like-Ligand

DML - Dorso-Medial Lip of the Dermomyotome

DMM - Dermomyotome/Myotome

Dmrt2 - Doublesex and Mab-Related Transcription Factor 2

DNA - Deoxyribonucleic Acid

Dsv - Dishevelled

ECM - Extracellular Matrix

EEE - Early Epaxial Enhancer

EGF - Epidermal Growth Factor

EMT - Epithelial-to-Mesenchymal Transition

E(n) - Embryonic day (number)

En1 - Engrailed Homeobox 1

ErbB3 - Erb-B2 Receptor Tyrosine Kinase 3

ERK - Extracellular Signal - Regulated Kinase

Eya - Eyes Absent Homolog

FGF- Fibroblast Growth Factor

FGFR - Fibroblast Growth Factor Receptor

Foxc1/2 - Forkhead Box C1/2

Fu - Fused

Fzd - Frizzled

GAG - Glycosaminoglycan

Gas1 - Growth Arrest-Specific Protein 1

GDF - Growth and Differentiation Factor

GDNF - Glial-Derived Neurotrophic Factor

GFP - Green Fluorescent Protein

Gli - Gli Family Zinc Finger

GPCR - G-Protein-Coupled Receptor-Like Protein

GSKβ3 - Glycogen Synthase Kinase 3 Beta

Hes - Hairy/Enhancer of Split

Hey - Hes Related Family BHLH Transcription Factor with YRPW Motif 1

HGF - -Hepatocyte Growth Factor

Hhip1 - Hedgehog Interacting Protein 1

HS -Heparan Sulphate

HSPG - Heparan Sulphate Proteoglycan

Ihh - Indian Hedgehog

INH - Inhibin

Jag - Jagged

JNK - C-Jun N-terminal Kinase

Kif7 - Kinesin-Like Protein 7

Lbx1 - Ladybird Homeobox 1

TCF1 /LEF - Transcription Factor 1 / Lymphoid Enhancer Binding Factor

Lefty - Left-Right Determination Factor

LRP5/6 - Low Density Lipoprotein - Related Protein 5/6

Mam - Mastermind-Like Protein

MAPK - Mitogen-Activated Protein Kinase

MET - MET Proto-Oncogene, Receptor Tyrosine Kinase

MHC - Myosin Heavy Chain

MRF - Myogenic Regulatory Factor

mTOR - Mechanistic Target of Rapamycin Kinase

MuSC - Muscle Stem Cell

Myf5 - Myogenic Factor 5

Myf6 /Mrf4 - Myogenic Factor 6

MyoD - Myogenic Differentiation 1

NCC - Neural Crest Cell

NECD - Notch Extracellular Domain

NFAT - Nuclear Factor of Activated T cell

Ngr -Neuregulin

NICD - Notch Intracellular Domain

Nodal - Nodal Growth Differentiation Factor

Notch -Notch Homolog 1, Translocation-Associated

NRR - Negative Regulatory Region

P (n) - Postnatal day (number)

Pax - Paired Box

PCP - Planar Cell Polarity

PDGF - Platelet-Derived Growth Factor

PDGFR - Platelet-Derived Growth Factor Receptor

PI3K - Phosphoinositide 3-Kinase

Pitx2 - Paired-like Homeodomain Transcription Factor 2

PKA - Protein Kinase A

PKC - Protein Kinase C

PLCγ - Phospholipase C, Gamma 1

PP2A - Protein Phosphatase 2

PSM - Presomitic Mesoderm

Ptch - Patched

RAS - Ras Family Small GTPase

RBPJ$_k$ - Recombining Binding Protein Suppressor of Hairless

RGD - Arginine-Glycine-Aspartic Acid

RL - Rostral Lip of the Dermomyotome

RNA - Ribonucleic Acid

RTK - Receptor-Linked Tyrosine Kinase

SCR- SCR Proto-Oncogene, Non-Receptor Tyrosine Kinase

Scx - Scleraxis bHLH Transcription Factor

Shh - Sonic Hedgehog

Sim1 - SIM bHLH Transcription Factor 1

Six - Sine Oculis Homeobox Homolog

Slit1 - Slit Guidance Ligand 1

SMAD - Mothers Against Decapentaplegic Homolog

Smo -Smoothened

Snail - Snail Family Transcriptional Repressor

SOX - Sex Determining Region Y-box

Spry - Sprouty RTK Signalling Antagonist

STAT - Signal Transducer and Activator of Transcription

SuFu - Suppressor of Fused

TCF1 /LEF - Transcription Factor 1 / Lymphoid Enhancer Binding Factor

TFIC - Transcription Factor Inhibitory Complex

TGFβ - Transforming Growth Factor Beta

TGFRβI/II - Transforming Growth Factor Beta Receptor Type I/II

VLL - Ventro-lateral Lip of the Dermomyotome

Wnt - Wingless/Integrated Family Member

Chapter 1

Introduction

I. General Introduction

1. The musculoskeletal system

1.1 The anatomy of the musculoskeletal system

Vertebrate movement depends on the musculoskeletal system which includes skeletal muscles, bones, connective tissue (including tendons), nerves and blood vessels. Of the three types of muscles in vertebrates (skeletal, cardiac and smooth muscle), skeletal muscle is the most abundant. To be functional, skeletal muscle tissue needs to be incorporated in the whole musculoskeletal system, i.e. linked to the skeleton through tendons, become innervated by motor neurons and sufficiently vascularised to sustain muscle homeostasis (Fig. 1.1A; Deries and Thorsteinsdóttir 2016; Frontera and Ochala, 2015; Hauschka, 1994).

Skeletal muscles consist of large multinucleated, elongated and striated cells that are coated by an extracellular matrix called a basement membrane (Fig. 1.1A, B). Basement membranes are composed of a combination of collagens, non-collagenous glycoproteins and proteoglycans and play key roles in cell polarisation, differentiation and homeostasis, and, in the case of skeletal muscle, synaptogenesis, tendinogenesis and regeneration (Sanes, 2003; Thorsteinsdóttir et al., 2011). Typically, skeletal muscle cells, also named myofibres, lie parallel to each other and are arranged in multiple cylindrical bundles named fascicles (Fig. 1.1A). Connective tissue contributes to support and organise the superstructure of the muscle by providing routes for nerve fibres and blood vessels and is stratified in three main layers: the endomysium, the perimysium and the epimysium. The endomysium is the most internal layer and wraps the individual muscle fibres, the perimysium organises the muscle fibres into multiple fascicles and the epimysium, the most external layer, delimits the whole muscle apparatus (Fig. 1.1A; Frontera and Ochala, 2015; Gillies and Lieber, 2011). These three sheaths are continuous with each other and extend to attach directly to the bone or to join the tendons that connect the muscles to bone or cartilage, thus enabling force transmission generated by skeletal muscles to move the skeleton (Fig. 1.1A).

The cellular components underlying the contractile capacity of muscle fibres are revealed upon microscopic analysis. The sarcoplasm (cytoplasm of the muscle fibre) contains repeated

contractile elements named sarcomeres, which in turn are formed by the organisation of thick (enriched in myosin) and thin (enriched in actin) cytoskeletal filaments (Frontera and Ochala, 2015). The alternated organisation of these two types of filaments gives skeletal muscles their striation pattern and underlies their contraction capacity as they slide along each other upon the release of Ca^{2+} from the sarcoplasmic reticulum, a process that is triggered by motor nerves (Frontera and Ochala, 2015). Hence, skeletal muscles are responsible for crucial biological functions such as breathing, body support, locomotion and their activity also contributes to the control of body temperature.

Muscle fibres associate with and maintain adult muscle stem cells (MuSCs), also known as satellite cells (Mauro, 1961), which are located between the muscle fibres and their overlying basement membrane (Fig. 1.1B). In healthy muscle they remain quiescent, but upon muscle injury, some satellite cells become activated and proliferate, thus expanding the population. Subsequently some of these MuSCs differentiate to repair the affected muscle area, while others return to their quiescence state under the basement membrane (Motohashi and Asakura, 2012).

1.2 Skeletal muscle development at a glance

Myogenesis, the process of building skeletal muscle is very complex. It is initiated during embryogenesis and continues throughout adulthood as a mechanism to maintain a healthy tissue. Most skeletal muscles of vertebrates (see section 4 for details) derive from paraxial mesodermal cells that have activated Pax3 and/or its paralogue Pax7, both members of the paired box (Pax)/homeodomain family of transcription factors, thus marking a subpopulation of mesodermal cells that can enter the myogenic lineage (Fig. 1.1C; Buckingham, 2006; Buckingham and Relaix, 2007). During development, first embryonic and then foetal MuSCs produce a sequential series of myogenic regulatory factors (MRFs), members of the MyoD family of myogenic basic helix-loop-helix (bHLH) transcription factors, thus initiating myogenic determination and differentiation. In vertebrates there are four MRFs named the myogenic factor 5 (Myf5), the myogenic factor 6 (Myf6, also known as Mrf4 or herculin), the myogenic differentiation 1 (MyoD, also known as MyoD1) and Myogenin (Asfour et al., 2018; Buckingham and Rigby, 2014; Pownall et al., 2002; Tajbakhsh, 2009) When an embryonic MuSC turns on the expression of Myf5, MyoD or Mrf4, it becomes committed to myogenesis and is termed a myoblast. Committed myoblasts can divide a few times (Fig. 1.1C) but as they

progress in the myogenic differentiation programme, they upregulate Myogenin which induces their exit from the cell cycle and their terminal differentiation into postmitotic myocytes as they elongate and start the synthesis of muscle structural proteins, such as desmin and several myosin

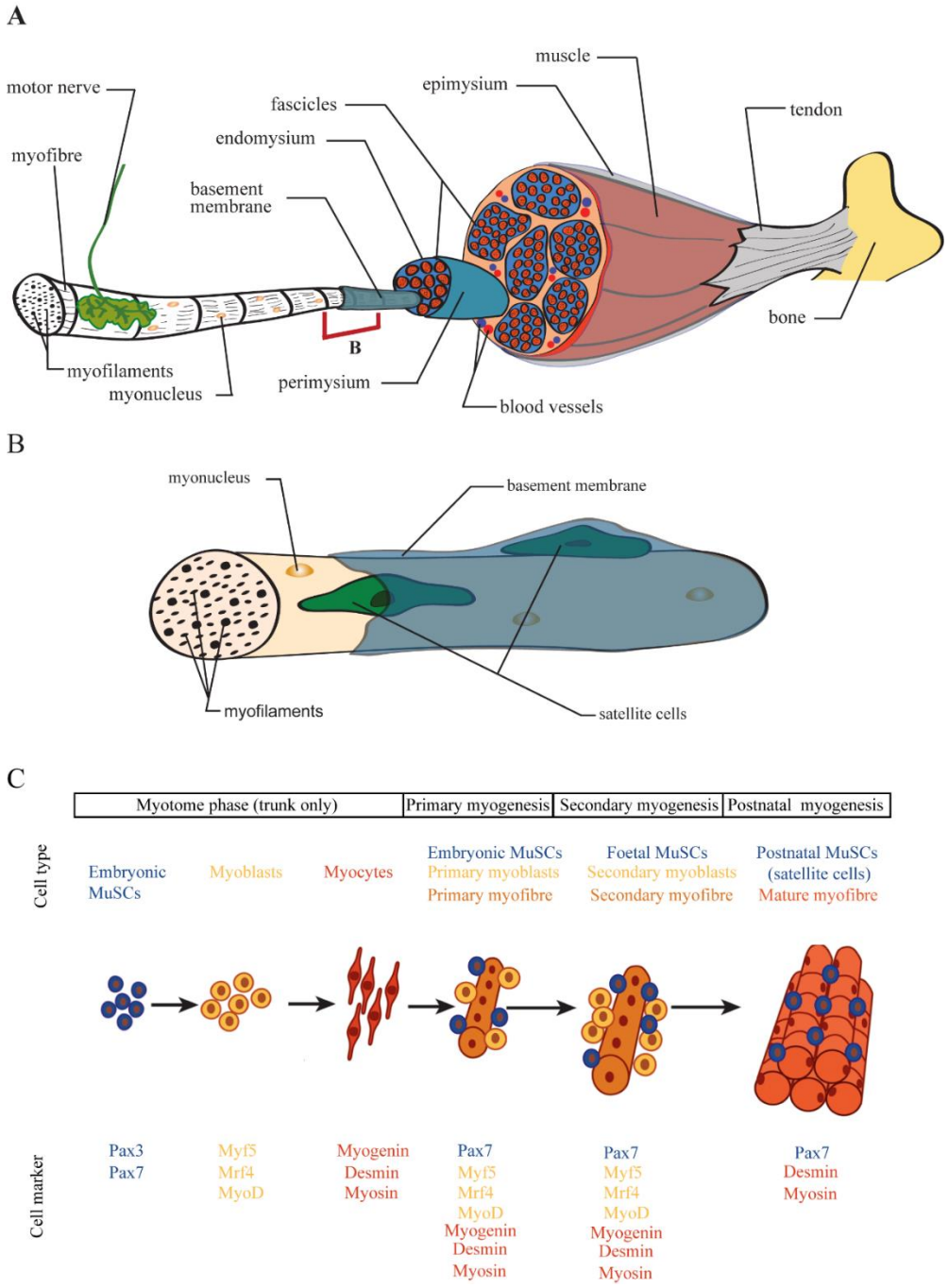

Figure 1.1: Anatomy of the vertebrate musculoskeletal system and development of skeletal muscles.
A: Adult skeletal muscle movements are directed by motor nerves that transmit nerve impulses at synaptic areas triggering the contraction of the muscle. Skeletal muscle is highly vascularised and is linked to bones through the tendons to transmit the force to the skeleton. It is composed of multiple multinucleated myofibres which contain contractile myofilaments and each myofibre is wrapped by its specific basement membrane. (**Continues next page**).

isoforms (Fig. 1.1C). Finally, terminally differentiated myocytes fuse with each other and/or with myoblasts to form multinucleated myotubes, named primary myofibres (Fig. 1.1C). This first wave of myofibre formation is termed primary myogenesis and sets the muscle pattern of the embryo (Biressi et al., 2007). Some MuSCs do not differentiate during this phase but continue proliferating. Some of these differentiate during foetal development through a process called secondary myogenesis, where foetal MuSCs differentiate into myoblasts which fuse forming new myotubes around the primary myofibres. These new myotubes are called secondary myofibres and their formation around primary myofibres leads to the growth of the muscles (Fig. 1.1C). Finally, in postnatal muscle, the MuSCs that are still undifferentiated enter quiescence and are called satellite cells. These can be activated and repair the muscle upon damage or disease (Almeida et al., 2016; Kuang and Rudnicki, 2008).

In the next section (section 2), I will give a general overview of the major cell-cell communication pathways that operate during development, focussing on those that are most relevant for muscle development. Then in sections 3 and 4, I will review skeletal muscle development, from the early stages in the somite, until birth. The major focus will be on the early stages of myogenesis *in vivo* in the mouse embryo. However, whenever appropriate, other vertebrate model systems will also be referred. The underlying mechanisms that lead to embryonic skeletal muscle differentiation and morphogenesis of the embryonic myotome will be described together with the main signals that influence the balance between proliferation and differentiation of embryonic MuSCs, and how this balance ensures the correct development of the skeletal musculature of the body.

(**Continued from previous page**). Myofibres are organised in fascicles and are surrounded by connective tissue in distinct layers (endomysium, perimysium and epimysium). **B:** Adult MuSCs (satellite cells) reside underneath the basement membrane of the myofibre in a quiescent state. Myonucleus refers to the nucleus of the muscle fibre. **C:** Simplified scheme illustrating the progression of myogenesis. The major cell types and respective myogenic markers involved in skeletal muscle differentiation are depicted. MuSCs: muscle stem cells. Adapted from Deries et al. (*in press*) (A, B) and Deries and Thorsteinsdóttir, 2016 (C).

---

2. Cell-cell communication in development

2.1 Types of cell-cell communication

During the development of multicellular organisms, cell behaviour is tightly regulated to assure an appropriate cellular response for successful morphogenesis of tissues and organs.

Cells communicate with each other (both within the same tissue and between distinct tissues) and this cell-cell communication is critical for the development of organisms, since it allows cellular coordination, cooperation, and organisation.

Cell-cell communications during the early stages of development can be divided into paracrine and juxtacrine communication events (Gilbert and Barresi, 2016). Paracrine communication events are usually mediated by paracrine factors, also called growth factors (Gilbert and Barresi, 2016). Paracrine factors are secreted extracellular-signalling proteins which act on neighbouring target cells by binding to specific high affinity plasma membrane receptors on these cells (Gilbert and Barresi, 2016; Sherbet, 2011). Upon binding, they usually trigger signal transduction pathways leading to the activation of effector mechanisms within the responding cell. Paracrine factors can be grouped into families or super families according to their structural characteristics (Gilbert and Barresi, 2016; Sherbet, 2011). Juxtacrine cell-cell communication events on the other hand depend on cell contact (Gilbert and Barresi, 2016). They include cell-cell adhesion processes (i.e. when a cell adheres to another cell), binding of the ligand on one cell to a receptor on the neighbouring cells (e.g. Notch signalling) or indirect cell-cell interactions mediated by the extracellular matrix (ECM).

2.2 Paracrine (growth) factor signalling

2.2.1 Fgf signalling

Fibroblast growth factors (Fgfs) form a big family of secreted proteins that are expressed in almost all tissues of our body and participate in a wide variety of crucial biological functions, such as proliferation, survival, migration and differentiation (Ornitz and Itoh, 2015).

Phylogenetic analysis led to the identification of a total of twenty-two structural related Fgf polypeptides and four Fgf receptors (Fgfrs) in humans and mice. This large Fgf family is further divided into subfamilies based on their structure and function which are conserved between vertebrates and invertebrates (Goetz and Mohammadi, 2013; Ornitz and Itoh, 2015). The seven subfamilies are grouped into three different groups, namely the canonical, endocrine and intracellular Fgfs (Fig. 1.2A; Goetz and Mohammadi, 2013; Ornitz and Itoh, 2015). Here, I will focus on the canonical Fgfs, their receptors and their downstream signalling pathways.

Canonical Fgfs are secreted molecules that can act in both an autocrine and paracrine manner. These Fgfs bind to Fgfrs on the cell surface and are very important during development. They synergise with heparin/heparan sulphate (HS) and heparan sulphate proteoglycans (HSPGs), which serve as co-factors that can modulate their binding to Fgfrs (Fig. 1.2B; Ornitz and Itoh, 2015; Yayon et al 1991).

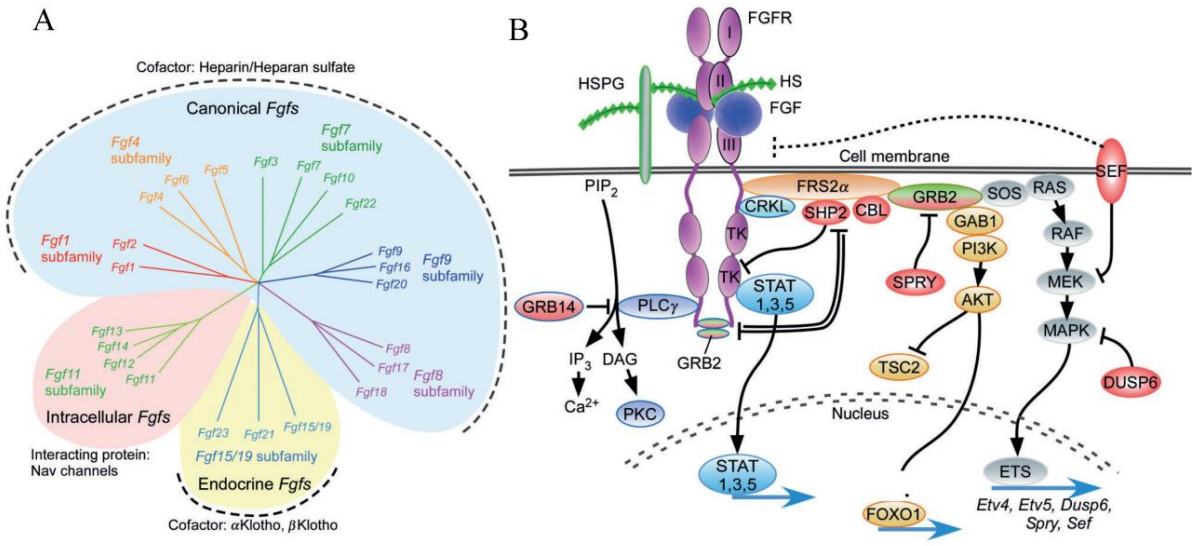

Figure 1.2: Overview of the Fgf signalling pathway.
A: Phylogenetic fibroblast growth factor (Fgf) tree including the twenty-two Fgfs that are grouped into seven distinct subfamilies according to their action mechanisms. Canonical Fgfs associate with heparin and heparan sulphate to bind to Fgf receptors (Fgfrs), while endocrine Fgfs bind to Fgfrs as well, but use α- and β-Klotho as co-factors. Intracellular Fgf are non-signalling proteins serving as co-factors for voltage gated sodium channels (Nav channels) and other molecules. Branch lengths are proportional to the evolutionary distance between each Fgf gene. **B:** A simplified perspective of the Fgf signalling pathway. Fgf-Fgfr association can trigger several signalling cascades including the PLCγ, STAT, PI3K/AKT/mTOR and the most common signalling cascade activated by Fgfs, the RAS/MAPK/ERK pathway. All these signalling cascades lead to the expression of target genes that codify proteins affecting cell behaviour. Some of these can act as activators or repressors of the Fgf signalling pathway. Based on Ornitz and Itoh, 2015.

Fgfrs are receptor-linked tyrosine kinases (RTKs) that possess three immunoglobulin-like domains. After binding to a specific Fgfr with its co-factors, canonical Fgfs induce the

phosphorylation of a subset of tyrosine kinase residues, which are coupled to and can activate intracellular signalling cascades (Fig. 1.2B; Goetz and Mohammadi, 2013; Ornitz and Itoh, 2015).

The binding of Fgfs to Fgfrs activates signalling platforms such as the RAS/MAPK/ERK (Ras/Mitogen-activated protein kinase/ Extracellular signal-regulated kinase) pathway involved in cell proliferation and differentiation, the PI3K/AKT/mTOR (phosphoinositide 3-kinase/ RAC-Alpha serine/threonine-protein kinase/ mechanistic target of rapamycin kinase) pathway involved in cell survival, the PLCγ (phospholipase C, gamma 1) signalling involved in cell adhesion and epithelial-to-mesenchymal transitions (EMTs) and the STAT (signal transducer and activator of transcription) pathway that controls for example cell motility (Fig. 1.2B; Ornitz and Itoh, 2015). These intracellular signalling cascades can be regulated by specific inhibitors such as those codified by the Sprouty (Spry) family of genes (Fig. 1.2B; Yang et al., 2013). Hence, the activation of Spry genes in a cell receiving Fgf signalling through the RAS/MAPK/ERK or PI3K/AKT/mTOR pathway dampens these signalling cascades and the respective cellular response (Fig. 1.2B; Yang et al., 2013). Phosphorylation of specific Fgfr residues recruit STAT proteins and PLCγ enzymes that initiate the STAT and PLCγ signalling cascades, respectively (Ornitz and Itoh, 2015). Thus, Fgf signalling activation can induce a variety of downstream effects in cells and the nature of these effects depends on the tissue type and on the biological context.

2.2.2 Pdgf signalling

Mammalian platelet-derived growth factors (Pdgfs) are a family of secreted proteins that encode four ligands (Pdgfa, Pdgfb, Pdgfc and Pdgfd) which bind to two receptors (Pdgfrα and Pdgfrβ). All Pdgf ligands consist of di-sulphide homodimers, but Pdgfa and Pdgfb types can also form functional heterodimers (Pdgfab) and the same happens with both Pdgfrs (Pdgfrαβ; Heldin and Westermark, 1999; Hoch and Soriano, 2003; Kazlauskas, 2017). Pdgfs are divided into two subfamilies according to structural differences and proteolytic processing, which determine ligand-receptor binding affinity (Fig. 1.3). The first subgroup includes Pdgfa and Pdgfb, which are cleaved and secreted in their active forms, while Pdgfc and Pdgfd are both activated after being secreted, therefore constituting another subgroup (Heldin and Westermark, 1999; LaRochelle et al., 2001; Li et al., 2000; Kazlauskas, 2017).

Like Fgfrs, Pdgfrs are RTKs exhibiting five immunoglobulin repeats and a split tyrosine domain in the cytoplasm (Fig. 1.3). Pdgf ligand binding induces the dimerization of Pdgfrs activating the cytoplasmic tyrosine kinase domains, which promotes the recruitment of signalling and adaptor proteins that consequently trigger downstream signalling pathways. These pathways are similar to the ones triggered by Fgf signalling as Pdgf ligands are able to trigger the PI3K/AKT/mTOR, STAT, RAS/MAPK/ERK and the PLCγ pathways (Fig. 1.2B) but they also are able to activate Scr family members (SRC proto-oncogene, non-receptor tyrosine kinase), the JNK (Jun N-terminal kinases) pathway and the N-Wasp proteins (Wiskott-Aldrich syndrome proteins) involved in the regulation of embryo development and cell growth, pro-inflammatory responses and filipodia formation, respectively (Claesson-Welsh, 1994). Structural differences between Pdgfrα and Pdgfrβ lead to the recruitment of distinct proteins that induce the activation of different signalling pathways. Thus, Pdgfrα and Pdgfrβ play distinct biological functions *in vivo* (Klinghoffer et al., 2001; Rosenkranz and Kazlauskas, 1999; Kazlauskas, 2017).

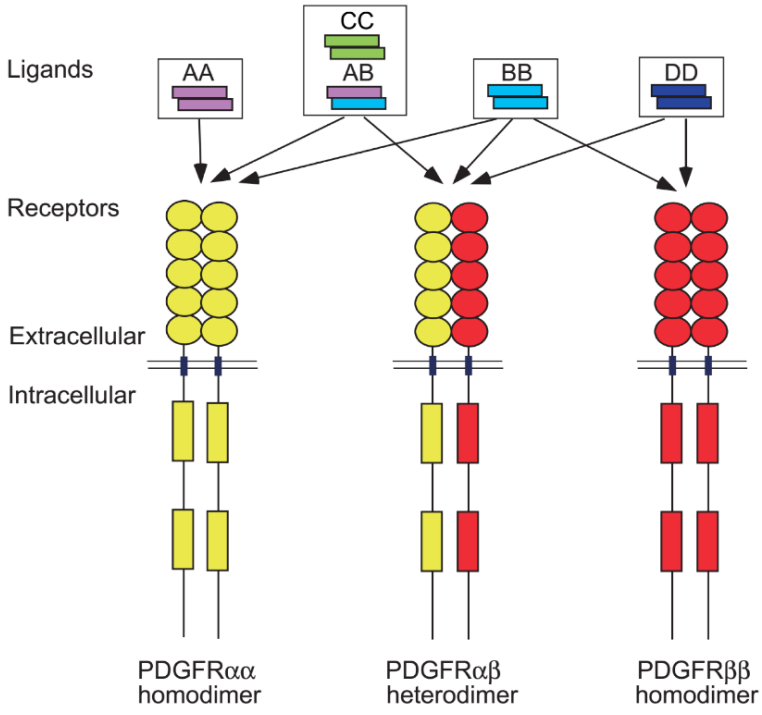

Figure 1.3: Pdgf ligands and Pdgfrs.
Platelet-derived growth factor (Pdgf) ligands form homo- or heterodimers that have distinct affinities for the different Pdgf receptors (Pdgfrs). Pdgf dimers are represented by the letters that compose their subunits. The arrows between ligands and receptors indicate the Pdgf/Pdgfr binding interactions. Based on Hoch and Soriano, 2003.

2.2.3 Wnt signalling

Wnt signalling is a well conserved pathway in Metazoans and plays a role in numerous important biological events, including cell proliferation, motility, polarisation, migration and determination, in the context of the establishment of the body plan as well as in the patterning of tissues and in organogenesis (Komiya and Habas, 2008; Teo and Kahn, 2010). The name Wnt derives from the fusion between the name of the *Drosophila* segment polarity gene *wingless* with the vertebrate homologue *integrated* or *int-1*. Wnts are secreted glycoproteins, which in humans and mice include a total of nineteen distinct Wnt proteins that share a core homology but exhibit distinct biological functions (Clevers and Nusse, 2012). Wnt ligands bind to Frizzled (Fzd) receptors, which are G protein-coupled receptor (GPCR)-like proteins that span the cell membrane seven times (Clevers and Nusse, 2012).

The best known Wnt signalling pathway operates through the activity of β-catenin and is termed the canonical Wnt pathway (Fig. 1.4). In the absence of Wnt ligands, cytoplasmic β-catenin is degraded through the activity of a degradation complex composed of Axin, APC (adenomatosis polyposis coli), PP2A (protein phosphatase 2A), CK1α (casein kinase 1α) and GSK3β (glycogen synthase kinase 3β). When Wnt ligands are present, they bind to the low-density lipoprotein-related protein 5/6 (LRP5/6) which acts as a co-factor to Fzd receptors and this coupling leads to the activation of Fzd (He et al., 2004; Fig. 1.4). The activation of Fzd is transduced by the phosphoprotein Dishevelled (Dsh) which directly interacts with Fzd (Wallingford and Habas, 2005). Activated Dsh recruits GSK3β and Axin to the membrane, thus dissociating the degradation complex, permitting the accumulation of β-catenin and its translocation to the nucleus, thereby inducing specific transcriptional gene expression (Fig. 1.4; Komiya and Habas, 2008). Wnt signalling can also occur through at least three so called non-canonical pathways (Fig. 1.4). These pathways are overall less well understood. Importantly, they are independent of LRP5/6 proteins and do not involve β-catenin activity. Rather they act through the PI3K/AKT/mTOR pathway, through G-protein mediated planar cell polarity (PCP) pathway or through the so called Wnt/Ca^{+2} pathway (Fig. 1.4) and are involved in a plethora of cellular responses crucial for tissue morphogenesis and organogenesis (Dale et al., 2009; De, 2011; Komiya and Habas, 2008; von Maltzahn et al., 2012a). Importantly, Wnt signalling can crosstalk with elements of other major signalling networks including Notch, Fgf and Shh pathways (Sethi and Vidal-Puig, 2010).

2.2.4 Hedgehog signalling

Hedgehog (Hh) signalling intervenes in a variety of important biological events such as cell differentiation, morphogenesis, tissue homeostasis and regeneration (Carballo et al., 2018; Lee et al., 2016). Hh proteins are found in a wide range of invertebrates and vertebrates and each Hh molecule is composed of a N-terminal domain, named "the Hedge" and a C-terminal domain termed "the Hog". The Hedge domain is responsible for the signalling activity, while the latter domain undergoes autoproteolytic cleavage and is lipidated before Hh is secreted (Briscoe and Thérond, 2013; Ingham et al., 2011). In mammals there are three different types of Hhs: Sonic-Hedgehog (Shh), Indian-Hedgehog (Ihh) and Desert-Hedgehog (Dhh). Shh is the the most common Hh protein in our body and is crucial for a myriad of developmental decisions, including the patterning of the neural tube and the limbs, whereas Ihh is more specific, playing a role in skeletogenesis for example (Cai and Liu, 2016; Dessaud et al., 2008; Tickle and Towers, 2017). Dhh is the most restricted of the Hhs in terms of expression, being important for the development of the gonads (Bitgood et al., 1996; Yao et al., 2002). In this section, I will review the Shh signalling pathway (Carballo et al., 2018).

Canonical Shh signalling occurs in a ligand-dependent manner (Fig. 1.5A). First, Shh ligand binds to its co-factors Cdo (cysteine dioxygenase), Boc (brother of Cdo) and Gas1 (growth arrest-specific protein 1) which promote its binding to the transmembrane receptor protein Patched1 (Ptch1; Allen et al., 2011). Ptch proteins are also involved in limiting Shh signalling by sequestering and endocytosing Shh ligands through Hhip1 (Hh interacting protein 1; Holtz et al., 2015). In the absence of Shh ligands, Ptch1 inhibits the G-protein coupled receptor Smoothened (Smo). When Shh binds to Ptch1, Ptch1 and its Shh ligand are internalised for degradation, lifting the Ptch1-induced repression on Smo that enters the membrane. When in the membrane, Smo initiates the Shh transduction signalling pathway (Fig. 1.5A; Carballo et al., 2018; Incardona et al., 2002; Lee et al., 2016).

In the absence of ligands, Smo is not detected in the membrane and the transcription factor inhibitory complex (TFIC) is active, which leads to the transformation of Gli family zinc finger (Gli) transcription factors from activator into repressors by inducing their proteolytic cleavage (Fig. 1.5B; Carballo et al., 2018; Lee et al., 2016). Repressor forms of Gli2 and Gli3 translocate into the nucleus and block Shh target genes, leading to processes such as differentiation, pro-

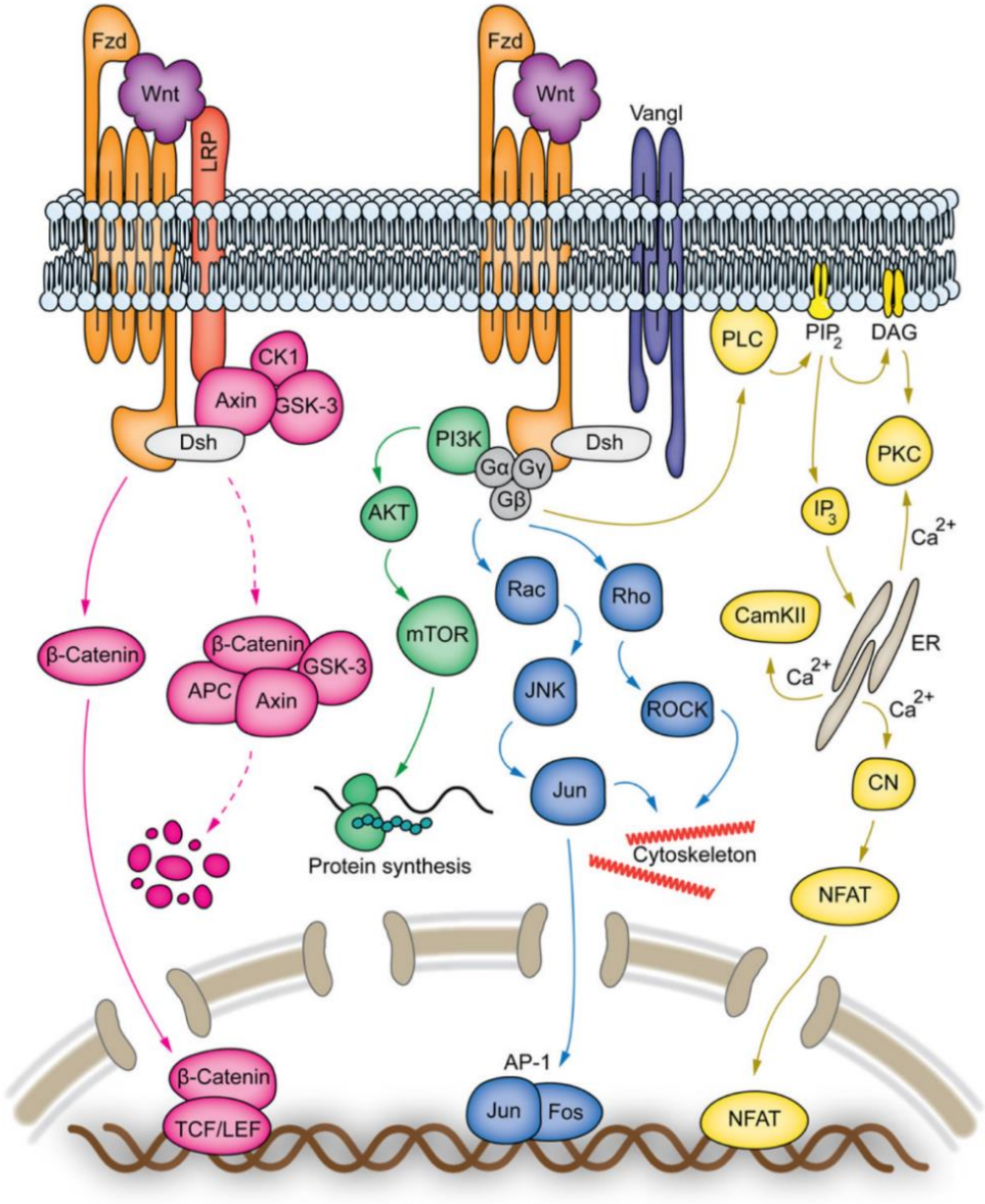

Figure 1.4: Wnt signalling pathway.
A: Wnt signalling can be transduced into a canonical pathway (pink signalling cascade), which leads to the intracellular accumulation of β-catenin, which is translocated to the nucleus where it acts as a transcription factor and associates with TCF/LEF (transcription factor 1 / lymphoid enhancer binding factor) proteins inducing the expression of target genes. Binding of certain Wnt ligands to Frizzled (Fzd) receptors can also trigger non-canonical Wnt pathways that are independent of LRP5/6 (low-density lipoprotein-related protein 5/6) proteins and β-catenin activity. These pathways are (1) the PI3K/AKT/mTOR (green signalling cascade), which is directly activated upon Wnt-Fzd binding and is involved in cellular proliferation, growth, survival and migration. (2) the G-protein mediated PCP (planar-cell-polarity) pathway, which leads to activation of several small-GTPases and activates a Jun kinases (JNK) cascade (blue signalling cascade) that causes cytoskeletal remodelling and cell migration. (3) the Wnt/Ca^{2+} pathway (yellow signalling cascade), which involves the activation of the PLC/PKC (phospholipase C/protein kinase C) signalling cascade leading to an increase of intracellular Ca^{2+} levels, which in turn culminate with the entry of NFAT (nuclear factor of activated T cell) into the nucleus where it drives the expression of genes involved in cell adhesion, motility, polarity and proliferation. Based on Dale et al., 2009; De, 2011; Komiya and Habas, 2008; von Maltzahn et al., 2012a, b.

apoptotic and anti-proliferative cellular responses (Fig. 1.5B; Carballo et al., 2018; Lee et al., 2016). When a Shh ligand is present, on the other hand, the activation of Smo induces the repression of the TFIC culminating in the inhibition of Gli2 and Gli3 protein cleavage, and their entry into the nucleus as transcriptional activators which promote processes such as cell proliferation, de-differentiation and survival (Fig. 1.5A; Carballo et al., 2018; Lee et al., 2016).

Patched2 (Ptch2) is another transmembrane receptor for Hh proteins. It shares more than 50% homology with Ptch1 and is also able to trigger the Shh signalling pathway. However, Ptch2 exhibits a lower efficiency in the inhibition of Smo and thus does not have the same effect as Ptch1 (Rahnama et al., 2004). Shh signalling can also be triggered in a non-canonical way, which is a process independent of Smo or Gli activity and can result in the modulation of the cytoskeleton and regulation of the cell cycle, respectively (Brennan et al., 2012).

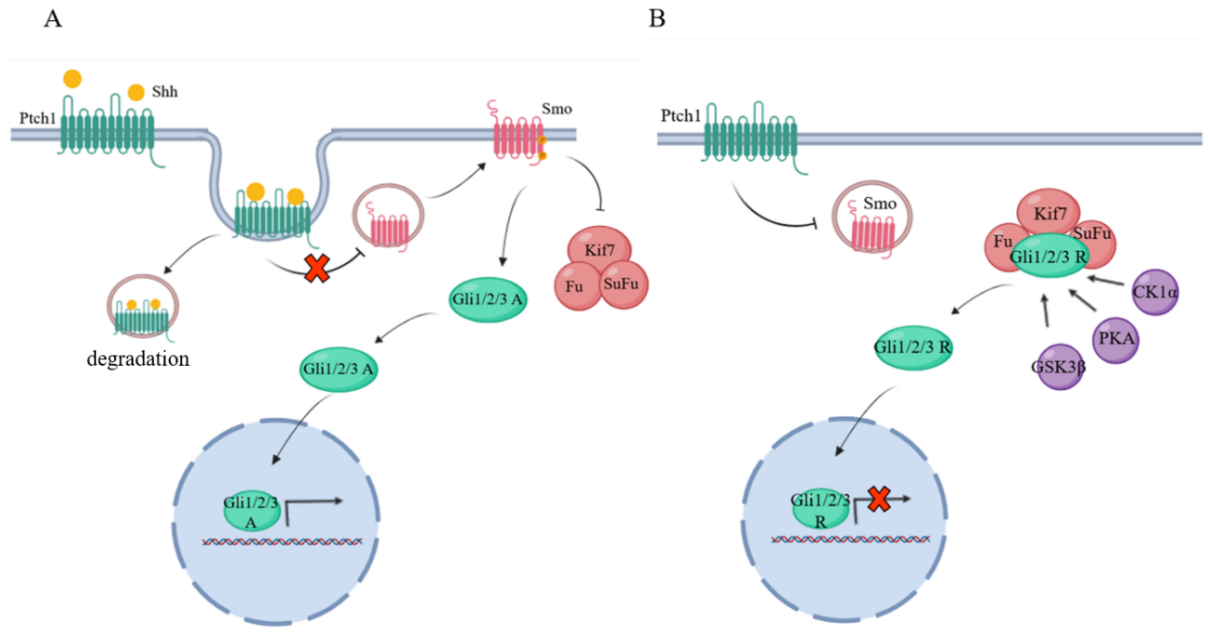

Figure 1.5: Generic overview of the Shh signalling pathway.
A: Secreted Sonic hedgehog (Shh) glycoproteins interact with transmembrane Patched (Ptch1) receptors. From these interactions Ptch1 and the Shh binding to it are internalised releasing the inhibition that Ptch1 exerted on Smoothened (Smo). Smo is stabilised and activated in the membrane, which results in the dissociation of the transcription factor inhibitory complex (TFIC) composed of Fu (Fused), SuFu (suppressor of Fused) and Kif7 (kinesin-like protein 7). proteins. This dissociation leads to the translocation of activated forms of Gli proteins (Gli1/2/3 A) leading to the activation of Shh target genes. **B:** In the absence of the ligand, Ptch1 remains inactive and inhibits Smo. With Smo inhibited the TFIC complex plus signalling cascades such as PKA (protein kinase A), CDK1 (cyclin dependent kinase 1) and GSK3β (glycogen synthase kinase 3β) promote the proteolytic change of Gli proteins, making them act as transcriptional repressors (Gli1/2/3 R). These forms of Gli proteins enter the nucleus and repress Shh target genes. Based on Carballo et al., 2018 and Lee et al., 2016.

2.2.5 Tgfβ/Bmp signalling

The transforming growth factor β (Tgfβ) superfamily is a conserved family of paracrine factors which include the Tgfβs, bone morphogenetic proteins (Bmps), growth and differentiation factors (Gdfs), glial-derived neurotrophic factors (Gdnfs) activins (Acts), inhibins (Inhs) and other ligands, such as anti-Müllerian hormone (Amh), left-right determination factor (Lefty) and nodal growth differentiation factor (Nodal) (Fig. 1.6A; Poniatowski et al., 2015). These different Tgfβ superfamily ligands induce multiple effects in the organism, being involved in a variety of critical cell decisions such as growth inhibition, cell differentiation, EMTs, ECM remodelling and immune suppression (Vortkamp et al., 1998; Zelzer et al., 2014). For the purposes of this thesis, I will focus on Tgfβs and Bmps.

Tgfβs are produced in a wide variety of cell types, including bone cells and the entire white blood cell lineage, in three major isoforms (Tgfβ1-3). In humans, they are encoded by genes located in distinct chromosomes, but the three proteins are highly homologous (Barton et al., 1988). More than a dozen of Bmp molecules are found in vertebrates and the Bmp family is divided into six main subgroups according to their structural characteristics and biological function (Katagiri and Watabe, 2016).

Tgfβs and Bmps family members are synthetised as inactive large homodimers in association with latent proteins. When these latent proteins are dissociated, Tgfβ and Bmp ligands become active (Schultz-Cherry et al., 1994). Other factors, such as changes in the pH environment or interactions with integrins (see section 2.3.2.) can also activate Tgfβ/Bmp ligands. After activation, Tgfβ ligands interact with a receptor complex forming a heterotetrameric combination containing two type I (TgfβrI) and two type II (TgfβrII) serine-threonine kinase receptors (Poniatowski et al., 2015). Bmps bind to Bmp type I (BmprI) receptors and type II (BmprII) serine-threonine kinase receptors but can also bind with less affinity to activin type II receptors (Katagiri and Watabe, 2016). Type II receptors for Bmps and Tgfβs ligands are constitutively active and control the binding of these ligands to type I receptors by inducing their phosphorylation. The specificities of the binding of Tgfβ /Bmps to their type I receptors depend on the identities of the interacting type II receptors and the cell type (Katagiri and Watabe, 2016; Poniatowski et al., 2015). After this, transduction of the Tgfβ or Bmp signalling pathways is initiated with the activation of Smad (mothers against decapentaplegic homolog) proteins. Smads can be classified as receptor (R-Smads), inhibitory

(I-Smads) or co-regulator Smads (Co-Smads). R-Smads are activated distinctly according to the sub-type of Tgfβ ligand that have triggered the pathway (Massagué, 2012). For example, Tgfβ ligands induce the activation of R-Smad2 or 3, while the R-Smads 1, 5 or 8 act as effectors of Bmp signalling (Fig. 1.6B). The I-Smads 6 and 7 act as negative regulators of the Tgfβ/Bmp signalling by binding and inhibiting the activity of R-Smads (Fig. 1.6B; Macias et al., 2015). If this inhibition does not occur, a final recruitment of the Co-Smad 4 to the activated effector R-Smad occurs and this complex enters the nucleus where it influences gene transcription (Fig. 1.6B; Shi et al., 1997). Some Tgfβ superfamily members bind extracellular antagonists (such as Noggin, Chordin and Follistatin) that inhibit their interaction with their receptors, thus dampening or blocking the cellular response to these factors (Chang, 2016).

Importantly, the Tgfβ/Bmp signalling pathway outcome is highly influenced by the cell type, the nature of the ligand, the receptors and the presence/absence of extracellular antagonists or agonists, as well as by the crosstalk with other signalling pathways, namely Notch, Wnt and Hh, (Chang, 2016; Luo, 2017).

2.3 Juxtacrine communication

2.3.1 Notch signalling

Notch (Notch homolog, translocation-associated) signalling mediates cell-cell communications between adjacent cells. It provides a simple, but effective system of communication in Metazoans and is commonly used to discriminate cell fate decisions (Andersson et al., 2011; Henrique and Schweisguth, 2019). This system involves a "signal-sending cell" that expresses a Notch ligand and presents it to a "signal-receiving cell", which possesses a Notch receptor. Notch receptors are transmembrane proteins composed of a Notch extracellular domain (NECD), a transmembrane segment and a Notch intracellular domain (NICD). In humans and mice, there are four Notch receptors (Notch1-4) and five distinct ligands, namely the Delta-like ligands (Dll1, Dll3 and Dll4) and the Jagged ligands (Jag1 and Jag2). Depending on the biological context, distinct Notch ligands can bind to more than one Notch receptor. Thus, according on the nature of the ligand binding to Notch receptors, Notch signalling can induce distinct cellular responses (Nandagopal et al., 2018). However, how this

regulation occurs remains unclear. In the absence of Notch ligands, Notch receptors are inactive. Activation of Notch signalling occurs when Dll or Jag ligands bind to the receptor and it involves several steps.

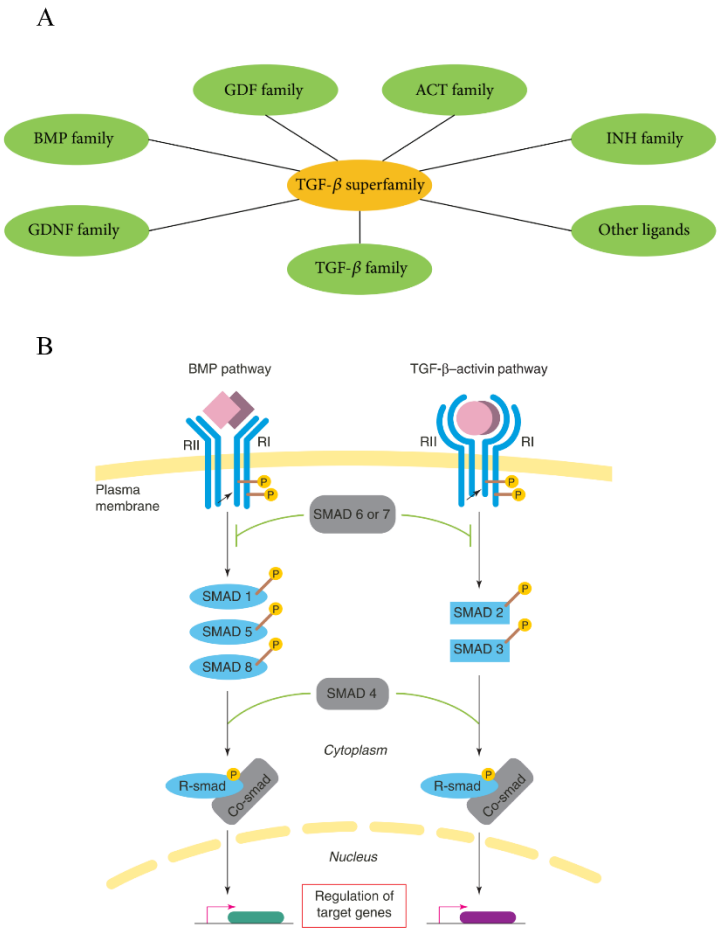

Figure 1.6: The Tgfβ member superfamily and the canonical, Smad-dependent Tgfβ/Bmp signalling pathway.
A: Schematic representation of the Tgfβ superfamily. Tgfβ members are divided into transforming growth factor-β (Tgfβ), inhibin (Inh), glial-derived neurotrophic factor (Gdnf), bone morphogenetic protein (Bmp), activin (Act) and growth and differentiation factor (Gdf) families. Other ligands, for example anti-Müllerian hormone (Amh), left-right determination factor (Lefy) and nodal growth differentiation factor (Nodal), are also included in this superfamily. **B:** Tgfβ and Bmps proteins are produced and secreted as a large latent homodimer complex. Upon activation, Tgfβ and Bmp ligands form a heteromeric complex with specific type II (RII) and type I (RI) receptors. Activation of RII induces the phosphorylation of RI releasing the signal to receptor-specific Smads (Smad 2 or 3 for Tgfβ ligands and Smad 1, 5 or 8 for Bmp ligands). Smad signalling transduction is modulated by inhibitory-Smads (Smad 6 and 7), but when this repression is not sustained, the co-mediator Smad 4 binds to activated receptor-Smad forming a complex that enters the nucleus and regulates the expression of target genes. Based on Lin et al., 2003 and Poniatowski et al., 2015.

First, the Notch receptor binds to a ligand in a juxtracrine fashion leading to the activation of the Notch receptor, a process also designated Notch trans-activation (Fig. 1.7; Henrique and

Schweisguth, 2019). This activation induces a mechanical stress, which triggers conformational changes in the negative regulatory region (NRR) of the NECD, unmasking a key proteolytic site (S2) that can be cleaved by a family of ADAM/TACE (a disintegrin and metalloproteinase) metalloproteases (Gordon et al., 2015; Stephenson and Avis, 2012). This initial cleavage exposes a γ-secretase- sensitive region on the intracellular side which is cleaved, releasing the NICD into the cytoplasm (Fig. 1.7; Mumm et al., 2000). NICD is transported to the nucleus and unlocks the repressor complex composed of mastermind-like protein (Mam) and DNA-binding domain protein CSL (also known as $RBPj_k$: recombining binding protein suppressor of Hairless), which culminates in the expression of Hes/Hey (Hairy/enhancer of Split/ Hes related family bHLH transcription factor with YRPW motif) genes that regulate gene expression (Fig. 1.7; Henrique and Schweisguth, 2019). Moreover, it was shown in *Drosophila* that Notch-ligand binding leads to the endocytosis of the ligand and the NECD of the Notch receptor by the "signal-sending cell" (Henrique and Schweisguth, 2019; Parks et al., 2000).

Notch signalling can also occur in a cis-manner and this case is observed when a Notch receptor of a given cell binds to a Notch ligand expressed by the same cell. However, this activation mode is not enough to trigger high mechanical stress and therefore does not expose the S2 site nor is NICD released intracellularly. Nevertheless, this mode of action has been described to recruit Notch receptors, thus competing with Notch receptor availability for ligands expressed on neighbouring cells and can thus indirectly modulate cell fate choices within a tissue (del Álamo et al., 2011).

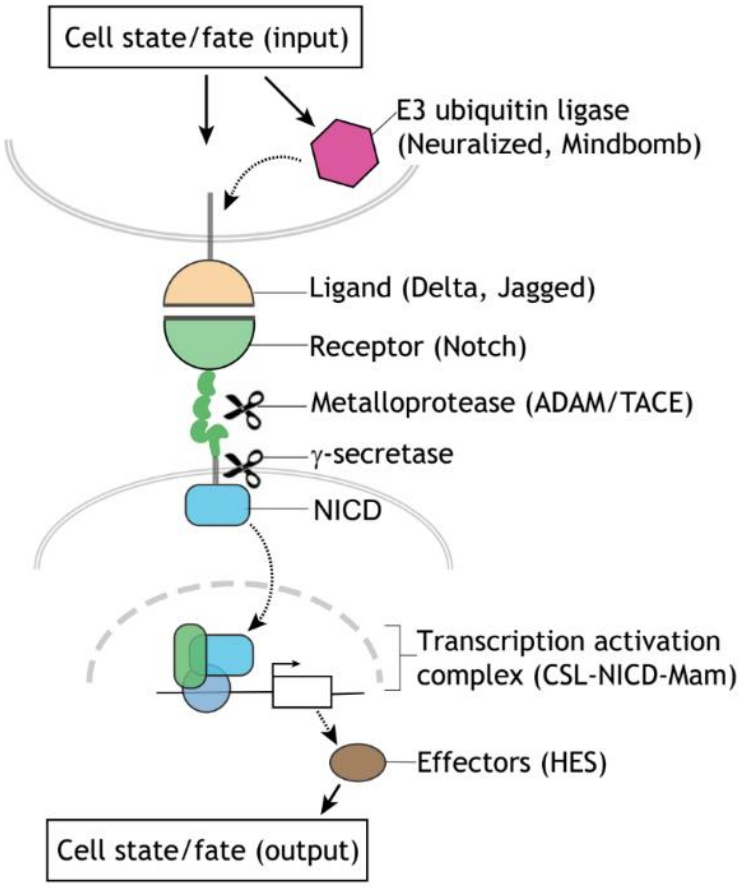

Figure 1.7: Overview of the Notch signalling pathway.
Canonical Notch signalling pathway is triggered when a "signal-sending" cell expressing a Notch ligand binds to a "signal-receiving" cell containing a Notch receptor. Notch ligand availability is tightly regulated by the E3 ubiquitin ligases group. Notch ligand-receptor binding triggers a series of structural changes of the Notch extracellular domain, which in turn activates two sequential cleavages of the Notch protein (one by the ADAM/TACE family of metalloproteases and another by the γ-secretase complex) releasing the Notch intracellular domain (NICD) into the cytoplasm of the cell. NICD translocates to the cell nucleus, where it forms a ternary protein regulatory complex with the DNA-binding proteins CSL and mastermind-like (Mam) that activate gene expression. Hes and Hey genes are the major Notch downstream effectors which modulate cell behaviour and fate in many biological scenarios. Adapted from Henrique and Schweisguth, 2019.

2.3.2 Cell adhesions

As described above, juxtacrine cell-cell communications can occur through the direct contact between cells which include (apart from the example of Notch signalling discussed above) cell-cell adhesions, or they can occur in an indirect fashion (cell-ECM adhesion). Cell adhesion receptors are divided into four major families that include the cadherins, immunoglobulin-like superfamily of cell adhesion molecules (Ig-CAMs), selectins and integrins (Gumbiner, 1996). These cell adhesion receptor proteins mediate adhesion in different

ways: For example, numerous cadherins and Ig-CAMs are homophilic cell adhesion receptors and only bind with another cell that expresses the same type of cadherin or Ig-CAM, while selectins and integrins are heterophilic and can interact with different receptors and/or extracellular matrix components (see section 2.4.1). Notably, mutations affecting the normal function of cell adhesion receptors are often associated with tissue pathology, including cancer (Farahani et al., 2014).

Cell-cell adhesion is mediated through cell junctions that can be divided into two main types: tight- and anchoring junctions. Tight junctions directly seal the space between cells and enable the creation of small paracellular pores between cells for selective ion trafficking, thus acting as small barriers (Steed et al., 2010). Anchoring junctions have the function of positioning cells within organised tissues, thereby maintaining cell and tissue morphology. This type of cell adhesion is mediated by cadherins, whose specific names often derives from the tissues where they were initially discovered (Oda and Takeichi, 2011). Cadherins are important in development since they bind to the F-actin cytoskeleton via three catenin proteins, providing cortical tension and dynamic stability of cell-cell junctions (Niessen et al., 2011). Two cadherins are particularly important for skeletal muscle: the neural- (N-) cadherin (also called cadherin-2) and myotubule- (M-) cadherin (also called cadherin-15). N-cadherin is present on all muscle cells, marking MuSCs, myoblasts and myofibres during development (Cifuentes-Diaz et al., 1993), while M-cadherin is particularly enriched during foetal myogenesis (Moore and Walsh, 1993). Conditional ablation of N- and M-cadherin in satellite cells leads to a break in satellite cell quiescence, with long-term expansion of a regeneration-proficient satellite cell pool, suggesting a role for these cadherins in maintaining satellite cell quiescence (Goel et al., 2017).

Connections between cells can also be mediated by the ECM (see section 2.4.). Cells bind to the ECM via a variety of receptors such as cell surface proteoglycans and sulfatides, but by far the most widespread receptors are the integrins. Integrins are present in all Metazoan animals (Lowell and Mayadas, 2012). They are heterodimeric transmembrane proteins composed of non-covalently associated α and β chains (Anderson et al., 2014; Barczyk et al., 2010; Hynes, 2002; Lowell and Mayadas, 2012). In mammals, the combination of eighteen α subunits with eight β subunits form twenty-four different integrin receptors which exhibit distinct binding affinities for ECM molecules and have a tissue-specific expression profile (Barczyk et al., 2010; Lowell and Mayadas, 2012). Integrins are very important because they connect the ECM with the intracellular cytoskeleton, via a myriad of intermediary proteins,

collectively called the integrin adhesome (Horton et al., 2016). Through this way, integrins mediate a wide array of cellular responses including adhesion, migration, proliferation, survival, differentiation, mechano-sensing and cytoskeletal organisation. Indeed, certain integrins are required for practically all developmental processes (Barczyk et al., 2010; Lowell and Mayadas, 2012), including skeletal muscle development (Thorsteinsdóttir et al., 2011).

2.4 The extracellular matrix

The macromolecular three-dimensional network of proteins that contacts almost all cells of multicellular organisms is called the extracellular matrix (ECM). For many years, it was thought that the ECM was a stable and mostly static non-cellular unit, which provided structural support to cells and influenced the hydrostatic pressure of tissues to sustain the morphology of the individuals (Frantz et al., 2010; Nelson and Bissell, 2006; Rozario and DeSimone, 2010). However, decades of research using cells in culture and the interpretation of genetic knock-outs in a wide range of model organisms led the scientific community to change this view and conclude that the ECM is a complex and highly dynamic entity. Apart from having biochemical properties which cells react to through receptors for specific ECM molecules, it can also act as a biochemical platform able to retain or release paracrine factors and hormones thus modulating local morphogen gradients (Frantz et al., 2010; Nelson and Bissell, 2006; Rozario and DeSimone, 2010). Furthermore, the physical nature of the ECM changes during development of the organisms being constantly remodelled not only during development but also in aging. This remodulation process is a consequence of a tightly regulated and balanced switching between ECM production, secretion, assembly, modification and degradation (Bonnans et al., 2014; Cox and Erler, 2011). Cells in turn react to the varying physical properties of the ECM, which modulates their responses at multiple levels (Wang, 2017).

Therefore, the ECM, in all its forms, directs cellular behaviour, being involved in directing the early morphogenesis of the embryo as well as that of practically all tissues and organs (Barros et al., 2011; Lockhart et al., 2011; Montano and Bushman, 2017; Thorsteinsdóttir et al., 2011; Zhou et al., 2018). Moreover, in addition to its importance during development, disruption in cell-ECM communications often leads to disease, such as chronic obstructive pulmonary disease, osteoarthritis, fibrosis and atherosclerosis, muscular

dystrophies, schizophrenia, Alzheimer´s disease, obesity and cancer (Bihlet et al., 2017; Lau et al., 2013; Sethi and Zaia, 2017; Sonbol, 2018; Williams et al., 2015).

2.4.1 A primer on extracellular molecules

Based on the composition and structure, the ECM can be divided into interstitial and pericellular matrices, the basement membranes being the most common form of pericellular matrices. The interstitial matrix is the matrix of the connective tissue and surrounds mesenchymal cells in the embryo, while basement membranes form a sheet-like structure that lines the basal side of epithelial and endothelial cells and surrounds muscle, neural and fat cells (Fig. 1.8; Frantz et al., 2010; Hynes and Naba, 2012; Rozario and DeSimone, 2010; Theocharis et al., 2016; Thorsteinsdóttir et al., 2011).

The ECM is primarily composed of two types of molecules: proteoglycans/glycosaminoglycans and glycoproteins. Proteoglycans are highly hydrophilic proteins covalently linked to carbohydrate polymers termed glycosaminoglycans (GAGs) which fill the interstitial space between cells. These include heparan-, chondroitin- and keratan sulphate. They absorb high compressive loads and additionally can bind to growth factors, chemokines and cytokines, protecting these factors from proteolysis. Furthermore, proteoglycans control specific signalling pathways and create morphogen gradients by sequestering ligands and balancing their turnover on the cell surface. They also can act as co-receptors for several RTKs (Frantz et al., 2010; Hynes and Naba, 2012; Rozario and DeSimone, 2010; Theocharis et al., 2016; Thorsteinsdóttir et al., 2011). Conversely glycoproteins are glycosylated fibrous proteins, which include collagens, fibronectin, laminins and tenascins. Glycoproteins play an important role in cell-ECM adhesion and are generally important for the assembly and supramolecular organisation of the ECM (Frantz et al., 2010; Hynes and Naba, 2012; Rozario and DeSimone, 2010; Theocharis et al., 2016; Thorsteinsdóttir et al., 2011).

Collagens are the most abundant proteins in mammals comprising 25%-35% of the total protein content of the body (Hynes and Naba, 2012; Theocharis et al., 2016). There are twenty-eight distinct collagen types in vertebrates. They consist of three polypeptide α-chains that assemble into homo- or heterotrimers exhibiting a triple helix-like structure. Depending on the biological context, collagens can vary in organisation, stiffness and density being associated

with basement membranes and/or interstitial matrix elements and support mechanical stress to several units of the musculoskeletal system (Theocharis et al., 2016; Thorsteinsdóttir et al., 2011). Most tissues have several collagens, but usually one type predominates in a given tissue. Mutations that affect the trimerization of collagens induce many chondrodysplasias, epidermolysis bullosa acquisita, several myopathies and Fuchs endothelia corneal dystrophy (Theocharis et al., 2016).

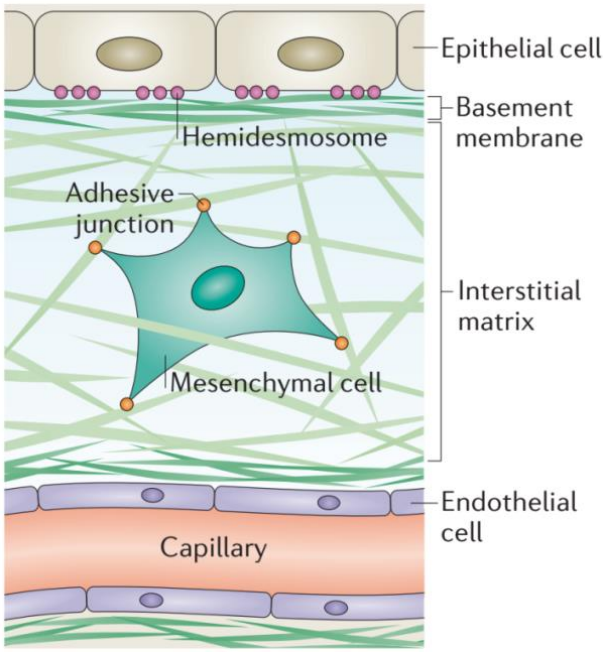

Figure 1.8: Extracellular matrix organisation in vertebrates.
Basement membranes are thin, sheet-like ECMs that line e.g. epithelial and endothelial cells, while the interstitial matrix is a three-dimensional network that surrounds and supports most mesenchymal cells. Based on Watt and Huck, 2013.

Laminins are large heterotrimeric cross-shaped glycoproteins (450-800 kDa) composed of an α, a β and a γ chain that are encoded by independent genes (Aumailley et al., 2005). In vertebrates, there are five distinct α chains (*Lama1-5*), three β (*Lamb1-3*) and three γ chains (*Lamc1-3*) forming at least sixteen different laminins, whose expression is tissue-specific. The nomenclature of laminins reflects their structural composition. For example, a laminin containing an α1, a β1 and a γ1 chain is termed laminin-111, while a laminin that is formed by an α5, a β2 and a γ1 chain is termed laminin-521 (Aumailley et al., 2005). β and γ chains exhibit

a coiled-coil domain that is necessary for laminin trimerization, however, this event is only concluded through the final incorporation of the α chain (Fig.1.9).

Laminins can self-assemble extracellularly independently of cells, however to have a biological role they need to attach to transmembrane receptors, which include the α3β1, α6β1 and α7β1 integrins, among others, as well as dystroglycans and syndecans (Hohenester and Yurchenco, 2013; Thorsteinsdóttir et al., 2011; Yurchenco, 2015). Importantly, laminins are the major components of basement membranes which together with collagen IV, nidogen and perlecan form the complete basement membrane structure. If laminin assembly fails, the remaining basement membrane components are not assembled. Laminins essentially are involved in governing cell-adhesions, proliferation, migration and differentiation and have a crucial role during earliest stages of embryonic development as well as during the development of a plethora of tissues and organs (Durbeej, 2010). Numerous congenital diseases are caused by deficiencies in one or more laminins, such as Merosin-deficient congenital muscular dystrophy type 1A, retinal ischemia, chronic kidney disease and Herlitz´s junctional epidermolysis bullosa (Aberdam et al., 1994; Nielsen et al., 2018; Reinhard et al., 2017).

Fibronectin matrices are widely distributed in early development and have crucial functions during the development of vertebrates (George et al., 1993; Georges-Labouesse et al., 1996; Snow et al., 2008; Singh et al., 2010). Fibronectin exists in two major forms: plasma fibronectin, a soluble inactive form which exists in blood plasma, and cellular fibronectin, a less soluble form which is produced within tissues and is assembled as a fibrillar fibronectin matrix (Mao and Schwarzbauer, 2005). Moreover, cells can assemble plasma fibronectin into a fibrillar insoluble fibronectin matrix (Moretti et al., 2007). In mammals, a single fibronectin (*Fn1*) transcript can undergo alternative splicing, producing several fibronectin variants (Schwarzbauer and DeSimone, 2011; Zollinger and Smith, 2017). Fibronectin is secreted as a dimer (of approximately 230-270 kDa, depending on the splice variant) where both subunits, composed of three types of modules: I, II and III, are linked by disulphide bonds (Fig. 1.10A). While type I and II repeats act mainly in the maintenance of the fibronectin dimer, the type III fibronectin module encompasses an Arginine-Glycine-Aspartic acid (RGD) domain which is crucial for cell-adhesion and can interact with tenascins, fibronectins, collagens, heparins and cell surface receptors (Schwarzbauer and DeSimone, 2011; Zollinger and Smith, 2017).

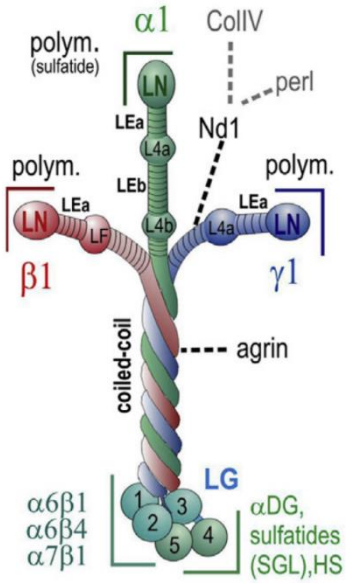

Figure 1.9: Structure of the laminin trimer.
Illustration showing laminin-111. The three laminin chains are united at the common coiled-coil domain, while the three N-terminal domains form the short arms which give laminins their cross-shaped structure and are responsible for laminin self-assembly. Laminins have specific binding domains to other ECM molecules, integrins, α-dystroglycan and sulfatides. Based on Yurchenco, 2015.

The fibronectin dimer is secreted as a folded and compacted dimer and the production of fibronectin matrix is dependent on a sequence of events: (1) fibronectin-integrin binding, (2) cell-mechanical stretching and (3) fibronectin-fibronectin interactions (Fig. 1.10B; Schwarzbauer and DeSimone, 2011; Zollinger and Smith, 2017).

Tenascins are part of the so called matricellular matrix, meaning that they do not have a structural function, but instead control the association of several ECM components to cells, thus balancing cell-adhesion (Bradshaw and Smith., 2014). There are four types of tenascins in vertebrates: tenascin-C, the most common type and the one addressed in this thesis, tenascin-R, tenascin-X, and tenascin-Y, each one with distinct tissue distribution (Chiquet-Ehrismann and Tucker, 2011). Tenascin-C is a modular glycoprotein composed of six dimers linked through disulphide bridges (Fig. 1.11; Midwood, 2016). Expression of tenascin-C is transient during embryonic development being restricted to certain types of tissues. In the adult it is sparse but is re-expressed at specific sites associated with tissue injury, inflammation and regeneration (Chiovaro et al., 2015). Typically, tenascin-C accumulates between the hard-soft

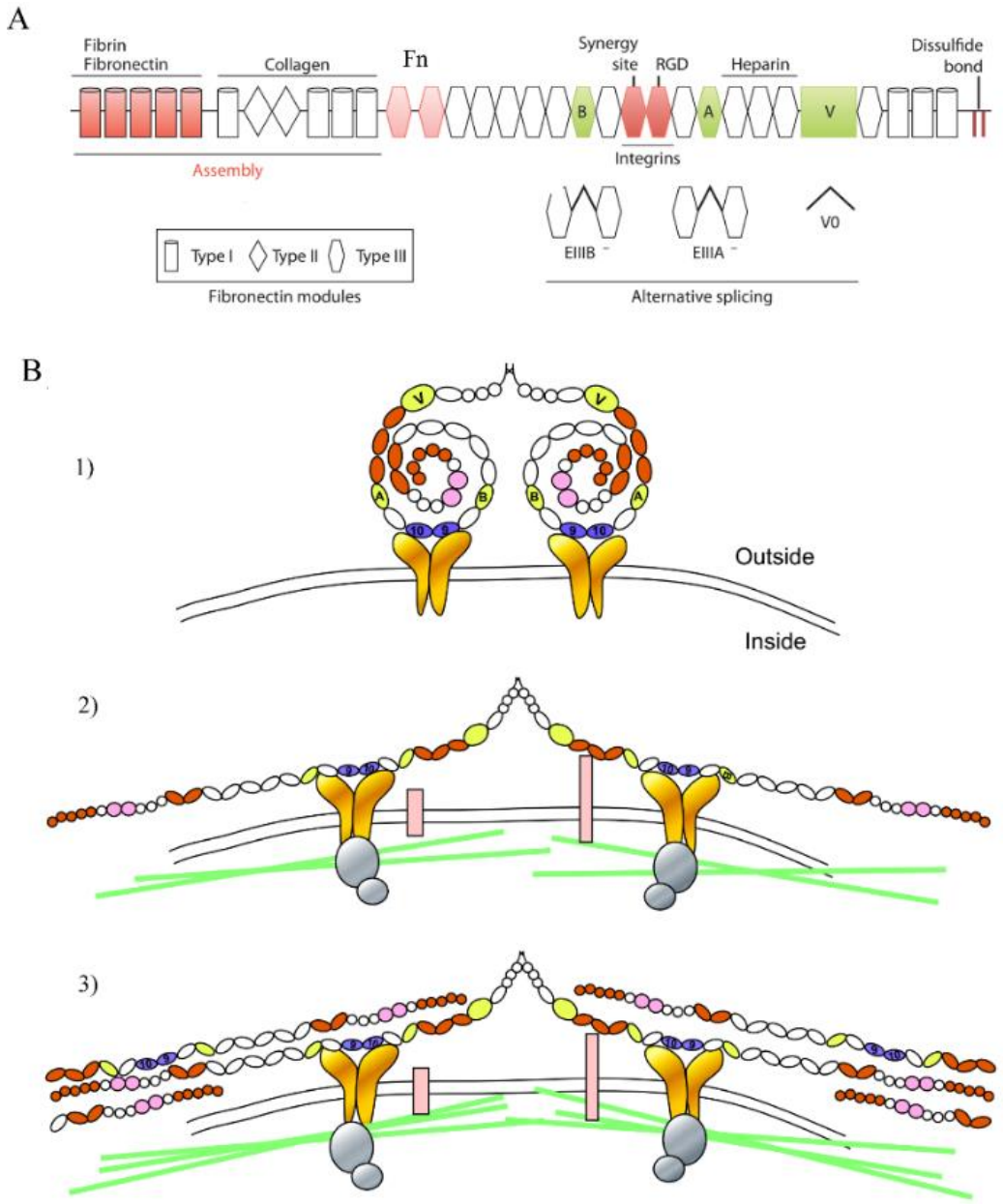

Figure 1.10: Fibronectin structure and assembly.
A: The fibronectin monomer is organised into three main modules (lower left) that include interaction sites with several ECM molecules and integrins (top) and alternative splicing isoforms (lower right). **B:** Schematic illustration showing the main steps of fibronectin assembly. 1) Initially, the secreted globular form of the fibronectin dimer attaches to integrin receptors specifically through the RGD motives (dark blue). 2) Integrin adhesome molecules (grey circles) link the cytoplasmic tails of integrins to the actin cytoskeleton (green lines) allowing the tensioned integrins to unfold and stretch the fibronectin molecule exposing the N-terminal fibronectin-fibronectin binding sites. 3) The exposure of these binding domains leads to fibronectin-fibronectin interactions culminating in the formation of a macromolecular fibrillar network composed of bonded fibronectin molecules. Fn: fibronectin. Adapted from Mao and Schwarzbauer, 2005 and Schwarzbauer and DeSimone, 2011.

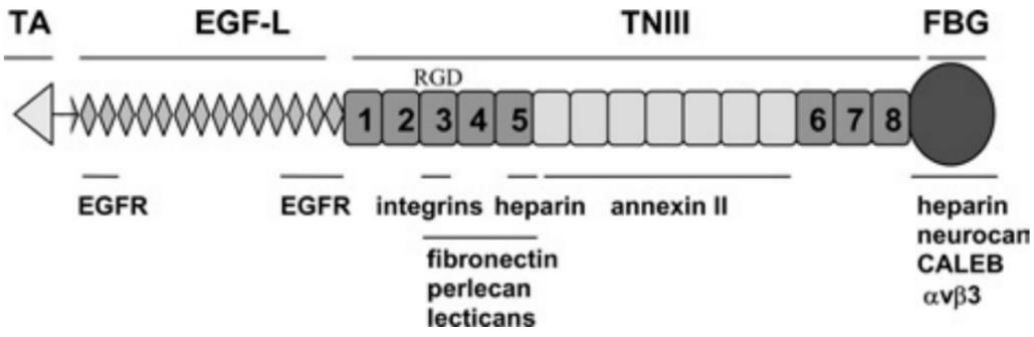

Figure 1.11: Structure of the tenascin-C molecule.
Each tenascin-C monomer comprises multiple binding domains that interact with cell surface receptors and other ECM molecules. The tenascin-C assembly domain is the TA region. Based on Trebaul et al., 2007.

tissue interface that includes higher mechanical loading, for instance at the myotendinous- and osteotendino-junctions (Chiquet-Ehrismann and Tucker., 2011). The true role of tenascin-C in development remains to be addressed since *TnC*$^{-/-}$ mice develop normally, albeit exhibiting some vascular and neuronal defects (Imanaka-Yoshida et al., 2003; Saga et al., 1992), possibly due to compensation from other tenascins (Chiquet-Ehrismann and Tucker, 2011). Moreover, tenascin-C is known to interact with cytokines, chemokines, retain certain growth factors such as Fgfs, Pdgfs and Egf (epidermal growth factors) and trigger specific signalling cascades (Midwood, 2016). Importantly, tenascin-C proteolytic fragments are modulators of fibronectin adhesion potential (Fig. 1.11) and are thus often associated with oncogenesis (Midwood, 2016; Midwood et al., 2004).

In the next sections, I will pinpoint the major functions of fibronectin, laminin and tenascin-C in the context of skeletal muscle development.

3. Embryonic origin of skeletal muscle

In vertebrates, all skeletal muscles of the body and some of the head derive from the segmented paraxial mesoderm, the somites (Fig. 1.12; Fig. 1.13A). MuSCs derive from the dorsal part of the somite, the dermomyotome (Fig. 1.13B) while the ventral region gives rise to the sclerotome, the precursor of the axial skeleton (Fig. 1.13B).

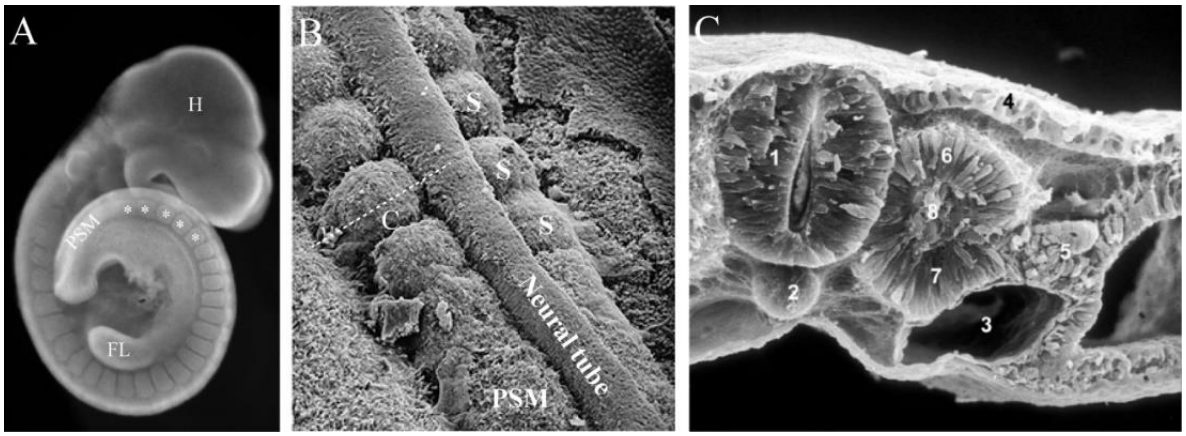

Figure 1.12: Somitogenesis.
A: Confocal microscopy image depicting the metameric organisation of somites (asterisks) along the axis of an E9.5 mouse embryo stained with Hoechst. **B:** Scanning electron microscopy image showing the segmentation of the anterior PSM into somites in a chick embryo. Line marks level depicted in C. **C:** Scanning electron microscopy image showing a transverse plane of an early chick epithelial somite. H: head; FL: forelimb; PSM: presomitic mesoderm; S: somites; 1: neural tube; 2: notochord; 3: dorsal aorta; 4: ectoderm; 5: intermediate mesoderm; 6: epithelial somite (dorsal); 7: epithelial somite (ventral); 8: mesenchymal somitocoel. Image A credits: James Ryall. Adapted from Gilbert, 2000 (B) and Christ et al., 2007 (C).

Skeletal muscles that derive from the somites can be classified in two groups: 1) muscles that form from MuSCs differentiating inside the segment, i.e. forming *in loco* (Fig. 1.13C); these muscles are the deep back muscles, intercostal, most lateral body wall and three out of four abdominal muscles and 2) muscles that form from MuSCs that undergo a long-range migration away from the segments (Fig. 1.13C) and only differentiate after arriving to their target sites; these muscles include the superficial back muscles, appendicular muscles, as well as the hypoglossal musculature (tongue and larynx) and diaphragm (Fig. 1.14; Huang et al., 1999). The craniofacial muscles (extraocular, masseter and pharyngeal muscles) do not derive from the somites. Rather they derive from the cephalic portion of the paraxial mesoderm and the prechordal mesoderm (Evans and Noden, 2006; Noden, 1983). Unlike the situation in the trunk, cephalic mesoderm is devoid of segmentation (Fig. 1.14; Sambasivan et al., 2011). Moreover, despite possessing some conserved elements, the molecular networks regulating cranial myogenesis are different from trunk myogenesis in several important aspects (Buckingham and Rigby, 2014; Sambasivan et al., 2011).

In this section, I will focus on the somites and their derivatives of relevance for the musculoskeletal system. Then in the following sections, I will focus on the mechanisms underlying the formation of axial and limb muscles in more detail.

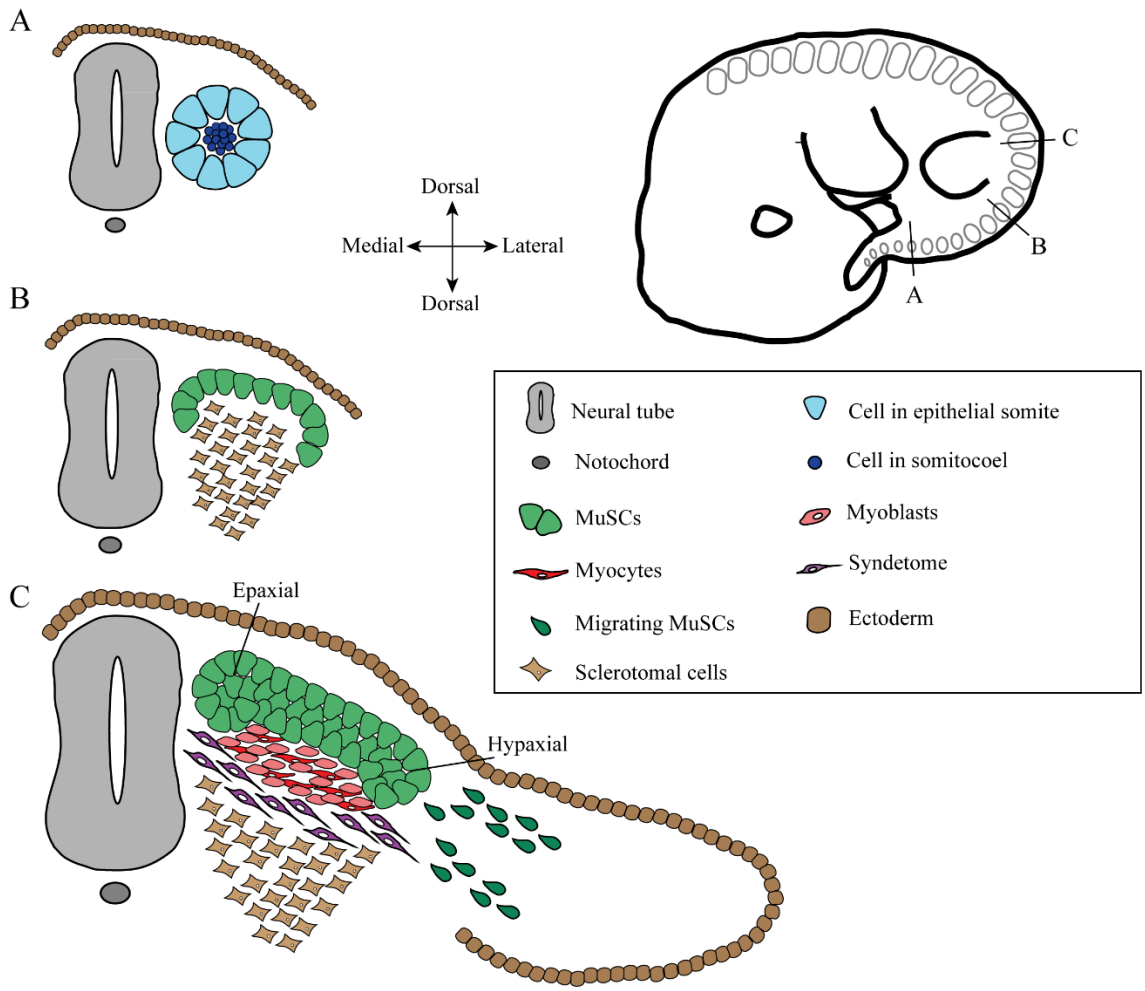

Figure 1.13: Illustration showing somite development at distinct axial levels along the caudal to rostral axis of an E11.5 mouse embryo.
A: Epithelial somites are rosettes of epithelioid cells (blue) with their apical side turned towards a central somitocoel which contains a few mesenchymal cells (dark blue). **B:** The ventral portion of the somite de-epithelializes to form the sclerotome (brown), while the dorsal portion remains epithelial and forms the dermomyotome (green). **C:** The dermomyotome originates cells for the formation of the myotome from its lips. These cells enter the area ventral to the dermomyotome, where they differentiate, first into myoblasts (pink cells), then into myotomal myocytes (red cells). At limb level, the ventro-lateral lip (VLL) of the dermomyotome gives rise to MuSCs that migrate long distance to their final destination like the limb bud (dark green cells). Communication between the myotome and the dorsal sclerotome induces the syndetome (purple cells). Adapted from Deries et al. (*in press*).

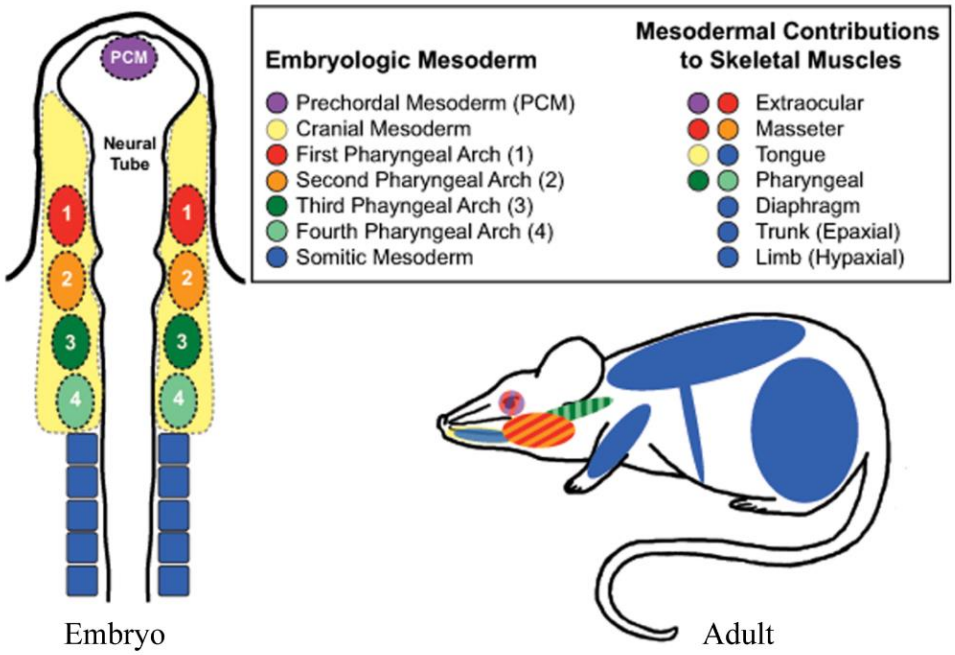

Figure 1.14: Embryonic origins of the adult skeletal musculature.
Distinct mesodermal regions of the embryo contribute to the formation of specific skeletal muscles in the mouse. Skeletal muscles of the trunk, limbs and diaphragm derive from the somitic mesoderm. The extraocular muscles arise from the pre-chordal mesoderm and the cranial paraxial mesoderm of the first pharyngeal arch. The first and second pharyngeal arches of the cranial paraxial mesoderm form the masseter muscles, while pharyngeal muscles derive from the third and fourth pharyngeal arches. Tongue muscles have their origins in the somitic mesoderm but migrate towards the cranial mesoderm niche. Adapted from Randolph and Pavlath, 2015.

3.1 Somitogenesis

Somites form from the paraxial mesoderm which flanks each side of the neural tube and the notochord (Pourquié, 2001; Fig. 1.12). The paraxial mesoderm arises bilaterally through gastrulation movements in the primitive streak (Iimura et al., 2007). The first cells to gastrulate form the cranial mesoderm. The portion of the paraxial mesoderm caudal to the head is initially unsegmented and is named the presomitic mesoderm (PSM). The PSM becomes segmented to form the epithelial somites (Pourquié, 2001). Soon after they form, somites differentiate, giving rise to several derivatives, including the progenitors of the trunk and appendicular skeletal musculature (Christ and Ordahl, 1995; Christ et al., 2007).

Somitogenesis is the first mark of the metameric pattern of the vertebrate body (Fig. 1.12A). This segmentation also contributes to the secondary metameric organisation of the

peripheral nervous system (Teillet et al., 1987). Somites are transient structures that are formed progressively in pairs, one on each side of the neural tube and the notochord (Fig. 1.12B). They bud off from the anterior portion of the PSM at regular intervals in a rostro-caudal fashion, as metameric spheres of epithelial cells surrounding a central cavity composed of mesenchymal cells, named the somitocoel (Fig. 1.12C; Fig. 1.13A; Christ and Ordahl, 1995). This rhythmic formation of somites is regulated by a complex network of events involving the interaction of a molecular clock with a wavefront of differentiation (Andrade et al., 2007; Aulehla and Pourquié, 2010; Saga, 2012; Mallo, 2016; Pais-de-Azevedo et al., 2018). The formation frequency of each somite (e.g. 30 minutes in zebrafish, 90 min in chicken, around 100 minutes in snakes, 120 minutes in mouse and 240-360 minutes in humans), as well as the total number of somites that are formed (e.g. 33 pairs in zebrafish, 50 in chicken, 65 in mouse, 38-44 in humans and from 300 up to 500 in snakes) is species-specific (Müller and O´Rahilly, 1986; Gomez et al., 2008). Importantly, newly formed somites located in the posterior regions of the embryo are less developed than the more rostral ones along the axis of the embryo, which permits the study of temporal somite differentiation within the same embryo (Fig. 1.13).

3.2 Somite compartmentalisation: the four major derivatives

As somites are formed, they immediately start to differentiate. This process of maturation leads to the formation of four major somite derivatives: first the sclerotome and the dermomyotome (Fig. 1.13B), then the myotome and finally the syndetome (Fig. 1.13C). These four somite compartments develop together to form the musculoskeletal system of the trunk (Brent and Tabin, 2002).

3.2.1 Sclerotome: the primordium of axial skeleton

The sclerotome contains all the precursors of the cartilage of the axial skeleton. Induction of sclerotome differentiation is dependent on extrinsic cues from the adjacent tissues (Chal and Pourquié, 2009; Christ et al., 2007). Shh produced by the notochord and the floor plate of the neural tube and Noggin, a Bmp antagonist, produced by the notochord, act directly on the ventral portion of the epithelial somite (Fan and Tessier-Lavigne, 1994; Fan et al., 1995;). These

cells undergo an EMT by downregulating N-cadherin (Duband et al., 1987), then they migrate to the perinotochordal space and together with somitocoel cells upregulate the transcription factors Paired box (*Pax*) *1* and later *Pax9,* the first sclerotomal markers (Ebensperger et al., 1995; Goulding et al., 1993). *Pax1* and *Pax9* transcripts synergise to ensure the maintenance of the sclerotomal lineage by activating Forkhead box C1/2 (*Foxc1/2)* transcription factors which promote cell proliferation and survival and sclerotomal vascularisation, prior to chondrogenic cell commitment. (Furumoto et a., 1999; Wilting et al., 1995).

As development proceeds, the sclerotome becomes divided into caudal and rostral halves (Fig. 1.15). A single vertebra is formed when the caudal half of one sclerotome joins the rostral half of the successive sclerotome along the body axis, a process known as sclerotome re-segmentation (Christ et al., 2004). The separation of the rostral and caudal sclerotomes within each segment originates a gap, the Von Ebner´s fissure that marks the definitive boundary between two adjacent vertebrae (Fig. 1.15; Christ et al., 2004). Thus, sclerotome re-segmentation is a vital step in early vertebrate development, allowing one muscular segment to attach to two adjacent vertebrae, a process that characterises the development of the axial musculoskeletal system in vertebrates (Chal and Pourquié, 2009; Christ et al., 2007). During this re-segmentation process, distinct subdomains defined by the expression of specific transcription factors characterise each single sclerotome (Chal and Pourquié, 2009; Christ et al., 2007) and each one of these sclerotomal subdomains will later contribute to the formation of distinct elements of the axial skeleton.

3.2.2 Dermomyotome: a progenitor epithelium

After sclerotome dispersal, the dorsal portion of each somite remains epithelial and forms the dermomyotome. The dermomyotome is composed of a central epithelial sheet, termed the central dermomyotome, which is surrounded by four contiguous lips defined as dorso-medial lip (DML) or epaxial lip, ventro-lateral lip (VLL) or hypaxial lip, rostral (RL) and caudal (CL) lip (Fig. 1.16A; Buckingham, 2006; Scaal and Christ, 2004). As development proceeds, the dermomyotome increases in size and elongates dorso-medially and ventro-laterally (compare Fig. 1.16A and C; Buckingham, 2006; Scaal and Christ, 2004). This elongation enables the regionalisation of the dermomyotome into distinct subdomains, the epaxial and hypaxial territories, which are characterised by the expression of specific markers (Fig. 1.16D; Spörle,

2001). The epaxial domain is localised above the notochord and includes the DML and the intercalated/central dermomyotome and is marked by the expression of *En1* (homeobox protein engrailed-1). The hypaxial domain is localised ventrally to the notochordal plane, is formed from the progressive growth of the VLL and expresses *Sim1* (single-minded homolog 1; Cheng et al., 2004; Gros et al., 2004; Spörle, 2001).

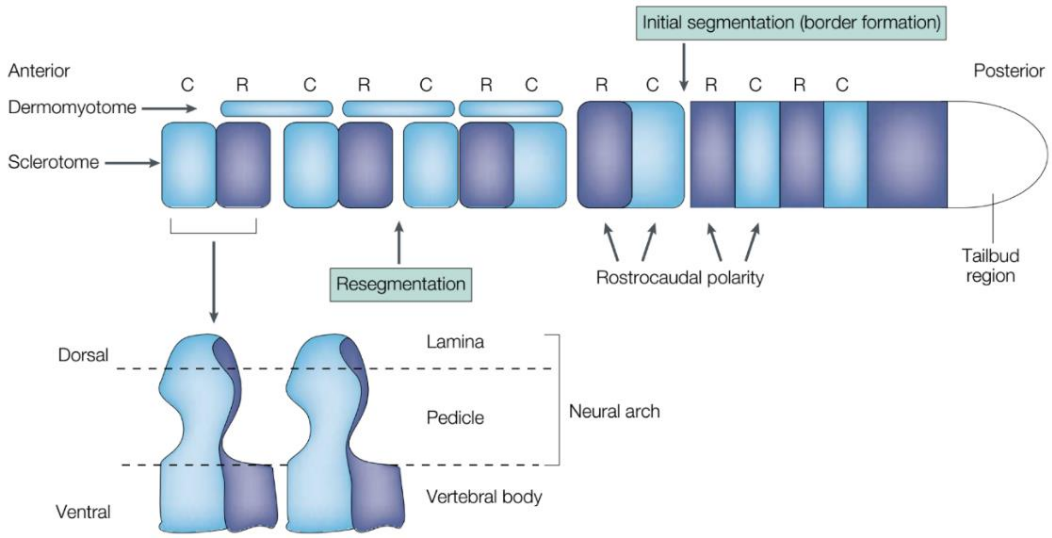

Figure 1.15: Sclerotome differentiation and vertebrae formation.
A: In the PSM, groups of cells acquire rostro-caudal polarity within the future segment. Later during development, sclerotomal cells undergo a re-segmentation process, during which a single sclerotome is divided into a rostral and caudal half, which will contribute to form distinct portions of the vertebrae. Thus, each vertebra is formed from the caudal and rostral halves of two adjacent sclerotomes. Adapted from Saga and Takeda, 2001.

The dermomyotome is composed of multipotent, highly proliferative and apoptosis-resistant epithelial cells (Delfini et al., 2000). These cells are marked by the expression of the transcription factors Pax3 and Pax7 and can give rise to several mesodermal lineages in addition to MuSCs, namely the dorsal dermis, endothelial cells, brown fat adipocytes and smooth muscle cells (Ben-Yair and Kalcheim, 2005, 2008; Relaix et al., 2005; Seale et al., 2008). *Pax3* transcripts are detected already in the unsegmented PSM and after that in the whole epithelial somite (Goulding et al., 1991; Williams and Ordahl, 1994). Later, Pax3 is downregulated in the ventral somite, concomitantly with the upregulation of Pax1 in the presumptive sclerotome and thus becomes confined to the dermomyotomal epithelium. Initially its expression extends through the whole dermomyotomal length, but eventually becomes enriched in the epaxial and

hypaxial extremities (Galli et al., 2008). Pax7 expression is turned on slightly later in development. It is first detected in the epithelial somites and later becomes restricted to the dermomyotome, becoming more strongly expressed in the central region of the dermomyotome (Galli et al., 2008; Relaix et al., 2006). Thus, Pax3 and Pax7 are evenly expressed in the early dermomyotome but later Pax3 becomes particularly enriched in the DML and VLL while Pax7 predominates in the central dermomyotome.

The epithelial cells of the dermomyotome are highly dynamic and can form filopodia-like protrusions that reach as far as the overlying ectoderm (Sagar et al., 2015). Trafficking of Fzd7 receptor along these filopodia allows dermomyotomal cell to receive Wnt signals (Sagar et al., 2015). triggered by ectodermal Wnt3a and Wnt6, which synergise with Bmp4 to maintain the epithelial integrity of the dermomyotome and promote the proliferation of the dermomyotomal

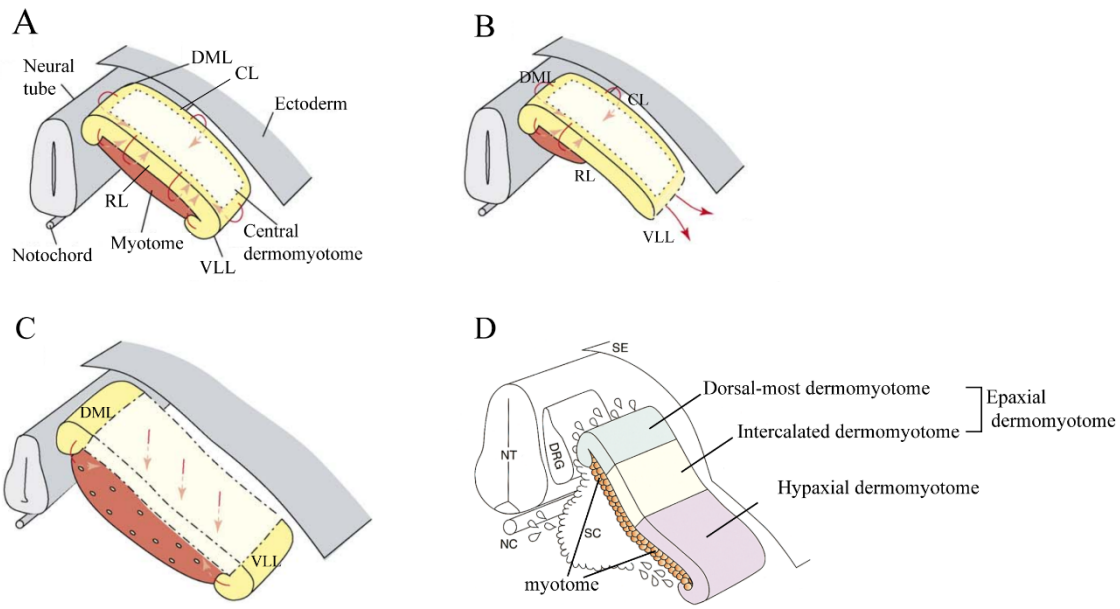

Figure 1.16: Dermomyotomal sources of MuSCs.
A: MuSCs from the dermomyotomal lips (yellow) undergo an epithelial-to-mesenchymal transition and delaminate first from the DML (also called the epaxial lip) of the dermomyotome (from E8.0 in the mouse) and later from the VLL (also called hypaxial lip) as well as the rostral and caudal lips. The MuSCs delaminating from the four lips form the myotome composed of differentiated mononucleated myocytes that span the segment. **B:** At certain axial levels, MuSCs of the VLL of the dermomyotome delaminate and undergo a long-range migration towards their target sites (limb bud, tongue or diaphragm). Therefore, at these levels, the hypaxial myotome does not develop. **C:** Starting at E10.5 in the mouse, cells from the central portion of the dermomyotome (cream) start to drop into the myotome. Then this central dermomyotomal sheet progressively dissociates to release proliferative MuSCs into the myotome. Some of these cells differentiate in the myotome while others conserve their MuSC status, thus becoming the MuSC pool of the axial muscles. **D:** The dermomyotome is divided into subdomains which relate to what region of the myotome they form. The epaxial region of the dermomyotome can be subdivided into two distinct regions: the dorsal-most (green) and the intercalated (yellow) dermomyotome. The remaining dermomyotome, is designated the hypaxial dermomyotome (purple). DML: dorso-medial lip (also called the epaxial lip) of the dermomyotome; VLL: ventro-lateral lip (also called the hypaxial lip) of the dermomyotome; RL: rostral lip of the dermomyotome; CL: caudal lip of the dermomyotome; SE: surface ectoderm; DRG: dorsal root ganglia; SC: sclerotome; NT: neural tube; NC: notochord Adapted from Buckingham, 2006 (A-C) and Tajbakhsh and Spörle, 1998 (D).

cells (Galli et al., 2004; Geetha-Loganathan et al., 2006). Furthermore, a discontinuous basement membrane containing laminins-111 and -511, known as the dermomyotomal basement membrane, lines the dermomyotome dorsally (Anderson et al., 2009; Bajanca et al., 2006; Deries et al., 2012; Rifes and Thorsteinsdóttir, 2012) and prevents its precocious differentiation (Bajanca et al., 2006).

Dermomyotomal Pax3/Pax7-positive cells have the potential to differentiate into skeletal muscle and are thus termed embryonic MuSCs (Tajbakhsh, 2009). As mentioned earlier, the dermomyotome is a transient embryonic epithelium that progressively releases MuSCs which colonise the space underneath it to establish the myotome (Buckingham, 2006). At certain axial levels, e.g. that of the limbs, the VLLs of the dermomyotomes contain MuSCs that undergo long-range migration to differentiate into the hypaxial muscles that develop away from the axial structures (limb muscles, diaphragm and tongue muscles; Fig. 1.16B; Babiuk et al., 2003; Buckingham et al., 2003). Thus, the hypaxial myotome does not develop at these axial levels. Once in their muscle mass (myotome, limb bud or other) these embryonic MuSCs have two possible fates: either they differentiate and get incorporated into muscle fibres, or they remain proliferative to maintain the MuSC pool within the muscle mass. Some of these proliferative MuSCs come to differentiate later during development while others are put aside as quiescent adult MuSCs (Ben-Yair and Kalcheim, 2005; Gros et al., 2005; Relaix et al., 2005; Kassar-Duchossoy et al., 2005). Importantly, as development proceeds, MuSC identity changes within the foetal and then postnatal environment (Messina et al., 2010; Mourikis et al., 2012). Thus, depending on the stage of development, MuSCs are termed embryonic, foetal, perinatal and finally adult MuSCs (Tajbakhsh, 2009). A summary of the terminology used for the different types of dermomyotome-derived MuSCs and their individual contribution for the specification of distinct skeletal muscles is provided in Table 1.2 (section 5.1; page 58).

3.2.3 Myotome: the first skeletal muscle

The myotome is the first skeletal muscle to form in vertebrate embryos. In anamniotes, the myotome is the first somite derivative to form (Scaal and Wiegreffe, 2006). In contrast, in birds and mammals, the myotome develops later in the somite differentiation programme through the delamination of temporally distinct waves of MuSCs from the different domains of the overlying dermomyotome (Gros et al., 2004; Spörle, 2001; Venters et al., 1999). To proceed

to myogenic differentiation, MuSCs downregulate the expression of Pax3 and Pax7 and initiate the muscle differentiation programme through the activation of a certain combination of MRFs: Myf5, Mrf4, MyoD, and Myogenin (see section 1.2; Buckingham, 1994; Pownall et al., 2002). The MRFs, discovered in the 1980s as being exclusively expressed in the skeletal muscle lineage, were also found to be able to convert non-muscle cells into muscle cells (Braun et al., 1989; Davis et al., 1987; Rhodes and Konieczny, 1989; Weintraub et al., 1989; Wright et al., 1989). Once produced, the MRFs activate a plethora of genes that encode proteins involved in the terminal differentiation of skeletal muscle cells.

In the mouse, *Myf5* is the first MRF to be expressed. Low levels of *Myf5* transcripts are detected in the PSM and epithelial somites *(*Kiefer and Kauschka, 2001) and at E8.0, at the onset of myotome formation, *Myf5* transcripts are upregulated in the DML of the dermomyotome (Ott et al., 1991; Teboul et al., 2002). These cells are the first to delaminate from the dermomyotome and they differentiate into elongated, mononucleated cells that span the segment, constituting the epaxial myotome (Fig. 1.16A; Eloy-Trinquet and Nicolas, 2002; Venters et al., 1999). As development proceeds, the DML grows dorsal-wards and more Myf5-positive cells delaminate and differentiate, thus adding new cells to the dorsally expanding epaxial myotome (Venters et al., 1999; Venters and Ordahl, 2002). After the epaxial myotomal domain is well established, a second wave of delamination of dermomyotomal MuSCs is observed in the VLL and these cells differentiate to form the beginning of the hypaxial myotome (Buckingham, 1994; Patapoutian et al., 1995; Smith et al., 1994). Subsequently, the ventral growth of the VLL provides more and more cells that delaminate and differentiate, thus adding cells to the ventrally expanding hypaxial myotome (compare Fig. 1.16A and C; Gros et al., 2004; Pu et al., 2013). While myotome growth is expanding both dorsally and ventrally, cells from the rostral and caudal lips of the dermomyotome turn on Myf5 and delaminate, migrate to the central segment where they differentiate and elongate bidirectionally, thus adding myocytes to the medial aspect of both the epaxial and hypaxial myotomal territories, contributing to the medio-lateral growth of the myotome (compare Fig. 1.16A and C; Gros et al., 2004; Venters et al., 1999).

It is interesting to note that although Myf5 is the first MRF to be expressed during the myotomal differentiation programme, *Mrf4* follows the expression of *Myf5*, being first detected at E9.0 in anterior somites and at E9.75 *Mrf4* transcripts accumulate in the epaxial myotome (Buckingham, 1994; Patapoutian et al., 1995; Smith et al., 1994). Moreover, in the epaxial region of the segment Myf5 and Mrf4 turn on Myogenin and thus drive myogenesis

independently of MyoD until E10.5 (Buckingham, 1994; Kassar-Duchossoy et al., 2004; Sassoon, 1993; Smith et al., 1994; see section 4.1). Hypaxially, both *Myf5* and *Mrf4* transcripts accumulate before MyoD is turned on but myogenic differentiation coincides with MyoD expression (Kassar-Duchossoy et al., 2004; Summerbell et al., 2002). However, MyoD is not required for the first stages of hypaxial myotome formation because mice lacking Myf5 and MyoD, but expressing Mrf4, express Myogenin and do form some hypaxial muscles (Kassar-Duchossoy et al., 2004). Thus, Myf5 and Mrf4 are thought to define a first phase of myotomal formation which lasts until E10.5 when MyoD expression comes up (Kassar-Duchossoy et al., 2004). However, it is interesting to note that this MyoD-independent phase lasts much longer in the epaxial myotome because epaxial myogenesis goes on for a full two days before MyoD expression comes up (E8.5-E10.5) whereas hypaxial myotome formation starts later, and MyoD expression comes up soon after (Bajanca et al., 2004; Tajbakhsh and Buckingham, 2000).

From E10.5 onwards, Pax3/Pax7-positive cells from the central dermomyotome start entering the myotome directly without going through the dermomyotomal lips. Then at around E11.0, the central dermomyotomal sheet progressively dissociates, releasing proliferative Pax3/Pax7-expressing MuSCs into the myotome (Fig. 1.16C; Ben-Yair and Kalcheim, 2005; Gros et al., 2005; Kassar-Duchossoy et al., 2005; Relaix et al., 2005).

The myotome is considered to have reached its terminal maturation point at E11.5 in the mouse (Deries et al., 2010, 2012; Tajbakhsh and Buckingham, 2000; Venters et al., 1999). This coincides with the time when the central dermomyotome sheet has dissociated fully and proliferative MuSCs have entered the myotomal muscle mass (Deries et al., 2012). It is also when the transformation of the segmented myotomes into the definitive axial muscle masses is about to begin (Deries et al., 2010; see section 4.4). Curiously, the mammalian myotome reaches its full maturation independently of innervation (Deries et al., 2008) contrarily to appendicular muscles (Hurren et al., 2015).

3.2.4 Syndetome: linking back muscles to the skeleton

The syndetome is the fourth derivative of the somites in amniotes and is characterised by the expression of the bHLH transcription factor Scleraxis (*Scx*), a marker of all tendon progenitors, mature tendons and muscle-tendon attachments (Brent et al., 2003; Cserjesi et al., 1995; Schweitzer et al., 2001). In the mouse embryos, *Scx* transcripts are first detected between

E9.5 and E10.5 and localise to the dorso-lateral sclerotome subdomain (Cserjesi et al., 1995). For many years, it was thought that axial tendons and cartilage shared the same Sox5/Sox6 (sex determining region Y-box factors 5/6)-expressing precursors. However, *Scx* expression is upregulated in *Sox5/Sox6* double mutants, showing that tendons develop from a Sox5/Sox6-independent lineage (Brent et al., 2005). This lineage, characterised by *Scx* expression and designated the syndetome, is specified by Fgfs secreted by the myotome (Brent et al., 2003). Moreover, *Scx* expression in restricted to cells in the area near the myotome by Pax1 activity, induced by Shh coming from the notochord (Brent et al., 2003). Thus, the syndetome domain is established between the sclerotome and the myotome (Fig. 1.17A). In fact, mouse embryos that do not form a myotome, fail to form a syndetome, demonstrating that the myotome is required to induce and sustain the syndetome lineage (Brent and Tabin, 2004; Brent et al., 2005).

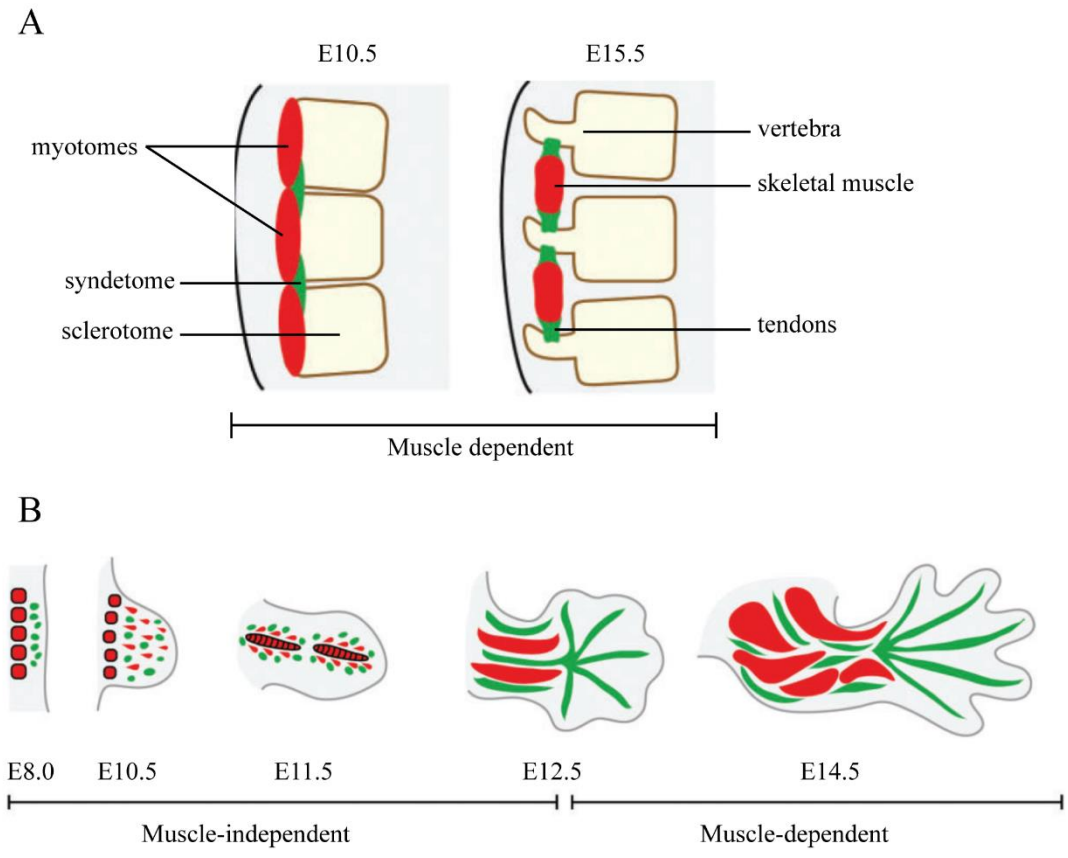

Figure 1.17: Trunk and limb tendon development.
A: In the trunk, tendon (green) differentiation requires signals from the muscle (red). **B:** In the limbs, tendinogenesis is initiated independently of the muscle, but in the stylo- and zeugopod regions, at later stages, tendon development requires signals from skeletal muscle cells. In the autopod, tendon differentiation is ensured through the developing cartilaginous centres and bones of this limb region. Adapted from Gaunt and Duprez, 2016.

4. Mechanisms of early stages of muscle differentiation

4.1 Transcriptional networks regulating myotomal populations

During the last decades, analysis of genetically altered mice with various combinations of targeted Pax and/or MRF gene mutations has contributed to an increased understanding of how transcriptional networks orchestrate myogenesis in the embryo (Buckingham and Rigby, 2014). Myf5, Mrf4 and MyoD were proven to be myogenic determination factors which specify the myogenic fate (Braun et al., 1992; Kassar-Duchossoy et al., 2004; Patapoutian et al., 1995; Rudnicki et al., 1992; Tajbakhsh et al., 1997), while Myogenin was shown to be a differentiation factor, causing terminal differentiation into myocytes and/or myotubes (Hasty et al., 1993; Nabeshima et al., 1993). Importantly, these studies have revealed that the relationships between the different transcription factors involved vary depending on the anatomical location where myogenesis occurs (Table 1.1). Here we will provide a brief overview of the transcriptional networks regulating myotome formation (Fig. 1.18; Buckingham and Rigby, 2014; Buckingham, 2017; Hernandez-Torres et al., 2017; Tajbakhsh, 2009).

It is generally believed that myotomal myogenesis is initiated through two pathways: first the epaxial pathway and then the hypaxial pathway (Fig. 1.18; Buckingham and Rigby, 2014). The earliest expression of Myf5 in the DML is regulated by the *Myf5* early epaxial enhancer (EEE; Teboul et al., 2002) whose activation occurs independently of Pax3 or Pax7 expression (Relaix et al., 2005). This enhancer appears to respond to Shh and Wnt signals from the notochord and dorsal neural tube, respectively (Fig. 1.18; also see section 4.2.1). Later on during epaxial myogenesis, Pax3 is, however, required and promotes Dmrt2 (doublesex and Mab-related transcription factor 2) expression which in turn turns on M*yf5* (Fig. 1.18; Sato et al., 2010) and hypaxially myogenesis is initiated by Pax3 and/or Pax7-expressing MuSCs (Buckingham and Relaix, 2015).

In the hypaxial dermomyotome, Pax3 needs other transcription factors to activate and regulate myogenesis. There, sine oculis homeobox transcription factors 1 and 4 (Six1/4) together with their co-activators Eya1/2 (eyes absent homolog 1 and 2) act with Pax3 to control *Myf5* activation (Fig. 1.18; Buckingham and Rigby, 2014; Giordani et al., 2007). Six1/4 proteins have also been shown to interact with *MyoD* regulatory elements and can thus directly control MyoD upregulation in the hypaxial dermomyotome (Fig. 1.18; Buckingham and Rigby,

2014). Hypaxial MuSCs also express the pituitary homeodomain transcription factor 2 (Pitx2) which lies genetically downstream to Pax3 and, when Myf5 and Mrf4 are mutated, they can activate *MyoD* in the hypaxial somite (L´Honoré et al., 2010; Marcil et al., 2003; Shih et al., 2007). There are important similarities between the transcriptional networks controlling hypaxial myotomal and limb muscle differentiation (Fig. 1.18; see section 4.5).

MuSCs coming into the myotome from the rostral and caudal dermomyotome lips are thought to first turn on Myf5 and then MyoD soon after (Venters et al., 1999). They migrate to the central segment where they turn on Myogenin and differentiate (Venters et al., 1999). Later, when the central dermomyotomal sheet dissociates, proliferating Pax3/Pax7-positive cells come into the muscle mass and some of those enter the myogenic differentiation programme, thus contributing to primary myogenesis (see section 5.1).

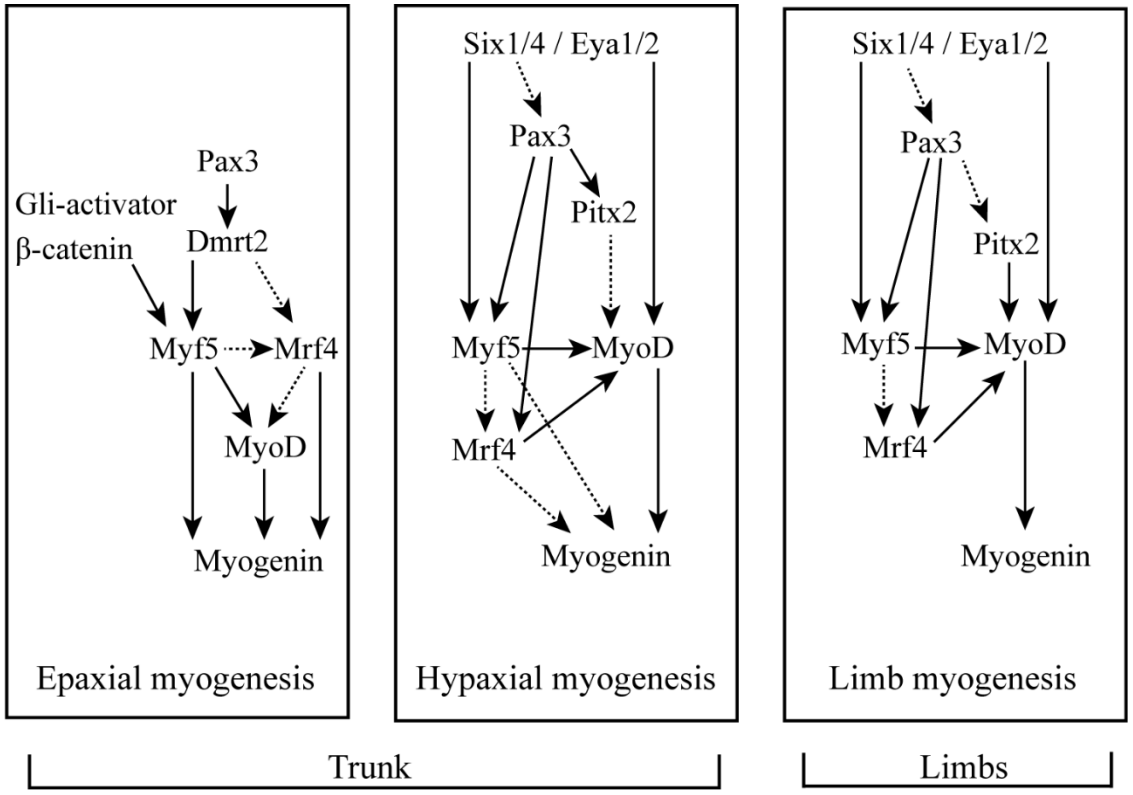

Figure 1.18: Transcriptional networks regulating myogenesis in the different regions of the myotome (trunk) and in the limb.
Full lines indicate core genetic networks and dashed lines correspond to complementary genetic networks. Based on Buckingham, 2017; Buckingham and Rigby, 2014; Hernandez-Torres et al., 2017; Sieiro et al., 2016 and Tajbakhsh, 2009.

Table 1.1: Phenotypes of loss of function (knock-outs) of MRFs.

Single gene knock-out	**Loss of function phenotype**	**References**
Myf5	Delay of the primary myotome development until Mrf4 and/or MyoD expression starts. Limb muscles develop normally.	Braun et al., 1992; Kablar et al., 1997, 1998; Kassar-Duchossoy et al., 2004
Mrf4	Variable skeletal defects depending on the allelic mutations. Phenotype is variable due to *Myf5* linkage. Affects a Myf5/Mrf4-dependent population that contributes to myotome growth between E9.0 and E10.5.	Olson et al., 1996; Patapoutian et al; 1995
MyoD	Normal primary myotome and epaxial muscle development. Hypaxial muscle development is delayed for 2.5 days. MuSCs delaminate and express Myf5, but limb myogenesis is delayed for 2.5 days as well and only starts at E13.5.	Kablar et al., 1997, 1998 Rudnicki et al., 1992;
Myogenin	Skeletal muscle develops normally but fail to differentiate.	Hasty et al., 1993; Nabeshima et al., 1993;
Combined gene knock-out	**Loss of function phenotype**	**References**
Myf5/Mrf4	Myotome formation is delayed. Perturbations in epaxial muscle development. MyoD expression is delayed for 1 day but is able to rescue myogenesis. Normal limb muscle development. Die perinatally.	Braun and Arnould, 1995; Kassar-Duchossoy et al., 2004; Tajbakhsh et al., 1996, 1997
Myf5/MyoD *(Mtf4 not affected)*	Epaxial and hypaxial myogenesis is delayed. Secondary myogenesis is impaired and newborns die at birth due to the lack of skeletal muscles in the body.	Kassar-Duchossoy et al., 2004, 2005
Myf5/MyoD *(Mrf4 affected)*	Lack of skeletal muscle in the body. Embryos not viable.	Kassar-Duchossoy et al., 2004; Rudnicki et al., 1993
Myf5/MyoG	Combination of both single mutation phenotypes	Rawls et al., 1998

4.2 Induction of myogenesis in the trunk

The morphogenesis of any tissue relies on the maintenance of the right balance between proliferation and differentiation of stem cells. Myogenesis is one of the best studied examples of this phenomenon. In fact, much is already known about how extrinsic signals from neighbouring tissues regulate the activation of the MRFs, thus assuring that muscle formation occurs in the right location at the right time.

4.2.1 Signalling molecules regulating epaxial myotome formation

During embryonic development, the dorso-ventral axis of the somite is patterned by several signals from adjacent tissues (Fig. 1.19A). One of these molecules is Shh, which at high levels induces sclerotome differentiation, while intermediate and low Shh levels influence myotome formation and MuSC maintenance, respectively (Cairns et al., 2008). Shh is produced and secreted by the notochord and the neural tube floor plate and finds its way through the sclerotome to reach the MuSCs of the DML where it induces *Myf5* expression (Borycki et al., 1999; Chiang et al 1996; Kahane et al., 2013). Shh signalling activates *Myf5* through Gli activator proteins that bind directly to the early epaxial enhancer within the *Myf5* locus (Fig. 1.19C; Gustafsson et al., 2002). However, the analysis of *Shh*-deficient mice revealed that Shh is necessary but not sufficient to drive *Myf5* activation in the DML of the dermomyotome (Teboul et al., 2003). It was later established that β-catenin regulates the expression of Gli factors and together they act synergistically to upregulate Myf5 (Fig. 1.19C; Borello et al., 2006). Evidence from in vitro experiments with chick and mouse embryos suggest that β-catenin is stabilised through signalling involving Wnt1/3a coming from the dorsal neural tube (Münsterberg et al., 1995; Tajbakhsh et al., 1998) and carried by migrating neural crest cells (NCCs) (Fig. 1.19B; Serralbo and Marcelle, 2014). However, more recently, an alternative hypothesis for β-catenin activity in the DML which uses the Notch pathway rather than Wnt pathway has been put forward for the chick embryo (Sieiro et al., 2016; see next paragraph). Bmps produced by the dorsal neural tube and surface ectoderm act as myogenic repressors (Fig. 1.19A; Ben-Yair and Kalcheim, 2008; Pourquié et al., 1996). However, myogenesis can proceed in the DML because Shh and β-catenin signalling in the dermomyotome DML activate

the expression of the Bmp antagonist Noggin (Fig. 1.19C; Marcelle et al., 1997; Reshef et al., 1998).

The Notch signalling pathway is also known to negatively regulate myogenesis (Kuroda et al., 1999; Schuster-Gossler et al., 2007). However, it was shown in the chick embryo that Notch signalling is transiently activated in the DML of the dermomyotome by migrating NCCs. NCCs delaminate from the dorsal neural tube and migrate to different target sites to differentiate into a variety of derivatives (Marmigère and Ernfors, 2007). NCCs express Dll1 which when they pass by the dermomyotomal MuSCs of the DML can bind to Notch receptors expressed on the surface of these cells. This transient Notch activation was shown to trigger epaxial myogenesis by activating Myf5 and MyoD in this region (Fig. 1.19B; Rios et al., 2011). Interestingly, it was later discovered that the activation of Notch by NCC-derived Dll1 does not lead to the transcriptional activation of Notch target genes (Sieiro et al., 2016). Rather, the transient Notch activation in the DML of the dermomyotome inhibits GSK3β activity, which stabilises the transcription factor Snail, an EMT regulator. The stabilisation of Snail leads to an EMT which releases β-catenin from the adherens junctions of dermomyotomal cells and this pool of β-catenin enters the nucleus to regulate transcription (Sieiro et al., 2016). The authors propose that it is this adherens junction β-catenin (and not β-catenin stabilised by canonical Wnt signalling) that synergises with Shh signalling and induces myogenesis in the DML (Fig. 1.19C).

This participation of NCCs in inducing myogenesis is particularly remarkable when one considers that after forming, the myotome assembles a basement membrane which the trunk NCCs use as a migration substrate (Tosney et al., 1994). Thus, at least in the chick embryo, the development of NCC and somites is interconnected and perfectly tuned since NCCs trigger myotome formation and the myotome then makes their path.

4.2.2 Signalling molecules regulating hypaxial myotome formation

Much less is known about hypaxial myotome formation but its formation is regulated by different signals compared to its epaxial counterpart. In mammals, the principal structure responsible for MRF induction in the VLL is the surface ectoderm. The surface ectoderm produces Wnt7a which is able to induce myogenesis through the non-canonical PCP pathway (Fig. 1.19A; Tajbakhsh et al., 1998). Although Myf5 is also the first MRF to be expressed in

the VLL, it is quickly followed by Mrf4 and MyoD expression, and MyoD is believed to be the major driver of myogenesis in the hypaxial myotome (Tajbakhsh and Buckingham, 2000).

It is interesting to note that the VLL grows much further and for a longer time than the DML. The lateral plate mesoderm secrets Bmp4 which blocks myogenesis and is thus believed to contribute to the proliferation of the hypaxial MuSC pool and the ventral expansion of the VLL (Fig. 1.19A; Amthor et al., 1996; Dietrich et al., 1998; Pourquié et al., 1996;). Noggin is absent in this region, but the effect of Bmp may be regulated by follistatin which is in a position to tune Bmp signalling, so as to allow for a balance between proliferation and differentiation in the hypaxial dermomyotome (Amthor et al., 1996).

4.2.3 Activation of myogenesis in the rostral and caudal dermomyotomal lips

Practically nothing is known about how myogenesis is activated in the rostral and caudal lips of the dermomyotome. This population of cells is, however, known to contribute differentiated cells to the medial aspect of both the epaxial and hypaxial regions of the myotome, thus increasing its size in the medio-lateral direction (Gros et al., 2004; Venters et al., 1999). The differentiation of cells in the rostral and caudal dermomyotomal lips is dependent on Myf5 (and possibly also Mrf4; Tajbakhsh and Buckingham, 2000; Tajbakhsh et al., 1996). However, it is presently unknown what signals turn on Myf5 in these cells. Soon after this Myf5-positive population of cells enters the myotomal space from the rostral and caudal lips, which occurs around E10.5 in the mouse, they turn on MyoD, followed by Myogenin (Venters et al., 1999). This observation together with the failure of these cells to undergo timely myogenesis in *Myf5/Mrf4* mutant embryos (Bajanca et al., 2006; Kassar-Duchossoy et al., 2004; Tajbakhsh and Buckingham, 2000), suggests that Myf5/Mrf4 are required to turn on MyoD and Myogenin in these cells.

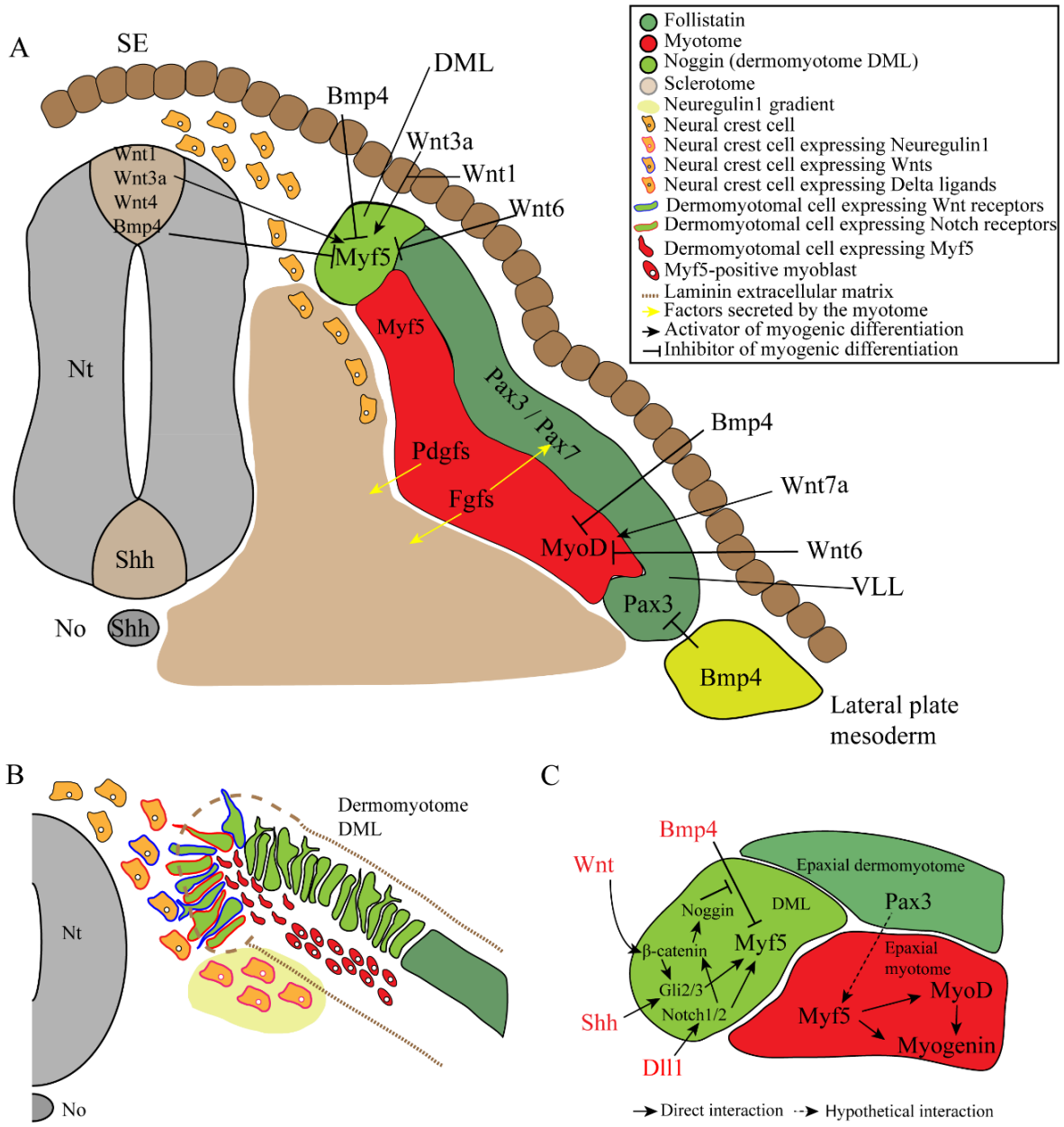

Figure 1.19: Induction of myogenesis by signals from neighbouring tissues.
A: Global overview of extrinsic signals produced by tissues adjacent to the somites and that regulate MRF activation in the myotome. **B:** Migratory neural crest cells expressing Delta briefly bind to filopodia of dermomyotomal MuSCs in the DML that express Notch. From that short interaction, myogenesis is activated and Myf5 is upregulated in the dermomyotome DML (red cells). Neural crest cells also bring Wnt ligands from the dorsal neural tube to DML cells which have the Fzd receptors. The brown dashed lines represent the incomplete dermomyotomal and myotomal basement membranes which enable cell-cell interactions between dermomyotomal/myotomal cells with other tissues. Neural crest cells also express Neuregulin-1 that represses myogenesis delimiting the myotome**. C:** Summarised and integrative model of Wnt, Bmp, Notch and Shh signalling interplay during induction of myogenesis in the DML of the dermomyotome. Note that recent data from the chick embryo suggest that Notch1 signalling acts directly on β-catenin (see text for details). DML: dorso-medial lip of the dermomyotome; VLL: ventro-lateral lip of the dermomyotome; SE: surface ectoderm; Nt: neural tube; No: notochord. Based on Deries et al. (*in press*).

4.2.4 The role of the myotomal basement membrane

As the myotome forms, a myotomal basement membrane is assembled by the developing myotomal cells (Tosney et al., 1984). This basement membrane contains three laminin variants, namely laminin-111, -211 and -511 (Nunes et al., 2017). The myotomal basement membrane separates the myotome from the sclerotome and prevents MuSCs and myoblasts from entering the sclerotome where chondrogenic cues predominate (Bajanca et al., 2006). It also acts as a containment structure that guides the myoblasts entering the myotome and may support the elongation of the differentiating myotomal myocytes (Bajanca et al., 2006). In fact, MuSCs of mouse embryos in which myotome formation was delayed failed to adopt myogenic fates (Tajbakhsh et al., 1996). Moreover, disruption of this basement membrane leads to major defects in myofibre elongation (Bajanca et al., 2006). Finally, as mentioned earlier, the basement membrane of the myotome is used as a substrate for NCC migration (Tosney et al., 1994).

4.3 Signalling molecules regulating myotome growth

After inducing the myogenic differentiation programme at early developmental stages, several signals interact to maintain skeletal muscle identity, myotomal development and growth (Deries and Thorsteinsdóttir, 2016). Analysis of *Shh*/*Gli* double mutant embryos has revealed that, with time, Shh loses the ability to induce myogenic differentiation of dermomyotomal MuSCs due to changes in Gli function from activator to repressor (McDermott et al., 2005). This mechanism of a loss in responsiveness to Shh enables the myotome to enter a growth phase (Kahane et al., 2013).

Notch signalling, which initially contributes to trigger epaxial myogenesis at least in the chick (see section 4.2.1; Rios et al., 2011; Sieiro et al., 2016), takes on its classical role at later stages, namely that of balancing differentiation and proliferation. In agreement with this, overexpression of Dll1 in chick somites leads to a block in myogenic differentiation in the myotome (Hirsinger et al., 2001) while dermomyotomal MuSCs in mouse embryos lacking Dll1 undergo accelerated differentiation, later leading to the exhaustion of the MuSC pool (Schuster-Gossler et al., 2007). More recently it was shown that overexpression of NICD under the control of a *Myf5* Cre driver (*Myf5*^{Cre}*:R26* $^{stop\text{-}NICD}$ embryos), which leads to constitutive Notch signalling in cells that express Myf5, blocks myogenesis in the embryo (Mourikis et al.,

2012). In these embryos, MuSCs are sustained in the presumptive muscle masses even in the absence of differentiated muscle cells and many of these cells, under these conditions, express high levels of Pax7 (Mourikis et al., 2012). These results strongly suggest that Notch signalling, which is normally induced by Notch-ligand expressing differentiated cells (Delfini et al., 2000; Schuster-Gossler et al., 2007), is enough to maintain MuSCs during muscle development.

Another signalling pathway that influences the equilibrium between proliferation and differentiation in the myotome is the Neuregulin (Ngr1) pathway. Nrg1 is produced by migrating NCCs, which, when these cells reach the area of the myotome, promote MuSC proliferation within the myotome through the ErbB3 (Erb-B2 receptor tyrosine kinase 3) receptor (Fig. 1.19B; Van Ho et al., 2011). In fact, when NCC migration is blocked or Ngr1 is lacking in mouse embryos, MuSC coming into the myotome tend to differentiate rather than proliferate (Van Ho et al., 2011).

Fgf signalling is also known to contribute to muscle development by triggering signalling pathways that modulate cell proliferation, survival, differentiation and motility (Goetz and Mohammadi, 2013). Myotomal cells express several Fgf ligands (Brent et al., 2005; deLapeyrière et al., 1993; Han and Martin 1993; Niswander and Martin, 1993). Fgfs from the myotome were shown to act on Fgfr1-expressing MuSCs of the chick central dermomyotome controlling their entry into the myotome through the activation of the MAPK/ERK/Snail pathway (Fig. 1.19A; Delfini et al., 2009). Indeed, Fgfr1 is expressed both in the dermomyotomal and myotomal territories (Yamaguchi et al., 1992). Fgfr4, which was shown to be a direct target of Pax3 in the mouse (Lagha et al., 2008) is expressed in the dermomyotome in the chick (Brent and Tabin, 2004; Kahane et al., 2001) and at the onset of myogenesis in the myotome in both chick and mouse (Brent and Tabin, 2004; Kahane et al., 2001; Marics et al., 2002; Stark et al., 1991). Moreover, myotomal Fgfs induce the development of the syndetome (see section 3.2.4; Fig. 1.19A; Brent et al., 2005). Members of the Pdgf family are also known to be present in somites. *Pdgfa* and *Pdgfrα* transcripts are expressed in the myotome and dermomyotome, respectively, and myotomal Pdgf signalling is involved in the development of the sclerotome (Fig. 1.19A; Mercola et al. 1990, Tallquist et al., 2000).

Interestingly, not only does the myotome affect the sclerotome, but the sclerotome also contributes to the development of the myotome. The caudal portion of each sclerotome secretes the Slit guidance ligand 1 (Slit1) protein which affects axonal migration (Wong et al., 2002). Slit1 interacts with its receptor Robo2 that is expressed by the myotomal Myf5-expressing myoblasts and induces their elongation in the rostral domain of the myotome (Halperin-Barlev

and Kalcheim, 2011). Currently, however, this is the only sclerotomal signal known to directly influence myotome development.

4.4 Myotome transformation and the formation of the trunk musculature

The mammalian myotome is a metameric transient structure that starts forming at E8.5 in the mouse embryo and then grows and differentiates for three days (Venters et al., 1999). A staging system divided into four stages has recently been proposed and is depicted in Fig. 1.20A-D (Deries et al., 2012). At the end of myotome development, the myotome transforms into the future adult muscle masses (Deries et al., 2010). Deries et al. (2010) studied the transformation of the epaxial myotome in detail and provide evidence to suggest that myotomal myocytes translocate to change their orientation and length to form the anlagen of epaxial muscle masses (Fig. 1.20E). The transformation of the hypaxial myotome into the hypaxial trunk muscles is less studied, but it also splits into different muscle masses (Christ et al., 1983; Cinnamon et al., 1999).

The epaxial myotome (red; Fig. 1.20F) transforms into the adult epaxial (deep back) muscles that in mammals are composed of four groups: the transversospinalis (the dorsal-most epaxial muscle), the longissimus; the iliocostalis (that lie more laterally) (Vallois, 1922), and lastly, but only at thoracic level, the ventro-medial levatores costarum (Sato, 1973; Smith and Hollyday, 1983). Together, the transversospinalis, longissimus and iliocostalis epaxial muscle groups compose the erector spinae muscle group, attaching to the vertebra acting mainly as flexor muscles, which is essential to support and stabilise the vertebral column (red; Fig. 1.20E, G). The levatores costarum muscle group has a major role in respiratory movements by attaching to the ribs (Sato, 1973; Smith and Hollyday, 1983).

The transformation of the epaxial myotome starts when the first myocytes are seen taking on a different orientation from that of the myotomal myocytes (Ontell et al., 1995; Venters et al., 1999; Deries et al., 2010). In the mouse and rat, the dorsal-most myocytes are the first to have a different orientation, not parallel to the axis of the embryo (Fig. 1.20D). This re-orientation marks the appearance of a first cleavage plane within the epaxial muscle masses, and they form a dorsal tilt, from which the transversospinalis masses will arise (Deries et al., 2010). At E12.0, a second cleavage plane appears ventrally to the first one to separate the future longissimus and iliocostalis muscle masses and at E12.5 all epaxial muscles are segregated (Fig. 1.20E; Deries et al., 2010). Although the epaxial musculature conserves some of the segmented features of the myotome, the

myotome itself has completely disappeared at E13.5 (Deries et al., 2010). In parallel, proliferative Pax3/Pax7-expressing MuSCs are found within the developing epaxial muscle masses in all phases of the myotome transformation (Deries et al., 2010; see section 5.1). Furthermore, *Scx*-expressing tendon precursor cells are moved along with the transformation of the epaxial myotome into the epaxial muscle masses. These cells accumulate between the developing muscle masses and within the cleavage points to form the definitive tendons at sites where the epaxial muscles later anchor to the axial skeleton (Deries et al., 2010).

The hypaxial myotome gives rise to the intercostal muscles and the abdominal muscles except for the rectus abdominis muscles which arise from the long-range migration of MuSCs (Christ et al., 1983; Tremblay et al., 1998). As mentioned earlier, while epaxial muscle morphogenesis is well documented, the transformation of the hypaxial myotome (blue; Fig. 1.20F) into adult hypaxial muscle masses remains poorly understood. Pioneering studies grafting quail cells into chick embryos described that the hypaxial myotome extends towards the lateral body wall (Christ et al., 1983; Rizk and Adieb, 1982). This extending myotome becomes segregated medio-laterally into four distinct layers which, at abdominal level, form the abdominal muscles (blue; Fig. 1.20G). Cinnamon and colleagues tracked the fate of individual quail myotomal cells through injection of stable fluorescent dyes and conclude that the hypaxial myotome also directly contributes to form the three main layers of intercostal muscle fibres (Cinnamon et al., 1999). Hence, the transformation of both the epaxial and hypaxial myotomes seems to be similar.

Interestingly, this *modus operandi* of forming a differentiated muscle and then transforming it is not “trunk-specific”. For example, the precursors of the extraocular muscles differentiate before translocating through the mesoderm-neural crest interface to reach the periocular environment, the extraocular muscle primordium (Noden and Francis-West, 2006).

The mammalian perineal muscles develop through two different mechanisms, first their MuSCs delaminate from the VLL of the dermomyotome in the hindlimb bud and migrate together with the limb muscle precursor cells. When they reach the limb, they start to differentiate and translocate towards the cloaca, their final destination, as differentiated cells (Evans et al., 2006; Valasek et al., 2005).

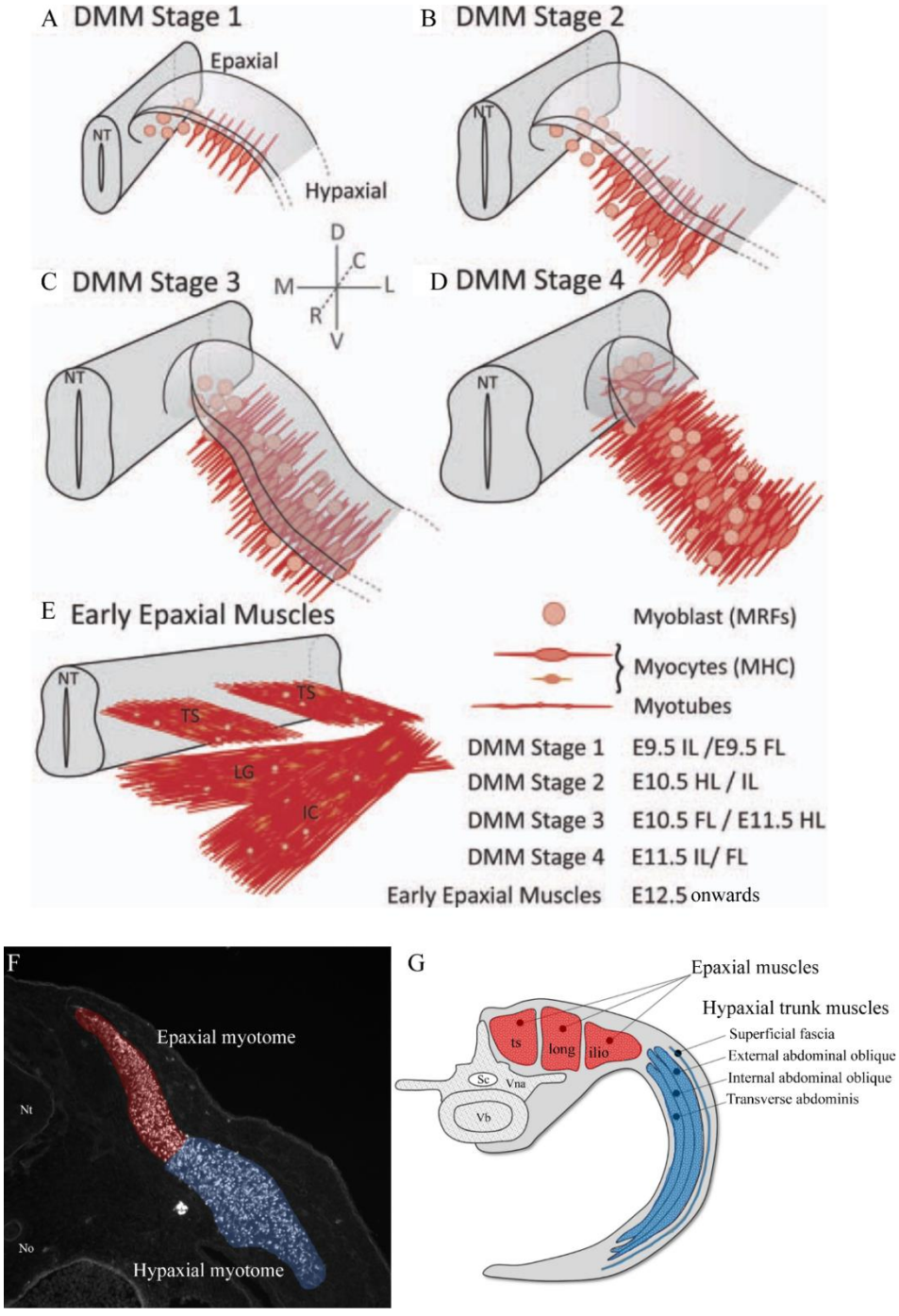

Figure 1.20: Developmental stages of the epaxial dermomyotome and myotome and segregation of the definitive axial musculature.
Four key dermomyotome/myotome stages (DMM stage 1-4) are represented beginning with the formation of the early epaxial myotome until the dissociation of the central dermomyotome. **A:** DMM stage 1 is marked by the emergence of the first fully differentiated myocytes. **B:** In DMM stage 2, the dermomyotome grows in a dorso-medial to ventro-lateral direction and myogenesis proceeds in the same direction with an accumulation of differentiated myocytes. **C:** In DMM stage 3, the dermomyotome has increased further in size and the dorso-medial lip becomes oblong. The myotome is thicker as myocytes arising from the rostral and caudal lips differentiate and contribute to its growth in the medio-lateral direction. At this stage, some Pax3/Pax7-positive cells parachute from the central dermomyotome, but the epithelium remains intact. **D:** DMM4 stage 4 marks the dissociation of the central dermomyotome. However, the dorso-medial (and ventro-lateral; not shown) lips still conserve their epithelial characteristics. Myoblasts increase in number throughout the myotome and in the dorsal-most region, epaxial myocytes begin to translocate. (**Continues next page**).

4.5 Limb myogenesis: migration and differentiation

Limb muscles arise from MuSCs of the VLLs of the dermomyotomes that are in the immediate vicinity to the limb buds. These MuSCs delaminate and undergo a long-range migration as undifferentiated cells that differentiate only after they have reached their target sites in the limb bud (Fig. 1.21A; Chevallier et al., 1977). This delamination is different from the one that forms the hypaxial myotome and, therefore, the MuSCs that originate the appendicular muscles will here be designated limb MuSCs in contrast to the trunk MuSCs. The dermomyotomal VLL contains two distinct cellular lineages, namely endothelial and myogenic cells, marked by the expression of the transcription factors Foxc2 and Pax3 respectively, which inhibit each other's expression (Lagha et al., 2009). Notch signalling has been shown to promote the endothelial lineage fate (Mayeuf-Louchart et al., 2014). At limb levels, Foxc2-expressing endothelial precursor cells are the first to migrate towards the limb bud and they have been shown to create a path composed of specific signals that are crucial for the correct migration of MuSCs (Yvernogeau et al., 2012). During their migration, limb MuSCs express Pax3, which is required for their survival (Relaix et al., 2005) and migration (Daston et al., 1996; Tremblay et al., 1998). They remain undifferentiated until reaching their target sites in the limb bud (Hutcheson et al., 2009). Limb MuSCs also express other factors that are also essential for MuSC migration.

VLL cells at all axial levels express the Met receptor (Met proto-oncogene, RTK), whose ligand, hepatocyte growth factor (Hgf) is expressed by the limb mesenchyme and acts as a paracrine factor triggering limb MuSC delamination from the VLL (Birchmeier and Brohmann, 2000; Scaal et al., 1999). Migratory limb MuSCs retain Met expression on their surface due to Pax3 (Yang et al., 1996).

(Continued from the previous page). E: The segmented myotome has disappeared since it has been transformed into the early epaxial muscles. **F:** Transverse perspective of an embryonic myotome of a E11.5 mouse embryo immunolabelled for myosin heavy chain (MHC). The epaxial and hypaxial myogenic populations are colour-coded in red and blue, respectively**. G:** Organisation of the definitive adult trunk muscle masses in a transverse view at the level of the abdomen after the transformation of the myotome. The epaxial and hypaxial muscle masses are shadowed with the same colours as in image F to better understand the origin of the adult musculatures. DMM: dermomyotome/myotome; R: rostral; C: caudal; D: dorsal; V: ventral; M: medial; L: lateral; FL: forelimb level; IL: interlimb level; HL: hindlimb level; MRFs: myogenic regulatory factors; Nt: Neural tube; No: Notochord; Sc: Spinal cord; ts: transversospinalis; long: longissimus; ilio: iliocostalis; Vna: ventral neural arch; Vb: vertebral body**.** For simplicity, the caudal and rostral lips of the dermomyotome are not drawn in A-E. The illustrations are schematic and are not intended to be to scale with each other. Adapted from Deries et al., 2012 (A-E) and Hall et al., 2017 (F-G).

Limb MuSCs also express Lbx1 (ladybird homeobox 1), which is crucial for the correct migration of MuSCs into the limb (Dietrich et al., 1999; Gross et al., 2000). Finally, the migratory route of limb MuSCs is ensured through the establishment of a chemoattractant signal involving the C-X-C-motif chemokine receptor 4 (Cxcr4) expressed by the migratory limb MuSCs and its ligand Cxcl12 (C-X-C-motif chemokine ligand 12; known also as Sdf1) secreted by the limb mesenchyme (Vasyutina et al., 2005).

By E11.5 in mouse embryos, limb MuSCs have migrated through the limb mesenchyme and, before myogenesis is initiated, they are arranged into the early dorsal and ventral muscle masses (Fig. 1.21B, C). The separation of dorsal and ventral pre-muscle masses is orchestrated by the limb mesenchyme located in the centre of the limb bud and which derives from the lateral plate mesoderm (Haase et al., 2002; Kramer et al., 2006). Once in the limb bud, Pax3-positive limb MuSCs first proliferate thus increasing the number of stem cells in these cellular aggregates. Indeed, the lateral plate mesoderm-derived limb mesenchyme expresses high levels of Bmps, which, as stated previously, act as myogenic repressors in this context (Duprez, 2002; Macias et al., 1997).

Not as much is known about how myogenesis is triggered in the limb compared to the trunk. Moreover, the signals differ depending on where in the limb MuSCs are (Deries and Thorsteinsdóttir, 2016). However, when limb MuSCs enter the myogenic programme, they first express Myf5 and later, MyoD, followed by Myogenin (Fig. 1.18). Later on during limb myogenesis, Pitx2 can also activate MyoD directly (Hernandez-Torres et al., 2017). Pax7-expressing limb MuSCs are detected later in development (at E12.5) first in the proximal region of the limb bud, near the entry point of the limb nerve (Lee et al., 2013) and they will originate the foetal MuSCs that drive secondary myogenesis (Hutcheson et al., 2009).

In contrast to the situation in the trunk, in the limb, myoblasts fuse into multinucleated myotubes immediately after their differentiation (Lee et al., 2013; Sieiro-Mosti et al., 2014). Muscle primordia arise from the muscle splitting of both the dorsal and ventral pre-muscle masses. Limb blood vasculature, which in amniotes is formed independently of limb muscle masses, promotes the muscle spitting event that occurs in the zones enriched in endothelial cells (Tozer et al., 2007). Endothelial cells express high levels of Pdgfb that attracts connective muscle precursor cells around muscle pre-masses to mark the future spitting area (Tozer et al., 2007).

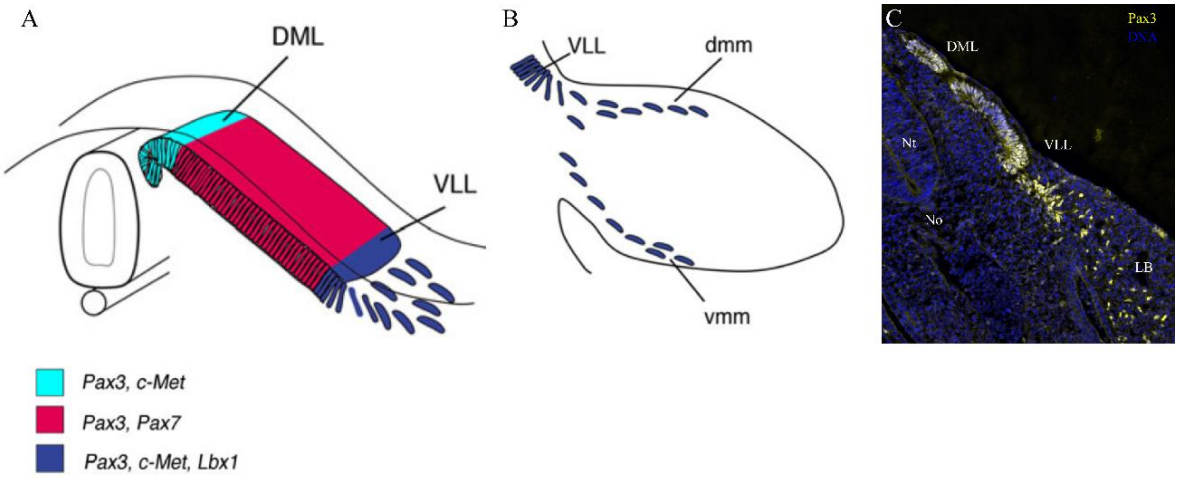

Figure 1.21: Specification and migration of limb MuSCs.
A: Scheme depicting the regionalisation of the dermomyotome at E10.5. MuSCs in the DML express Pax3 and c-Met. Central dermomyotomal cells express both Pax3 and Pax7. Migratory limb MuSCs expressing Pax3, c-Met and Lbx1 (dark blue) migrate from the VLL of the dermomyotome towards the limb bud. **B:** In the limb bud, limb MuSCs migrate dorsally or ventrally to form the dorsal and ventral muscle masses, respectively. **C:** Transverse view of a cryosectioned E10.5 mouse embryo at the forelimb level showing immunolabelled Pax3-positive cells (in yellow) delaminating from the dermomyotome VLL and colonising the limb bud. DML: dorso-medial lip of the dermomyotome; VLL: ventro-lateral lip of the dermomyotome; dmm: dorsal muscle masses; vmm: ventral muscle masses; LB: limb bud; Nt: neural tube; No: notochord. Adapted from Yokoyama and Asahara, 2011.

4.6 Limb tendinogenesis

In contrast to deep back and intercostal muscle masses, tendons of abdominal and limb musculatures arise from the lateral plate mesoderm and not from the somites (Kardon, 1998; Kieny and Chevallier 1979; Tozer and Duprez, 2005). In tetrapods, each limb is organised in three main zones, which are from proximal to distal: the stylopod (upper arm/thigh), the zeugopod (forearm/calf) and the autopod (fingers/toes). In the mouse embryo, during early limb bud formation, tendon progenitor cells and limb MuSCs are physically mixed within the limb mesenchyme. Induction of *Scx* starts in proximal regions and expands towards the distal domains. In contrast to the situation in the trunk, *Scx* expression in the limb occurs independently of the presence of skeletal muscle (Gaunt and Duprez, 2016) and is first observed in dorsal and ventral sub-ectodermal regions that are in proximity to the already segregated dorsal and ventral pre-muscle masses (Fig. 1.17B; Murchison et al., 2007; Schweitzer et al., 2001). At E12.5 proximal tendon progenitor cells undergo a re-organisation and they become intermingled between the developing limb muscles and cartilage (Gaunt and Duprez, 2016),

while ventrally, these progenitors form a dorsal and ventral blastema instead (Rothrauff et al., 2015). Further tendon development involves the organisation of cells by a mesenchymal ECM that is particularly enriched in tenascin (Hurle et al., 1989). Later, at E13.5, tendon progenitor cells condensate to form the definitive tendons of the main limb regions (Murchison et al., 2007).

The regulatory mechanisms underlying limb tendon formation are also distinct from that of the trunk (Fig. 1.17B). As mentioned above, limb skeletal muscle signals are not necessary to induce limb tendon differentiation, because muscle-deficient mutant mice initially show normal *Scx* expression in the limbs (Brent et al., 2005). Rather, Scx appears to be induced by Wnt signals from the surface ectoderm (Yamamoto-Shiraishi and Kuroiwa, 2013). Nevertheless, at later stages, limb tendon differentiation is governed in two independent ways: stylopod and zeugopod tendons depend on Fgfs produced by skeletal muscle (Edom-Vovard et al., 2002; Eloy-Trinquet et al., 2009; Kardon, 1998), while autopod tendons do not require skeletal muscle signals. Instead, signals from cartilage are important to drive autopod limb tendinogenesis (Huang et al., 2015).

5. Later stages of skeletal myogenesis

5.1 Primary myogenesis

Primary (or embryonic) myogenesis is essential to organise the basic muscle pattern of multinucleated myotubes and to establish the connection between muscles and their tendons and nerves. In the trunk, primary myogenesis starts after myotome development at E11.5, when MuSCs from the dissociating dermomyotome enter the myotome, and it ends at E14.5 in the mouse (Fig. 1.22; Table 1.2; Biressi et al., 2007; Stockdale et al., 1992). Primary myogenesis therefore accompanies the transformation of the embryonic myotome into the definitive epaxial and hypaxial muscle masses (see section 4.4; Deries et al., 2010). In the limbs, and other regions receiving migrating dermomyotome-derived MuSCs, primary myogenesis starts after the arrival of the MuSCs to their target sites (Fig, 1.22; Table 1.2; Buckingham, 2001; Christ and Brand-Saberi, 2002; Goulding et al., 1994).

In the limb, primary myoblasts (also called embryonic myoblasts) develop from Pax3-expressing MuSCs (Table 1.2) whereas in the trunk, a mixture of Pax3- and Pax7-positive MuSCs are released from the dermomyotome, and some of these cells differentiate into myoblasts that fuse with the existing myotomal myocytes (Fig. 1.22; Biressi et al., 2007; Kassar-Duchossoy et al., 2005; Relaix et al., 2005). Since many of these cells co-express Pax3 and Pax7 (Fig. 1.22; Table 1.2; Kassar-Duchossoy et al., 2005; Relaix et al., 2005), it is unclear whether Pax3 and Pax7 play similar or different roles in this context. Knock-in of Pax7 into the Pax3 locus leads to normal myogenesis in the trunk, indicating that Pax7 can compensate for the absence of Pax3 in trunk MuSCs (Relaix et al., 2004). However, limb MuSCs fail to migrate in the absence of Pax3, showing that Pax7 is not able to induce the migratory behaviour normally regulated by Pax3 (Relaix et al., 2004).

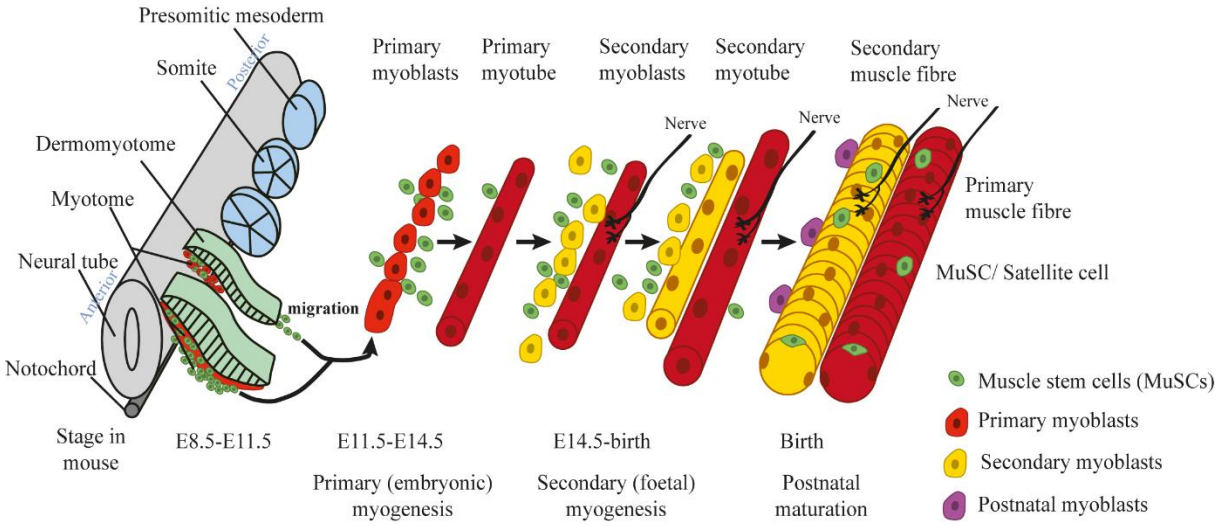

Figure 1.22: Summary of skeletal muscle development.
Scheme showing primary and secondary myogenesis and postnatal maturation of muscle fibres. All skeletal muscles of the vertebrate body arise from the dermomyotomal MuSCs of the somites (green). These cells either undergo long-range migration and differentiate after reaching their target site or translocate underneath the dermomyotome and differentiate there to form the segmented myotomes which will later transform into axial muscles. In their differentiation zones, MuSCs either remain proliferative and undifferentiated or they differentiated into primary (red) then secondary (yellow) and finally into postnatal (perinatal or adult) myoblasts (purple), depending on when during development they enter the differentiation programme. Multinucleated primary myotubes (dark red) arise from the fusion between primary myoblasts, then secondary multinucleated myotubes (yellow cell with cylindrical shape) are formed from the fusion of secondary myoblasts to each other. Later during foetal development, after the formation of all the secondary myotubes, secondary myoblasts fuse with all existing myotubes, increasing their size. After birth, myotubes mature into myofibres and the MuSCs present at those stages come to enter quiescence and occupy a position as satellite cells along the fibres. Adapted from Deries et al. (*in press*).

Primary myoblasts fuse extensively with each other and/or with the already existing myotomal myocytes in the trunk and form the multinucleated primary myotubes (Fig. 1.22). Primary myotubes are few in number and have a small cross-sectional area but their formation sets the muscle pattern, connects muscles to tendon and nerves and serves as a scaffold for the subsequent stages of muscle development (Fig. 1.22; Duxson et al., 1989).

Very little is known about what molecules regulate the orientation of primary myogenesis that sets the muscle pattern. These extensive cellular rearrangements are thought to be at least partially influenced by ECM remodelling and cell-ECM interactions. In the trunk, the segmentally organised tenascin-C matrix is completely remodelled and become confined to the tendon anchor points (Deries et al., 2012).

In the limb, a tenascin-C matrix is initially assembled in the absence of muscle, but communication between differentiated muscle and tendinocytes is required to produce the final tendon pattern (Kardon, 1998). Muscle cells express several fibronectin-specific receptors during primary myogenesis (Cachaço et al., 2005; Hirsch et al., 1994), so it is possible that myoblasts and/or differentiated muscle cells use the surrounding fibronectin matrix as a guidance cue for their orientation. Indeed, during primary myogenesis, a fibronectin matrix fills the space around and between nascent myofibers both in the trunk and limbs (Cachaço et al., 2005; Deries et al., 2012; Kosher et al., 1982). Moreover, a fibronectin matrix may play a role in limb MuSC migration to the limb bud because blocking cell-fibronectin interaction in the chick impairs this migration (Brand-Saberi et al., 1993).

Remarkably, primary myogenesis is a laminin-independent process. In the trunk, laminin and other components of the myotomal basement membrane are disassembled (Deries et al., 2012) and laminins are lacking from the limb mesenchyme (Cachaço et al., 2005). Laminin assembly around myotubes starts when primary myogenesis is completed and secondary myogenesis commences (Nunes et al., 2017).

Primary myogenesis is also characterised by the onset of innervation, where motor nerves invade the differentiating muscle anlagen (Hurren et al., 2015). In the limb, the first neural markers correlate with myogenic differentiation and the emergence of the first myocytes expressing MHC (Hurren et al., 2015). Motor neurons exit the ventral part of the neural tube, mix with the sensory neurons to form the spinal nerves and they migrate together towards their targets (Marmigère and Ernfors, 2007). During nerve growth, NCCs migrate along the nerve and when they reach a specific target they differentiate into Schwann cells which produce the

myelin layer that comes to surround neuronal axons, thus contributing to the maturation of the peripheral nervous system (Jessen et al., 2015). Motor neurons contact skeletal muscle fibres through synapses and this intercommunication occurs through reciprocal communication between these two cell types leading to the development of neuromuscular junctions at specific sites along the muscle fibres (Lai and Ip, 2003).

Table 1.2: MuSC terminology.
Simplified terminology of the different types of dermomyotome-derived MuSCs (head MuSCs are not included). Six major MuSCs types have been defined, but it is important to appreciate that each MuSC type is heterogeneous and that the significance of this heterogeneity is presently unclear. E8.5: embryonic day 8.5; P21: postnatal day 21. Based on Deries et al., 2019 (*in press*).

MuSC type (/alternative name)	Pax gene expression	Stage (in mouse)	Location	Arises from	Differentiates into
MuSCs from dermomyotome lips / Founder MuSCs[1]	First none[1], then Pax3	E8.5/9.0 – E11.0	Trunk	Dorso-medial, rostral, caudal and ventro-lateral dermomyotome lips (in trunk)	Myotome
Embryonic MuSCs (trunk) / Founder MuSCs[2]	Pax3/ Pax7	E11.0-E14.5	Trunk	Central dermomyotome	Primary (embryonic) myofibres in trunk
Embryonic MuSCs (limbs) / Founder MuSCs	Pax3	E10.5-E14.5	Limb-levels	Ventro-lateral dermomyotome lip (limb levels)	Primary (embryonic) myofibres in limbs
Foetal MuSCs	Pax7	E14.5-Birth	Trunk and limbs	Embryonic MuSCs[2]	Secondary (foetal) myofibres. Also contribute to growth of all myofibres.
Perinatal MuSCs / Juvenile satellite cell	Pax7	Birth-P21	Trunk and limbs	Foetal MuSCs[2]	Contribute to growth of all myofibres. Generate some new myofibres.
Adult MuSCs / Satellite cells	Pax7	P21 onwards	Trunk and limbs	Perinatal MuSCs[2]	Enter quiescence. Activated upon growth, exercise or injury and contribute to muscle repair. After repair, some of them re-enter quiescence.

[1] The first cells to differentiate from the dermomyotome lips do not express Pax3. They may not be true MuSCs.

[2] Although the current view is that one MuSC type develops into the next type, the possibility that different subpopulations within the dermomyotome originate the different MuSC types cannot be excluded.

5.2 Secondary myogenesis

Secondary (or foetal) myogenesis starts at E14.5 and extends until birth (Fig. 1.22). When secondary myogenesis starts, MuSCs have downregulated Pax3 and express only Pax7 (Deries and Thorsteinsdóttir, 2016; Tajbakhsh, 2009) and are termed foetal MuSCs (Table 1.2). Some of these MuSCs undergo a wave of myogenic differentiation and give rise to secondary myoblasts which fuse with each other to form secondary (or foetal) myotubes (Fig. 1.22). Interestingly, differentiation and fusion of secondary myoblasts starts at the innervation point of the primary myotubes, which is located near their centre (Fig. 1.22; Duxson et al., 1989). Fusion of an increasing number of secondary myoblasts to the nascent secondary myotubes then leads to their extension in both directions along the primary myotubes to finally run their whole length, after which the secondary myotubes attach to the tendons (Duxson and Usson, 1989; Duxson et al., 1989). In parallel, all myofibres become surrounded by a laminin-containing basement membrane (Duxson et al., 1989; Nunes et al., 2017) and at around E16.5 in the mouse, foetal MuSCs migrate underneath the myofibre basement membrane (Kassar-Duchossoy et al., 2005; Ontell and Kozeka, 1984).

Towards the end of foetal development, the formation of new secondary myofibres slows down, as differentiated myoblasts start to preferentially fuse with all existing myofibres (cell-mediated hypertrophy) and increase their size (Fig. 1.22). This pattern of growth continues perinatally, after which some of the MuSCs will enter quiescence and become satellite cells (Table 1.2; Mauro, 1961; White et al., 2010; Yablonka-Reuveni, 2011).

5.3 Neonatal and adult myogenesis

After birth, hypertrophic muscle growth is the main feature observed in skeletal muscles until they reach their final size (Ontell and Kozeka, 1984; Sparrow and Schöck, 2009). In the mouse, hypertrophy is ensured by myoblast fusion with muscle fibres (Fig. 1.22) until postnatal day 21 (P21; White et al., 2010). From P21 stage onwards, skeletal muscle growth is achieved through protein synthesis, without incorporation of new myonuclei (Lepper and Fan, 2010). However, if the muscle is damaged, satellite cells are activated and proliferate. Some of them enter the myogenic programme and fuse with each other or existing myofibres to repair the

damage to the muscles, while others return to quiescence, thus replenishing the MuSC pool (Dumont et al., 2015; Yin et al., 2013).

II. Aims and objectives

The above introduction highlights that skeletal myogenesis is highly complex, involving the coordination and cooperation of multiple signals and cell types. One question that has only been incompletely answered is about the specific role of the myotome in the early stages of axial myogenesis. In this work, I address the question whether the myotome is required for normal axial myogenesis, by focussing on the cellular and molecular mechanisms underlying axial muscle morphogenesis, from the time that myogenesis is triggered in the somite until the formation of the definitive axial muscle masses.

In **chapter 2** we developed an *in vivo ex utero* culture system that allows for the study of myotome development in culture. It is of general interest to develop fast and cheap *in vitro* strategies that satisfy the criteria of studying the development of embryonic structures *in vivo*. We compared the development of *ex utero* cultured mouse explants with same stage embryos that had developed *in utero* by using markers for proliferation and apoptosis and by assessing the three-dimensional morphology of the muscle masses and the organisation of the ECM that surrounds the muscle. We show that, under our serum-free culture conditions, and within a time window of 12 hours, myotome morphogenesis proceeds in the same way as in embryos that developed *in utero*, even though a slight delay in development occurs.

We also show that this system, although limited to a specific time window, is very simple and quick in terms of practical demands and suggest that it can be used not only to study myotome development, but also that of other embryonic structures in the early embryo. Moreover, importantly, this culture system is a practical system to test for the effect of inhibitors of numerous signalling pathways on specific developmental events. This culture system was used for this purpose in chapter 3. The output of this research was published in *Differentiation* (2016) 91, 57-67.

In **chapter 3,** we addressed the role of the myotome in axial muscle morphogenesis by studying axial muscle development in $Myf5^{nlacZ/nlacZ}$ embryos where myotome formation is delayed (Kassar-Duchossoy et al., 2004; Tajbakhsh et al., 1996). Previous studies have shown

that in these embryos, MuSCs are mislocalised and that the myogenic differentiation programme is delayed until MyoD is activated at E11.5 (Tajbakhsh and Buckingham, 2000; Tajbakhsh et al., 1996). Our detailed analysis of these embryos showed that they lack three of the four epaxial muscle groups. We further demonstrate that when MyoD expression comes up at E11.5, only the hypaxial muscles and the dorsal-most epaxial muscle group, the transversospinalis, form; the transient myotome *per se* never develops. We find that this dramatic impairment in epaxial muscle morphogenesis most likely occurs because MuSCs that enter the myotomal area upon central dermomyotome dissociation lose their myogenic identity in the absence of the myotome. We then go on to show that Fgfs, normally expressed by the differentiated myotome, are required to maintain Pax3- and Pax7- expression in MuSCs after their de-epithelialization. This chapter is a manuscript in preparation for publication.

In chapter 4, we thoroughly describe, using 3D reconstructions of images obtained through whole mount immunohistochemistry, how the ECM environment, specifically the laminin, fibronectin and tenascin-C matrices, accompany the de-epithelialization of the central dermomyotomal MuSCs and their entry into the myotome in wild type embryos. We found that MuSCs of the dermomyotome and the myotome have specific relationship with each type of ECM.

In chapter 5, we address whether the distribution patterns of the matrices analysed in chapter 4 are altered in *Myf5*$^{nlacZ/nlacZ}$ embryos, which do not form a myotome. First, we show that some laminins and fibronectin are not secreted by the myotome even if they are assembled by it. In fact, we show that the myotome is required to assemble and organise its own ECM. When the myotome is missing, the myotomal laminin basement membrane does not form and fibronectin and tenascin-C are organised in accordance to the absence of the myotome. However, when the transversospinalis muscle masses form, they are not only able to produce their own adequate ECMs, but they also induce *Scx* expression, an early tendinocyte marker in the surrounding mesenchyme. Parts of these results of this chapter were included in the article by Gomes de Almeida et al. *Developmental Dynamics* (2016) 235, 520-535.

In **chapter 6**, we discuss the main findings described in the previous chapters and integrate them with the existing literature. We place a particular focus on the role of the myotome in the embryo and the particularities of the mechanism of development of the transversospinalis muscles.

III. References

Aberdam, D., Galliano, M. F, Vailly, J., Pulkkinen, L., Bonifas, J., Christiano, A. M., Tryggvason, K., Uitto, J., Epstein Jr, E. H., Ortonne, J.P. and Meneguzzi, G. (1994). Herlitz's junctional epidermolysis bullosa is linked to mutations in the gene (LAMC2) for the gamma 2 subunit of nicein/kalinin (LAMININ-5). *Nat. Genet.* **6**, 299-304.

Allen, B. L., Song, J. Y., Izzi, L., Althaus, I. W., Kang, J., Charron, F., Krauss, R. S. and Mcmahon, A. P. (2011). Overlapping roles and collective requirement for the coreceptors Gas1, Cdo and Boc in Shh pathway function *Dev. Cell* **20**, 775-787.

Almeida, C. F., Fernandes, S. A., Junior, A. F. R., Okamoto, O. K. and Vainzof, M. (2016). Muscle satellite cells : exploring the basic biology to rule them. *Stem Cells Int.* **2016**, 1078686.

Amthor, H., Connolly, D., Patel, K., Brand-Saberi, B., Wilkinson, D. G., Cooke, J. and Christ, B. (1996). The expression and regulation of follistatin and a Ffollistatin-like gene during avian somite compartmentalization and myogenesis. *Dev. Biol.* **178**, 343-362.

Anderson, C., Thorsteinsdóttir, S. and Borycki, A. G. (2009). Sonic hedgehog-dependent synthesis of laminin 1 controls basement membrane assembly in the myotome. *Development* **136**, 3495–3504.

Anderson, L. R., Owens, T. W. and Naylor, M. J. (2014). Structural and mechanical functions of integrins. *Biophys. Rev.* **6**, 203-213.

Andersson, E. R., Sandberg, R. and Lendahl, U. (2011). Notch signaling: simplicity in design, versatility in function. *Development* **138**, 3593-3612.

Andrade, R. P., Palmeirim, I. and Bajanca, F. (2007). Molecular clocks underlying vertebrate embryo segmentation: A 10-year-old hairy-go-round. *Birth Defects Res. Part C - Embryo Today Rev.* **81**, 65-83.

Asfour, H. A., Allouh, M. Z. and Said, R. S. (2018). Myogenic regulatory factors : the orchestrators of myogenesis after 30 years of discovery. *Exp. Biol. Med*. **243**, 18-128.

Aulehla, A. and Pourquie, O. (2010). Signaling gradients during paraxial mesoderm development. *Cold Spring Harb. Perspect. Biol.* **2**, a000869.

Aumailley, M., Bruckner-Tuderman, L., Carter, W. G., Deutzmann, R., Edgar, D., Ekblom, P., Engel, J., Engvall, E., Hohenester, E., Jones, J. C. R., et al. (2005). A simplified laminin nomenclature. *Matrix Biol.* **24**, 326-332.

Babiuk, R. P., Zhang, W., Clugston, R., Allan, D. W. and Greer, J. J. (2003). Embryological origins and development of the rat diaphragm. *J. Comp. Neurol.* **455**, 477-487.

Bajanca, F., Luz, M., Duxson, M. J. and Thorsteinsdóttir, S. (2004). Integrins in the mouse myotome: developmental changes and differences between the epaxial and hypaxial lineage. *Dev. Dyn.* **231**, 402-415.

Bajanca, F., Luz, M., Raymond, K., Martins, G. G., Sonnenberg, A., Tajbakhsh, S., Buckingham, M. and Thorsteinsdóttir, S. (2006). Integrin α6β1-laminin interactions regulate early myotome formation in the mouse embryo. *Development* **133**, 1635-1644.

Barczyk, M., Carracedo, S. and Gulberg, D. (2010). Integrins. *Cell Tissue Res.* **339**, 269-280.

Barros, C. S., Franco, S. J. and Müller, U. (2011). Extracellular matrix: functions in the nervous system. *Cold Spring Harb. Perspect. Biol.* **3**, a00510.

Barton, D. E., Foellmer, B. E., Du, J., Tamm, J., Derynck, R. and Francke, U. (1988). Chromosomal mapping of genes for transforming growth factors beta 2 and beta 3 in man and mouse: dispersion of TGF-beta gene family. *Oncogene Res.* **3**, 323-331.

Ben-Yair, R. and Kalcheim, C. (2005). Lineage analysis of the avian dermomyotome sheet reveals the existence of single cells with both dermal and muscle progenitor fates. *Development* **132**, 689-701.

Ben-Yair, R. and Kalcheim, C. (2008). Notch and bone morphogenetic protein differentially act on dermomyotome cells to generate endothelium, smooth, and striated muscle. *J. Cell Biol.* **180**, 607-618.

Bihlet, A. R., White, W., Bowler, R., Roberts, M., Karsdal, M. A., Leeming, D. J. and Sand, J. M. B. (2017). Biomarkers of extracellular matrix turnover are associated with emphysema and eosinophilic-bronchitis in COPD. *Respir. Res.* **18**, 1-11.

Birchmeier, C. and Brohmann, H. (2000). Genes that control the development of migrating muscle precursor cells. *Curr. Opin. Cell Biol.* **12**, 725-730.

Biressi, S., Molinaro, M. and Cossu, G. (2007). Cellular heterogeneity during vertebrate skeletal muscle development. *Dev. Biol.* **308**, 281-293.

Bitgood, M. J., Shen, L. and Mcmahon, A. P. (1996). Sertoli cell signaling by Desert hedgehog regulates the male germline. *Curr. Biol.* **6**, 298-304.

Bonnans, C., Chou, J. and Werb, Z. (2014). Remodelling the extracellular matrix in development and disease. *Nat. Rev. Mol. Cell Biol.* **15**, 786-801.

Borello, U., Berarducci, B.,, Murphy, P., Bajard, L., Buffa, V., Piccolo, S., Buckingham. M. and Cossu G. (2006). The Wnt/β-catenin pathway regulates Gli-mediated Myf5 expression during somitogenesis. *Development* **133**, 3723-3732.

Borycki, A. G., Brunk, B., Tajbakhsh, S., Buckingham, M., Chiang, C. and Emerson, C. P. (1999). Sonic hedgehog controls epaxial muscle determination through Myf5 activation. *Development* **126**, 4053-4063.

Bradshaw, M. J. and Smith, M. L. (2014). Multiscale relationships between fibronectin structure and functional properties. *Acta Biomater.* **10**, 1524-1531.

Brand-Saberi, B., Krenn, V., Grim, M. and Christ, B. (1993). Differences in the fibronectin-dependence of migrating cell populations. *Anat. Embryol. (Berl).* **187**, 17-26.

Braun, T. and Arnold, H. H. (1995). Inactivation of Myf-6 and Myf-5 genes in mice leads to alterations in skeletal muscle development. *EMBO J.* **14**, 1176-1186.

Braun, T., Buschhausen-Denker, G., Bober, E., Tannich, E., Arnold, H. H. and Buckingham, M. (1989). A novel human muscle factor related to but distinct from MyoD1 induces myogenic conversion in 1OT1/2 fibroblasts. *EMBO J.* **8**, 701-709.

Braun, T., Rudnicki, M. A., Arnold, H. H. and Jaenisch, R. (1992). Targeted inactivation of the muscle regulatory gene Myf-5 results in abnormal rib development and perinatal death. *Cell* **71**, 369-382.

Brennan, D., Chen, X., Cheng, L., Mahoney, M. and Riobo, N. A. (2012). Noncanonical hedgehog signaling. *Vitam. Horm.* **88**, 55-72.

Brent, A. E. and Tabin, C. J. (2002). Developmental regulation of somite derivatives: muscle, cartilage and tendon. *Curr. Opin. Genet. Dev.* **12**, 548-557.

Brent, A. E. and Tabin, C. J. (2004). FGF acts directly on the somitic tendon progenitors through the Ets transcription factors Pea3 and Erm to regulate scleraxis expression. *Development* **131**, 3885-3896.

Brent, A. E., Braun, T. and Tabin, C. J. (2005). Genetic analysis of interactions between the somitic muscle, cartilage and tendon cell lineages during mouse development. *Development* **132**, 515-528.

Brent, A. E., Schweitzer, R. and Tabin, C. J. (2003). A somitic compartment of tendon progenitors. *Cell* **113**, 235-248.

Briscoe, J. and Thérond, P. P. (2013). The mechanisms of Hedgehog signalling and its roles in development and disease. *Nat. Rev. Mol. Cell Biol.* **14**, 416-429.

Buckingham, M. (1994). Which myogenic factors make muscle?. *Curr. Biol.* **4**, 61-63.

Buckingham, M. (2001). Skeletal muscle formation in vertebrates. *Curr. Opin. Genet. Dev.* **11**, 440-448.

Buckingham, M. (2006). Myogenic progenitor cells and skeletal myogenesis in vertebrates. *Curr. Opin. Genet. Dev.* **16**, 525-532.

Buckingham, M. (2017). Gene regulatory networks and cell lineages that underlie the formation of skeletal muscle. *Proc. Natl. Acad. Sci.* **114**, 5830-5837.

Buckingham, M. and Relaix, F. (2007). The role of Pax genes in the development of tissues and organs : Pax3 and Pax7 regulate muscle progenitor cell functions. *Annu. Rev. Cell Dev. Biol.* **23**, 645-673.

Buckingham, M. and Relaix, F. (2015). PAX3 and PAX7 as upstream regulators of myogenesis. *Semin. Cell Dev. Biol.* **44**, 115-125.

Buckingham, M. and Rigby, P. W. J. (2014). Gene regulatory networks and transcriptional mechanisms that control myogenesis. *Dev. Cell* **28**, 225-238.

Buckingham, M., Bajard, L., Chang, T., Daubas, P., Hadchouel, J., Meilhac, S., Montarras, D., Rocancourt D. and Relaix, F. (2003). The formation of skeletal muscle: from somite to limb. *J. Anat.* **202**, 59-68.

Cachaço, A. S., Pereira, C. S., Pardal, R. G., Bajanca, F. and Thorsteinsdóttir, S. (2005). Integrin repertoire on myogenic cells changes during the course of primary myogenesis in the mouse. *Dev. Dyn.* **232**, 1069-1078.

Cai, H. and Liu, A. (2016). Spop promotes skeletal development and homeostasis by positively regulating Ihh signaling. *Proc. Natl. Acad. Sci. U S A.* **113**, 14751-14756.

Cairns, D. M., Sato, M. E., Lee, P. G., Lassar, A. B. and Zeng, L. (2008). A gradient of Shh establishes mutually repressing somitic cell fates induced by Nkx3.2 and Pax3. *Dev. Biol.* **323**, 152-165.

Carballo, G. B., Honorato, J. R., Pinto, G., Lopes, F. De, Cristina, T. and Sampaio, L. De (2018). A highlight on Sonic hedgehog pathway. *Cell Commun. Signal.* **16**, 11.

Chal, J. and Pourquié, O. (2009). Patterning and differentiation of the vertebrate spine. In the skeletal system Cold Spring Harbor Monograph. pp41-116.

Chang, C. (2016). Agonists and antagonists of TGF-β family ligands. *Cold Spring Harb. Perspect. Biol.* **8**, a021923.

Cheng, L., Alvares, L. E., Ahmed, M. U., El-Hanfy, A. S. and Dietrich, S. (2004). The epaxial-hypaxial subdivision of the avian somite. *Dev. Biol.* **274**, 348-369.

Chevallier, A., Kieny, M. and Mauger, A. (1977). Limb-somite relationship: origin of the limb musculature. *J. Embryol. Exp. Morphol.* **41**, 245-258.

Chiang, C., Litingtung, Y., Lee, E., Young, K. E., Corden, J. L., Westphal, H. and Beachy, P. A. (1996). Cyclopia and defective axial patterning in mice lacking Sonic hedgehog gene function. *Nature* **383**, 407-413.

Chiovaro, F., Chiquet-Ehrismann, R. and Chiquet, M. (2015). Transcriptional regulation of tenascin genes. *Cell Adh. Migr.* **9**, 34-47.

Chiquet-Ehrismann, R. and Tucker, R. P. (2011). Tenascins and the importance of adhesion modulation. *Cold Spring Harb. Perspect. Biol.* **3**, a004960.

Christ, B. and Brand-Saberi, B. (2002). Limb muscle development. *Int. J. Dev. Biol.* **46**, 905-914.

Christ, B. and Ordahl, C. P. (1995). Early stages of chick somite development. *Anat. Embryol. (Berl).* **191**, 381-396.

Christ, B., Huang, R. and Scaal, M. (2004). Formation and differentiation of the avian sclerotome. *Anat. Embryol. (Berl).* **208**, 333-350.

Christ, B., Huang, R. and Scaal, M. (2007). Amniote somite derivatives. *Dev. Dyn.* **236**, 2382–2396.

Christ, B., Jacob, M. and Jacob, H. J. (1983). On the origin and development of the ventrolateral abdominal muscles in the avian embryo. *Anat. Embryol. (Berl).* **166**, 87-101.

Cifuentes-Diaz, C., Nicolet, M., Goudou, D., Rieger, F. and Mège, R. M. (1993). N-cadherin and N-CAM-mediated adhesion in development and regeneration of skeletal muscle. *Neuromuscul. Disord.* **3**, 361-365.

Cinnamon, Y., Kahane, N. and Kalcheim, C. (1999). Characterization of the early development of specific hypaxial muscles from the ventrolateral myotome. *Development* **126**, 4305-4315.

Claesson-Welsh, L. (1994). Signal transduction by the Pdgf receptors. *Prog. Growth Factor Res.* **5**, 37-54.

Clevers, H. and Nusse, R. (2012). Wnt/β-catenin signaling and disease. *Cell* **149**, 1192-1205.

Cox, T. R. and Erler, J. T. (2011). Remodeling and homeostasis of the extracellular matrix: implications for fibrotic diseases and cancer. *Dis. Model. Mech.* **4**, 165-178.

Cserjesi, P., Brown, D., Ligon, K. L., Lyons, G. E., Copeland, N. G., Gilbert, D. J., Jenkins, N. A. and Olson, E. N. (1995). Scleraxis: a basic helix-loop-helix protein that prefigures skeletal formation during mouse embryogenesis. *Development* **121**, 1099-1110.

Dale, R. M., Sisson, B. E. andTopczewski, J. (2009). The emerging role of Wnt/PCP signaling in organ formation. *Zebrafish* **6**, 9-14.

Daston, G., Lamar, E., Olivier, M. and Goulding, M. (1996). Pax-3 is necessary for migration but not differentiation of limb muscle precursors in the mouse. *Development* **122**, 1017-1027.

Davis, R. L., Weintraub, H. and Lassar, A. B. (1987). Expression of a single transfected cDNA converts fibroblasts to myoblasts. *Cell* **51**, 987-1000.

De, A. (2011). Wnt/Ca2+ signaling pathway: a brief overview. *Acta. Biochim. Biophys. Sin.* (Shanghai). **43**, 745-756.

del Álamo, D., Rouault, H. and Schweisguth, F. (2011). Mechanism and significance of cis-inhibition in notch signalling. *Curr. Biol.* **21**, 40-47.

deLapeyrière, O., Ollendorff, V., Planche, J., Ott, M. O., Pizette, S., Coulier, F. and Birnbaum, D. (1993). Expression of the Fgf6 gene is restricted to developing skeletal muscle in the mouse embryo. *Development* **118**, 601-611.

Delfini, M. C., De La Celle, M., Gros, J., Serralbo, O., Marics, I., Seux, M., Scaal, M. and Marcelle, C. (2009). The timing of emergence of muscle progenitors is controlled by an FGF/ERK/SNAIL1 pathway. *Dev. Biol.* **333**, 229-237.

Delfini, M. C., Hirsinger, E., Pourquie, O., Duprez, D. and Pourquié, O. (2000). Delta 1-activated notch inhibits muscle differentiation without affecting Myf5 and Pax3 expression in chick limb myogenesis. *Development* **127**, 5213-5224.

Deries, M. and Thorsteinsdóttir, S. (2016). Axial and limb muscle development: dialogue with the neighbourhood. *Cell. Mol. Life Sci.* **73**, 4415-4431.

Deries, M., Collins, J. J. P. and Duxson, M. J. (2008). The mammalian myotome: A muscle with no innervation. *Evol. Dev.* **10**, 746-755.

Deries., M., Gonçalves, A. B. and Thorsteinsdóttir, S. (*in press*). Skeletal muscle development - from stem cells to body movement. In Rodrigues, G. and Roelen, B. A. J. (Eds). Springer Learning Series: "Concepts and application of stem cell biology: a guide for students".

Deries, M., Gonçalves, A. B., Vaz, R., Martins, G. G., Rodrigues, G. and Thorsteinsdóttir, S. (2012). Extracellular matrix remodeling accompanies axial muscle development and morphogenesis in the mouse. *Dev. Dyn.* **241**, 350-364.

Deries, M., Schweitzer, R. and Duxson, M. J. (2010). Developmental fate of the mammalian myotome. *Dev. Dyn.* **239**, 2898-2910.

Dessaud, E., McMahon, A. P. and Briscoe, J. (2008). Pattern formation in the vertebrate neural tube: a sonic hedgehog morphogen-regulated transcriptional network. *Development* **135**, 2489-2503.

Dietrich, S., Abou-Rebyeh, F., Brohmann, H., Bladt, F., Sonnenberg-Riethmacher, E., Yamaai, T., Lumsden, A., Brand-Saberi, B. and Birchmeier, C. (1999). The role of SF/HGF and c-Met in the development of skeletal muscle. *Development* **126**, 1621-1629.

Dietrich, S., Schubert, F. R., Healy, C., Sharpe, P. T. and Lumsden, A. (1998). Specification of the hypaxial musculature. *Development* **125**, 2235–2249.

Duband, J. L., Dufour, S., Hatta, K., Takeichi, M., Edelman, G. M. and Thiery, J. P. (1987). Adhesion molecules during somitogenesis in the avian embryo. *J. Cell Biol.* **104**, 1361-1374.

Dumont, N. A., Wang, Y. X. and Rudnicki, M. A. (2015). Intrinsic and extrinsic mechanisms regulating satellite cell function. *Development* **142**, 1572-1581.

Duxson, M. J. and Usson, Y. (1989). Cellular insertion of primary and secondary myotubes in embryonic rat muscles. *Development* **107**, 243-251.

Duxson, M. J., Usson, Y. and Harris, A. J. (1989). The origin of secondary myotubes in mammalian skeletal muscles: ultrastructural studies. *Development* **107**, 743-750.

Duprez, D. (2002). Signals regulating muscle formation in the limb during embryonic development. *Int. J. Dev. Biol.* **46**, 915-925.

Durbeej, M. (2010). Laminins. *Cell Tissue Res.* **339**, 259-268.

Ebensperger, C., Wilting, J., Brand-Saberi, B., Mizutani, Y., Christ, B., Balling, R. and Koseki, H. (1995). Pax-1, a regulator of sclerotome development is induced by notochord and floor plate signals in avian embryos. *Anat. Embryol. (Berl).* **191**, 297-310.

Edom-Vovard, F., Schuler, B., Bonnin, M. A., Teillet, M. A. and Duprez, D. (2002). Fgf4 positively regulates scleraxis and tenascin expression in chick limb tendons. *Dev. Biol.* **247**, 351-366.

Eloy-Trinquet, S. and, Nicolas, J. F. (2002). Clonal separation and regionalisation during formation of the medial and lateral myotomes in the mouse embryo. *Development* **129,** 111-122.

Eloy-Trinquet, S., Wang, H., Edom-Vovard, F. and Duprez, D. (2009). Fgf signaling components are associated with muscles and tendons during limb development. *Dev. Dyn.* **238**, 1195-1206.

Evans, D. J. R. and Noden, D. M. (2006). Spatial relations between avian craniofacial neural crest and paraxial mesoderm cells. *Dev Dyn* **235**, 1310-1325.

Evans, D. J. R., Valasek, P., Schmidt, C. and Patel, K. (2006). Skeletal muscle translocation in vertebrates. *Anat. Embryol. (Berl).* **211**, 43-50.

Fan, C. M. and Tessier-Lavigne, M. (1994). Patterning of mammalian somites by surface ectoderm and notochord: Evidence for sclerotome induction by a hedgehog homolog. *Cell* **79**, 1175-1186.

Fan, C. M., Porter, J. A., Chiang, C., Chang, D. T., Beachy, P. A. and Tessier-Lavigne, M. (1995). Long-range sclerotome induction by sonic hedgehog: Direct role of the amino-terminal cleavage product and modulation by the cyclic AMP signaling pathway. *Cell* **81**, 457-465.

Farahani, E., Patra, H. K., Jangamreddy, R. and Kawalec, M. (2014). Cell adhesion molecules and their relation to (cancer) cell stemness. **35**, 747-759.

Frantz, C., Stewart, K. M. and Weaver, V. M. (2010). The extracellular matrix at a glance. *J. Cell Sci.* **123**, 4195-4200.

Frontera, W. R. and Ochala, J. (2015). Skeletal Muscle : A brief review of structure and function. *Calcif. Tissue Int.* **96**, 183-195.

Furumoto, T. A., Miura, N., Akasaka, T., Mizutani-Koseki, Y., Sudo, H., Fukuda, K., Maekawa, M., Yuasa, S., Fu, Y., Moriya, H., et al. (1999). Notochord-dependent expression of Mfh1 and Pax1 cooperates to maintain the proliferation of sclerotome cells during the vertebral column development. *Dev. Biol.* **210**, 15-29.

Galli, L. M., Knight, S. R., Barnes, T. L., Doak, A. K., Kadzik, R. S. and Burrus, L. W. (2008). Identification and characterization of subpopulations of Pax3 and Pax7 expressing cells in developing chick somites and limb buds. *Dev. Dyn.* **237**, 1862-1874.

Galli, L. M., Willert, K., Nusse, R., Yablonka-Reuveni, Z., Nohno, T., Denetclaw, W. and Burrus, L. W. (2004). A proliferative role for Wnt-3a in chick somites. *Dev. Biol.* **269**, 489-504.

Gaut, L. and Duprez, D. (2016). Tendon development and diseases. *Wiley Interdiscip. Rev. Dev. Biol.* **5**, 5-3.

Geetha-Loganathan, P., Nimmagadda, S., Huang, R., Christ, B. and Scaal, M. (2006). Regulation of ectodermal Wnt6 expression by the neural tube is transduced by dermomyotomal Wnt11: a mechanism of dermomyotomal lip sustainment. *Development* **133**, 2897-2904.

George, E. L., Georges-Labouesse, E. N., Patel-King, R. S., Hynes, R. O. and Rayburn, H. (1993). Defects in mesoderm, neural tube and vascular development in mouse embryos lacking fibronectin. *Development* **119**, 1079-1091.

Georges-Labouesse, E. N., George, E. L., Rayburn, H. and Hynes, R. O. (1996). Mesodermal development in mouse embryos mutant for fibronectin. *Dev. Dyn.* **207**, 145-156.

Gilbert, S. F. (2000). Developmental Biology. 6th ed, Sunderland (MA), USA: Sinauer Associates, Inc.

Gilbert, S. F. and Barresi, M. J. F. (2016). Developmental biology. 11th ed, Sunderland (MA), USA: Sinauer Associates, Inc.

Gillies, A. R. and Lieber, R. L. (2011). Structure and function of the skeletal muscle extracellular matrix. *Muscle Nerve* **44**, 318-331.

Giordani, J., Bajard, L., Demignon, J., Daubas, P., Buckingham, M. and Maire, P. (2007b). Six proteins regulate the activation of Myf5 expression in embryonic mouse limbs. *Proc. Natl. Acad. Sci. USA* **104**, 11310-1135.

Goel, A. J., Rieder, M. K., Arnold, H. H., Radice, G. L. and Krauss, R. S. (2017). Niche cadherins control the quiescence-to-activation transition in muscle stem cells. *Cell Rep.* **21**, 2236-2250.

Goetz, R. and Mohammadi, M. (2013). Exploring mechanisms of FGF signalling through the lens of structural biology. *Nat. Rev. Mol. Cell Biol.* **14**, 166-180.

Gomez, C., Özbudak, E. M., Wunderlich, J., Baumann, D., Lewis, J. and Pourquié, O. (2008). Control of segment number in vertebrate embryos. *Nature* **454**, 335-39.

Gordon, W. R., Zimmerman, B., He, L., Miles, L. J., Huang, J., Tiyanont, K., McArthur, D. G., Aster, J. C., Perrimon, N., Loparo, J. J. and Blacklow, S. C. (2015). Mechanical allostery: evidence for a force requirement in the proteolytic activation of Notch. *Dev. Cell.* **33**, 729-736.

Goulding, M. D., Erselius, J. R., Chalepakis, G., Gruss, P. and Deutsch, U. (1991). Pax-3, a novel murine DNA binding protein expressed during early neurogenesis. *EMBO J.* **10**, 1135-1147.

Goulding, M. D., Lumsden, A. and Gruss, P. (1993). Signals from the notochord and floor plate regulate the region-specific expression of two Pax genes in the developing spinal cord. *Development* **117**, 1001-1016.

Goulding, M. D., Lumsden, A. and Paquette, A. J. (1994). Regulation of Pax-3 expression in the dermomyotome and its role in muscle development. *Development* **120**, 957-971.

Gros, J., Manceau, M., Thomé, V. and Marcelle, C. (2005). A common somitic origin for embryonic muscle progenitors and satellite cells. *Nature* **435**, 954-958.

Gros, J., Scaal, M. and Marcelle, C. (2004). A two-step mechanism for myotome formation in chick. *Dev. Cell* **6**, 875-882.

Gross, M. K., Moran-Rivard, L., Velasquez, T., Nakatsu, M. N., Jagla, K. and Goulding, M. (2000). Lbx1 is required for muscle precursor migration along a lateral pathway into the limb. *Development* **127**, 413-427.

Gumbiner, B. M. (1996). Cell adhesion: the molecular basis of tissue architecture and morphogenesis. *Cell* **84**, 345-357.

Gustafsson, M. K., Pan, H., Pinney, D. F., Liu, Y., Lewandowski, A., Epstein, D. J. and Emerson, C. P. (2002). Myf5 is a direct target of long-range Shh signaling and Gli regulation for muscle specification. *Genes Dev.* **16**, 114-126.

Haase, G., Dessaud, E., Garcès, A., De Bovis, B., Birling, M. C., Filippi, P., Schmalbruch, H., Arber, S. and DeLapeyrière, O. (2002). GDNF acts through PEA3 to regulate cell body positioning and muscle innervation of specific motor neuron pools. *Neuron* **35**, 893-905.

Hall, M. I., Rodriguez-Sosa, J. R. and Plochocki, J. H. (2017). Reorganization of mammalian body wall patterning with cloacal septation. *Sci. Rep.* **7**, 1-7.

Halperin-Barlev, O. and Kalcheim, C. (2011). Sclerotome-derived Slit1 drives directional migration and differentiation of Robo2-expressing pioneer myoblasts. *Development* **138**, 2935-2945.

Han, J. K. and Martin, G. R. (1993). Embryonic expression of Fgf-6 is restricted to the skeletal muscle lineage. *Dev. Biol.* **158**, 549-554.

Hasty, P., Bradley, A., Morris, J. H., Edmondson, D. G., Venuti, J. M., Olson, E. N. and Klein, W. H. (1993). Muscle deficiency and neonatal death in mice with a targeted mutation in the myogenin gene. *Nature* **364**, 501-506.

Hauschka, S. D. (1994). The embryonic origin of muscle. In Engel, A. G. and Franzini-Armstrong, C. (Eds). Myology, 2nd ed. McGraw-Hill. New York. Pp 3-73.

He, X., Semenov, M., Tamai, K. and Zeng, X. (2004). LDL receptor-related proteins 5 and 6 in Wnt/β -catenin signaling : arrows point the way. *Development* **131**, 1663-1677.

Heldin, C. and Westermark, B. (1999). Mechanism of action and in vivo role of platelet-derived growth factor. *Physiol. Rev.* **79**, 1283-1316.

Henrique, D. and Schweisguth, F. (2019). Mechanisms of Notch signaling: a simple logic deployed in time and space. *Development* **146**, dev172148.

Hernandez-Torres, F., Rodríguez-Outeiriño, L., Franco, D. and Aranega, A. E. (2017). Pitx2 in embryonic and adult myogenesis. *Front. Cell Dev. Biol.* **5**, 46.

Hirsch, E., Gullberg, D., Balzac, F., Altruda, F., Silengo, L. and Tarone, G. (1994). α v Integrin subunit is predominantly located in nervous tissue and skeletal muscle during mouse development. *Dev. Dyn.* **201**, 108-120.

Hirsinger, E., Malapert, P., Dubrulle, J., Delfini, M. C., Duprez, D., Henrique, D., Ish-Horowicz, D. and Pourquié, O. (2001). Notch signalling acts in postmitotic avian myogenic cells to control MyoD activation. *Development* **128**, 107-116.

Hoch, R. V and Soriano, P. (2003). Roles of PDGF in animal development. *Development* **130**, 4769-4784.

Hohenester, E., Yurchenco, P. D. (2013). Laminins in basement membrane assembly. *Cell Adh. Migr.* **7**, 56-63.

Holtz, A. M., Griffiths, S. C., Davis, S. J., Bishop, B., Siebold, C. and Allen, B. L. (2015). Secreted HHIP1 interacts with heparan sulfate and regulates Hedgehog ligand localization and function. *J. Cell Biol.* **209**, 739-757.

Horton, E. R., Humphries, J. D., James, J., Jones, M. C., Askari, J. A. and Humphries, M. J. (2016). The integrin adhesome network at a glance. *J. Cell Sci.* **129**, 4159-4163.

Huang, A. H., Riordan, T. J., Pryce, B., Weibel, J. L., Watson, S. S., Long, F., Lefebvre, V., Harfe, B. D., Stadler, H. S., Akiyama, H., et al. (2015). Musculoskeletal integration at the wrist underlies the modular development of limb tendons. *Development* **142**, 2431-2441.

Huang, R., Zhi, Q., Izpisua-Belmonte, J. C., Christ, B. and Patel, K. (1999). Origin and development of the avian tongue muscles. *Anat. Embryol. (Berl).* **200**, 137-152.

Hurle, J. M., Ros, M. A., Hinchliffe, J. R., Critchlow, M. A. and Genis-Galvez, J. M. (1989). The extracellular matrix architecture relating to myotendinous pattern formation in the distal part of the developing chick limb: An ultrastructural, histochemical and immunocytochemical analysis. *Cell Differ. Dev.* **27**, 103-120.

Hurren, B., Collins, J. J. P., Duxson, M. J. and Deries, M. (2015). First neuromuscular contact correlates with onset of primary myogenesis in rat and mouse limb muscles. *PLoS One* **10**, 1-18.

Hutcheson, D. A., Zhao, J., Merrell, A., Haldar, M. and Kardon, G. (2009). Embryonic and fetal limb myogenic cells are derived from developmentally distinct progenitors and have different requirements for β-catenin. *Genes Dev.* **23**, 997-1013.

Hynes, R. O. (2002). Integrins : bidirectional, allosteric signaling machines in their roles as major adhesion receptors , integrins. *Cell* **110**, 673-687.

Hynes, R. O. and Naba, A. (2012). Overview of the matrisome-an inventory of extracellular matrix constituents and functions. *Cold Spring Harb. Perspect. Biol.* **4**, a004903.

Iimura, T., Yang, X., Weijer, C. J. and Pourquié, O. (2007). Dual mode of paraxial mesoderm formation during chick gastrulation. *Proc. Natl. Acad. Sci. U S A.* **104**, 2744-2749.

Imanaka-Yoshida, K., Matsumoto, K., Hara, M., Sakakura, T. and Yoshida, T. (2003). The dynamic expression of tenascin-C and tenascin-X during early heart development in the mouse. *Differentiation.* **71**, 291-298.

Incardona, J. P., Gruenberg, J. and Roelink, H. (2002). Sonic hedgehog induces the segregation of patched and smoothened in endosomes. *Curr. Biol.* **12**, 983-995.

Ingham, P. W., Nakano, Y. and Seger, C. (2011). Mechanisms and functions of Hedgehog signalling across the metazoa. *Nat. Publ. Gr.* **12**, 393-406.

Jessen, K. R., Mirsky, R. and Lloyd, A. C. (2015). Schwann Cells: development and role in nerve repair. *Cold Spring Harb. Perspect. Biol.* **7**, a020487.

Kablar, B., Asakura, A., Krastel, K., Ying, C., May, L. L., Goldhamer, D. J. and Rudnicki, M. A. (1998). MyoD and Myf-5 define the specification of musculature of distinct embryonic origin. *Biochem. Cell Biol.* **76**, 1079-1091.

Kablar, B., Krastel, K., Ying, C., Asakura, a, Tapscott, S. J. and Rudnicki, M. a (1997). MyoD and Myf-5 differentially regulate the development of limb versus trunk skeletal muscle. *Development* **124**, 4729-4738.

Kahane, N., Cinnamon, Y., Bachelet, I. and Kalcheim, C. (2001). The third wave of myotome colonization by mitotically competent progenitors: regulating the balance between differentiation and proliferation during muscle development. *Development* **128**, 2187-2198.

Kahane, N., Ribes, V., Kicheva, A., Briscoe, J. and Kalcheim, C. (2013). The transition from differentiation to growth during dermomyotome-derived myogenesis depends on temporally restricted hedgehog signaling. *Development* **140**, 1740-1750.

Kardon, G. (1998). Muscle and tendon morphogenesis in the avian hind limb. *Development* **125**, 4019-4032.

Kassar-Duchossoy, L., Gayraud-Morel, B., Gomès, D., Rocancourt, D., Buckingham, M., Shinin, V. and Tajbakhsh, S. (2004). Mrf4 determines skeletal muscle identity in Myf5:Myod double-mutant mice. *Nature* **431**, 466-471.

Kassar-Duchossoy, L., Giacone, E., Gayraud-morel, B., Jory, A., Gomès, D. and Tajbakhsh, S. (2005). Pax3 / Pax7 mark a novel population of primitive myogenic cells during development. *Genes Dev.* **19**, 1426-1431.

Katagiri, T. and Watabe, T. (2016). Bone morphogenetic proteins. *Cold Spring Harb. Perspect. Biol.* **8**, a021899.

Kazlauskas, A. (2017). PDGFs and their receptors. *Gene* **614**, 1-7.

Kiefer, J. C. and Hauschka, S. D. (2001). Myf-5 is transiently expressed in nonmuscle mesoderm and exhibits dynamic regional changes within the presegmented mesoderm and somites I-IV. *Dev. Biol.* **232**, 77-90.

Kieny, M. and Chevallier, A. (1979). Autonomy of tendon development in the embryonic chick wing. *J. Embryol. Exp. Morphol.* **49**, 153-165.

Klinghoffer, R. A., Mueting-Nelsen, P. F., Faerman, A., Shani, M. and Soriano, P. (2001). The two PDGF receptors maintain conserved signaling in vivo despite divergent embryological functions. *Mol. Cell* **7**, 343-354.

Komiya, Y. and Habas, R. (2008). Wnt signal transduction pathways. *Organogenesis* **4**, 68-75.

Kosher, R. A., Walker, K. H. and Ledger, P. W. (1982). Temporal and spatial distribution of fibronectin during development of the embryonic chick limb bud. *Cell Differ.* **11**, 217-228.

Kramer, E. R., Knott, L., Su, F., Dessaud, E., Krull, C. E., Helmbacher, F. and Klein, R. (2006). Cooperation between GDNF/Ret and ephrinA/EphA4 signals for motor-axon pathway selection in the limb. *Neuron* **50**, 35-47.

Kuang, S. and Rudnicki, M. A. (2008). The emerging biology of satellite cells and their therapeutic potential. *Trends Mol. Med.* **14**, 82-91.

Kuroda, K., Tani, S., Minoguchi, S., Honjo, T., Tamura, K. and Kurooka, H. (1999). Delta-induced Notch signaling mediated by RBP-J inhibits MyoD expression and myogenesis. *J. Biol. Chem.* **274**, 7238-7244.

L'Honoré, A., Ouimette, J.-F., Lavertu-Jolin, M. and Drouin, J. (2010). Pitx2 defines alternate pathways acting through MyoD during limb and somitic myogenesis. *Development* **137**, 3847-856.

Lagha, M., Brunelli, S., Messina, G., Cumano, A., Kume, T., Relaix, F. and Buckingham, M. E. (2009). Pax3:Foxc2 reciprocal repression in the somite modulates muscular versus vascular cell fate choice in multipotent progenitors. *Dev. Cell* **17**, 892-899.

Lagha, M., Kormish, J. D., Rocancourt, D., Manceau, M., Epstein, J. A., Zaret, K. S., Relaix, F. and Buckingham, M. E. (2008). Pax3 regulation of FGF signaling affects the progression of embryonic progenitor cells into the myogenic program. *Genes Dev.* **22**, 1828-1837.

Lai, K.-O. and Ip, N. Y. (2004). Postsynaptic signaling of new players at the neuromuscular junction. *J. Neurocytol.* **32**, 727-741.

LaRochelle, W. J., Jeffers, M., Mcdonald, W. F., Chillakuru, R. A., Giese, N. A., Lokker, N. A., Sullivan, C., Boldog, F. L., Yang, M., Vernet, C., et al. (2001). PDGF-D , a new protease-activated growth factor. *Nat. Cell Biol.* **3**, 517-521.

Lau, L. W., Cua, R., Keough, M. B., Haylock-Jacobs, S. and Yong, V. W. (2013). Pathophysiology of the brain extracellular matrix: A new target for remyelination. *Nat. Rev. Neurosci.* **14**, 722-729.

Lee, A. S. J., Harris, J., Bate, M., Vijayraghavan, K., Fisher, L., Tajbakhsh, S. and Duxson, M. (2013). Initiation of primary myogenesis in amniote limb muscles. *Dev. Dyn.* **242**, 1043-1055.

Lee, R. T., Zhao, Z. and Ingham, P. W. (2016). Hedgehog signalling. *Development* **143**, 367-372.

Lepper, C. and Fan, C. (2010). Inducible lineage tracing of Pax7-descendant cells reveals embryonic origin of adult satellite cells. *Genesis* **48**, 424-436.

Li, X., Pontén, A., Aase, K., Karlsson, L., Abramsson, A., Uutela, M., Hellström, M., Boström, H., Li, H., Soriano, P., Betsholtz, C., Heldin, C. H., Alitalo, K., Ostman, A. and Eriksson, U. (2000). PDGF-C is a new protease-activated ligand for the PDGF α -receptor. *Nat. Cell Biol.* **2**, 302-309.

Lin, S. Y., Morrison, J. R., Phillips, D. J. and de Krestser, D. M. (2003). Regulation of ovarían function by lhe TGF-beta superfamily and follistatin. *Reproduction* **126**, 133-148.

Lockhart, M., Wirrig, E., Phelps, A. and Wessels, A. (2011). Extracellular matrix and heart development. *Birth Defects Res. A Clin. Mol. Teratol.* **91**, 535-550.

Lowell, C. and Mayadas, T. (2012). Integrin and cell adhesion molecules. *Methods Mol Biol* **757**, 3-14.

Luo, K. (2017). Signaling cross talk between TGF-β/Smad and other signaling pathways. *Cold Spring Harb. Perspect. Biol.* **9**, a022137.

Macias, D., Gañan, Y., Sampath, T. K., Piedra, M. E., Ros, M. A. and Hurle, J. M. (1997). Role of BMP-2 and OP-1 (BMP-7) in programmed cell death and skeletogenesis during chick limb development. *Development* **124**, 1109-1117.

Macias, M. J., Martin-malpartida, P., Companys, P. L. and Program, G. (2015). Structural determinants of SMAD function in TGF-β signaling. *Trends Biochem. Sci.* **40**, 296-308.

Mallo, M. (2016). Revisiting the involvement of signaling gradients in somitogenesis. *FEBS J.* **283**, 1430-1437.

Mao, Y. and Schwarzbauer, J. E. (2005). Fibronectin fibrillogenesis, a cell-mediated matrix assembly process. *Matrix Biol.* **24**, 389-399.

Marcelle, C., Stark, M. R. and Bronner-fraser, M. (1997). Coordinate actions of BMPs , Wnts , Shh and Noggin mediate patterning of the dorsal somite. *Development* **3963**, 3955-3963.

Marcil, A., Dumontier, E., Chamberland, M., Camper, S.A and, Drouin, J. (2003). Pitx1 and Pitx2 are required for development of hindlimb buds. *Development* **130**, 45-55.

Marics, I., Padilla, F., Guillemot, J., Scaal, M. and Marcelle, C. (2002). FGFR4 signaling is a necessary step in limb muscle differentiation. *Development* **129**, 4559-4569.

Marmigère, F. and Ernfors, P. (2007). Specification and connectivity of neuronal subtypes in the sensory lineage. *Nat. Rev. Neurosci.* **8**, 114-127.

Massagué, J. (2012). TGFβ signalling in context *Nat Rev Mol Cell Biol* **13**, 616-630.

Mauro, A. (1961). Satellite cell of skeletal muscle fibers. *J. Biophys. Biochem. Cytol.* **9**, 493-495.

McDermott, A., Gustafsson, M., Elsam, T., Hui, C.-C., Emerson, C. P. and Borycki, A.-G. (2005). Gli2 and Gli3 have redundant and context-dependent function in skeletal muscle formation. *Development* **132**, 345-357.

Mayeuf-Louchart, A., Vincent, S. D., Rocancourt, D., Danckaert, A., Lagha, M., Buckingham, M. and Relaix, F. (2014). Notch regulation of myogenic versus endothelial fates of cells that migrate from the somite to the limb. *Proc. Natl. Acad. Sci. USA* **111**, 8844-8849.

Mercola, M., Wang, C. Y., Kelly, J., Brownlee, C., Jackson-Grusby, L., Stiles, C. and Bowen-Pope, D. (1990). Selective expression of PDGF A and its receptor during early mouse embryogenesis. *Dev. Biol.* **138**, 114-122.

Messina, G., Biressi, S., Monteverde, S., Magli, A., Cassano, M., Perani, L., Roncaglia, E., Tagliafico, E., Starnes, L., Campbell, C. E., et al. (2010). Nfix regulates fetal-specific transcription in developing skeletal muscle. *Cell* **140**, 554-566.

Midwood, K. S., Chiquet, M., Tucker, R. P. and Orend, G. (2016). Tenascin-C at a glance. *J. Cell Sci.* **129**, 4321-4327.

Midwood, K. S., Valenick, L. V, Hsia, H. C. and Schwarzbauer, J. E. (2004). Coregulation of fibronectin signaling and matrix contraction by tenascin-C and syndecan-4. *Mol. Biol. Cell* **15**, 5670-5677.

Montano, M. and Bushman, W. (2017). Morphoregulatory pathways in prostate ductal development. *Dev. Dyn.* **246**, 89-99.

Moore, R. and Walsh, F. S. (1993). The cell adhesion molecule M-cadherin is specifically expressed in developing and regenerating, but not denervated skeletal muscle. *Development* **117**, 1409-1420.

Moretti, F. A., Chauhan, A. K., Iaconcig, A., Porro, F., Baralle, F. E. and Muro, A. F. (2007). A major fraction of fibronectin present in the extracellular matrix of tissues is plasma-derived. *J. Biol. Chem.* **282**, 28057-28062.

Motohashi, N. and Asakura, A. (2012). Molecular regulation of muscle satellite cell self-renewal. *J. Stem. Cell Res. Ther.* **Suppl 11,** e002.

Mourikis, P., Gopalakrishnan, S., Sambasivan, R. and Tajbakhsh S. (2012). Cell-autonomous Notch activity maintains the temporal specification potential of skeletal muscle stem cells. *Development.* **139**, 4536-4548.

Müller, F. and O'Rahilly, R. (1986). Somitic-vertebral correlation and vertebral levels in the human embryo. *Am. J. Anat.* **177**, 3-19.

Mumm, J. S., Schroeter, E. H., Saxena, M. T., Griesemer, A., Tian, X., Pan, D. J., Ray, W. J. and Kopan, R. (2000). A ligand-induced extracellular cleavage regulates γ-secretase-like proteolytic activation of Notch1. *Mol. Cell* **5**, 197-206.

Münsterberg, A. E., Kitajewski, J., Bumcrot, D. A., McMahon, A. P. and Lassar, A. B. (1995). Combinatorial signaling by Sonic hedgehog and Wnt family members induces myogenic bHLH gene expression in the somite. *Genes Dev.* **9**, 2911-2922.

Murchison, N. D., Price, B. A., Conner, D. A., Keene, D. R., Olson, E. N., Tabin, C. J. and, Schweitzer R. (2007). Regulation of tendon differentiation by scleraxis distinguishes force-transmitting tendons from muscle-anchoring tendons. *Development* **134**, 2697-2708.

Nabeshima, Y., Hanaoka, K., Hayasaka, M., Esumi, E., Li, S., Nonaka, I. and Nabeshima Y. (1993). Myogenin gene disruption results in perinatal lethality because of severe muscle defect. *Nature* **364**, 532-535.

Nandagopal, N., Santat, L. A., LeBon, L., Sprinzak, D., Bronner, M. E. and Elowitz, M. B. (2018). Dynamic ligand discrimination in the Notch signaling pathway. *Cell* **172**, 869-880.e19.

Nelson, C. M. and Bissell, M. J. (2006). Of extracellular matrix, scaffolds, and signaling: tissue architecture regulates development, homeostasis, and cancer. *Annu. Rev. Cell De.v Biol.* **22**, 287-309.

Nielsen, S. H., Rasmussen, D. G. K., Brix, S., Fenton, A., Jesky, M., Ferro, C. J., Karsdal, M., Genovese, F. and Cockwell, P. (2018). A novel biomarker of laminin turnover is associated with disease progression and mortality in chronic kidney disease. *PLoS One* **13**, e0204239.

Niessen, C. M., Leckband, D. and Yap, A. S. (2011). Tissue organization by cadherin adhesion molecules: dynamic molecular and cellular mechanisms of morphogenetic regulation. *Physiol. Rev.* **91**, 691-731.

Niswander, L. and Martin, G. R. (1993). FGF-4 and BMP-2 have opposite effects on limb growth. *Nature* **361**, 68-71.

Noden, D. M. (1983). The role of the neural crest in patterning of avian cranial skeletal, connective, and muscle tissues. *Dev. Biol.* **96**, 144-165.

Noden, D. M. and Francis-west, P. (2006). The differentiation and morphogenesis of craniofacial muscles. *Dev. Dyn.* **235,** 1194-1218.

Nunes, A. M., Wuebbles, R. D., Sarathy, A., Fontelonga, T. M., Deries, M., Burkin, D. J. and Thorsteinsdóttir, S. (2017). Impaired fetal muscle development and JAK-STAT activation mark disease onset and progression in a mouse model for merosin-deficient congenital muscular dystrophy. *Hum. Mol. Genet.* **26**, 2018-2033.

Oda, H. and Takeichi, M. (2011). Structural and functional diversity of cadherin at the adherens junction. *J. Cell Biol.* **193**, 1137-1146.

Olson, E. ., Arnold, H.-H., Rigby, P. W. . and Wold, B. . (1996). Know your neighbors: three phenotypes in null mutants of the myogenic bHLH gene MRF4. *Cell* **85**, 1-4.

Ontell, M. and Kozeka, K. (1984). The organogenesis of murine striated muscle: A cytoarchitectural study. *Am. J. Anat.* **171**, 133-148.

Ontell, M., Ontell, M. P. and Buckingham, M. (1995). Muscle-specific gene expression during myogensis in the mouse. *Microsc. Res. Tech.* **30**, 354-365.

Ornitz, D. M. and Itoh, N. (2015). The fibroblast growth factor signaling pathway. *Wiley Interdiscip. Rev. Dev. Biol.* **4**, 215-266.

Ott, M. O., Bober, E., Lyons, G., Arnold, H. and Buckingham, M. (1991). Early expression of the myogenic regulatory gene, myf-5, in precursor cells of skeletal muscle in the mouse embryo. *Development* **111**, 1097-1107.

Pais-de-Azevedo, T., Magno, R., Duarte, I. and Palmeirim, I. (2018). Recent advances in understanding vertebrate segmentation. *F1000Research* **7**, 97.

Parks, A. L., Klueg, K. M., Stout, J. R. and Muskavitch, M. A. (2000). Ligand endocytosis drives receptor dissociation and activation in the Notch pathway. *Development* **127**, 1373-1385.

Patapoutian, A., Yoon, J. K., Miner, J. H., Wang, S., Stark, K. and Wold, B. (1995). Disruption of the mouse MRF4 gene identifies multiple waves of myogenesis in the myotome. *Development* **121**, 3347-3358.

Poniatowski, L. A., Wojdasiewicz, P., Gasik, R. and Szukiewicz, D. (2015). Transforming growth factor beta family: Insight into the role of growth factors in regulation of fracture healing biology and potential clinical applications. *Mediators Inflamm. Mediators Inflamm.* **2015**, 137823.

Pourquié, O. (2001). Vertebrate somitogenesis. *Annu. Rev. Cell Dev. Biol.* **17**, 311-350.

Pourquié, O., Fan, C. M., Coltey, M., Hirsinger, E., Watanabe, Y., Bréant, C., Francis-West, P., Brickell, P., Tessier-Lavigne, M. and Le Douarin, N. M. (1996). Lateral and axial signals involved in avian somite patterning: A role for BMP4. *Cell* **84**, 461-471.

Pownall, M. E., Gustafsson, M. K. and Emerson, C. P. (2002). Myogenic regulatory factors and the specification of muscle progenitors in vertebrate embryos. *Annu. Rev. Cell Dev. Biol.* **18**, 747-783.

Pu, Q., Abduelmula, A., Masyuk, M., Theiss, C., Schwandulla, D., Hans, M., Patel, K., Brand-Saberi, B. and Huang, R. (2013). The dermomyotome ventrolateral lip is essential for the hypaxial myotome formation. *BMC Dev. Biol.* **13**, 37.

Rahnama, F., Toftgård, R. and Zaphiropoulos, P. G. (2004). Distinct roles of PTCH2 splice variants in Hedgehog signalling. *Biochem J.* **378**, 325-334.

Randolph, M. E. and Pavlath, G. K. (2015). A muscle stem cell for every muscle : variability of satellite cell biology among different muscle groups. *Front. Aging Neursosci.* **7**, 190.

Rawls, A., Valdez, M., Zhang, W., Richardson, J., Klein, W. and Olson, E. (1998). Overlapping functions of the myogenic bHLH genes MRF4 and MyoD revealed in double mutant mice. *Development* **125**, 2349-2358.

Reinhard, J.R., Lin, S., McKee, K. K., Meinen, S., Crosson, S. C., Sury, M., Hobbs, S., Maier, G., Yurchenco, P. D. and Rüegg, M. A. (2017). Linker proteins restore basement membrane and correct LAMA2-related muscular dystrophy in mice. *Sci. Transl. Med.* **9**, eaal4649.

Relaix, F., Montarras, D., Zaffran, S., Gayraud-Morel, B., Rocancourt, D., Tajbakhsh, S., Mansouri, A., Cumano, A. and Buckingham, M. (2006). Pax3 and Pax7 have distinct and overlapping functions in adult muscle progenitor cells. *J. Cell Biol.* **172**, 91-102.

Relaix, F., Rocancourt, D., Mansouri, A. and Buckingham, M. (2004). Divergent functions of murine Pax3 and Pax7 in limb muscle development. *Genes Dev.* **18**, 1088-1105.

Relaix, F., Rocancourt, D., Mansouri, A. and Buckingham, M. (2005). A Pax3/Pax7-dependent population of skeletal muscle progenitor cells. *Nature* **435**, 948-953.

Reshef, R., Maroto, M. and Lassar, A. B. (1998). Regulation of dorsal somitic cell fates: BMPs and Noggin control the timing and pattern of myogenic regulator expression. *Genes Dev.* **12**, 290-303.

Rhodes, S. J. and Konieczny, S. F. (1989). Identification of MRF4: A new member of the muscle regulatory factor gene family. *Genes Dev.* **3**, 2050-2061.

Rifes, P. and Thorsteinsdóttir, S. (2012). Extracellular matrix assembly and 3D organization during paraxial mesoderm development in the chick embryo. *Dev. Biol.* **368**, 370-381.

Rios, A. C., Serralbo, O., Salgado, D. and Marcelle, C. (2011). Neural crest regulates myogenesis through the transient

activation of NOTCH. *Nature* **473**, 532-535.

Rizk, N. N. and Adieb, N. (1982). The development of the anterior abdominal wall in the rat in the light of a new anatomical description. *J. Anat.* **134**, 237-242.

Rosenkranz, S. and, Kazlauskas, A. (1999). Evidence for distinct signaling properties and biological responses induced by the PDGF receptor alpha and beta subtypes. *Growth Factors* **16,** 201-216.

Rothrauff, B. B., Yang, G. and Tuan, R. S. (2015). Tendon resident cells- biology and physiology of tendons. In Tendon regeneration: understanding tissue physiology and development to engineer functional substitutes. Academic Press. pp 41-76,.

Rozario, T. and DeSimone, D. W. (2010). The extracellular matrix in development and morphogenesis: A dynamic view. *Dev. Biol.* **341**, 126-140.

Rudnicki, M. A., Braun, T., Hinuma, S. and Jaenisch, R. (1992). Inactivation of MyoD in mice leads to up-regulation of the myogenic HLH gene Myf-5 and results in apparently normal muscle development. *Cell* **71**, 383-390.

Rudnicki, M. A., Schnegelsberg, P. N. J., Stead, R. H., Braun, T., Arnold, H. H. and Jaenisch, R. (1993). MyoD or Myf-5 is required for the formation of skeletal muscle. *Cell* **75**, 1351-1359.

Saga, Y. (2012). The mechanism of somite formation in mice. *Curr. Opin. Genet. Dev.* **22**, 331-338.

Saga, Y. and Takeda, H. (2001). The making of the somite: molecular events in vertebrate segmentation. *Nat. Rev. Genet.* **2**, 835-845.

Saga, Y., Yagi, T., Ikawa, Y., Sakakura, T. and Aizawa, S. (1992). Mice develop normally without tenascin. *Genes Dev.* **6**, 1821-1831.

Sagar, Prols, F., Wiegreffe, C. and Scaal, M. (2015). Communication between distant epithelial cells by filopodia-like protrusions during embryonic development. *Development* **142**, 665-671.

Sambasivan, R., Kuratani, S. and Tajbakhsh, S. (2011). An eye on the head : the development and evolution of craniofacial muscles. *Development* **138**, 2401-2415.

Sanes, J. R. (2003). The basement membrane/basal lamina of skeletal muscle. *J. Biol. Chem.* **278**, 12601-1264.

Sassoon, D. A. (1993). Myogenic regulatory factors: dissecting their role and regulation during vertebrate embryogenesis. *Dev. Biol.* **156**, 11-23.

Sato, T. (1973). Innervation and Morphology of the Musculi Levatores Costarum Longi. *Proc. Japan Acad.* **49**, 555-558.

Sato, T., Rocancourt, D., Marques, L., Thorsteinsdóttir, S. and Buckingham, M. (2010). A Pax3/Dmrt2/Myf5 regulatory cascade functions at the onset of myogenesis. *PLoS Genet.* **6**, e1000897.

Scaal, M. and Christ, B. (2004). Formation and differentiation of the avian dermomyotome. *Anat. Embryol. (Berl).* **208**, 411-424.

Scaal, M. and Wiegreffe, C. (2006). Somite compartments in anamniotes. *Anat. Embryol. (Berl).* **211 Suppl 1**, 9-19.

Scaal, M., Bonafede, A., Dathe, V., Sachs, M., Cann, G., Christ, B. and Brand-Saberi, B. (1999). SF/HGF is a mediator between limb patterning and muscle development. *Development* **126**, 4885-4893.

Schultz-Cherry, S., Lawler, J. and Murphy-Ullrich, J. E. (1994). The type 1 repeats of thrombospondin 1 activate latent transforming growth factor-β. *J. Biol. Chem.* **269**, 26783-26788.

Schuster-Gossler, K., Cordes, R. and Gossler, A. (2007). Premature myogenic differentiation and depletion of progenitor cells cause severe muscle hypotrophy in Delta1 mutants. *Proc. Natl. Acad. Sci.* **104**, 537-542.

Schwarzbauer, J. E. and DeSimone, D. W. (2011). Fibronectins, their fibrillogenesis, and in vivo functions. *Cold Spring Harb. Perspect. Biol.* **3**, 1-19.

Schweitzer, R., Chyung, J. H., Murtaugh, L. C., Brent, E., Rosen, V., Olson, E. N., Lassar, A. and Tabin, C. J. (2001). Analysis of the tendon cell fate using Scleraxis, a specific marker for tendons and ligaments. *Development* **128**, 3855-3866.

Seale, P., Bjork, B., Yang, W., Kajimura, S., Chin, S., Kuang, S., Scimè, A., Devarakonda, S., Conroe, H. M., Erdjument-

Bromage, H., et al. (2008). PRDM16 controls a brown fat/skeletal muscle switch. *Nature* **454**, 961-967.

Serralbo, O. and Marcelle, C. (2014). Migrating cells mediate long-range WNT signaling. *Development* **141**, 2057-2063.
Sethi, J. K. and Vidal-Puig, A. (2010). Wnt signalling and the control of cellular metabolism. *Biochem. J.* **427**, 1-17.

Sethi, M.K. and Zaia, J. (2017). Extracellular matrix proteomics in schizophrenia and Alzheimer's disease. *Anal. Bioanal. Chem.* **409**, 379-394.

Sherbet, G. V. (2011). Growth factors and their receptors in cell differentiation, cancer and cancer therapy. Elsavier Inc.

Shi,Y., Hata, A., Lo, R. S., Massagué, J. and Pavletich, N.P. (1997). A structural basis for mutational inactivation of the tumour suppressor Smad4. *Nature* **388**, 83-93.

Shih, H. P., Gross, M. K. and Kioussi, C. (2007). Expression pattern of the homeodomain transcription factor Pitx2 during muscle development. *Gene Expr. Patterns* **7**, 441-451.

Sieiro-Mosti, D., De La Celle, M., Pelé, M. and Marcelle, C. (2014). A dynamic analysis of muscle fusion in the chick embryo. *Development* **141**, 3605-3611.
Sieiro, D., Rios, A. C., Hirst, C. E. and Marcelle, C. (2016). Cytoplasmic NOTCH and membrane-derived β-catenin link cell fate choice to epithelial-mesenchymal transition during myogenesis. *Elife* **5**, 1-21.

Singh, P., Carraher, C. and Schwarzbauer, J. E. (2010). Assembly of fibronectin extracellular matrix. *Annu. Rev. Cell Dev. Biol.* **26**, 397-419.

Smith, C. L. and Hollyday, M. (1973). The development and postnatal organization of motor nuclei in the rat thoracic spinal cord. *J. Comp. Neurol.* **220**, 16-28.

Smith, T. H., Kachinsky, A. M. and Miller, J. B. (1994). Somite subdomains, muscle cell origins, and the four muscle regulatory factor proteins. *J. Cell Biol.* **127**, 95-105.

Snow, C. J., Peterson, M. T., Khalil, A. and Henry, C. A. (2008). Muscle development is disrupted in zebrafish embryos deficient for fibronectin. *Dev. Dyn.* **237**, 2542-2553.

Sonbol, H. (2018). Extracellular matrix remodeling in human disease. *J. Microsc. Ultrastruct.* **6**, 123-125.

Sparrow, J. C. and Schöck, F. (2009). The initial steps of myofibril assembly: Integrins pave the way. *Nat. Rev. Mol. Cell Biol.* **10**, 293-298.

Spörle, R. (2001). Epaxial-adaxial-hypaxial regionalisation of the vertebrate somite: Evidence for a somitic organiser and a mirror-image duplication. *Dev. Genes Evol.* **211**, 198-217.

Stark, K. L., McMahon, J. A. and McMahon, A. P. (1991). FGFR-4, a new member of the fibroblast growth factor receptor family, expressed in the definitive endoderm and skeletal muscle lineages of the mouse. *Development* **113**, 641-651.

Steed, E., Balda, M. S. and Matter, K. (2010). Dynamics and functions of tight junctions. *Trends Cell Biol.* **20**, 142-149.

Stephenson, N. L. and Avis, J. M. (2012). Direct observation of proteolytic cleavage at the S2 site upon forced unfolding of the Notch negative regulatory region. *Proc. Natl. Acad. Sci.* **109**, E2757-E2765.

Stockdale, F. E. (1992). Myogenic cell lineages. *Dev. Biol.* **154**, 284-298.

Summerbell, D., Halai, C. and Rigby, P. W. J. (2002). Expression of the myogenic regulatory factor Mrf4 precedes or is contemporaneous with that of Myf5 in the somitic bud. *Mech. Dev.* **117**, 331-335.

Tajbakhsh, S. (2009). Skeletal muscle stem cells in developmental versus regenerative myogenesis. *J. Intern. Med.* **266**, 372-389.

Tajbakhsh, S. and Buckingham, M. (2000). The birth of muscle progenitor cells in the mouse: spatiotemporal considerations. *Curr. Top. Dev. Biol.* **48**, 225-268.

Tajbakhsh, S. and Spörle, R. (1998). Somite development: constructing the vertebrate body. Cell **92**, 9-16.

Tajbakhsh, S., Borello, U., Vivarelli, E., Kelly, R., Papkoff, J., Duprez, D., Buckingham, M. E. and Cossu, G. (1998). Differential activation of Myf5 and MyoD by different Wnts in explants of mouse paraxial mesoderm and the later activation of myogenesis in the absence of Myf5. *Development* **125**, 4155-4162.

Tajbakhsh, S., Rocancourt, D. and Buckingham, M. (1996). Muscle progenitor cells failing to respond to positional cues

adopt non- myogenic fates in myf-5 null mice. *Nature* **384**, 266-270.

Tajbakhsh, S., Rocancourt, D., Cossu, G. and Buckingham, M. (1997). Redefining the genetic hierarchies controlling skeletal myogenesis: Pax- 3 and Myf-5 act upstream of MyoD. *Cell* **89**, 127-138.

Tallquist, M. D., Weismann, K. E., Hellstrom, M. and Soriano, P. (2000). Early myotome specification regulates PDGFA expression and axial skeleton development. *Development* **127**, 5059-5070.

Teboul, L., Hadchouel, J., Daubas, P., Summerbell, D., Buckingham, M. and Rigby, P. W. J. (2002). The early epaxial enhancer is essential for the initial expression of the skeletal muscle determination gene Myf5 but not for subsequent, multiple phases of somitic myogenesis. *Development* **129**, 4571-4580.

Teboul, L., Summerbell, D. and Rigby, P. W. J. (2003). The initial somitic phase of Myf5 expression requires neither Shh signaling nor Gli regulation. *Genes Dev.* **17**, 2870-2874.

Teillet, M. A., Kalcheim, C. and Le Douarin, N. M. (1987). Formation of the dorsal root ganglia in the avian embryo: segmental origin and migratory behavior of neural crest progenitor cells. *Dev. Biol.* **120**, 329-347.

Teo, J. and Kahn, M. (2010). The Wnt signaling pathway in cellular proliferation and differentiation : A tale of two coactivators. *Adv. Drug Deliv. Rev.* **62**, 1149-1155.

Theocharis, A. D., Skandalis, S. S., Gialeli, C. and Karamanos, N. K. (2016). Extracellular matrix structure. *Adv. Drug Deliv. Rev.* **97**, 4-27.

Thorsteinsdóttir, S., Deries, M., Cachaço, A. S. and Bajanca, F. (2011). The extracellular matrix dimension of skeletal muscle development. *Dev. Biol.* **354**, 191-207.

Trebaul, A., Chan, E. K. and Midwood, K. S. (2007). Regulation of fibroblast migration by tenascin-C. *Biochem. Soc. Trans.* **35**, 695-697.

Tremblay, P., Dietrich, S., Mericskay, M., Schubert, F. R., Li, Z. and Paulin, D. (1998). A crucial role for Pax3 in the development of the hypaxial musculature and the long-range migration of muscle precursors. *Dev. Biol.* **203**, 49-61.

Tickle, C. and Towers, M. (2017). Sonic hedgehog signaling in limb development. *Front. Cell Dev. Biol.* **5**, 14.

Tosney, K. W., Dehnbostel, D. B. and Erickson, C. A. (1994). Neural crest cells prefer the myotome's basal lamina over the sclerotome as a substratum. *Dev. Biol.* **163**, 389-406.

Tozer, S., Bonnin, M.A., Relaix, F., Di Savino, S., García-Villalba, P., Coumailleau, P. and Duprez, D. (2007). Involvement of vessels and PDGFB in muscle splitting during chick limb development. *Development* **134**, 2579-2591.

Tozer, S. and Duprez, D. (2005). Tendon and ligament: Development, repair and disease. *Birth Defects Res. Part C - Embryo Today Rev.* **75**, 226-236.

Valasek, P., Evans, D.J. , Maina, F., Grim, M., Patel, K. (2005). A dual fate of the hindlimb muscle mass: cloacal/perineal musculature develops from leg muscle cells. *Development* **132**, 447-458.

Vallois, H. V. (1922). Les transformations de la musculature de l'épisome chez les vertébrés. Paris: Faculté des sciences de l'université de Paris.

Van Ho, A. T., Hayashi, S., Bröhl, D., Auradé, F., Rattenbach, R. and Relaix, F. (2011). Neural crest cell lineage restricts skeletal muscle progenitor cell differentiation through Neuregulin1-ErbB3 signaling. *Dev Cell.* **21**, 273-287.

Vasyutina, E., Stebler, J., Brand-Saberi, B., Schulz, S., Raz, E. and Birchmeier, C. (2005). CXCR4 and Gab1 cooperate to control the development of migrating muscle progenitor cells. *Genes Dev.* **19**, 2187-2198.

Venters, S. J. and Ordahl, C. P. (2002). Persistent myogenic capacity of the dermomyotome dorsomedial lip and restriction of myogenic competence. *Development* **129**, 3873-3885.

Venters, S. J., Thorsteinsdóttir, S. and Duxson, M. J. (1999). Early development of the myotome in the mouse. *Dev. Dyn.* **216**, 219-232.

von Maltzahn, J., Bentzinger, C. F. and Rudnicki, M. A. (2012a). Wnt7a-Fzd7 signalling directly activates the Akt/mTOR anabolic growth pathway in skeletal muscle. *Nat Cell Biol.***14**, 186-191.

von Maltzahn, J., Chang, N. C., Bentzinger, C. F. and Rudnicki, M. A. (2012b). Wnt signaling in myogenesis. *Trends Cell Biol.* **22**, 602-609.

Vortkamp, A., Pathi, S., Peretti, G. M., Caruso, E. M., Zaleske, D. J. and Tabin, C. J. (1998). Recapitulation of signals regulating embryonic bone formation during postnatal growth and in fracture repair. *Mech. Dev.* **71**, 65-76.

Wallingford, J. B. and Habas, R. (2005). The developmental biology of Dishevelled : an enigmatic protein governing cell fate and cell polarity. *Development* **132**, 4421-4436.

Wang, N. (2017). Review of cellular mechanotransduction. *J. Phys. D. Appl. Phys.* **50**, 407-420.

Watt, F. M. and Huck, W. T. S. (2013). Role of the extracellular matrix in regulating stem cell fate. N*at. Rev. Mol. Cell Biol.* **14**, 467-473.

Weintraub, H., Tapscott, S. J., Davis, R. L., Thayer, M. J., Adam, M. A., Lassar, A. B. and Miller, A. D. (1989). Activation of muscle-specific genes in pigment, nerve, fat, liver, and fibroblast cell lines by forced expression of MyoD. *Proc. Natl. Acad. Sci. USA* **86**, 5434-5438.

White, R. B., Biérinx, A., Gnocchi, V. F. and Zammit, P. S. (2010). Dynamics of muscle fibre growth during postnatal mouse development. *BMC Dev. Biol.* 22, 10-21.

Williams, A. S., Kang, L. and Wasserman, D. H. (2015). The Extracellular matrix and insulin resistance. *Trends Endocrinol. Metab.* **26**, 357-366.

Williams, B. A., Ordahl, C. P., Burke, A. C., Nelson, C. E., Morgan, B. A. and Tabin, C. (1994). Pax-3 expression in segmental mesoderm marks early stages in myogenic cell specification. *Development* **120**, 785-796.

Wilting, J., Brand-Saberi, B., Huang, R., Zhi, Q., Köntges, G., Ordahl, C. P. and Christ, B. (1995). Angiogenic potential of the avian somite. *Dev. Dyn.* **202**, 165-171.

Wong, K., Park, H. T., Wu, J. Y. and Rao, Y. (2002). Slit proteins: Molecular guidance cues for cells ranging from neurons to leukocytes. *Curr. Opin. Genet. Dev.* **12**, 583-591.

Wright, W. E., Sassoon, D. A. and Lin, V. K. (1989). Myogenin, a factor regulating myogenesis, has a domain homologous to MyoD. *Cell* **56**, 607-617.

Yablonka-Reuveni, Z. (2011). The skeletal muscle satellite cell. *J. Histochem. Cytochem.* **59**, 1041-1059.

Yamaguchi, T. P., Conlon, R. a and Rossant, J. (1992). Expression of the fibroblast growth factor receptor FGFR-1/flg during gastrulation and segmentation in the mouse embryo. *Dev. Biol.* **152**, 75-88.

Yamamoto-Shiraishi, Y. I. and Kuroiwa, A. (2013). Wnt and BMP signaling cooperate with Hox in the control of Six2 expression in limb tendon precursor. *Dev. Biol.* **377**, 363-374.

Yang, X., Gong, Y., Tang, Y., Li, H., He, Q., Gower, L. and Liaw, L. (2013). Spry1 and Spry4 differentially regulate human aortic smooth muscle cell phenotype via Akt/FoxO/myocardin signaling. *PLoS One* **8**, e58746.

Yang, X. M., Vogan, K., Gros, P. and Park, M. (1996). Expression of the met receptor tyrosine kinase in muscle progenitor cells in somites and limbs is absent in Splotch mice. *Development* **122**, 2163-2171.

Yao, H. H., Whoriskey, W. and Capel, B. (2002). Desert Hedgehog/Patched 1 signaling specifies fetal Leydig cell fate in testis organogenesis. *Genes Dev.* **16**, 1433-1440.

Yayon, A., Klagsbrun, M., Leder, P. and Ornitz, D. M. (1991). Cell surface, heparin-like molecules are required for binding of basic fibroblast growth factor to its high affinity receptor. *Cell* **64**, 841-848.

Yin, H., Price, F. and Rudnicki, M. A. (2013). Satellite cells and the muscle stem cell niche. *Physiol. Rev.* **93**, 23-67.

Yokoyama, S. and Asahara, H. (2011). The myogenic transcriptional network. *Cell. Mol. Life Sci.* **68**, 1843-1849.

Yurchenco, P. D. (2015). Integrating activities of laminins that drive basement membrane assembly and function.*Curr. Top Membr.* **76**, 1-30.

Yvernogeau, L., Auda-Boucher, G. and Fontaine-Perus, J. (2011). Limb bud colonization by somite-derived angioblasts is a crucial step for myoblast emigration. *Development* **139**, 277-287.

Zelzer, E., Blitz, E., Killian, M. L. and Thomopoulos, S. (2014). Tendon-to-bone attachment: from development to maturity. *Birth Defects Res. C Embryo Today* **102**, 101-112.

Zhou, Y., Horowitz, J. C., Naba, A., Ambalavanan, N., Atabai, K., Balestrini, J., Bitterman, P. B., Corley, R. A., Ding, B. Sen, Engler, A. J., et al. (2018). Extracellular matrix in lung development, homeostasis and disease. *Matrix Biol.* **73**, 77-104.

Zollinger, A. J. and Smith, M. L. (2017). Fibronectin, the extracellular glue. *Matrix Biol.* **60**–**61**, 27-37.

Chapter 2

Rapid and simple method for *in vivo ex utero* development of mouse embryo explants

Rapid and simple method for *in vivo ex utero* development of mouse embryo explants

André B. Gonçalves[a], Sólveig Thorsteinsdóttir[a,b] and Marianne Deries[a]

Differentiation 91, 57-67, 2016

[a] Centro de Ecologia, Evolução e Alterações Ambientais, Faculdade de Ciências, Departamento de Biologia Animal, Universidade de Lisboa, 1749-016 Lisboa, Portugal.

[b] Instituto Gulbenkian de Ciência, 2781-901 Oeiras, Portugal.

Contribution for the publication:

	Experimental work depicted in Fig.					Manuscript writing
	2.1	2.2	2.3	2.4	2.5	
Design and concept	III	O	III	III	III	III
Execution	III	O	III	III	III	
Analysis and interpretation	III	III	III	III	III	

Legend:

- ..... non-applicable
O ..... no intervention
I ..... minor contribution
II ..... moderate contribution
III .... major contribution/full execution

Note: this contribution does not exclude other contributions, similar or not, from the remaining authors

Differentiation 91 (2016) 57–67

Contents lists available at ScienceDirect

Differentiation

journal homepage: www.elsevier.com/locate/diff

Rapid and simple method for in vivo ex utero development of mouse embryo explants

André B. Gonçalves [a,*], Sólveig Thorsteinsdóttir [a,b], Marianne Deries [a,*]

[a] Centro de Ecologia, Evolução e Alterações Ambientais, Departamento de Biologia Animal, Faculdade de Ciências, Universidade de Lisboa, Lisbon, Portugal
[b] Instituto Gulbenkian de Ciência, Oeiras, Portugal

ARTICLE INFO

Article history:
Received 23 November 2015
Accepted 4 December 2015
Available online 17 February 2016

Keywords:
Ex utero
Explant culture
Floating membranes
Muscle morphogenesis
Extracellular matrix
Mouse embryo

ABSTRACT

The in utero development of mammals drastically reduces the accessibility of the mammalian embryo and therefore limits the range of experimental manipulation that can be done to study functions of genes or signaling pathways during embryo development. Over the past decades, tissue and organ-like culture methods have been developed with the intention of reproducing in vivo situations. Developing accessible and simple techniques to study and manipulate embryos is an everlasting challenge. Herein, we describe a reliable and quick technique to culture mid-gestation explanted mouse embryos on top of a floating membrane filter in a defined medium. Viability of the cultured tissues was assessed by apoptosis and proliferation analysis showing that cell proliferation is normal and there is only a slight increase in apoptosis after 12 h of culture compared to embryos developing in utero. Moreover, differentiation and morphogenesis proceed normally as assessed by 3D imaging of the transformation of the myotome into deep back muscles. Not only does muscle cell differentiation occur as expected, but so do extracellular matrix organization and the characteristic splitting of the myotome into the three epaxial muscle groups. Our culture method allows for the culture and manipulation of mammalian embryo explants in a very efficient way, and it permits the manipulation of in vivo developmental events in a controlled environment. Explants grown under these ex utero conditions simulate real developmental events that occur in utero.

1. Introduction

During embryogenesis, pluripotent cells differentiate into highly specified cells, which form tissues and organs of a whole organism through the tight regulation of gene expression, cell–cell communication and cell–extracellular matrix (ECM) interactions. These events, underlying development, and in particular morphogenesis, are fascinating and understanding them is the challenge of developmental biologists. Many different organisms are used as models to study developmental biology, from the easiest to grow and genetically manipulate such as fruit fly, nematode or zebrafish, to more complex models such as chick and mouse (Bolker, 1995; Jenner and Wills, 2007). Experiments on these organisms help to draw fundamental developmental biology concepts that not only expand our knowledge in biology but are also useful to understand human cancer and genetic diseases which share basic mechanisms with developmental biology.

Functional experiments on mammalian embryos have allowed the mapping of gene interactions, lineage tracing and morphogenetic events of mammalian development (Bueno et al., 1996; Ellington, 1991; Muñoz-Espín et al., 2013; Petersen et al., 2006; Tam and Behringer, 1997). Among several studied species, the mouse is considered to be the prime mammalian model system. The mouse is a small and relatively easy animal to keep and breed. Its embryo shares genetic, physiological and metabolic characteristics with human embryos, as would any mammal, but more importantly the great majority of the molecular tools available to study mammalian embryos, including gene targeting in embryonic stem cells, have been developed in the mouse (Bedell et al., 1997; Capecchi, 2005). All these technical reasons made the mouse embryo an efficient model to study not only developmental events but also tissue homeostasis and disease mechanisms (Allamand and Campbell, 2000; Elder et al., 2010; Murry and Keller, 2008).

A major drawback of using the mouse as a model is that genetic manipulation of mice implies intense labor and a large investment, both financially and logistically, besides raising some ethical constraints (Bradley, 2002; Ormandy et al., 2011). Developing more accessible and cheaper experimental approaches which mimic

* Corresponding authors.
E-mail addresses: abrgoncalves@fc.ul.pt (A.B. Gonçalves), mederies@fc.ul.pt (M. Deries).

http://dx.doi.org/10.1016/j.diff.2015.12.002
Join the International Society for Differentiation (www.isdifferentiation.org)
0301-4681/

in vivo biological processes is a challenging issue. Because of the viviparous development of placental mammals, the inaccessibility of the post-implantation embryo limits its direct manipulation. In vitro culture techniques were established long before gene targeting experiments (Carrel, 1912; Carrel and Burrows, 1911) enabling the growth of cells, tissues or even organs outside the body in an artificially controlled environment (Freshney, 2000). These model systems have been of utmost importance and have contributed to a significant number of relevant discoveries (e.g. Miller et al., 1993; Karpas et al., 2001; Masters et al., 2002). Methods involving primary culture of embryonic and adult stem cells have also been developed and have provided invaluable data on the mechanisms of cell fate choices and cell differentiation (Evans and Kaufman, 1981; Solter, 2006; Pittenger, 1999; Bianco et al., 2008). Nonetheless, 2D cell culture cannot fully reproduce in vivo conditions and efforts have thus been made to develop 3D cultures in order to create conditions that are closer to the situation in vivo (Edmondson et al., 2014; Fournier and Martin, 2006; Mazzoleni et al., 2009; Ravi et al., 2014). Although 2D and 3D cell culture systems are excellent models for many applications, in other situations they are not representative of the whole embryonic tissue. For example, no multinucleated muscle fibers form in the limbs of *myogenin*-null mouse embryos, but when mutant myoblasts are isolated and grown in vitro, they differentiate and fuse into multinucleated myotubes (Nabeshima et al., 1993). This example shows how completely different the behavior of cells can be in culture compared to in the complex environment of the whole organism.

In the present work, we describe a simple and quick in vivo ex utero mouse embryo explant culture method which can be used to follow the normal development of explanted embryos and, due to their accessibility ex utero, to experimentally manipulate developmental pathways or processes. The technique is built on the chick embryo explant method developed by Palmeirim et al. (1997) and was adapted in our laboratory to enable the culture of mouse embryo explants to study early developmental events such as somite development (Bajanca et al., 2006). Here, we have further improved the technique to enable culture of explants of later embryonic stages and use the development of deep back muscles (epaxial muscles) as an illustration of the success of this system. During the time of culture, cell proliferation, differentiation and extracellular matrix (ECM) assembly proceed as normal and apoptosis levels are low. Furthermore, the epaxial muscles of the explanted embryos not only maintain a normal morphology as assessed by 3D imaging, but also undergo the same morphogenetic transformations as those in embryos developing in utero.

2. Methods and results

2.1. Retrieval and dissection of in vivo ex utero mouse explants: a step by step description

Embryos are produced by crossing wild-type adult mice (Charles-River CD1; Envigo) and the day of the vaginal plug is designated as embryonic day (E) 0.5. Pregnant females are sacrificed by cervical dislocation after isoflurane anesthesia. Animal handling procedures were performed according to EU law and the guidelines recommended and monitored by the Faculty of Sciences University of Lisbon ethics (ORBEA) committee and the Direção-Geral de Alimentação e Veterinária (DGAV).

Here we describe the retrieval and dissection of E11.75 mouse embryos for explant cultures. This stage is of particular interest to us because it marks the beginning of the transformation of the myotome into the deep back muscle masses (Deries et al., 2010; Deries et al., 2012). However, this explant culture method is not limited to this particular stage, in fact we have used it to culture explants prepared from E8.0 up to E12.5 embryos.

Table 1 summarizes the materials needed to successfully perform embryo collection, manipulation and the culture technique. A careful and adequate embryo manipulation and dissection are key steps to successfully perform explant cultures. To extract embryos, each uterine horn is isolated from the pregnant female and placed in a sterile phosphate-buffered saline solution (PBS) containing 0.9 mM $CaCl_2$ and 0.5 mM $MgCl_2$ (complete PBS) at room temperature (Fig. 1A). During all the following procedures, embryos are manipulated under a dissecting stereoscope to avoid unnecessary damage. Embryos together with their extraembryonic membranes and the placenta are isolated from the uterus with sterilized tools and transferred into sterile, prewarmed (37 °C) Dissecting medium (Table 2): Dulbecco's Modified Eagle Medium/Ham's F12 GlutaMax medium (DMEM/F12) with a final concentration of 25 mM HEPES to maintain a physiological pH during dissection, further supplemented with sodium pyruvate as a carbon source and penicillin and streptomycin antibiotics (see Table 2).

The uterus and the decidua are opened to release the embryo (Fig. 1B). All extraembryonic membranes are then removed one after the other. Reichert's membrane is the first to be removed, but the placenta is kept intact as long as possible. At the end of this step the embryo is visible through the yolk sac and the amnion (Fig. 1C). It is then possible to tear the yolk sac off after making a small puncture with the tips of the forceps thus exposing the amniotic sac and the umbilical cord. Finally, the amnion and placenta are removed and the umbilical cord is cut (Fig. 1D).

It is important to mention that embryos are processed differently depending on their stages (Table 3): as development increases, embryos need to be more dissected to allow penetration of the medium into the tissues of interest. In the case of E11.75 embryos, they are beheaded and the internal organs are removed (Fig. 1E). This dissection ensures the viability of the tissues of interest (in this case the axial tissues) during culture (see below). At the end of the dissection, each new explant is set aside in a new, warm (37 °C) dissecting medium until all the remaining embryos are processed.

2.2. Explant culture

After dissection, each explant is positioned either on their side (E9.5–E10.5) or ventrally (older than E10.5; Table 3) on a 0.8 μm pore size polycarbonate hydrophilic Isopore membrane filter laid in the lid of a six-well cell culture plate (Fig. 1F and G). Several explants can be placed on the same filter, but care has to be taken not to put too many to avoid sinking the filter when floated onto the medium (see Table 3 for recommended number of embryos per filter).

When the desired number of embryo explants has been transferred (Fig. 1H), the filter is placed floating on top of

Table 1
Materials for mouse embryo explant culture.

10.5 cm straight fine iris scissor
12.5 cm, 0.4 mm × 0.2 mm thick inox forceps
11 cm, 0.05 mm × 0.02 mm thick inox fine forceps with biology tips
15 mm diameter Moria MC17 BIS perforated spoon
4.5 cm cutting edge, 0.15 mm thick, 22.5° cutting angle thick micro knife
Plastic Petri dishes
Pasteur pipettes
25 mm, 0.8 μm pore size, white plain Isopore hydrophilic polycarbonate membrane filters
Six-well cell culture plates

Table 2.1: Materials for mouse embryo explant culture.

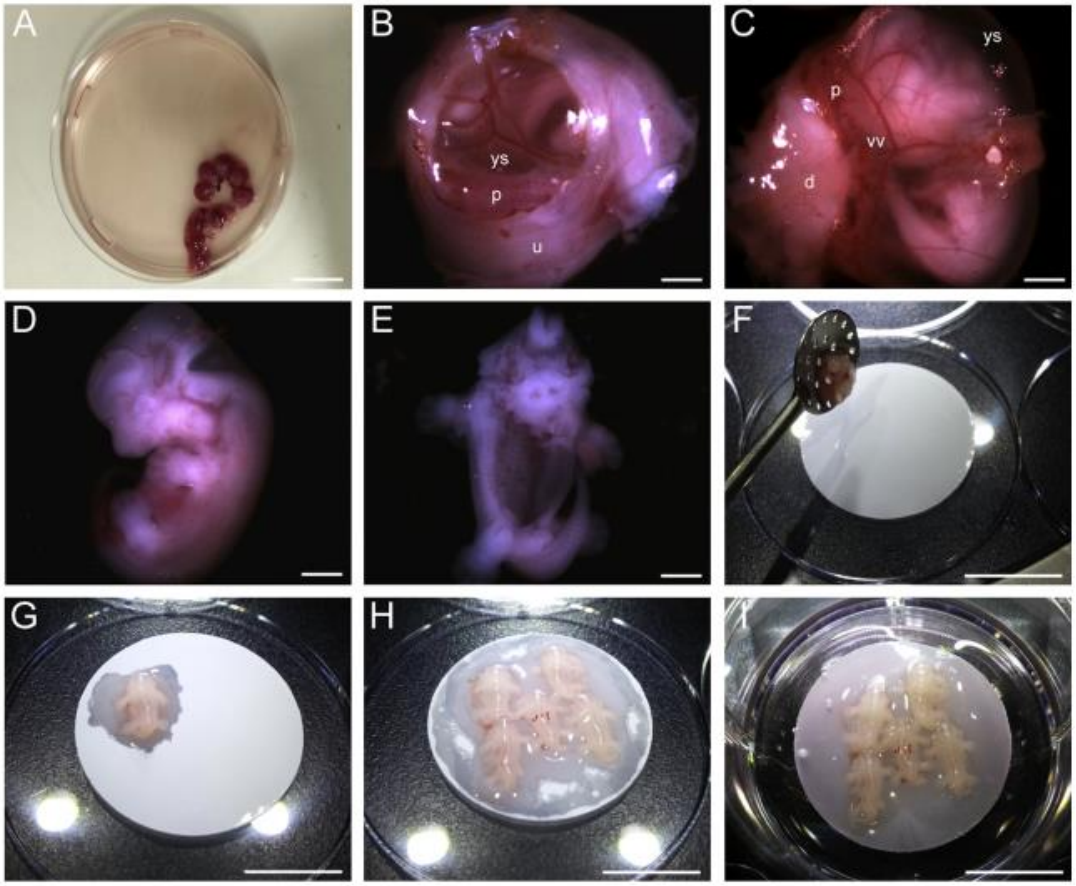

Fig. 1. Dissection of an E11.75 mouse conceptus for explant culture. After opening the visceral cavity of the female mouse with a midline laparotomy and moving the viscera to the side, the uterus containing all the embryos is cut near the oviducts and across the cervix, is then gently pulled out with forceps, and transferred into a Petri dish containing complete PBS (A). After dissecting away the uterine blood vessels, transverse cuts are made in the uterine wall in between each conceptus and these are transferred into Dissecting medium (B). The uterine wall, decidua and Reichert's membrane are then removed by gently grasping them with forceps and pulling these tissues apart. After this step, the embryo and placenta are visible through the yolk sac and amnion (C). The yolk sac is pierced and removed, the placenta is separated from the embryo and the umbilical cord cut to free the embryo from all extraembryonic tissues (D). Embryos are beheaded and eviscerated (E) and placed individually with a perforated spoon on the membrane filter which is resting in the lid of a six-well culture plate (F). Each embryo is placed with the ventral side down on the membrane filter (G) and this procedure is repeated until the filter is full (H). The membrane filter with the explants is carefully transferred into a well with Culture medium, floating on top of Culture medium (I) and placed in an incubator for the desired time. d – decidua; p – placenta; u – uterine wall; vv – vitelline vessels; ys – yolk sac. Scale bars: 10 mm in A, F–I and 1 mm in B–E.

prewarmed Culture medium (Table 2) in the six-well plate (Fig. 1I). Finally, some drops of Culture medium are placed on top of the explants (and the filter) to prevent them from drying and explants are then incubated at 37 °C in a 5% CO_2 humidified atmosphere. After 6 or 12 h of culture, the filter is transferred into PBS to release the explants and they are processed according to the desired experimental approach protocol.

We have tested and optimized two culture time periods, 6 and 12 h, and present results for 12 h here. Two control groups were named "No culture-E11.75" and "No Culture-E12.25". The first one is composed of embryos of the same litter as the cultured explants but fixed and stained without culture (therefore stage E11.75). This control allows the assessment of the stage of development of the cultured tissues before culture. The second control group comprises embryos that have developed in utero until E12.25 and were collected and fixed without culture. This stage of development corresponds to the theoretical stage of the explants after 12 h in culture and thus allows us to compare the development and

Table 2
Media for mouse embryo explant culture.

Dissecting medium	DMEM-F12 Glutamax (with 15 mM HEPES and 2.5 mM L-glutamine)-Lonza; 1 mM sodium pyruvate (from a 100 mM stock solution)-Lonza 100 U/ml; penicillin/streptomycin (from a 10,000 U/ml stock solution)-Lonza 10 mM; HEPES (from a 1 M HEPES stock solution in distilled water)-Sigma-Aldrich
Culture medium	DMEM-F12 Glutamax (with 15 mM HEPES and 2.5 mM L-glutamine)-Lonza; 1 mM sodium pyruvate (from a 100 mM stock solution)-Lonza 100 U/ml; penicillin/streptomycin (from a 10,000 U/ml stock solution)-Lonza

Figure 2.1: Dissection of an E11.5 mouse conceptus for explant culture.

Table 2.2: Media for mouse embryo explant culture.

Table 3
Description of embryo dissection and number of embryos per filter according to their age.

Developmental stage	Embryo processing description after removal of extraembryonic membranes	Number of explanted embryos/ filter
E8.0–E9.5	No embryo dissection needed. Explants are placed positioned sideways on top of the floating membrane filters.	7–10
E10.5	Head and heart are removed (optional). Explants are placed positioned sideways on top of the floating membrane filter.	5–6
E11.5–E12.5	Head, heart and internal organs are removed. Explants are placed ventrally on top of the floating membrane filter.	3–5

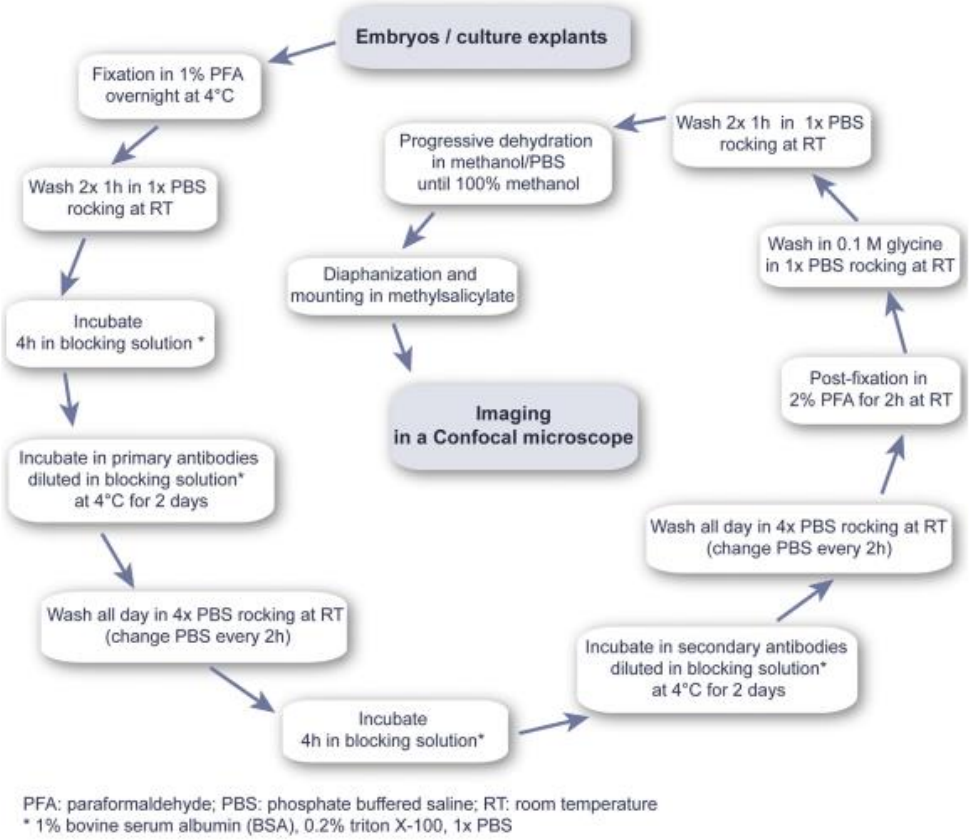

Fig. 2. Whole mount immunohistochemistry protocol. Schematic representation of the whole mount immunohistochemistry protocol (adapted from Ordahl et al. (2001) and Martins et al. (2009)). Antibodies and their dilutions are displayed in Table 4.

Table 4
Antibodies.

	Antibody	Clone/ reference	Company	Dilution
Primary antibodies	Monoclonal mouse anti-myosin heavy chain	MF20	Developmental Studies Hybridoma Bank	1:50
	Monoclonal mouse anti-myogenin	F5D	Developmental Studies Hybridoma Bank	1:50
	Polyclonal rabbit anti-myogenin	F5D	Santa Cruz Biotechnology	1:50
	Monoclonal rat anti-tenascin-C	LAT-2	Courtesy of Arnoud Sonnenberg	1:50
	Polyclonal rabbit anti-cleaved caspase-3 (Asp175) conjugated with Alexa Fluor 488	9669	Cell Signaling Technology	1:100
	Polyclonal rabbit anti-phospho-Histone H3 (Ser 10)	06-570	Merck Millipore	1:100
Secondary antibodies and nuclear staining	Alexa Fluor 568-conjugated anti-mouse IgG	A-11019	Molecular Probes	1:500
	Alexa Fluor 488-conjugated anti-rabbit IgG	A-11070	Molecular Probes	1:500
	Alexa Fluor 488-conjugated anti-rat IgG	A-11006	Molecular Probes	1:500
	TO-PRO-3	T3605	Molecular Probes	1:500

Figure 2.2: Whole mount immunohistochemistry protocol.

Table 2.3: Description of embryo dissection and number of embryos per filter according to their age.

Table 2.4: Antibodies.

.

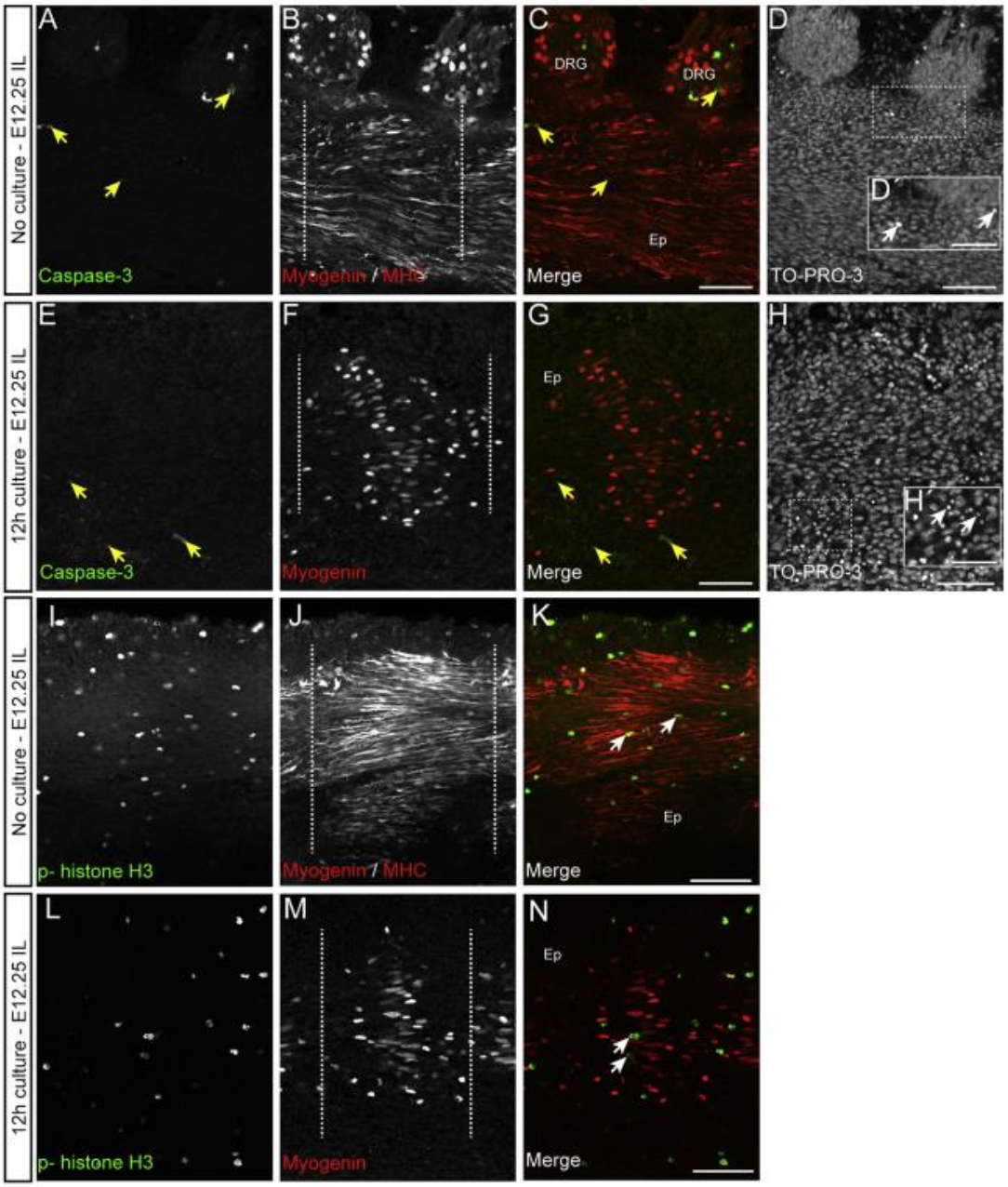

Fig. 3. Apoptosis and proliferation in cultured explant embryos. Optical 0.5 μm sections obtained from confocal stacks representing the middle of an axial myotomal segment at interlimb level (IL; A–N) of an E12.25 embryo fixed without culture (A–D and I–K) and a representative E11.75 embryo explant cultured for 12 h (E–H and L–N). Embryos were labeled using antibodies against myogenin and MHC (B, J; both red in C, K), and explants were labeled for myogenin only (F, M; red in G, N), combined with either activated caspase-3 (A, E; green in C, G) to detect apoptosis or phospo-histone H3 (p-histone H3; I, L; green in K, N) to detect cells in mitosis. TO-PRO-3 nuclear staining was used (D, H) to detect pyknotic nuclei, a maker of terminal stages of apoptosis. The epaxial (Ep, dorsal) side is upwards in all figures. Dashed lines outline a single muscle segment (B, F, J, M). A–D: E12.25 embryos that have developed in utero exhibit low levels of apoptosis (A, C). A few caspase-3-positive cells are found within the tissues (yellow arrows in A, C). Higher levels of apoptosis are always detected in the dorsal root ganglia (DRG, C). TO-PRO-3 nuclear staining show pyknotic nuclei (arrows in D′) both within the muscle segment and in the DRG. E–H: There is a slight increase in caspase-3 staining in explants cultured for 12 h (yellow arrows in E, G) and in the number of pyknotic nuclei (arrows in H′), mainly localized in the tissues surrounding the myotomal segment. I–N: No differences were detected in the proliferation of the cells during the time of the culture. p-histone H3 staining reveals that cells in the tissues of both E12.25 control embryo (I–K) and explants cultured for 12 h (L–N) are proliferating (arrows in K, N). DRG-Dorsal root ganglia. Scale bars: 50 μm in A–N and 25 μm in D′ and H′.

Figure 2.3: Apoptosis and proliferation in cultured explant embryos.

health of the tissues in explant culture with the development of the same tissues in embryos in utero.

Control embryos and cultured explants are fixed overnight and processed for whole-mount immunolabeling using the method of Ordahl et al. (2001) with some minor changes (for protocol, see Fig. 2). The diaphanization step of the tissue was performed

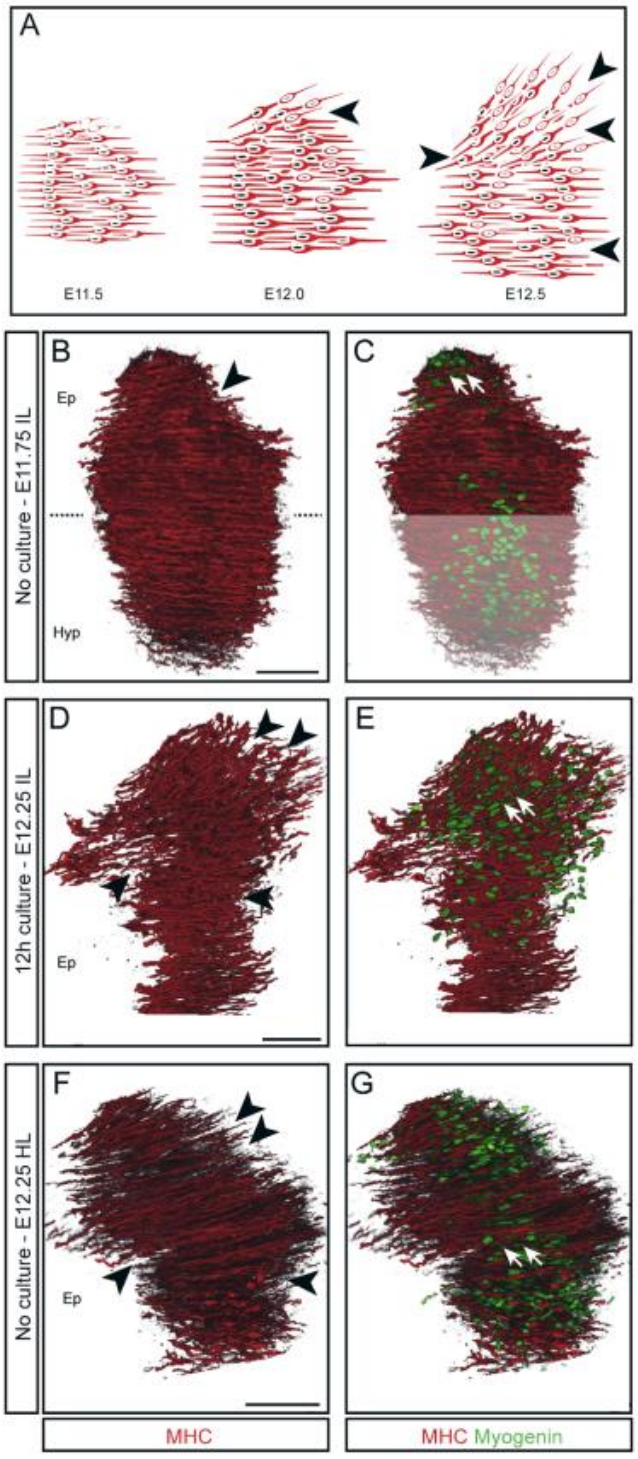

Figure 2.4: Morphogenesis of deep back muscles occurs normally in cultured explants.

.

according to Martins et al. (2009). Table 4 shows the antibodies and dilutions used in the whole-mount immunolabeling protocol. Immunostained tissues were analyzed by confocal microscopy. Images were acquired with a 40x ACS APO 1.15 oil-immersion lens. 2D images were obtained from the original confocal stacks, in which one representative optical section (0.5 µm) was selected using ImageJ 1.49a. To show the morphology of the muscles, confocal stacks were 3D reconstructed and analyzed using the Amira v5.3.3 software (Visage Inc.), in which one individual segment and/or its associated matrix were isolated by manual contouring of confocal stacks (i.e. other cells and the matrix from surrounding tissues were "digitally erased").

2.3. The tissue of cultured embryo explants is healthy after 12 h of culture

After incubation, the general appearance of the tissue was observed to verify whether it looked healthy. Most of the time explants looked healthy, but occasionally a specimen did not develop and degenerated (data not shown). We find that this is most likely due to death coming from a developmental malformation (which would have occurred in utero as well) or due to error or damage during the procedure, as for example the tissue becoming dehydrated due to evaporation of the culture medium from the top of the explant during incubation.

To further assess the health of the explants after culture we verified the level of apoptosis in whole mounts of "No culture-E12.25" control embryos (Fig. 3A–D) stained with antibodies against myogenin and myosin heavy chain (MHC) and compared with explants fixed after 12 h of culture and stained for myogenin (Fig. 3E–H) using two approaches: (1) Co-immunostaining with an antibody against cleaved caspase-3, which is an early marker of the apoptosis pathway; and (2) Detection of the terminal stage of apoptosis, characterized by the condensation of the chromatin in the nucleus, a process called karyopyknosis, followed by the fragmentation of the nuclei, which is visible when DNA is stained. To this end we used a fluorescent nuclear dye (TO-PRO-3) to assess the shape of the nuclei in tissues (Fig. 3D and H). Overall caspase-3 staining is slightly increased in the cultured explants compared to the in utero controls (compare Fig. 3A and C with 3E, G; yellow arrows). Activated caspase-3 is an early marker of apoptosis, and does not always lead to cell death (Khalil et al., 2012). We therefore also counted the number of pyknotic nuclei in 20 optical sections per embryo and found that on average 0.5% of nuclei were pyknotic in embryos developing in utero ($n=2$ embryos) whereas in cultured explants 0.9% of nuclei were pyknotic ($n=3$ explants). We therefore conclude that there is a slight increase in cell death in the cultured explants, but that the level of cell death is still very low.

Proliferation was assessed by immunohistochemistry (Fig. 3I–N) using an antibody against histone H3 phosphorylated on serine 10 residue (designated p-histone H3; a marker for mitosis) combined with myogenin (explants) or myogenin/MHC (controls). No striking differences were found between non-cultured and cultured embryos. In general, histone H3-positive cells are evenly distributed throughout all the tissues (compare Fig. 3I, K with L, N) and within the differentiated muscle masses in both experimental groups (arrows; Fig. 3K and N), indicating that the tissues are healthy and viable.

Thus, these results show that the described technique can be successfully applied to culture embryo explants in ex utero conditions for up to 12 h with only a slight augmentation of apoptosis.

2.4. Epaxial muscle morphology is normal and morphogenesis occurs properly during culture

Embryos are dissected before being incubated and explants are either incubated on their side (E9.5 – 10.5) or with the ventral region down (E11.0 – E11.5; Table 3). Thus they are not floating as in the uterus or in a rolling tube but they rest on a filter. We therefore asked whether morphogenesis occurs normally during culture. To answer this question, we analyzed the development of the epaxial muscles.

All epaxial muscles derive from myotomes, segmented muscles with mononucleated myocytes parallel to each other and to the axis of the embryo (Fig. 4A). In amniote embryos, the epaxial (dorsal) part of the segmented myotomes transforms into the epaxial (deep back) muscle masses. During this process, myocytes change their orientation and cleavages appear within the segments (arrowheads Fig. 4A), dividing them into three epaxial muscle groups: transversospinalis, longissimus and iliocostalis groups (Deries et al., 2010). Meanwhile, fusion between myocytes and/or myoblasts leads to the formation of primary myotubes, which form the scaffold of the definitive epaxial muscle groups (Deries et al., 2010). In the mouse, this process starts approximately at E11.5 and extends until E12.5 (Fig. 4A; Deries et al., 2012). These morphological characteristics are easy to observe and evaluate in 3D reconstructions of confocal images of explants where myocytes are immunostained with an anti-MHC antibody and the nuclei of differentiating muscle cells are visualized with an anti-myogenin antibody (Fig. 4B–G).

The stage of the embryo at the beginning of the culture, E11.75, was chosen to catch the transformation of the myotome. After 12 h of culture and in the "No culture control – E12.25", the myotome had grown significantly compared to E11.75 embryos (Fig. 4D–G). To verify whether epaxial muscle development and morphogenesis were normal, we focused on the dorsal-most part of the segment, i.e. where the translocation begins. Before culture, E11.75 myotomes are mature and the myocytes are predominantly mononucleated and parallel to each other (Fig. 4B). Only a small number of myocytes in the epaxial-most region have become multinucleated (white arrows; Fig. 4C), and have begun to change

Fig. 4. Morphogenesis of deep back muscles occurs normally in cultured explants. Lateral views of 3D reconstructions of interlimb (B–E) and hindlimb myotomes (F, G) of freshly collected E11.75 (no culture) embryos (B, C), E11.75 embryo explants cultured for 12 h (E11.75 + 12 h; D, E) and freshly collected E12.25 (no culture) embryos (F, G) stained by whole mount immunofluorescence with antibodies against MHC (red in B–G) and myogenin (green in C, E, G). The dorsal side is upwards in all figures. A: Scheme representing the first steps of the transformation of the myotome into the deep back muscles. Arrowheads mark the first emerging cleavages, separating groups of myocytes, which will later become the different epaxial muscle groups. Initially most myocytes are mononucleated (large nuclei with dark nucleolus) but as development proceeds more and more multinucleated cells are visible (addition of smaller, light nuclei). B–C: The myotome of E11.75 embryos is mainly composed of mononucleated myocytes fully extended through the whole segment and parallel to each other and to the axis of the embryo. The most dorsal myocytes have tilted to create the first sign of a cleavage (arrowhead in B) and have become multinucleated (white arrows in C). The dashed line indicates the separation between the epaxial (Ep) and hypaxial (Hyp) region of the E11.75 myotome (B) and the hypaxial region was covered with a transparent white box to better appreciate the size of the epaxial (non-covered) region (C). D–E: After 12 h of culture, the epaxial myotome (Ep) has grown significantly and now occupies the full figure (compare with epaxial part in B, C). The translocation of the dorsal-most epaxial myocytes is now accentuated and the cleavages individualizing the epaxial muscle masses are visible (arrowheads in D). Myogenin positive nuclei are abundant throughout the whole epaxial segment, indicating that cells were able to differentiate during culture and a large number of myocytes have become multinucleated (white arrows in E). F–G: The hindlimb-level myotome of an E12.25 embryo developed in utero displays the same cleavages (arrowheads in F) as the interlimb segment in the cultured embryo explant (compare arrowheads in F and D) and their orientation is similar (compare F and D). A similar number of myogenin positive cells (compare G and E) and multinucleated myocytes (compare white arrows in G and E) are also seen. Thus an interlimb segment of a cultured E12.25 embryo corresponds to the hindlimb segment of an E12.25 developing in utero. Scale bars: 50 µm.

their orientation, exposing the first cleavages (black arrowhead; Fig. 4B), as expected (Deries et al., 2010; Deries et al., 2012). Myogenin positive cells are abundant in the epaxial myotome (Fig. 4C) indicating that the progenitor cells are differentiating to contribute to the growth of the myotome. After 12 h in culture, the muscle masses have grown significantly. The epaxial region has dramatically increased in size (compare epaxial -nonshaded- area in Fig. 4C with epaxial region shown in Fig. 4E). The muscle masses also clearly present a different shape. Myocytes are no longer parallel to the axis of the embryo, but rather form the characteristic tilt in the dorsal-most tip of the muscle (Fig. 4D and E). Several cleavages can be observed among the myocytes (black arrowheads, Fig. 4D), which mark the individualization of the three epaxial muscle masses (Deries et al., 2010). Myogenin positive cells are present throughout the whole epaxial myotome, indicating that cells committed to myogenesis were able to differentiate during the culture period (Fig. 4E). Furthermore, the majority of the epaxial myocytes are now bi- or multinucleated (white arrows; Fig. 4E).

All these features are characteristic of E12.25 embryos developing in utero (Fig. 4F, G). However, the stage of the cultured explants resemble more a hindlimb level segment (Fig. 4F, G) than an interlimb segment as it should be, showing that the development of the cultured embryo explants is slightly delayed compared to in utero development. This delay is probably due to the extraction and the dissection of the tissue before culture, which may induce several physicochemical stress factors such as the dissection procedure itself, a change in medium composition and temperature. Although we use warmed Dissection medium, it is difficult to maintain a constant temperature during the whole extraction and dissection and the explants may thus take some time to recover a constant body temperature after being placed in the incubator. These factors are known to have an impact on the rate of preimplantation embryo metabolism and development (Feuer and Rinaldo, 2012) and are likely to also affect post-implantation embryos.

Despite the slight developmental delay, most likely due to the dissection procedure, all these observations strongly indicate that normal differentiation and morphogenesis of the muscle tissue has occurred during culture.

2.5. Assembly and organization of the ECM proceed normally during culture.

The effect of the culture system on the integrity of the ECM associated with the myotome was also analyzed through the staining of tenascin-C, which is present in the sclerotome and later becomes confined to the forming myotendinous junction regions (Crossin et al., 1986; Deries et al., 2012). Tissues were immunolabeled with antibodies against MHC and tenascin-C (Fig. 5).

3D reconstructions of the immunostaining show that before culture, tenascin ECM is abundant at the intersegmental borders (asterisks; Fig. 5A, B) and tenascin cables extend from these borders through the whole myotomal segment (arrows; Fig. 5A, B). After 12 h of culture, the tenascin cables of the explants are more numerous (arrows; Fig. C, D) and the thickness of the matrix at the intersegmental borders, where the tips of the elongated myocytes are inserted, increases dramatically (asterisks; Fig. 5C, D). This corresponds to the normal pattern of tenascin matrix growth in embryos developing in utero (Deries et al., 2012). Thus, our data reveal that the explants keep a normal temporal and spatial organization of tenascin ECM during the 12 h of culture. In addition, other ECMs (namely laminins and fibronectin) were analyzed revealing that they also develop normally during culture of the explant tissue (data not shown). All these data corroborate to demonstrate that our method does not interfere with tissue intrinsic cell–ECM interactions, since both skeletal muscle and its ECM develop normally when cultured using this system.

3. Discussion

Mammalian embryos are by essence complicated to manipulate during their development. Consequently, a large proportion of experiments on mammalian embryos have been restricted to the mouse and are done resorting to gene targeting methodologies in embryonic stem cells or zygotes, followed by the development of the manipulated cells/embryos in utero. These methodologies are generally very powerful, but have the disadvantage of being both costly and time-consuming. Moreover, sometimes gene ablations or insertions can unexpectedly produce different results in gene expression or protein function (Mourikis et al., 2012; Yutzey and Robins, 2007) and thus the large investment made is not a guarantee of success. Cell culture has been used for over a century and has contributed vastly towards increasing our knowledge on cell and molecular biology. Furthermore, the culture and differentiation of embryonic cells has provided a multitude of essential data that have greatly advanced our understanding of mammalian developmental biology (Solter, 2006). However, the complexity of the embryo, including potential interactions between different cell types (e.g. Rios et al., 2011; Van Ho et al., 2011) and between cells and their surrounding ECMs (e.g. Blaess et al., 2004; Bajanca et al., 2006) cannot easily be achieved in these systems.

The best way to keep the in vivo environment of embryonic cells in culture is of course to grow the whole embryo. This has been achieved with good results for post-implantation embryos collected at E7.5–E11.5 and cultured for periods between 36 and 72 h, depending on the starting stage (up to 72 h for the earliest stages and down to a maximum of 36 h for E11.5; Cockroft, 1990; Takahashi et al., 2008). However, this technique has the disadvantages that embryos are cultured in a non-defined medium, pure rat serum, and specific embryo culture equipment is required (Cockroft, 1990; Takahashi et al., 2008).

In this work we describe a simple but efficient method of culturing mouse embryo explants which maintains the 3D organization of the tissues, including their ECM. Using axial deep back muscle development as an illustration, we show that the cultured tissues are able to develop in a healthy way with normal morphology and morphogenesis. Moreover, we have successfully cultured explants derived from embryos ranging from E8.0 to E12.5 using this method demonstrating that this technique is versatile. In addition, it may be particularly suitable as an alternative for studying developing tissues of mid-gestation stage embryos, which are difficult to culture using whole embryo culture (Cockroft, 1990; Takahashi et al., 2008).

A major advantage of this method is that we use a defined culture medium, without any serum supplement. Serum contains undefined components such as growth factors, growth inhibitors as well as the ECM component, fibronectin, which can all influence the behavior and differentiation status of cells (Freshney, 2000). To avoid these uncharacterized factors, our protocol uses a complex medium (DMEM/F12 Glutamax medium) which is a medium rich in vitamins and amino acids, specifically designed to culture cells without serum (Barnes and Sato, 1980) and we add pyruvate as an extra carbon source (Webb et al., 2002). Furthermore, the controlled environment of a defined medium is highly suitable for experiments aimed at blocking or activating developmental signaling pathways. For example, we have successfully used function-blocking antibodies to the α6 integrin subunit to block the binding of the α6β1 integrin to laminin in explants of E9.5 embryos (Bajanca et al., 2006; Fournier-Thibault et al., 2009). Our serum-free culture method is also useful to study the role of paracrine

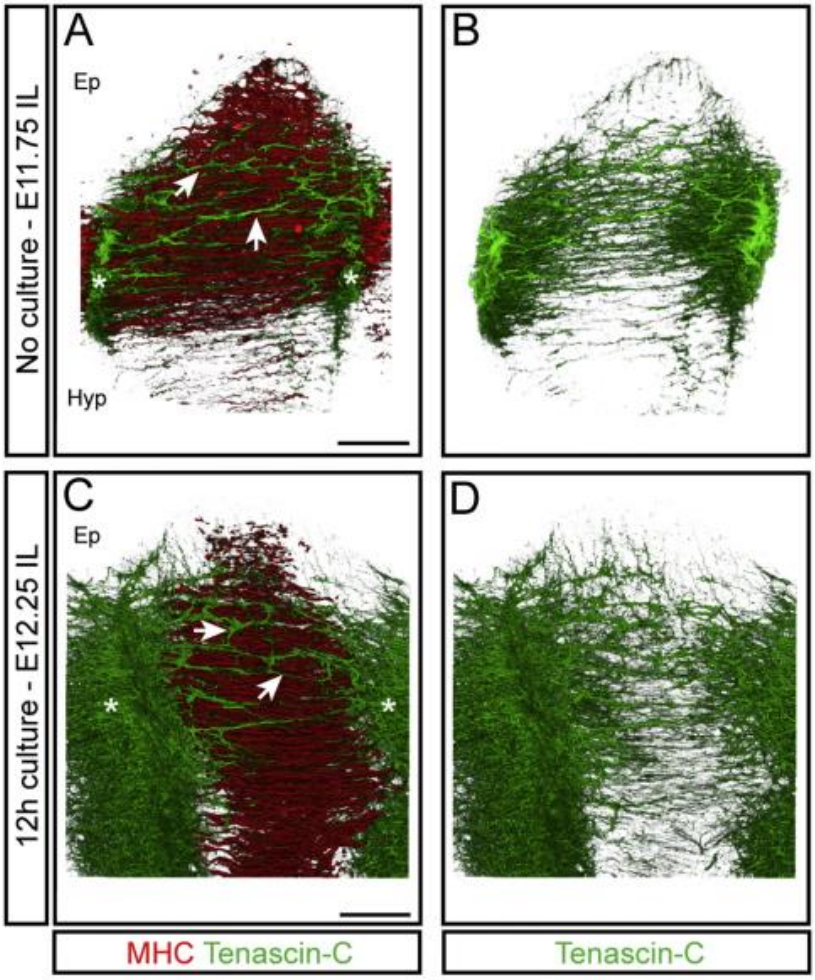

Fig. 5. The tenascin ECM of deep back muscles grows with the muscles during the 12 h culture period. Lateral views of 3D reconstructions of interlimb myotomes of E11.75 embryos fixed before culture (A, B) and E11.75 embryos cultured for 12 h (C, D). Antibodies against MHC (red, A, C) and tenascin-C (green, A–D) were used to immunolabel embryos and explants. In all images, the epaxial (Ep, dorsal) side is upwards and the hypaxial (Hyp, ventral) side downwards. A–B: Tenascin ECM is abundant at the intersegmental borders of E11.75 non-cultured embryos (asterisks in A), where tenascin cables emerge to extend throughout the whole myotome (arrows in A). C–D: After 12 h of culture, the tenascin matrix at the intersegmental borders has grown extensively with the muscle masses and fibers are now thicker (asterisks in C). The cables extending through the myotome are both denser and more numerous (arrows in C). Scale bars: 50 μm.

signaling pathways in developmental events by incubating explants with drugs blocking these pathways and/or by adding certain paracrine factors, their antagonists or agonists to the culture medium. The fact that the drug/protein is added to the whole embryo explant can be considered as a downside of the method. However, since the explants are easily accessible, it is possible to deliver specific molecules on beads and place them in precise locations to restrict their action to a certain region of the explant, a technique frequently used in chick embryo explant culture (e.g. Lorda-Diez et al., 2010; Sheeba et al., 2012).

Globally, apoptosis levels are slightly higher in cultured versus in utero developing tissues. Cell proliferation, tissue morphology and morphogenetic movements are, however, normal after 12 h of culture, and comparable to those of embryos developing in utero. These developmentally normal changes in tissue morphology that occur during the culture period strongly indicate that the three basic processes of development, cell proliferation, differentiation and morphogenesis, occur correctly in time and space within the explants. Nevertheless we consider that a 12 h culture period as being the maximum advisable culture period, at least from the stage E11.75, under the described serum-free conditions. It is possible that younger embryos can be cultured for longer periods, as is the case for whole embryo culture (Cockroft, 1990; Takahashi et al., 2008). In fact, we have cultured E9.5 embryos for up to 24 h with good results (Bajanca et al., 2006). To ensure that culture conditions are satisfactory, we nevertheless recommend that apoptosis levels be assessed for each experimental setup. Finally, it is likely that adding serum to the medium increases the usable time-frame of culture. This may be advisable in certain experimental situations, but would also remove the advantages of having a defined culture medium.

Our culture method is very simple and quick to perform allowing the study of in vivo mouse embryo development more

Figure 2.5: The tenascin ECM of deep back muscles grows with the muscles during the 12h culture period.

easily than by any other experimental method currently in use. It does not need a big investment, using only basic embryo dissection and cell culture equipment. The method can be used for several post-implantation stages and a relatively large number of embryos can be cultured at once, with different treatments, permitting several replicates, as is necessary when performing functional studies through the use of chemical inhibitors or activators of signaling pathways. In fact, since it is simple and effective, this culture method can also be used for pilot experiments to validate experimental strategies before a gene targeting methodology is applied.

4. Conclusion

In conclusion, our mouse embryo explant culture method not only allows the manipulation and culture of explants in a very efficient way, but also enables the experimental analysis of in vivo developmental events ranging from molecular pathways to actors of morphogenesis in a controlled environment. Explants grown under these conditions simulate real developmental events which occur in utero, including the morphogenesis of the cultured tissue and its extracellular matrix.

Acknowledgments

We thank present and past members of our group, in particular Gabriela Rodrigues, Luís Marques, Raquel Vaz and Fernanda Bajanca, for their contributions in different phases of this study. We also thank Arnoud Sonnenberg for the LAT-2 antibody. The MF20 and F5D antibodies were developed by DA Fischman and WE Wright, respectively, and were obtained from the Developmental Studies Hybridoma Bank, developed under the auspices of the NICHD and maintained by the University of Iowa, Department of Biology, Iowa City, IA52242, USA. This study was financed by Fundação para Ciência e Tecnologia (FCT, Portugal) project PTDC/SAU-BID/120130/2010 and PEst-OE/BIA/UI0329/2011. ABG and MD were supported by fellowships SFRH/BD/90827/2012 and SFRH/BPD/65370/2009 from FCT.

References

Allamand, V., Campbell, K.P., 2000. Animal models for muscular dystrophy: valuable tools for the development of therapies. Hum. Mol. Genet. 9, 2459–2467. http://dx.doi.org/10.1093/hmg/9.16.2459.

Bajanca, F., Luz, M., Raymond, K., Martins, G.G., Sonnenberg, A., Tajbakhsh, S., Buckingham, M., Thorsteinsdóttir, S., 2006. Integrin α6β1-laminin interactions regulate early myotome formation in the mouse embryo. Development 133, 1635–1644. http://dx.doi.org/10.1242/dev.02336.

Barnes, D., Sato, G., 1980. Methods for growth of cultured cells in serum-free medium. Anal. Biochem. 102, 255–270. http://dx.doi.org/10.1016/0003-2697(80)90151-7.

Blaess, S., Graus-Porta, D., Belvindrah, R., Radakovits, R., Pons, S., Littlewood, E., Senften, M., Guo, H., Li, Y., Miner, J.H., Reichardt, L.F., Müller, U., 2004. β1-integrins are critical for cerebellar granule cell precursor proliferation. J. Neurosci. 24, 3402–3412. http://dx.doi.org/10.1523/JNEUROSCI.5241-03.2004.

Bedell, M.A., Jenkins, N.A., Copeland, N.G., 1997. Mouse models of human disease. Part I: techniques and resources for genetic analysis in mice. Genes. Dev. 11, 1–10. http://dx.doi.org/10.1101/gad.11.1.1.

Bianco, P., Robey, P.G., Simmons, P.J., 2008. Mesenchymal stem cells: revisiting history, concepts and assays. Cell Stem Cell 2, 313–319. http://dx.doi.org/10.1016/j.stem.2008.03.002.

Bolker, J.A., 1995. Model systems in developmental biology. BioEssays 17, 451–455. http://dx.doi.org/10.1002/bies.950170513.

Bradley, A., 2002. Mining the mouse genome: we have the draft sequence-but how do we unlock its secrets? Nature 420, 512–514. http://dx.doi.org/10.1038/420512a.

Bueno, D., Skinner, J., Abud, H., Heath, J.K., 1996. Spatial and temporal relationships between Shh, Fgf4, and Fgf8 gene expression at diverse signalling centers during mouse development. Dev. Dyn. 207, 291–299. http://dx.doi.org/10.1002/(SICI)1097-0177(199611)207:3<291::AID-AJA6>3.0.CO;2-C.

Capecchi, M.R., 2005. Gene targeting in mice: functional analysis of the mammalian genome for the twenty-first century. Nat. Rev. Genet. 6, 507–512. http://dx.doi.org/10.1038/nrg1619.

Carrel, A., 1912. On the permanent life of tissues outside of the organism. J. Exp. Med. 15, 516–528. http://dx.doi.org/10.1084/jem.15.5.516.

Carrel, A., Burrows, M.T., 1911. Cultivation of tissues in vitro and its technique. J. Exp. Med. 13, 387–396. http://dx.doi.org/10.1084/jem.13.3.387.

Cockroft, D.L., 1990. Dissection and culture of postimplantation embryos. In: Copp, A.J., Cockroft, D.L. (Eds.), Postimplantation Mammalian Embryos: A Practical Approach. IRL Press, Oxford, pp. 15–40.

Crossin, K.L., 1986. Site-restricted expression of cytotactin during development of the chicken embryo. J. Cell Biol. 102, 1917–1930. http://dx.doi.org/10.1083/jcb.102.5.1917.

Deries, M., Gonçalves, A.B., Vaz, R., Martins, G.G., Rodrigues, G., Thorsteinsdóttir, S., 2012. Extracellular matrix remodeling accompanies axial muscle development and morphogenesis in the mouse. Dev. Dyn. 241, 350–364. http://dx.doi.org/10.1002/dvdy.23703.

Deries, M., Schweitzer, R., Duxson, M.J., 2010. Developmental fate of the mammalian myotome. Dev. Dyn. 239, 2898–2910. http://dx.doi.org/10.1002/dvdy.22425.

Edmondson, R., Broglie, J.J., Adcock, A.F., Yang, L., 2014. Three-dimensional cell culture systems and their applications in drug discovery and cell-based biosensors. Assay. Drug Dev. Technol. 12, 207–218. http://dx.doi.org/10.1089/adt.2014.573.

Elder, G.A., Sosa, M.A.G., De Gasperi, R., 2010. Transgenic mouse models of Alzheimer's disease. Mt. Sinai J. Med. 77, 69–81. http://dx.doi.org/10.1002/msj.20159.

Ellington, S.K.L., 1991. Use of embryo culture to study development and developmental mechanisms. Reprod. Toxicol. 5, 229–235. http://dx.doi.org/10.1016/0890-6238(91)90056-l.

Evans, M.J., Kaufman, M.H., 1981. Establishment in culture of pluripotential cells from mouse embryos. Nature 292, 154–156. http://dx.doi.org/10.1038/292154a0.

Feuer, S., Rinaudo, P., 2012. Preimplantation stress and development. Birth Defects Res. C. Embryo Today 96, 299–325. http://dx.doi.org/10.1002/bdrc.21022.

Fournier, M.V., Martin, K.J., 2006. Transcriptome profiling in clinical breast cancer: from 3D culture models to prognostic signatures. J. Cell Physiol. 209, 625–635. http://dx.doi.org/10.1002/jcp.20787.

Fournier-Thibault, C., Blavet, C., Jarov, A., Bajanca, F., Thorsteinsdóttir, S., Duband, J. L., 2009. Sonic Hedgehog regulates integrin activity, cadherin contacts, and cell polarity to orchestrate neural tube morphogenesis. J. Neurosci. 29, 12506–12520. http://dx.doi.org/10.1523/jneurosci.2003-09.2009.

Freshney, R.I., 2000. Culture of Animal Cells-a Manual of Basic Technique, fourth ed. Wiley-Liss, New York.

Jenner, R.A., Wills, M.A., 2007. The choice of model organisms in evo–devo. Nat. Rev. Genet. 8, 311. http://dx.doi.org/10.1038/nrg2062.

Karpas, A., Dremucheva, A., Czepulkowski, B.H., 2001. A human myeloma cell line suitable for the generation of human monoclonal antibodies. Proc. Natl. Acad. Sci. USA 98, 1799–1804. http://dx.doi.org/10.1073/pnas.98.4.1799.

Khalil, H., Peltzer, N., Walicki, J., Yang, J.Y., Dubuis, G., Gardiol, N., Held, W., Bigliardi, P., Marsland, B., Liaudet, L., Widmann, C., 2012. Caspase-3 protects stressed organs against cell death. Mol. Cell. Biol. 32, 4523–4533. http://dx.doi.org/10.1128/mcb.00774-12.

Lorda-Diez, C.I., Montero, J.A., Garcia-Porrero, J.A., Hurle, J.M., 2010. *Tgfβ2* and *3* are coexpressed with their extracellular regulator *Ltbp1* in the early limb bud and modulate mesodermal outgrowth and BMP signaling in chicken embryos. BMC Dev. Biol. 10, 69–78. http://dx.doi.org/10.1186/1471-213X-10-69.

Martins, G.G., Rifes, P., Amândio, R., Rodrigues, G., Palmeirim, I., Thorsteinsdóttir, S., 2009. Dynamic 3D cell rearrangements guided by a fibronectin matrix underlie somitogenesis. Plos. ONE 4, e7429. http://dx.doi.org/10.1371/journal.pone.0007429.

Masters, J.R., 2002. HeLa cells 50 years on: the good, the bad and the ugly. Nat. Rev. Cancer 2, 315–319. http://dx.doi.org/10.1038/nrc775.

Mazzoleni, G., Di Lorenzo, D., Steimberg, N., 2009. Modelling tissues in 3D: the next future of pharmaco-toxicology and food research? Genes. Nutr. 4, 13–22. http://dx.doi.org/10.1007/s12263-008-0107-0.

Miller, J.B., Everitt, E.A., Smith, T.H., Block, N.E., Dominov, J.A., 1993. Cellular and molecular diversity in skeletal muscle development: news from in vitro and in vivo. BioEssays 15, 191–196. http://dx.doi.org/10.1002/bies.950150308.

Mourikis, P., Gopalakrishnan, S., Sambasivan, R., Tajbakhsh, S., 2012. Cell-autonomous Notch activity maintains the temporal specification potential of skeletal muscle stem cells. Development 139, 4536–4548. http://dx.doi.org/10.1242/dev.084756.

Muñoz-Espín, D., Cañamero, M., Maraver, A., Gómez-López, G., Contreras, J., Murillo-Cuesta, S., Rodríguez-Baeza, A., Varela-Nieto, I., Ruberte, J., Collado, M., Serrano, M., 2013. Programmed cell senescence during mammalian embryonic development. Cell 155, 1104–1118. http://dx.doi.org/10.1016/j.cell.2013.10.019.

Murry, C.E., Keller, G., 2008. Differentiation of embryonic stem cells to clinically relevant populations: lessons from embryonic development. Cell 132, 661–680. http://dx.doi.org/10.1016/j.cell.2008.02.008.

Nabeshima, Y., Hanaoka, K., Hayasaka, M., Esumi, E., Li, S., Nonaka, I., Nabeshima, Y., 1993. Myogenin gene disruption results in perinatal lethality because of severe muscle defect. Nature 364, 532–535. http://dx.doi.org/10.1038/364532a0.

Ordahl, C.P., Berdougo, E., Venters, S.J., Denetclaw, W.F., 2001. The dermomyotome dorsomedial lip drives growth and morphogenesis of both the primary myotome and dermomyotome epithelium. Development 128, 1731–1744. http://dx.

doi.org/10.1186/1471-213X-13-37.
Ormandy, E.H., Dale, J., Griffin, G., 2011. Genetic engineering of animals: ethical issues, including welfare concerns. Can. Vet. J. 52, 544–550.
Palmeirim, I., Henrique, D., Ish-Horowicz, D., Pourquié, O., 1997. Avian hairy gene expression identifies a molecular clock linked to vertebrate segmentation and somitogenesis. Cell 91, 639–648. http://dx.doi.org/10.1016/s0092-8674(00)80451-1.
Petersen, P.H., Tang, H., Zou, K., Zhong, W., 2006. The enigma of the Numb–Notch relationship during mammalian embryogenesis. Dev. Neurosci. 28, 156–168. http://dx.doi.org/10.1159/000090761.
Pittenger, M.F., 1999. Multilineage potential of adult human mesenchymal stem cells. Science 284, 143–147. http://dx.doi.org/10.1126/science.284.5411.143.
Ravi, M., Paramesh, V., Kaviya, S.R., Anuradha, E., Solomon, F.D.P., 2014. 3D cell culture systems: advantages and applications. J. Cell. Physiol. 230, 16–26. http://dx.doi.org/10.1002/jcp.24683.
Rios, A.C., Serralbo, O., Salgado, D., Marcelle, C., 2011. Neural crest regulates myogenesis through the transient activation of NOTCH. Nature 473, 532–535. http://dx.doi.org/10.1038/nature09970.
Sheeba, C.J., Andrade, R.P., Palmeirim, I., 2012. Joint interpretation of AER/FGF and ZPA/SHH over time and space underlies hairy2 expression in the chick limb. Biol. Open 1, 1102–1110. http://dx.doi.org/10.1242/bio.20122386.
Solter, D., 2006. From teratocarcinomas to embryonic stem cells and beyond: a history of embryonic stem cell research. Nat. Rev. Genet. 7, 319–327. http://dx.doi.org/10.1038/nrg1827.
Takahashi, M., Nomura, T., Osumi, N., 2008. Transferring genes into cultured mammalian embryos by electroporation. Dev. Growth Differ. 50, 485–497. http://dx.doi.org/10.1006/meth.2001.1154.
Tam, P.P.L., Behringer, R.R., 1997. Mouse gastrulation: the formation of a mammalian body plan. Mech. Dev. 68, 3–25. http://dx.doi.org/10.1016/S0925-4773(97)00123-8.
Van Ho, A.T., Hayashi, S., Bröhl, D., Auradé, F., Rattenbach, R., Relaix, F., 2011. Neural crest cell lineage restricts skeletal muscle progenitor cell differentiation through neuregulin1-ErbB3 signaling. Dev. Cell 21, 273–287. http://dx.doi.org/10.1016/j.devcel.2011.06.019.
Webb, D.J., Asmussen, H., Murase, S., Horwitz, A.F., 2002. Cell migration in slice cultures. In: Adams, J.C. (Ed.), Methods in Cell–Matrix Adhesion. Academic Press, San Diego, pp. 341–358.
Yutzey, K.E., Robbins, J., 2007. Principles of genetic murine models for cardiac disease. Circulation 115, 792–795. http://dx.doi.org/10.1161/circulationaha.106.682534.

Chapter 3

The myotome is necessary for epaxial muscle development and provides essential cues for the maintenance of muscle stem cells

The myotome is necessary for epaxial muscle development and provides essential cues for the maintenance of muscle stem cells

André B. Gonçalves[a,b], Sólveig Thorsteinsdóttir[a,b*] and Marianne Deries[a*]
([*]equal contribution)

[a] Centro de Ecologia, Evolução e Alterações Ambientais, Faculdade de Ciências, Departamento de Biologia Animal, Universidade de Lisboa, 1749-016 Lisboa, Portugal.
[b] Instituto Gulbenkian de Ciência, 2781-901 Oeiras, Portugal.

Contribution for the publication:

	Experimental work depicted in Fig.						Manuscript writing
	3.1	3.2	3.3	3.4	3.5	3.6	
Design and concept	I	III	III	III	III	III	III
Execution	III	III	III	III	III	III	
Analysis and interpretation	III	III	III	III	III	III	

	Experimental work depicted in Sup. Fig.		Manuscript writing
	S3.1	S3.2	
Design and concept	III	III	III
Execution	III	III	
Analysis and interpretation	III	III	

Legend:

- ..... non-applicable
O ..... no intervention
I ..... minor contribution
II ..... moderate contribution
III .... major contribution/full execution

Note: this contribution does not exclude other contributions, similar or not, from the remaining authors

Abstract

Myogenesis in the embryo starts with the formation of the epaxial myotome, which later gives rise to the epaxial (deep back) muscles. The differentiation of the epaxial myotome is initially driven by the myogenic regulatory factors Myf5 and Mrf4 and consequently, when these transcription factors are absent, epaxial myogenesis is delayed. However, it is presently unclear whether the observed delay affects the normal development of the epaxial muscle groups and, if so, in what way.

Here, we address this question using *Myf5*$^{nlacZ/nlacZ}$ mouse embryos in which trunk myogenesis is initiated after a two-day delay, through the Myf5/Mrf4-independent activation of MyoD. Remarkably, our data show that in *Myf5*$^{nlacZ/nlacZ}$ embryos, epaxial myotome development is skipped altogether. When myogenesis is activated, muscle stem cells (MuSCs) only differentiate in the dorsal-most region of the segments, leading to the development of one epaxial muscle group, the transversospinalis, which does not go through a myotome stage. In contrast, the three remaining epaxial muscle groups never form. Moreover, when the dissociation of the central dermomyotome releases proliferating MuSCs into the myotomal space, the Pax7-positive MuSCs that enter the area where the myotome is missing lose their myogenic identity, suggesting that cues from the myotome may be required to maintain their myogenic potential. Consistent with this hypothesis, blocking fibroblast growth factor signalling (through Fgfr1 or Fgfr4) in wild type embryo explants leads to a significant reduction in the number of Pax3- and Pax7-positive MuSCs indicating a role for myotomal Fgfs in maintaining these cells.

We conclude that normal epaxial muscle development requires the formation of the epaxial myotome and that Fgfs secreted by the differentiated myotome seem to provide crucial cues for the maintenance of MuSCs upon central dermomyotome dissociation. Our data also suggest that the development of the epaxial-most muscle, the transversospinalis, differs from that of the three remaining groups.

Keywords: Muscle development, Epaxial muscles; Muscle stem cells; Pax7; Pax3; Myf5; Mrf4; MyoD; Myotome; Fibroblast growth factors; Mouse embryo.

Introduction

The segmented myotomes are the first differentiated skeletal muscles in vertebrate embryos (Buckingham, 2006; Christ et al., 2007; Devoto et al., 2006; Ikeda et al., 1968; Williams, 1910). They develop from the somites, transient mesodermal segments that form in pairs on both sides of the neural tube and notochord (Christ et al., 2007; Pourquié, 2001; Stickney et al., 2000). The myotomes are the first, and most dominant, somite derivatives to develop in anamniotes and incremental growth of the myotomes originates their definitive trunk musculature (Rescan, 2008; Scaal and Wiegreffe, 2006). In contrast, in amniotes, the myotome only starts forming after the separation of the embryonic somite into the dorsal epithelial dermomyotome and the ventral mesenchymal sclerotome (Pownall et al., 2002; Scaal and Christ, 2004; Spörle, 2001). The amniote dermomyotome, which expresses the transcription factors Pax3 and/or Pax7, gives rise to the progenitors of all skeletal muscles in the trunk and limbs while also contributing cells to the dorsal dermis, brown fat, and some endothelial and smooth muscle cells (Deries and Thorsteinsdóttir, 2016; Kalcheim, 2015; Tajbakhsh, 2009). Sclerotomal cells on the other hand, express Pax1 and Pax9 and originate the axial skeleton and associated tendons (Christ et al., 2007).

Myotome formation in amniotes starts when cells originating from the epaxial (dorso-medial) lip of the dermomyotome epithelium delaminate and differentiate into elongated mononucleated myocytes that span the full segment parallel to the neural tube (Denetclaw et al., 1997; Gros et al., 2004; Kahane et al., 1998; Venters et al., 1999;). Moreover, at certain axial levels, cells from the hypaxial (ventro-lateral) lip delaminate and migrate e.g. to the limbs where muscle differentiates away from the somites (Buckingham, 2003). Subsequently, in the trunk, waves of dermomyotomal cells from all four lips of the dermomyotome contribute to the growth of the myotome (Gros et al., 2004; Spörle, 2001; Venters et al., 1999). Then the dermomyotome dissociates and releases Pax3- and/or Pax7-positive muscle stem cells (MuSCs) into the myotome (Ben-Yair and Kalcheim, 2005; Gros et al., 2005; Kassar-Duchossoy et al., 2005; Relaix et al., 2005). These Pax3- and/or Pax7-positive MuSCs either differentiate and fuse with each other or existing myocytes or stay undifferentiated and give rise to the MuSCs of later developmental stages, including the satellite cells of adult muscles (Kassar-Duchossoy et al., 2005; Relaix et al., 2005). Thus, although the myocytes of the segmented amniote myotome contribute to the definitive axial musculature (Cinnamon et al., 1999; Deries et al., 2010), their contribution is much more modest than that observed for the myocytes of the

anamniote myotome (Scaal and Wiegreffe, 2006). Given that myogenesis can occur in the absence of a myotome (e.g. in the limbs), the question arises whether the formation of the segmented myotomes is a prerequisite for normal axial muscle development in amniotes.

Myogenic determination and differentiation are controlled by four myogenic regulatory factors (MRFs): Myf5, Mrf4 (also called Myf6), MyoD and Myogenin (Buckingham and Rigby, 2014). Inactivation of these transcription factors in mice revealed that specification of the myogenic lineage is driven by Myf5, Mrf4 and/or MyoD (Kassar-Duchossoy et al., 2004; Kaul et al., 2000; Rudnicki et al., 1993) and Myogenin is crucial for myoblast terminal differentiation and the formation of myotubes (Hasty et al., 1993; Nabeshima et al., 1993). During myotome formation in the mouse embryo, Myf5, Mrf4 and MyoD have distinct spatiotemporal expression patterns. Myf5 is the first MRF to be expressed and its activation in the epaxial lip of the dermomyotome triggers myogenesis and the subsequent activation of Myogenin (and/or Mrf4 and Myogenin) leading to the formation of the epaxial myotome (Gros et al., 2004; Kassar-Duchossoy et al., 2004; Spörle, 2001; Venters et al., 1999). MyoD is expressed considerably later during axial myogenesis in the mouse, first in cells entering the myotome from the hypaxial dermomyotome and eventually in differentiating myoblasts within the whole myotome (Sassoon et al., 1989; Smith et al., 1994; Venters et al., 1999). In contrast, during limb myogenesis, after Pax3-positive MuSCs have reached their destination, Myf5 and MyoD activation occurs almost simultaneously (Ott et al., 1991; Sassoon et al., 1989).

While myogenesis in the limbs proceeds normally in mouse embryos lacking expression of Myf5 and Mrf4, trunk myogenesis in these embryos is delayed (Braun and Arnold, 1995; Kablar et al., 1997; Kassar-Duchossoy et al., 2004; Tajbakhsh et al., 1996, 1997). In fact, MyoD expression is delayed compared to control embryos, indicating that the earliest MyoD expression depends on Myf5/Mrf4, but then a later Myf5/Mrf4-independent activation of MyoD in first the ventral and then the dorsal dermomyotomal lips triggers trunk myogenesis (Tajbakhsh et al., 1997). This delay in myotome formation has been shown to impact sclerotome development, as fibroblast growth factors (Fgfs) and platelet-derived growth factors (Pdgfs) from the myotome are needed for timely syndetome (Brent et al., 2005) and rib (Vinagre et al., 2010) development. Moreover, in the chick, Fgf8 from the myotome has been shown to be required for the dissociation of the central dermomyotome (Delfini et al., 2009). However, although some perturbations in deep back muscle development have been noted in the mouse (Kassar-Duchossoy et al., 2004; Tajbakhsh and Buckingham, 2000) it is unclear whether, and if so how, the observed delay in trunk myogenesis in Myf5/Mrf4 mutants impacts axial muscle development.

To clarify whether the Myf5/Mrf4-dependent myotome is required for normal axial muscle development in the mouse, we performed a detailed analysis of muscle development in *Myf5*$^{nlacZ/nlacZ}$ mouse embryos (Tajbakhsh et al., 1996), which are functional double knock-outs for *Myf5* and *Mrf4* (Kassar-Duchossoy et al., 2004). We show that epaxial muscle morphogenesis is severely affected in these mutants, in that three out of the four epaxial muscle groups fail to form. The dorsal-most epaxial muscle group, the transversospinalis, is the only group to develop in *Myf5*$^{nlacZ/nlacZ}$ embryos and, remarkably, it forms without going through a myotome stage. Moreover, our results demonstrate that the MuSCs that normally contribute to the formation of the three missing epaxial muscles (longissimus, iliocostalis and levatores costarum) fail to maintain their MuSC identity when the central dermomyotome dissociates. We further show that blocking Fgfr1 or Fgfr4 activity in wild-type mouse embryo explants leads to a severe decrease in the number of both Pax7- and Pax3-positive MuSCs, indicating that in *Myf5*$^{nlacZ/nlacZ}$ embryos, the maintenance of MuSC identity may be dependent on Fgfs secreted by the differentiated cells of the Myf5/Mrf4-dependent epaxial myotome.

Experimental procedures

Mice, embryo collection and phenotyping

Myf5^{nlacZ} (C57BL/6J) mice have a *nlacZ-neo* cassette insertion replacing the coding sequence of the endogenous *Myf5* locus (Tajbakhsh and Buckingham, 1994). Due to its proximity to *Myf5* within the same locus, *Mrf4* expression is directly affected in *Myf5*$^{nlacZ/nlacZ}$ embryos. Therefore, *Myf5*$^{nlacZ/nlacZ}$ embryos are functional double-knockouts for both *Myf5* and *Mrf4* (Kassar-Duchossoy et al., 2004). Explant culture experiments were performed with mouse embryos obtained from outbred Hsd:ICR mice (CD-1; Charles River Laboratories International, Inc.). Heterozygous *Myf5*$^{+/nlacZ}$ mice or outbred CD-1 mice were crossed and dated pregnancies were obtained with the day of the vaginal plug defined as embryonic day 0.5 (E0.5). Pregnant females were sacrificed by cervical dislocation after isoflurane anaesthesia.

Embryos from heterozygous *Myf5*$^{+/nlacZ}$ crossings were phenotyped by staining cervical somites to detect the β-galactosidase activity as described in Hogan et al. (1986) with minor modifications. Briefly, all embryos were collected in phosphate buffer saline (PBS) and decapitated. The neck regions, containing the cervical somites of each embryo, were incubated overnight (O/N) in a 0.5 mg/ml X-Gal (5-bromo-4-chloro-3-indolyl-β-D-galactoside), 5 mM

potassium ferricyanide, and 5 mM potassium ferrocyanide staining solution at 37 °C. Wild type embryos remained unstained, while *Myf5*$^{+/nlacZ}$ and *Myf5*$^{nlacZ/nlacZ}$ somites stained blue. *Myf5*$^{nlacZ/nlacZ}$ somites are clearly distinguishable from *Myf5*$^{+/nlacZ}$ somites in that X-Gal-positive cells are blocked in the dermomyotomal lips and do not form a myotome (Tajbakhsh and Buckingham, 2000).

To precisely define the different stages of dermomyotome and myotome development in our study, we used a recently described DMM stage system (Deries et al., 2012) when describing our observations.

All experiments and manipulations conducted on animals including housing, husbandry and welfare were performed according to the recommended guidelines provided by Direção Geral de Alimentação e Veterinária (DGAV) and approved through protocol 3/2016 from the Animal Welfare Body (ORBEA) of the Faculty of Sciences of the University of Lisbon.

In situ hybridisation

For whole mount *in situ* hybridisation, embryos were fixed in 4% paraformaldehyde (PFA) in PBS containing 0.05% of diethyl pyrocarbonate (PBS-DEPC) O/N at 4°C. They were then washed in PBT-DEPC (PBS-DEPC with 1% Tween 20), dehydrated in a gradient of methanol and stored at -20°C. Whole mount *in situ* hybridisation was performed as described in Bajanca et al. (2004). Proteinase K (Roche; 10 µg/ml PBS) digestion treatment was 25 min for E10.5 embryos, 35 min for E11.0 embryos, 45 min for E11.5 embryos and 75 min for E12.5 embryos. Chromogenic detection of DIG-labelled riboprobes was performed with 4-Nitro blue tetrazolium chloride (NBT, Roche; 450 µg/ml PBT) and 5-bromo-4-chloro-3-indolyl-phosphate, 4-toluidine salt (BCIP, Roche; 175 µg/ml PBT). Tissues were then washed in PBS, immediately processed for cryoembedding in sucrose and gelatine (Bajanca et al., 2004) and stored at -80°C until sectioning in a Leica CM1860 UV cryostat.

For *in situ* hybridisation on sections, embryos were fixed in 4% PFA in PBS-DEPC O/N at 4°C, washed in PBS-DEPC and processed for cryoembedding as described above. The hybridisation was then performed as described in Gomes de Almeida et al. (2016). After staining, slides were mounted in Aquatex (Merck Millipore).

Antisense probes used in this study were mouse *Myod1* (Sassoon et al., 1989), *Pax3* (Tajbakhsh et al., 1997), *Pax7* (Jostes et al., 1990), *Fgf6* (Han and Martin et al., 1993), *Fgfr1*

(Yamaguchi et al., 1992), *Fgfr4* (Stark et al., 1991), *Pdgfrα* (Orr-Urtreger and Lonai, 1992) and *Pdgfa* (Mercola et al., 1990).

Immunohistochemistry

For immunohistochemistry on sections, all tissues were fixed in 0.2% PFA in PBS O/N at 4°C, washed in PBS and processed for cryoembedding as described above. The skin of E16.5 foetuses was removed before fixation to improve the penetration of the tissues. Immunohistochemistry was performed as previously described in Bajanca et al. (2004) with minor modifications. Briefly, after drying followed by two PBS washes, cryosections were blocked for 20 min in 1% or 5% bovine serum albumin (for embryos and foetuses, respectively) in PBS at room temperature (RT). Primary antibodies were incubated O/N at 4°C and secondary antibodies for 2 hours at RT. All antibodies were diluted in the previously described blocking solutions. Cryosections were counterstained with 4,6-diamidine-2-phenylidole-dihydrochloride (DAPI, 5 µg/ml in PBS with 0.1% Triton X-100). Sections were mounted in 5 mg/ml propyl gallate in glycerol/PBS (9:1) with 0.01% azide and the coverslips sealed with nail varnish.

Whole mount immunohistochemistry was performed as described in Gonçalves et al. (2016). The diaphanization of the tissues was performed according to Martins et al. (2009).

Primary and secondary antibodies used in this work are listed in Table 3.1. We used a polyclonal antibody raised against laminin-111, which we designate pan-muscle laminin antibody, because it detects all laminin isoforms containing either the α1-, β1- or γ1 chains. Since all laminin isoforms present in developing skeletal muscle contain at least the γ1 chain (Patton et al., 1997), this antibody was sometimes used to identify skeletal muscle masses in sectioned embryos and foetuses.

Explant Culture

Litters of E10.75 CD-1 embryos were collected in PBS containing 0.9 mM $CaCl_2$ and 0.5 mM $MgCl_2$. Embryo explants were prepared and placed on top of membrane filters as previously described (Gonçalves et al. 2016) followed by culture for 12 hours in the presence of Fgfr and/or Pdgfr inhibitors or with an equal amount of the vehicle, dimethyl sulfoxide (DMSO), diluted in the culture medium. The names, specificity and concentrations of the inhibitors used in explant culture experiments are displayed in Table 3.2**.** After culture, explants were washed in PBS-DEPC and processed for immunohistochemistry or *in situ* hybridisation

as described above. The developmental stages occurring in culture (i.e. E10.75 + twelve hours) include the normal entry of central dermomyotome-derived cells into the myotome (i.e. DMM stage 3 to 4; Buckingham, 2006; Deries et al., 2012). The health of each explant was assessed after culture and dead or abnormally developed explants were excluded from the analysis. Moreover, since developmental variabilities can be observed between littermates, we established a morphological criterion, based on counting somite pairs and using morphological markers characteristic of the desired stage (e.g. limb bud morphology and the length of the explant; Kaufman, 1992) at the beginning (E10.75) and the end (E11.25) of culture. Embryos that were younger or older than this established developmental stage were not included in the analyses.

Table 3.1: Primary and secondary antibodies used for immunohistochemistry on sections (IHC) and in whole mount immunohistochemistry (WMIHC).
DSHB: Developmental Studies Hybridoma Bank.

Antibody type	Antibody name	Company/ Catalogue	Dilution
Primary antibodies	Cleaved caspase-3 (Asp-175)	Cell Signalling Technology (9661)	1:800 (IHC)
	Myosin heavy chain (MHC)	DSHB (MF20)	1:400 (IHC); 1:100 (WMIHC)
	MyoD	Gift from J. Harris	1:200 (IHC); 1:100 (WMIHC)
	Myogenin (M-225)	Santa Cruz Biotechonolgy (sc-576)	1:200 (IHC)
	Laminin	Sigma (L9393)	1:400 (IHC)
	Pax3	DSHB (Pax3)	Supernatant (1:20; IHC)
	Pax7	DSHB (Pax7)	1:100 (IHC)
	Phospho-histone H3 (Ser10) (H3S10p)	Upstate (06-570)	1:800 (IHC)

(**Continues next page**)

(**Continued from previous page**)

Antibody type	Antibody name	Company/ Catalogue	Dilution
Secondary antibodies	Alexa Fluor 488- conjugated goat anti mouse IgG F(ab´)2 fragments	Life Technologies (A-11017)	1:1000 (IHC)
	Alexa Fluor 488- conjugated goat anti rabbit IgG F(ab´)2 fragments	Life Technologies (A-11070)	1:1000 (IHC); 1:500 (WMIHC)
	Alexa Fluor 568- conjugated goat anti mouse IgG F(ab´)2 fragments	Life Technologies (A-11019)	1:1000 (IHC); 1:500 (WMIHC)
	Alexa Fluor 568- conjugated goat anti rabbit IgG F(ab´)2 fragments	Life Technologies (A-21069)	1:1000 (IHC)

Table 3.2: Chemical inhibitors used in explant cultures of wild type embryos.

Compound	Source	Targets	Concentration used	References
SU5402	Calbiochem (572631)	Fgfr1; Pdgfrβ	20 µM	Mohammadi et al., 1997
PD173074	Selleckchem (S1264)	Fgfr1; Vegfr2	20 µM	Mohammadi et al., 1998
Ponatinib (AP24534)	Selleckchem (S1490)	Fgfr1; Vegfr2; Pdgfrα	20 µM	Gozgit et al., 2011
Crenolanib (CP-868596)	Selleckchem (S2730)	Pdgfrα; Pdgfrβ	20 µM	Heinrich et al., 2012
BLU9931	Selleckchem (S7819)	Fgfr4; Fgfr3	50 µM	Hagel et al., 2015
DMSO	Sigma-Aldrich (D2438)	Vehicle control	Same volume as the inhibitor	Rodríguez-Burford et al., 2003

Image analysis and quantifications

Sections processed for *in situ* hybridisation were photographed with a DFK 23U274 camera (The Imaging Source) coupled to an Olympus BX51 microscope. Images of sections processed for immunohistochemistry were acquired with a Hamamatsu Orca R2 camera coupled to an Olympus BX60 microscope with epifluorescence. Images were subsequently analysed and treated using Fiji version 1.52i. When necessary, images were stitched together using Adobe Photoshop CS5 Extended programme or the pairwise sticking Fiji plugin (Preibisch et al., 2009). Whole mount immunolabelled embryos were imaged with a Leica TCS SPE confocal microscope, producing stacks of images with a 0.5 mm z-step. Confocal z-stacks were analysed and treated with Amira v5.3.3 software (Visage Imaging Inc.). 3D surface volumes were acquired by rendering and by digital manual segmentation of raw stacks of images.

Transverse sections of mouse explants processed for immunohistochemistry were used to quantify the number of Pax3-, Pax7-, MyoD- and Myogenin-positive cells. All quantifications were performed at interlimb level and a minimum of four images (containing a transverse section of a full segment) per staining and per explant were analysed. Quantifications were performed in a blinded fashion using the Fiji plugin Cell Counter (http://imagej.net/Cell_Counter).

Statistical analyses

Normal distribution of the data obtained within each control and experimental group was assessed using Shapiro-Wilk test. To compare the number of Pax3-, Pax7-, MyoD- and Myogenin-positive cells in interlimb sections of control explants with those of explants treated with the inhibitors mentioned above, a Student´s t-test was performed. In all *a priori* and *a posteriori* performed tests, $P<0.05$ was considered as statistically significant. Statistical analyses and graph plots were performed using PAST (version 3.20) and R (version 3.5.1) software.

Results

Myf5$^{nlacZ/nlacZ}$ embryos fail to develop three of the four epaxial muscle groups

To understand whether timely myotome formation is necessary for the normal development of epaxial skeletal muscles, we analysed epaxial muscle development in *Myf5$^{nlacZ/nlacZ}$* embryos, where myotomal myogenesis is initially blocked (Tajbakhsh et al., 1996), and compared it to that of their normal heterozygous littermates. Immunohistochemistry with antibodies against myosin heavy chain (MHC) and pan-muscle laminin were used to mark differentiated myocytes and myofibres in sections or in whole mount embryos/foetuses from E11.5 to E14.5 (Fig. 3.1).

At E11.5 (DMM stage 4), the myotome of *Myf5$^{+/nlacZ}$* embryos is fully mature with extensive MHC-staining marking differentiated myocytes (Fig. 3.1A). In contrast, no MHC-positive cells are detected in *Myf5$^{nlacZ/nlacZ}$* embryos (Fig. 3.1B; Tajbakhsh et al., 1996). During normal axial muscle development, myotomal myocytes, together with the early multinucleated myotubes present at late myotomal stages, segregate and transform into the definitive epaxial and hypaxial muscles (Deries et al., 2010). At E12.5, the segregation of the epaxial muscle groups is well underway in *Myf5$^{+/nlacZ}$* heterozygous embryos and the different muscle masses are partially individualised (Fig. 3.1E). In E12.5 *Myf5$^{nlacZ/nlacZ}$* embryos, myogenesis has started (Tajbakhsh et al., 1996), but differentiated myocytes are detected only in the epaxial-most (red arrowhead; Fig. 3.1F) and in the hypaxial regions (yellow arrowhead; Fig. 3.1F). Thus, a major portion of the epaxial musculature is missing in E12.5 *Myf5$^{nlacZ/nlacZ}$* embryos (white arrowheads; Fig. 3.1F).

Epaxial or deep back muscles are composed of transversospinalis, longissimus and iliocostalis muscle groups and, at thoracic level, also levatores costarum (Sato, 1973; Smith and Hollyday, 1983). To comprehend the *Myf5$^{nlacZ/nlacZ}$* phenotype better, the morphology of the epaxial muscle masses of the mutant embryos was analysed in 3D reconstructions of MHC-stained epaxial regions at E12.5 and E13.5 and compared to that of their normal littermates (Fig. 3.1G, H, K, L). This analysis revealed that the isolated epaxial muscle mass observed in *Myf5$^{nlacZ/nlacZ}$* embryos at E12.5 has the same gross morphology and orientation as the transversospinalis of *Myf5$^{+/nlacZ}$* embryos (compare Fig. 3.1G and H), while the remaining epaxial muscles, evident in *Myf5$^{+/nlacZ}$* embryos, (Fig. 3.1G) are absent in *Myf5$^{nlacZ/nlacZ}$* embryos (Fig. 3.1H). Between E12.5 and E13.5, all epaxial muscles grow significantly, both by addition

of myonuclei to existing myocytes and fibres and by the formation of new myofibres (compare Fig. 3.1E and I; G and K). In *Myf5*$^{nlacZ/nlacZ}$ embryos, the transversospinalis muscle grows to a similar extent as observed in control embryos (compare Fig. 3.1K and L), but in contrast, longissimus, ilicostalis and levatores costarum muscles remain completely absent (compare Fig. 3.1I and J; K and L). We conclude that the single epaxial muscle mass that develops in *Myf5*$^{nlacZ/nlacZ}$ embryos corresponds to the transversospinalis muscle.

During normal muscle development, the first differentiated muscle cells to arise in the embryo are the elongated mononucleated myocytes of the myotome (Deries et al., 2010; Sieiro-Mosti et al., 2014; Venters et al., 1999). By E11.5, bi- and tri-nucleated myocytes are detected (Deries et al., 2010; Venters et al., 1999), most likely formed by the fusion of rostral and caudal-lip derived myoblasts with the mononucleated myocytes of the myotome (Sieiro-Mosti et al., 2014; Venters et al., 1999;). Then, as the central dermomyotomal sheet de-epithelializes, more and more fusion events occur in the myotome (Relaix et al., 2005; Sieiro-Mosti et al., 2014). Indeed, by E12.5, the epaxial muscle masses of *Myf5*$^{+/nlacZ}$ embryos are composed of multinucleated myocytes (arrowheads; Fig. 3.1C). In contrast to this sequence of events, the first differentiated muscle cells to appear in *Myf5*$^{nlacZ/nlacZ}$ embryos are not elongated mononucleated myocytes; rather they are initially short multinucleated cells (arrowheads; Fig. 3.1D´). Therefore, these muscles are not myotomes, but appear to arise through the fusion of differentiating myoblasts into progressively longer myotubes, which is evocative of what occurs in the muscles of the limbs (Sieiro-Mosti et al., 2014). Close examination of the transversospinalis muscle in *Myf5*$^{+/nlacZ}$ embryos show that they are also not composed of elongated mononucleated cells but are like the differentiated cells observed in *Myf5*$^{nlacZ/nlacZ}$ embryos (arrowheads; Fig. 3.1C´). These observations suggest that *Myf5*$^{nlacZ/nlacZ}$ embryos do not develop a myotome. Moreover, they show that, in contrast to the three other epaxial muscles, the development of the transversospinalis muscle proceeds in the absence of a myotome.

From E12.5 onwards, the only epaxial muscles that develop in *Myf5*$^{nlacZ/nlacZ}$ embryos are the transversospinalis muscles (compare red arrowheads; Fig. 3.1E, F, I, J; ts in Fig. 3.1M, N). No muscle groups corresponding to longissimus, iliocostalis or levatores costarum (outlined areas in Fig. 3.1E, I, M) are observed in *Myf5*$^{nlacZ/nlacZ}$ embryos (white arrowheads; Fig. 3.1F, J). Moreover, MuSCs and differentiating muscle cells, marked by the presence of Pax7 and Myogenin, respectively, are only present in the transversospinalis muscles (Fig. 3.1P), and are absent in the area of the missing epaxial muscles (outlined area; Fig. 3.1O; arrowheads in Fig. 3.1P).

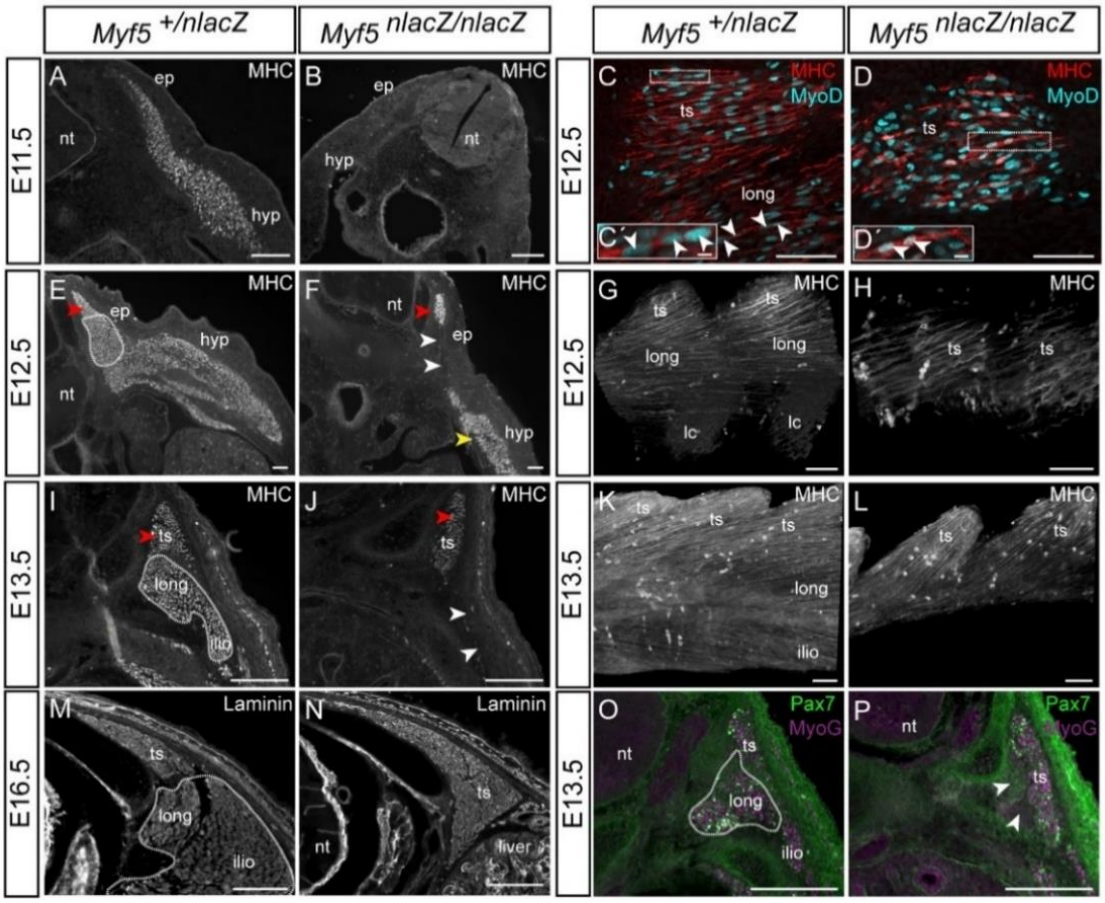

Figure 3.1: Epaxial muscle morphogenesis in *Myf5*$^{nlacZ/nlacZ}$ embryos is incomplete.
Transverse interlimb level cryosections (A, B, E, F, I, J, M-P), sagittal images selected among full digital z-stacks (C, D) and snapshots of 3D reconstructions showing the lateral views of whole mount immunolabelled interlimb epaxial segments (G, H, K, L) of *Myf5*$^{+/nlacZ}$ and *Myf5*$^{nlacZ/nlacZ}$ embryos/foetuses at E11.5, E12.5, E13.5 and E16.5. Embryos and foetuses were stained with antibodies against MHC (A, B, E-L; red in C, D), MyoD (cyan in C, D), laminin (M, N), Pax7 (green in O, P) and Myogenin (MyoG; magenta in O, P). **A, B:** At E11.5, the myotome is fully matured and developed in *Myf5*$^{+/nlacZ}$ embryos (A), while in *Myf5*$^{nlacZ/nlacZ}$ embryos myogenesis is delayed and the myotome is absent (B). **C, D:** At E12.5 in *Myf5*$^{+/nlacZ}$ embryos, longissimus and iliocostalis muscle fibres are multinucleated and have started fusing across segments (C), while these muscles are absent in *Myf5*$^{nlacZ/nlacZ}$ embryos (D). Notably the first differentiated muscle cells present in *Myf5*$^{nlacZ/nlacZ}$ embryos are already multinucleated (arrowheads in D´, insert) just like the transversospinalis muscle fibres of same stage *Myf5*$^{+/nlacZ}$ embryos (arrowheads in C´, insert). **E-N:** At E12.5 the epaxial musculature in control embryos is segregated (E, G, I, K, M). In G, iliocostalis muscle masses were observed but are not visible in this plane. In *Myf5*$^{nlacZ/nlacZ}$ embryos all epaxial muscle groups are missing (F, J, H, L, N; white arrowheads in F, J) except the transversospinalis muscle group which has developed in the epaxial-most region (F, J, H, L, N; red arrowheads; compare E, I with F, J). The hypaxial musculature appears to develop normally in *Myf5*$^{nlacZ/nlacZ}$ embryos (yellow arrowhead in F). **O, P:** At E13.5, Pax7-positive MuSCs in *Myf5*$^{+/nlacZ}$ embryos are detected within all epaxial muscle masses (O). In contrast, in *Myf5*$^{nlacZ/nlacZ}$ embryos, MuSCs are only detected in the transversospinalis muscle mass and are absent in the areas where epaxial muscle morphogenesis in *Myf5*$^{nlacZ/nlacZ}$ embryos is impaired (arrowheads in P). White dashed lines in E, I, M, O indicate the epaxial muscle masses in *Myf5*$^{+/nlacZ}$ embryos that are absent in *Myf5*$^{nlacZ/nlacZ}$ embryos. nt: neural tube; ts: transversospinalis; long: longissimus; ilio: iliocostalis; lc: levatores costarum. Dorsal is up and left is either medial (A, B, E, F, I, J, M-P) or caudal (C, D, G, H, K, L) Scale bars: 100 µm in A, B, E, F, I, J, M-P, 50 µm in C, D, G, H, K, L an 5 µm in C´and D´.

Thus, the MuSCs and myoblasts, which normally contribute to the formation of the longissimus, iliocostalis and levatores costarum muscles, are absent in *Myf5*$^{nlacZ/nlacZ}$ embryos. In fact, as seen on a section of an E16.5 *Myf5*$^{nlacZ/nlacZ}$ foetus (Fig. 3.1N), not only are the muscle

cells missing, but the space for these putative muscle masses (outlined area in Fig. 3.1M) ceases to exist and becomes occupied by the liver (Fig. 3.1N).

We conclude that epaxial myogenesis of *Myf5*$^{nlacZ/nlacZ}$ embryos is impaired in that only one out of four epaxial muscle groups forms. Moreover, we provide evidence to suggest that *Myf5*$^{nlacZ/nlacZ}$ embryos do not produce an epaxial myotome and thus do not follow the normal sequence of events, i.e. formation of a myotome, segregation of the myotome and formation of epaxial muscles. Rather the only muscle that forms, the transversospinalis, appears to develop without going through a myotome stage.

MyoD expression does not fully rescue epaxial myogenesis in Myf5$^{nlacZ/nlacZ}$ *embryos*

Since *Myf5*$^{nlacZ/nlacZ}$ embryos are functional double mutants for *Myf5* and *Mrf4* (Kassar-Duchossoy et al., 2004), the myogenic differentiation programme can only be triggered through MyoD expression, which in *Myf5*$^{nlacZ/nlacZ}$ embryos is delayed by about one day (Tajbakhsh et al., 1997; Sassoon et al., 1989). To better understand why longissimus, iliocostalis and levatores costarum muscle groups fail to form in *Myf5*$^{nlacZ/nlacZ}$ embryos, we compared the expression pattern of MyoD in *Myf5*$^{+/nlacZ}$ and *Myf5*$^{nlacZ/nlacZ}$ embryos from E11.0 (DMM stage 3) to E12.5 (Fig. 3.2).

In E11.0 and E11.5 *Myf5*$^{+/nlacZ}$ embryos (DMM stages 3 and 4), MyoD mRNA and protein are present throughout the whole segment (Fig. 3.2A, B, E, F) and remain expressed in the epaxial and hypaxial muscle masses after their segregation at E12.5 (red and yellow arrowheads; Fig. 3.2I, J). In contrast, at the same interlimb level in E11.0 *Myf5*$^{nlacZ/nlacZ}$ embryos, MyoD transcripts and protein are only detected in the hypaxial region of the segment (Fig. 3.2 C, D). At E11.5, MyoD expression is also detected in the dorsal-most part of the segment (red arrowheads; Fig. 3.2G, H). Occasionally, a faint signal is also detected in the ventral part of the epaxial region (white arrowheads; Fig. 3.2G, H), but this expression is not sustained (Fig. 3.2K, L). Rather, at E12.5, MyoD mRNA and protein expression is always restricted to the transversospinalis (red arrowheads; Fig. 3.2K, L) and hypaxial (yellow arrowheads; Fig. 3.2 K, L) muscles and is never observed in the putative region of longissimus, iliocostalis and levatores costarum muscle groups (white arrowheads; Fig. 3.2K, L).

We conclude that MyoD expression is both delayed and spatially restricted in *Myf5*$^{nlacZ/nlacZ}$ embryos. MyoD activates the differentiation programme of the hypaxial muscles,

as it does in wild type embryos. However, epaxially it is only activated in the dorsal-most epaxial region, which gives rise to the transversospinalis muscles.

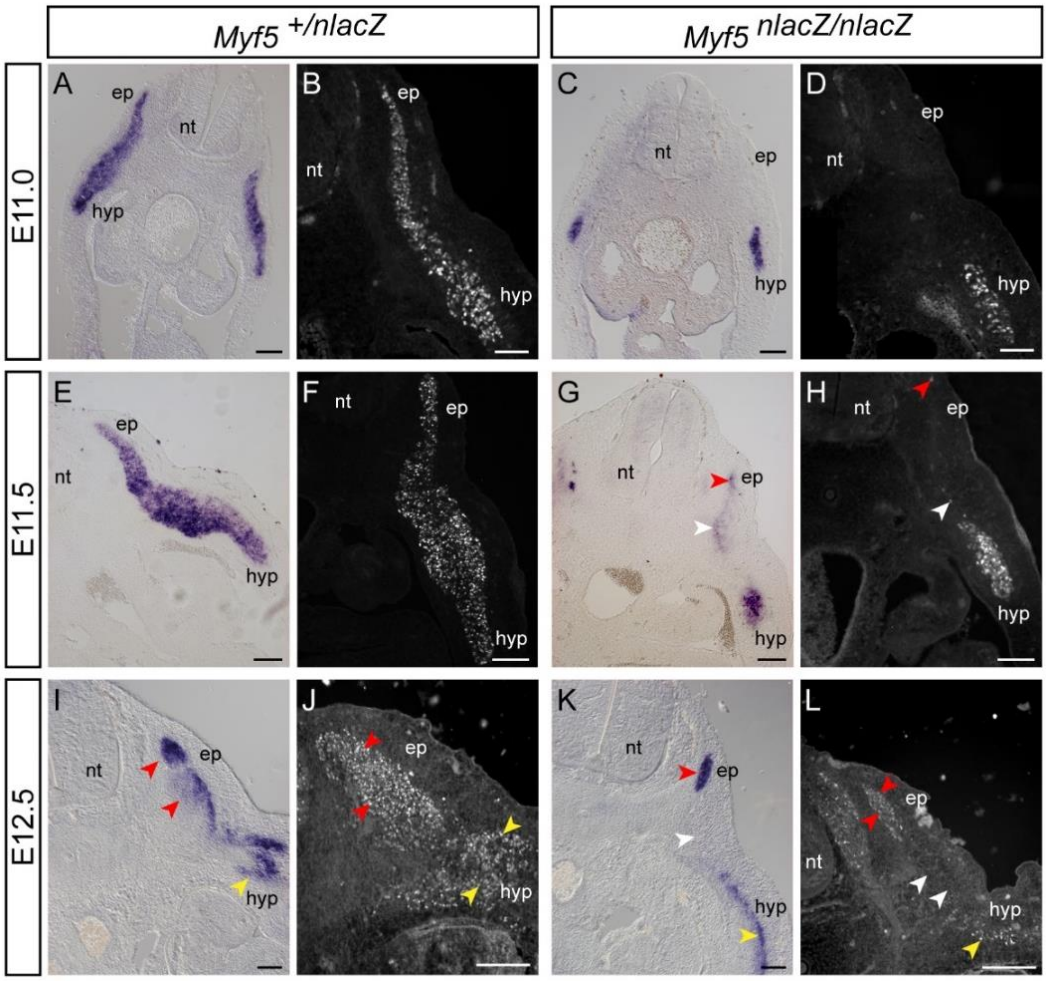

Figure 3.2: MyoD expression is spatially restricted in *Myf5*$^{nlacZ/nlacZ}$ embryos.
Detection of *MyoD* transcripts by *in situ* hybridisation (A, C, E, G, I, K) and MyoD immunolocalisation (B, D, F, H, J, L) on cryosections of interlimb segments of *Myf5*$^{+/nlacZ}$ and *Myf5*$^{nlacZ/nlacZ}$ embryos at E11.0, E11.5 and E12.5. **A-D:** In E11.0 *Myf5*$^{nlacZ/nlacZ}$ embryos, the myogenic differentiation programme is delayed compared to the control (compare C, D with A, B), and MyoD is only detected hypaxially (C, D). **E-H:** In E11.5 *Myf5*$^{+/nlacZ}$ embryos, MyoD (mRNA and protein) is present in the whole myotome (E, F). In *Myf5*$^{nlacZ/nlacZ}$ embryos, MyoD expression is maintained hypaxially and can now be detected epaxially, but only in the dorsal-most part of the segment (red arrowheads in G, H). Despite a faint expression in the central portion of the segment at this stage (white arrowheads in G, H), MyoD expression is not sustained in this region. **E-L:** At E12.5, after the segregation of the epaxial muscle masses, MyoD (mRNA and protein) remains expressed in both the developing hypaxial (yellow arrowheads in I, J) and the epaxial muscle masses (red arrowheads in I, J) of *Myf5*$^{+/nlacZ}$ embryos. In same stage *Myf5*$^{nlacZ/nlacZ}$ embryos, MyoD expression is detected within the hypaxial muscle masses (yellow arrowheads in K, L), but epaxially it is spatially confined to the dorsal-most part (red arrowheads in K, L) and MyoD mRNA and protein are absent in the areas where epaxial muscle development fails to occur (white arrowheads in K, L). Dorsal is up and medial on the left. ep: epaxial; hyp: hypaxial; nt: neural tube. Scale bars: 100 µm.

Myf5$^{nlacZ/nlacZ}$ embryos fail to maintain Pax7-expressing cells after the dissociation of the central dermomyotome

In E13.5 *Myf5$^{nlacZ/nlacZ}$* embryos, Pax3- and Pax7-positive MuSCs are absent from the putative longissimus, iliocostalis and levatores costarum muscle areas (Fig. 3.1O, P), raising the question of what happened to these cells. To address this issue, we analysed the expression of Pax3 and Pax7 by *in situ* hybridisation and immunohistochemistry before, during and after the dissociation of the central dermomyotome in both *Myf5$^{+/nlacZ}$* and *Myf5$^{nlacZ/nlacZ}$* embryos. (Fig. 3.3).

In E10.5 *Myf5$^{+/nlacZ}$* embryos, i.e. before the dissociation of the central dermomyotome, *Pax3* transcripts are detected throughout the whole dermomyotome (Fig. 3.3A) and a few Pax3-positive MuSCs have de-epithelialized and entered the myotome in the central domain (arrowheads; Fig. 3.3G; Relaix et al., 2005). At the same stage, *Pax7* mRNA is more spatially restricted, being localised in the epaxial and central dermomyotome (Fig. 3.3M) and a considerable number of Pax7-positive cells can be detected inside the epaxial myotome (arrowheads; Fig. 3.3S). During the dissociation of the central dermomyotome which starts at E11.0 (DMM stage 3) in interlimb somites (Deries et al., 2012), *Pax3* transcripts become further downregulated in the central dermomyotome while becoming enriched in the epaxial and hypaxial dermomyotomal lips in *Myf5$^{+/nlacZ}$* embryos (Fig. 3.3C; Goulding et al., 1994). Also, more Pax3-positive MuSCs are now detected within the myotome (arrowheads; Fig. 3.3I). At this same stage, Pax7 mRNA and protein are abundantly expressed within the whole myotome and few Pax7-positive cells remain in the epithelial parts of the dermomyotome (Fig. 3.3O, U). At E11.5 (DMM stage 4), when the central dermomyotome is fully dissociated, Pax3 transcripts and protein remain expressed in the epaxial and hypaxial regions, but only a faint expression is detectable in the central myotome (Fig.3. 3E, K). At this same stage, strong *Pax7* mRNA expression persists in the myotome (Fig. 3.3Q) and Pax7-expressing MuSCs have become even more abundant throughout the whole segment (Fig. 3.3W).

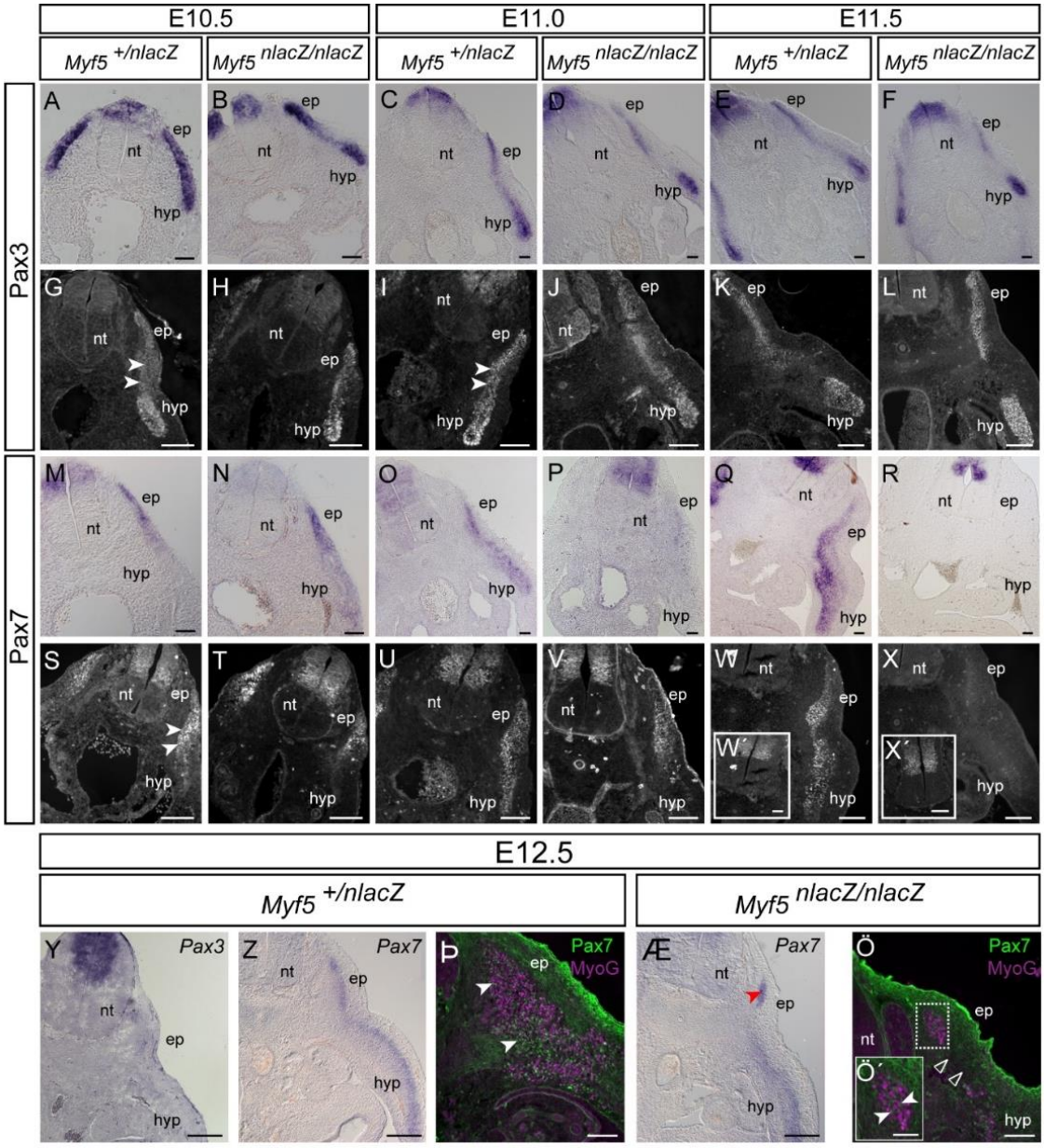

Figure 3. 3: MuSCs of *Myf5* $^{nlacZ/nlacZ}$ embryos fail to maintain Pax7 expression after central dermomyotome dissociation.

In situ hybridisation for *Pax3* (A-F, Y) and *Pax7* (M-R, Z, Æ) and immunohistochemistry on cryosections of interlimb segments (G-L, S-X´, Þ, Ö, Ö') of *Myf5*$^{+/nlacZ}$ and *Myf5*$^{nlacZ/nlacZ}$ embryos at E10.5, E11.0, E11.5 and E12.5. Antibodies against Pax3 (G-L), Pax7 (S-X´; green in Þ, Ö, Ö') and Myogenin (MyoG; magenta in Þ, Ö, Ö') were used on cryosections. **A-L:** As myogenesis progresses, Pax3 is consistently expressed by the MuSCs in the dermomyotome of both *Myf5*$^{+/nlacZ}$ (A, C, E, G, I, K) and *Myf5*$^{nlacZ/nlacz}$ (B, D, F, H, J, L) embryos, and in *Myf5*$^{+/nlacZ}$ embryos, a few Pax3-positive cells are localised in the myotome (arrowheads in G). At E11.0, some Pax3-positive MuSCs are detected in the central myotome (arrowheads in I) but Pax3 expression has become enriched in the epaxial-most and hypaxial portion of the segments in both types of embryos. Thus, there are no differences in the spatial expression of Pax3 between *Myf5*$^{+/nlacZ}$ (E, K) and *Myf5*$^{nlacZ/nlacZ}$ (F, L) embryos. **M-X:** At E10.5, prior to the dissociation of the central dermomyotome, the majority of Pax7-positive MuSCs are epithelial within the dermomyotome sheet (N, T), while in control embryos some Pax7-positive MuSCs are located within the myotome (arrowheads; S). At E11.0, when the central dermomyotome dissociates, only a few Pax7-positive MuSCs are detected in *Myf5*$^{nlacZ/nlacZ}$ segments (compare O with P and U with V) and at E11.5, Pax7 expression (transcripts and protein) has been almost totally lost in the mutant embryos (compare Q with R and W with X). Note that Pax7 is always normally expressed in the dorsal neural tube of *Myf5*$^{nlacZ/nlacZ}$ embryos (M-V, W´, X´). (**Continues next page**).

In fact, double immunohistochemistry for Pax3 or Pax7 with MyoD at E11.5 reveals that MuSCs that remain epithelial in the dermomyotomal lips tend to express Pax3 rather than Pax7 (compare supplementary Fig. 3.1A and D with C and F). In contrast, most MuSCs within the myotomal space at this stage are Pax7-positive while only relatively few are Pax3-positive (supplementary Fig. 3.1A-F), with this difference being particularly striking in the central myotomal domain (compare supplementary Fig. 3.1B with E; Deries et al., 2010; Galli et al., 2008).

In *Myf5*$^{nlacZ/nlacZ}$ embryos, Pax3 mRNA and protein expression in the dermomyotome is indistinguishable from that of normal embryos at the stages under study (Fig. 3.3A-L). Also, at E10.5, *Pax7* mRNA and protein are expressed in the epaxial and central dermomyotome of *Myf5*$^{nlacZ/nlacZ}$ embryos (Fig. 3.3N, T) in a pattern similar to the one observed in control embryos (Fig. 3.3M, S). However, at E11.0, a sharp downregulation of *Pax7* mRNA has occurred in the segments of *Myf5*$^{nlacZ/nlacZ}$ embryos (compare Fig. 3.3P with O). Importantly, this downregulation is specific for the segments since the expression of *Pax7* mRNA in the neural tube is unchanged (compare Fig. 3.3P with O; Lacosta et al., 2005; Murdoch et al., 2012). At this same stage *Myf5*$^{nlacZ/nlacZ}$ embryos also appear to have fewer Pax7-positive cells in the myotome than *Myf5*$^{+/nlacZ}$ embryos (compare Fig. 3.3V with U). Strikingly, at E11.5, Pax7 mRNA and protein expression is completely absent from the segments of *Myf5*$^{nlacZ/nlacZ}$ embryos (compare Fig. 3.3R with Q and X with W), while Pax7 expression in the dorsal neural tube is unaffected (compare Fig. 3.3R with Q and X´ with W´). We conclude that Pax7 mRNA and protein expression in the segments of *Myf5*$^{nlacZ/nlacZ}$ embryos is essentially normal at E10.5 (DMM stage 2), becomes reduced at the time of the onset of central dermomyotome dissociation (E11.0; DMM stage 3) and has disappeared completely when this dissociation is completed (E11.5; DMM stage 4). In contrast, the expression of Pax3 mRNA and protein, which normally becomes restricted to the epaxial and hypaxial dermomyotomal lips and the myotome near these lips at E11.5 (Fig. 3.3E, K; supplementary Fig. 3.1A-C), is normal in *Myf5*$^{nlacZ/nlacZ}$ embryos (Fig. 3.3F, L).

(Continued from previous page). Y- Ö: At E12.5 in *Myf5*$^{+/nlacZ}$ embryos, *Pax3* expression has been downregulated (Y), while *Pax7* expression remains (Z) and Pax7-positive MuSCs intermingle with Myogenin-positive myoblasts in all the muscle masses (arrowheads in Þ). At E12.5, Pax7 mRNA and protein expression has reappeared in *Myf5*$^{nlacZ/nlacZ}$ embryos, in areas where differentiated, Myogenin-positive muscle cells are found (Æ-Ö´). However, epaxially, Pax7 mRNA and protein expression is restricted to the transversospinalis muscles (red arrowheads in Æ and arrowheads in Ö´), while, hypaxially, *Pax7* transcripts are detected in the same pattern as in *Myf5*$^{+/nlacZ}$ embryos (compare Z with Æ). No Pax7-positive MuSCs are detected in the areas where the remaining epaxial muscles are missing (empty arrowheads in Ö). Dorsal is up and medial on the left. ep: epaxial; hyp: hypaxial; nt: neural tube. Scale bars: 100 µm in A- Ö and 50 µm in W´, X´, Ö´.

To test whether the loss of Pax7-positive cells in *Myf5*$^{nlacZ/nlacZ}$ embryos was due to impaired cell proliferation in the central dermomyotome and/or increased cell death, we performed co-immunolocalisation experiments for Pax7 and a phosphorylated form of histone H3 (H3S10p-pH3; a marker of mitosis) or cleaved caspase-3 (an apoptosis marker) in E10.5-E11.5 *Myf5*$^{+/nlacZ}$ and *Myf5*$^{nlacZ/nlacZ}$ embryos. Co-immunolabelling for H3S10p-pH3 and Pax7 does not reveal any obvious differences in proliferation of Pax7-positive cells in *Myf5*$^{+/nlacZ}$ and *Myf5*$^{nlacZ/nlacZ}$ embryos (supplementary Fig. 3.2A-F). Moreover, no massive increase in caspase-3 staining was detected, (supplementary Fig. 3.2G-L) indicating that the dramatic loss of Pax7-positive cells observed in *Myf5*$^{nlacZ/nlacZ}$ embryos between E10.5 and E11.5 is not due to apoptosis.

We conclude that between E10.5 and E11.5 *Myf5*$^{nlacZ/nlacZ}$ embryos display a normal spatio-temporal expression pattern of Pax3 and that, as in control embryos, during this period, Pax3 expression gets progressively restricted to the epaxial and hypaxial lips. In contrast, during this same period, Pax7 expression is gradually lost in the segments of *Myf5*$^{nlacZ/nlacZ}$ embryos, becoming practically undetectable at E11.5. Since there is no simultaneous increase in apoptosis, our results suggest that Pax7-positive cells which upon the dissociation of the central dermomyotome are released into the area where the myotome should have been, are unable to maintain their Pax7 expression.

Pax7-positive cells become detectable concomitantly with myogenic differentiation in the transversospinalis and hypaxial muscles of Myf5$^{nlacZ/nlacZ}$ *embryos*

During normal epaxial myogenesis beyond E11.5 (DMM stage 4), the epaxial dermomyotomal lips de-epithelialize, releasing MuSCs into the developing epaxial muscle masses (Deries et al., 2010, 2012). Since at E11.5 the great majority of cells of the epaxial lips are Pax3-positive and only very few cells are Pax7-positive (Fig. 3.3K, W; supplementary Fig. 3.1A, D), it would be expected that most cells released upon the de-epithelialization of the epaxial lip would be Pax3-positive cells. However, at E12.5 *Pax3* expression has been downregulated in *Myf5*$^{+/nlacZ}$ embryos (Fig. 3.3Y; Bober et al., 1994) while *Pax7* expression is maintained throughout the segment (Fig. 3.3Z) and Pax7-expressing MuSCs are intermingled among differentiated cells within the muscle masses (arrowheads; Fig. 3.3Þ). Thus, it appears that during normal development epaxial lip-derived cells downregulate Pax3 and upregulate Pax7 after they de-epithelialize and populate the developing muscle masses.

Myf5$^{nlacZ/nlacZ}$ embryos do not express Pax7 at E11.5 (Fig. 3.3R, X). However, cells in the epaxial lip express Pax3 at E11.5 (Fig. 3.3F, L) and by E12.5 *Myf5*$^{nlacZ/nlacZ}$ embryos have started forming the transversospinalis as well as the hypaxial muscles (Fig. 3.1F). We thus asked whether MuSCs within these *Myf5*$^{nlacZ/nlacZ}$ E12.5 muscles express Pax7. Indeed, we found that *Pax7* mRNA is expressed in both the transversospinalis (red arrowheads; Fig. 3.3Æ) and the hypaxial muscles (compare Fig. 3.3Æ and 3.1F) and Pax7-positive cells can be seen intermingled among the differentiated cells (arrowheads; Fig. 3.3Ö'). These results suggest that in *Myf5*$^{nlacZ/nlacZ}$ embryos, the de-epithelializing Pax3-positive cells that enter an area where muscle differentiation is occurring are maintained as MuSCs. Moreover, as observed in heterozygous embryos between E11.5 and E12.5, these MuSCs undergo a switch from being Pax3- to Pax7-positive. In contrast, no Pax7-positive cells are detected in the area where the remaining epaxial muscles should have been (empty arrowheads; Fig. 3.3Ö). These results suggest that the MuSCs that entered this area, which in *Myf5*$^{nlacZ/nlacZ}$ embryos does not have a myotome, fail to maintain their MuSC identity.

Expression of Fgf6 and Pdgfa is disrupted in Myf5$^{nlacZ/nlacZ}$ *embryos*

We next hypothesised that the abnormal downregulation of Pax7 expression in *Myf5*$^{nlacZ/nlacZ}$ embryos might be due to the absence of the myotome. We thus turned our attention to what factors, normally produced by the myotome, could be important for the maintenance of MuSC identity. The mouse myotome is known to express *Fgf4* and *Fgf6*, which have identical expression patterns (de Lapeyrière et al., 1993; Grass et al., 1996; Han and Martin, 1993; Niswander and Martin, 1992), as well as *Pdgfa*, the gene codifying for platelet-derived growth factor A protein (Orr-Utreger and Lonai, 1992; Tallquist et al., 2000). Myotome-derived Fgfs and Pdgfs are known to play a crucial role in the patterning of the sclerotome (Brent et al., 2005; Grass et al., 1996; Tallquist et al., 2000; Vinagre et al., 2010), but whether they also play a role in the maintenance of MuSCs within the segment is unknown.

Previous studies have shown that *Fgf4*, *Fgf6* and *Pdgfa* expression is delayed in embryos lacking *Myf5* (Brent et al. 2005; Grass et al., 1996; Tallquist et al., 2000). To characterise this delay in more detail, we analysed the expression of *Fgf6* and *Pdgfa* in *Myf5*$^{+/nlacZ}$ and *Myf5*$^{nlacZ/nlacZ}$ embryos. In control embryos, *Fgf6* transcripts are present in the myotome (Fig. 3.4A, C, E; de Lapeyrière et al., 1993) and then, at E12.5, *Fgf6* mRNA is present in all muscle masses (de Lapeyrière et al., 1993) including the epaxial (red arrowheads; Fig. 3.4G) and the

hypaxial ones (yellow arrowheads; Fig. 3.4G). As expected, *Myf5*$^{nlacZ/nlacZ}$ embryos, which lack a myotome of differentiated cells, are negative for *Fgf6* transcripts (Fig. 3.4B, D, F; Grass et al., 1996). Only at E12.5, when MHC-positive cells are detected hypaxially (yellow arrowheads; Fig. 3.4L) and in the transversospinalis (red arrowheads; Fig. 3.4L), is *Fgf6* expression observed in these muscles (yellow and red arrowheads; Fig. 3.4H) but is absent in the area where the missing epaxial muscles should have been (white arrowheads; Fig. 3.4H, L). *Pdgfa* is also expressed by the whole myotome (Fig. 3.4I; Orr-Utreger and Lonai, 1992; Tallquist et al., 2000). Interestingly, *Pdgfa* expression in *Myf5*$^{nlacZ/nlacZ}$ embryos comes up earlier than *Fgf6* expression. At E11.5 *Pdgfa* expression is very similar to the MyoD protein expression pattern of *Myf5*$^{nlacZ/nlacZ}$ embryos, both epaxially (red arrowheads; Fig. 3.4J, K) and hypaxially (yellow arrowheads; Fig. 3.4J, K), while no expression is detected in the central aspect of the segment (white arrowheads; Fig. 3.4J, K).

We next turned our attention to what Fgf and Pdgf receptors are expressed in the dermomyotome and myotome before and after the dissociation of the central dermomyotome. The mouse dermomyotome has been reported to express *Fgfr1* and *Pdgfrα*, while the myotome is negative for both receptors (Orr-Urtreger et al., 1992; Yamaguchi et al., 1992). However, we detect a weak expression of *Fgfr1* transcripts in the myotome of *Myf5*$^{+/nlacZ}$ embryos (red arrowhead; Fig. 3.5A) and this transcript is strongly expressed in the sclerotome (yellow arrowhead; Fig. 3.5A). This expression pattern was also detected in the sclerotome of *Myf5*$^{nlacZ/nlacZ}$ embryos (yellow arrowhead; Fig. 3.5B) but myotomal *Fgfr1* expression is missing in these embryos (Fig. 3.5B). *Fgfr4* is expressed in the mouse myotome (Stark et al., 1991) and is detected in the dermomyotomal lips (Lagha et al., 2008). In avians *Fgfr4* is detected in the central dermomyotome as well as in proliferating cells within the myotome (Delfini et al., 2009; Kahane et al., 2001). We confirmed that *Fgfr1*, *Fgfr4* and *Pdgfrα* are indeed expressed in the E10.5 (DMM stage 2) dermomyotome of both *Myf5*$^{+/nlacZ}$ and *Myf5*$^{nlacZ/nlacZ}$ embryos (white arrowheads, Fig. 3.5A-F), but since *Myf5*$^{nlacZ/nlacZ}$ embryos lack a myotome, myotomal *Fgfr4* expression was only detected in *Myf5*$^{+/nlacZ}$ embryos (red arrowhead; compare Fig. 3.5C and D). At E11.5 (DMM stage 4), *Fgfr1* appears not to be expressed within the myotome of *Myf5*$^{+/nlacZ}$ embryos (Fig. 3.5G). *Myf5*$^{nlacZ/nlacZ}$ embryos display a lateral extension of *Fgfr1* expression compared to control embryos (yellow arrowheads; compare Fig. 3.5G with H). However, since the sclerotomal domain reaches the dermomyotome in *Myf5*-null embryos (Grass et al., 1996) it is not possible to determine whether this expression is exclusively sclerotomal or if it also includes dermomyotome-derived cells. *Fgfr4* mRNA is exclusively expressed in the myotome of E11.5 *Myf5*$^{+/nlacZ}$ embryos (red arrowheads; Fig. 3.5I) and is absent in *Myf5*$^{nlacZ/nlacZ}$ embryos

(Fig. 3.5J; Lagha et al., 2008). At E11.5, expression of *Pdgfra* mRNA in *Myf5*$^{+/nlacZ}$ embryos is essentially confined to the dermis and the dorsal sclerotome (Fig. 3.5K). *Myf5*$^{nlacZ/nlacZ}$ embryos have a similar *Pdgfra* expression pattern except expression in the sclerotome appears more widespread than in control embryos (yellow arrowhead; Fig. 3.5L).

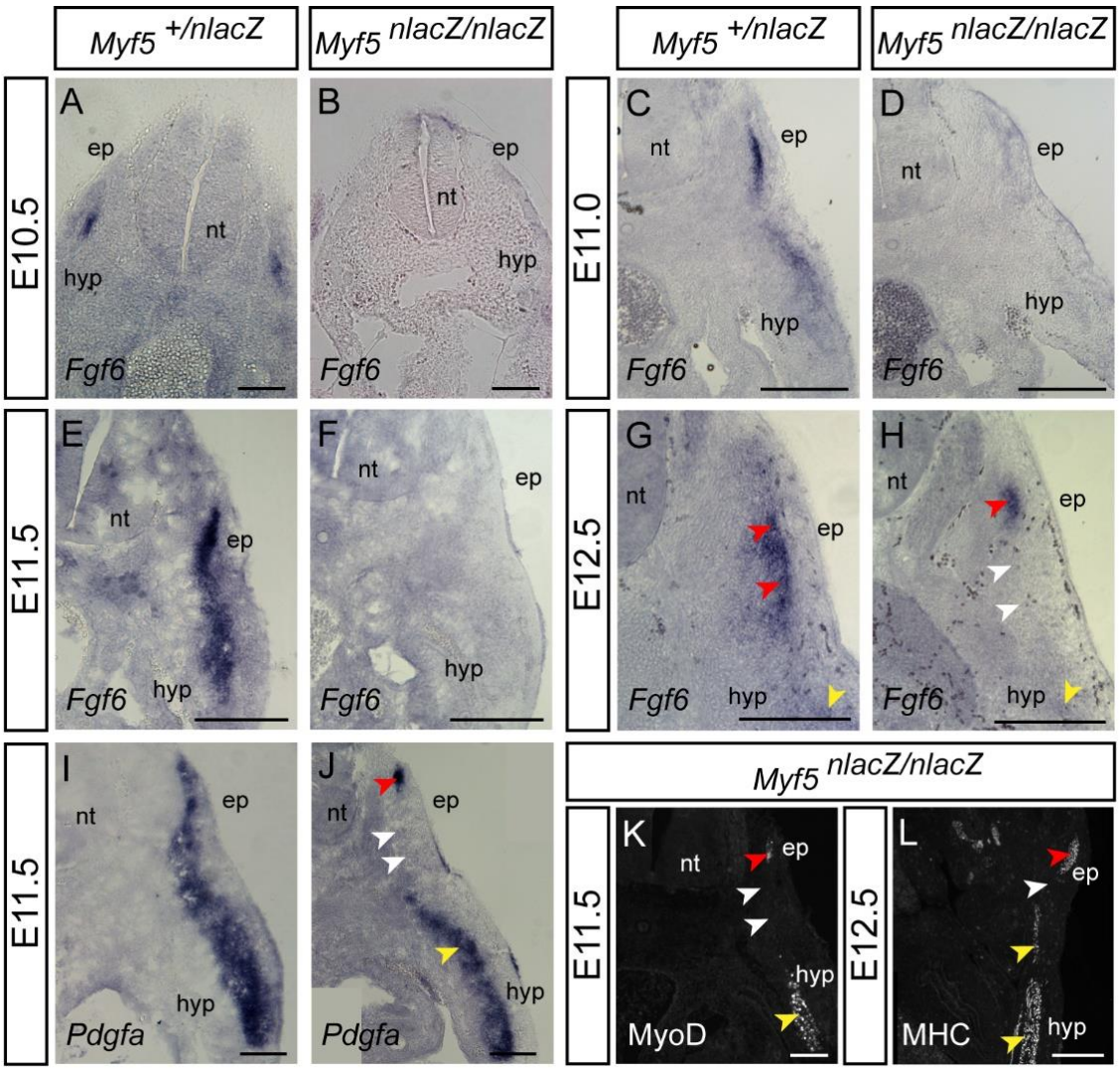

Figure 3.4: *Myf5*$^{nlacZ/nlacZ}$ embryos express *Fgf6* and *Pdgfa* upon myogenic differentiation.
Cryosections of interlimb segments of E10.5, E11.0, E11.5 and E12.5 *Myf5*$^{+/nlacZ}$ and *Myf5*$^{nlacZ/nlacZ}$ embryos hybridised for *Fgf6* in (A-H) and E11.5 *Myf5*$^{+/nlacZ}$ and *Myf5*$^{nlacZ/nlacZ}$ embryos hybridised for *Pdgfa* (I, J). Immunostaining for MyoD in an E11.5 *Myf5*$^{nlacZ/nlacZ}$ embryo (K) and for MHC in a E12.5 *Myf5*$^{nlacZ/nlacZ}$ embryo (L). In *Myf5*$^{+/nlacZ}$ embryos when myotomal cells start to be differentiated, *Fgf6* in expressed in the myotome (A, C) and *Fgf6* expression increases with the growth and maturation of the myotome (A, C, E). At E12.5, *Fgf6* transcripts are present in both epaxial (red arrowheads in G) and hypaxial (yellow arrowhead in G) muscle masses. By contrast, *Myf5*$^{nlacZ/nlacZ}$ embryos do not express *Fgf6* (B, D, F) until E12.5 (H) when *Fgf6* start to be expressed in a pattern similar to MHC protein expression in the transversospinalis (red arrowheads in H, L) and hypaxial muscle masses (yellow arrowhead in H, L). No *Fgf6* expression can be seen in the area where longissimus, iliocostalis and levatores costrarum muscles are missing (white arrowheads in H, L). *Pdgfa* expression is abundant in the *Myf5*$^{+/nlacZ}$ myotome at E11.5 (I). *Myf5*$^{nlacZ/nlacZ}$ embryos also express *Pdgfa* at E11.5 (J) in a pattern very similar to that of MyoD protein expression at the same stage (K). Expression of *Pdgfa* like MyoD is seen in the transversospinalis (red arrowheads in J, K) and hypaxial (yellow arrowheads in J, K) muscle masses, but expression is absent in between (white arrowheads in J, K). Dorsal is up and medial to the left. ep: epaxial; hyp: hypaxial; nt: neural tube. Scale bars: 100 µm.

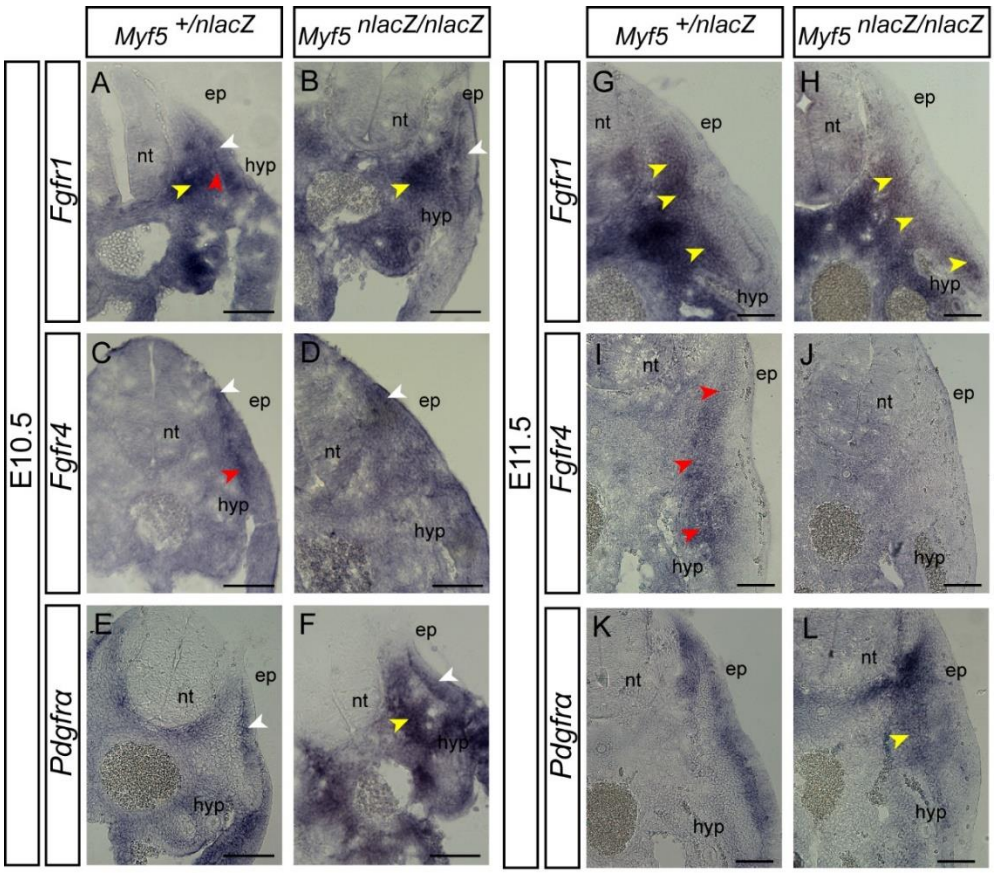

Figure 3.5: Comparative expression pattern of *Fgfr1*, *Fgfr4* and *Pdgfrα* in *Myf5*$^{+/nlacZ}$ and *Myf5*$^{nlacZ/nlacZ}$ embryos.
In situ hybridisation for *Fgfr1* (A, B, G, H), *Fgfr4* (C, D, I, J) and *Pdgfα* (E, F, K, L) in *Myf5*$^{+/nlacZ}$ and *Myf5*$^{nlacZ/nlacZ}$ embryos at E10.5 and E11.5 followed by cryosectioning of interlimb segments. **A-F:** In E10.5 *Myf5*$^{+/nlacZ}$ and *Myf5*$^{nlacZ/nlacZ}$ embryos *Fgfr1* mRNA is detected in the dermomyotome (white arrowheads in A, B) and weakly in the myotome of the *Myf5*$^{+/nlacZ}$ embryos (red arrowheads in A), while the myotomal expression is absent in *Myf5*$^{nlacZ/nlacZ}$ embryos (B). Expression of *Fgfr1* mRNA is high in the sclerotome of both types of embryos (yellow arrowheads in A, B). *Fgfr4* mRNA is also expressed in the dermomyotome (white arrowheads in C, D) of both *Myf5*$^{+/nlacZ}$ and *Myf5*$^{nlacZ/nlacZ}$ embryos and is strongly expressed in the myotome of the *Myf5*$^{+/nlacZ}$ embryos (red arrowheads in C), which is absent in *Myf5*$^{nlacZ/nlacZ}$ embryos (D). *Pdgfrα* mRNA is detected in the dermomyotome of both *Myf5*$^{+/nlacZ}$ and *Myf5*$^{nlacZ/nlacZ}$ embryos (white arrowheads in E, F). Faint *Pdgfrα* expression can be seen in the *Myf5*$^{+/nlacZ}$ sclerotome (E) and this sclerotomal expression appears to be stronger in the *Myf5*$^{nlacZ/nlacZ}$ embryos (yellow arrowhead in F). **G-L:** In E11.5 *Myf5*$^{+/nlacZ}$ and *Myf5*$^{nlacZ/nlacZ}$ embryos the central dermomyotome has de-epithelialized. *Fgfr1* remains strongly expressed in the sclerotome (yellow arrowheads in G, H) which in the *Myf5*$^{nlacZ/nlacZ}$ embryos reaches the dermomyotome (yellow arrowheads in H). *Fgfr4* mRNA is expressed in the myotome of *Myf5*$^{+/nlacZ}$ embryos (red arrowheads in I), but no *Fgfr4* mRNA is detected in E11.5 *Myf5*$^{nlacZ/nlacZ}$ segments by *in situ* hybridisation (J). *Pdgfrα* transcripts are expressed in the dermis and dorsal sclerotome zones in E11.5 *Myf5*$^{+/nlacZ}$ embryos, but the myotome is negative (K), while in *Myf5*$^{nlacZ/nlacZ}$ embryos, *Pdgfrα* expression remains high in the sclerotome (yellow arrowhead in L). Dorsal is up and medial on the left. ep: epaxial; hyp: hypaxial; nt: neural tube. Scale bars: 100 µm.

Our data show that the expression of *Fgf6* and *Pdgfa* in *Myf5*$^{nlacZ/nlacZ}$ embryos correlates in space and time with myogenic differentiation; *Pdgfa* expression coincides with MyoD protein expression while *Fgf6* expression comes up later, at a stage where MHC-positive myocytes/myotubes are present in the muscle masses. Moreover, we find that *Fgfr1*, *Fgfr4* and *Pdgfrα* are all expressed in the dermomyotome prior to its dissociation and are thus in a position to transduce Fgf and Pdgf signals in dermomyotome-derived MuSCs.

Blocking Fgfr1 or Fgfr4, but not Pdgfrα, in wild type embryo explant cultures leads to a reduction in the number of MuSCs

We next asked whether Fgfs and Pdgfs from the myotome, acting through Fgfr1, Fgfr4, and/or Pdgfrα, play a role in the maintenance of MuSCs as they enter the myotomal space. To address this question, we prepared explants from E10.75 wild type mouse embryos (i.e. embryos which have an Fgf- and Pdgf-expressing myotome) and cultured them for 12 hours (until E11.25) in the presence of chemical antagonists targeting Fgfr1, Fgfr4 or Pdgfrα (see Table 3.2) or a DMSO control (Fig. 3.6A; also see Materials and Methods). Fixed explants were then either processed for *in situ* hybridisation for *Pax7* or *Pax3* or for immunohistochemistry against Pax7, Pax3, MyoD and/or Myogenin. To assess for differences between treatments, the number of Pax7-, Pax3-, MyoD- and Myogenin-positive cells were quantified in transverse sections of control versus chemical inhibitor-treated explants.

Fgfr1 activity was blocked using three different compounds (SU5402, PD173074 or Ponatinib; see Table 3.2). All three compounds caused a significant reduction in the number of both Pax7- and Pax3-positive cells (Fig. 3.6B, C). SU5402 treatment leads to a dramatic downregulation of *Pax7* mRNA (compare Fig. 3.6J with Q) and a 68% reduction in the number of Pax7-positive cells (n=8; P=0.0016; Fig. 3.6B, also compare Fig. 3.6K with R) compared to controls (n=14). PD173074 treatment induces a 55% reduction in the number of Pax7-positive cells (n=4; P=0.00014, Fig. 3.6B), while incubation with Ponatinib leads to a reduction of 38% in the number of Pax7-positive cells (n=3; P=0.011; Fig. 3.6B). The number of Pax3-positive cells are reduced by 54% and *Pax3* mRNA is reduced (data not shown) when explants are cultured with SU5402 (n=8; P=0.0011; Fig. 3.6C; also compare Fig. 3.6L with S), PD173074 treatment leads to a 51% reduction in the number of Pax3-positive cells (n=4; P=0.010; Fig. 3.6C) and Ponatinib treatment leads to a reduction of 35% in the number of Pax3-positive cells (n=3; P=0.00075; Fig. 3.6C). In addition to blocking Fgfr1, Ponatinib also blocks Pdgfrα (Gozgit et al., 2011; Table 3.2) and therefore the effect of blocking Pdgfrα was analysed independently using Crenolanib, which blocks both Pdgfrα and Pdgfrβ, but has no effect on Fgfr1 (Table 3.2). A slight reduction in the number of Pax7- and Pax3-positive MuSCs is detected in explants cultured with Crenolanib relative to DMSO controls, but this difference is not statistically significant (n=5; P=0.059 and P=0.068, respectively; Fig. 3.6B, C; also compare Fig. 3.6M, N with T, U), suggesting that the effect of Ponatinib treatment on MuSCs at these stages of development is mostly due to its inhibitory effect on Fgfr1 signalling. Finally,

BLU9931 was used to specifically inhibit Fgfr4. BLU9931 had a considerably milder effect than the Fgfr1 inhibitors, with the reduction in the number of Pax7- and Pax3-expressing cells being mostly localised to the central myotome (compare Fig. 3.6 O, P with V, W). Inhibition of Fgfr4 activity with BLU9931 leads to a 30% reduction in the number of Pax7-positive cells (n=5; P=0.026; Fig. 3.6F) and a more modest (17%), but statistically significant, reduction in the number of Pax3-positive cells (n=6; P=0.042; Fig. 3.6G) in comparison with control explants (n=6).

Both SU5402 and Ponatinib treatment leads to a significant (44% and 52%, respectively) decrease in the number of MyoD-positive myoblasts (n=8; P=0.0027 and n=3; P=0.008, respectively; Fig. 3.6D) relative to controls (n=14). Of these two compounds, Ponatinib also caused a significant reduction in the number of Myogenin-positive cells (n=3; P=0.025; Fig. 3.6E), while SU5402 treatment did not (n=8; P=0.085; Fig. 3.6E). PD173074 treatment on the other hand, did not significantly influence either the number of MyoD- (n=4; P=0.27, Fig. 3.6D) or Myogenin-positive cells (n=4; P=0.71; Fig. 3.6E), nor does Crenolanib (n=5; P=0.78 and P=0.68, respectively; Fig. 3.6D, E) or BLU9931 (n=5; P=0.49 and P=0.57 respectively; Fig. 3.6H, I).

Our results demonstrate that blocking Fgfr1 in mouse embryo explants at the time when MuSCs are entering the myotome from the central dermomyotome has a dramatic effect on the number of both Pax7- and Pax3-positive MuSCs, while blocking Fgfr4 activity has a comparatively modest, but nevertheless significant effect, on these cells. Two of the Fgfr1 inhibitors used also caused a significant reduction in the number of MyoD-positive myoblasts and one of them affected the number of Myogenin-positive myocytes, suggesting that the failure to maintain adequate numbers of MuSCs may lead to the generation of fewer differentiated cells. However, a direct effect of these inhibitors on differentiation cannot be excluded. Our results further indicate that Pdgfs either do not contribute or play only a minor role in maintaining Pax7- and Pax3-positive MuSCs at the stages under study. We conclude that Fgf signalling, mostly acting through Fgfr1 but also through Fgfr4, is crucial for the maintenance of the identity of MuSCs during central dermomyotome dissociation.

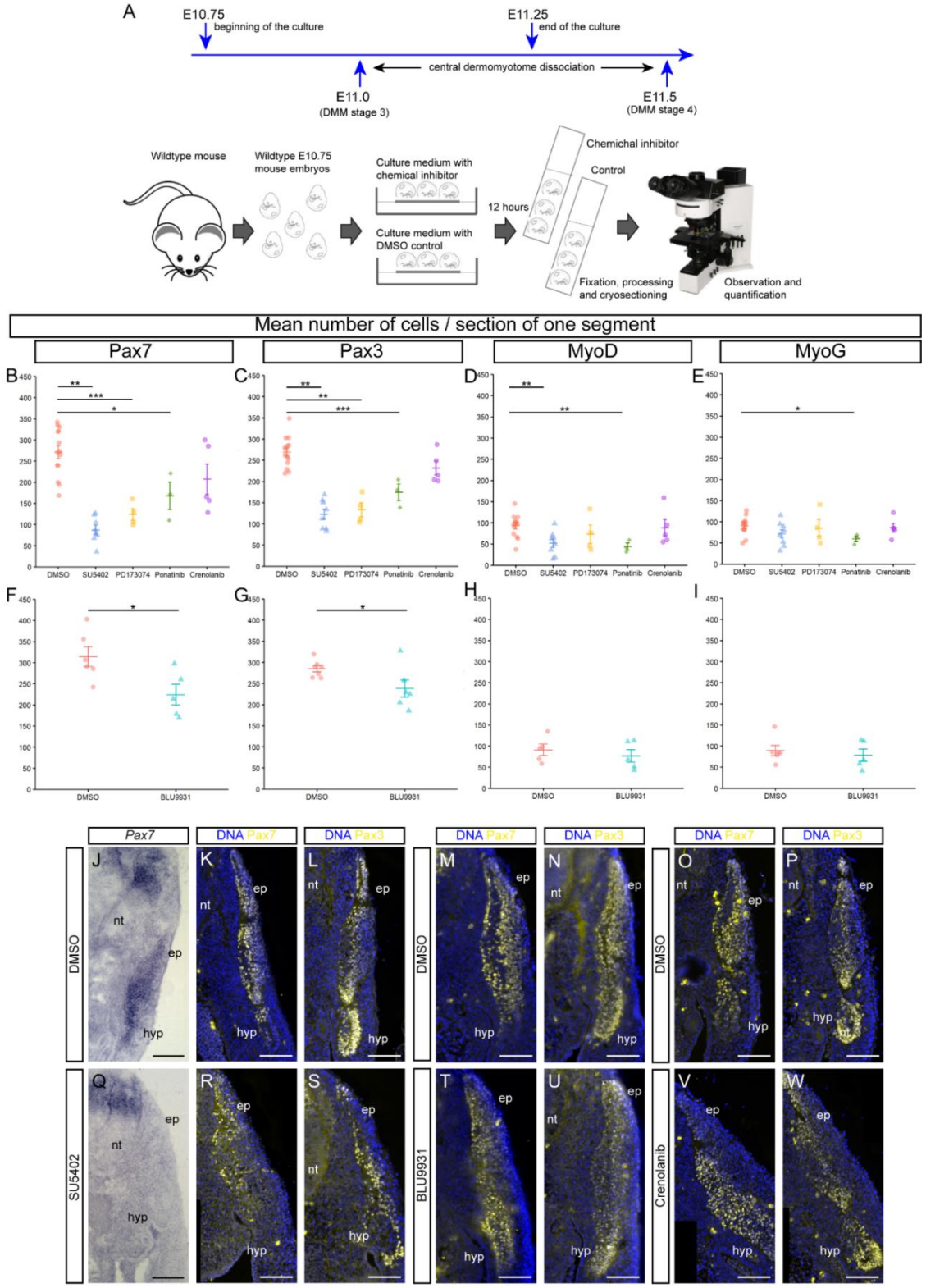

Figure 3.6: Fgf signalling through Fgfr1 and Fgfr4 maintain MuSC identity after central dermomyotome dissociation. **A:** Experimental design of mouse explant culture assays**.** E10.75 wild type embryos were collected, dissected and placed in culture medium containing SU5402, PD173074, Ponatinib, Crenolanib or BLU9931 or their DMSO controls. Explants were cultured for 12 hours, after which they were processed for whole mount *in situ* hybridisation or immunohistochemistry on cryosections of interlimb segments. (**Continues next page**).

Discussion

Myf5$^{nlacZ/nlacZ}$ embryos do not form an epaxial myotome

In normal embryos, the epaxial myotome starts forming at E8.0 when cells in the epaxial lip turn on Myf5, induced by β-catenin and Shh signalling as well as Dmrt2, which bind to the Myf5 early epaxial enhancer (EEE; Sato et al., 2010; Teboul et al., 2002). These cells enter the myotome from the rostral and caudal edges of the epaxial lip, migrate to the central region of the segment where they turn on Myogenin and differentiate into mononucleated myocytes that span the segment, parallel to the axis of the embryo (Venters et al., 1999). This myotome initially grows in a dorsal direction, concomitantly with the dorsal-wards growth of the epaxial lip, but it remains thin in the medio-lateral aspect (Patapoutian et al., 1995; Venters et al., 1999). This early myotome does not form in *Myf5$^{nlacZ/nlacZ}$* embryos; rather β-gal positive cells can be seen undergoing an epithelium-to-mesenchyme transition (EMT), but they fail to colonise the myotomal space, and instead migrate aberrantly (Tajbakhsh et al., 1996). In normal embryos, Mrf4 expression starts epaxially at E9.5 and contributes together with Myf5 to turn on Myogenin and promote myotomal myocyte differentiation (Kassar-Duchossoy et al., 2004; Summerbell et al., 2002).

(Continued from previous page). B-I: Graphical representation of the average number of Pax3-, Pax7-, MyoD- and Myogenin (MyoG) -positive cells detected per section of individual explants cultured with SU5402 PD173074, Ponatinib or Crenolanib compared with the DMSO control (B-E) or with BLU9931 compared with the DMSO control (F-I). Inhibition of Fgfr1 activity with SU5402, PD173074 or Ponatinib (all at 20 μM) leads to a dramatic and statistically significant reduction in the number of both Pax7- and Pax3-positive MuSCs (B, C). Moreover, the number of MyoD-positive myoblasts is also significantly reduced in the presence of SU5402 and Ponatinib, but not with PD173074 (D) and Ponatinib caused a small, but significant reduction in the number of Myogenin-positive cells (E). Blocking the activity of Pdgfrs with Crenolanib did not influence the number of cells expressing any of the myogenic markers (B-E). Blocking Fgfr4 activity with 50 μM BLU9931 caused a significant reduction in the number of Pax7 and Pax3-positive cells (F, G), but the number of MyoD- and Myogenin-positive cells is unchanged compared to the DMSO control (H, I). **J-W:** Representative transverse cryosections of wild type embryo explants shows a dramatic downregulation of *Pax7* mRNA in the SU5402-treated explant (Q) compared to the DMSO control (J). Representative images of cryosections of explants cultured with DMSO (K-P), SU5402 (R, S), BLU9931 (T, U) or Crenolanib (V, W) and immunostained for Pax7 or Pax3 (yellow) and with DAPI (blue). SU5402-treated explants show much fewer Pax7- and Pax3- positive cells (R, S) compared to control explants (K, L). Culture with BLU9931 induces a milder reduction in the number of Pax7- and Pax3-positive cells, which is most noticeable in the central segment (M, N, T, U). In contrast, culture with Crenolanib does not appear to have an effect the number of Pax7- and Pax3-positive cells (O, P, V, W). Dorsal is up and medial to the left. ep: epaxial; hyp: hypaxial; nt: neural tube. Scale bars: 100 μm. Data are means ± SEM. *P≤0.05, **P≤0.01, ***P≤0.001.

Then a second phase of epaxial myotome formation starts around E10.0, when cells at the rostral and caudal lips of the dermomyotome turn on Myf5 and migrate medially to the early myotome (Gros et al., 2004; Venters et al., 1999). In the mouse, these cells turn on MyoD soon after entering the myotomal space, migrate to the centre of the segment where they turn on Myogenin and differentiate into mononucleated myocytes spanning the whole segment, thus contributing to myotome growth in the medio-lateral direction (Venters et al., 1999). These cells, which turn on Myf5 followed by MyoD and then Myogenin, are the first MyoD-positive cells in the embryo (Sassoon et al., 1989; Venters et al., 1999). This second phase of myotome formation also does not happen in *Myf5*$^{nlacZ/nlacZ}$ embryos. β-gal positive cells can be seen stuck in the rostral and caudal lips of the dermomyotome (Tajbakhsh and Buckingham, 2000) and here we demonstrate that these cells also never turn on MyoD because MyoD expression remains absent epaxially until E11.5. Moreover, when MyoD expression starts in *Myf5*$^{nlacZ/nlacZ}$ embryos, it is only detected in the epaxial-most region of the segment. These results strongly indicate that cells from the rostral and caudal lips of the dermomyotome cannot turn on MyoD independently of Myf5/Mrf4 and thus remain in the lips.

Finally, a third wave of myogenesis occurs in the epaxial-most lip which remains epithelial for a while after central dermomyotome dissociation. This differentiation event goes ahead in *Myf5*$^{nlacZ/nlacZ}$ embryos and starts with the Myf5/Mrf4-independent activation of MyoD at E11.5. However, unlike the situation in the epaxial myotome, these differentiating cells do not originate elongated mononucleated myocytes that span the segment. Rather, they quickly fuse and form multinucleated myotubes. Moreover, these myotubes translocate to a position that is not aligned with the axis of the embryo and form the transversospinalis muscles (also see Deries et al., 2010). Indeed, upon close examination of the dorsal-most cells in normal embryos, their behaviour appears to be identical, suggesting that the dorsal-most epaxial muscle is not myotome-derived and rather forms through *de novo* differentiation of the epaxial dermomyotomal lip MuSCs.

The myotome is a special muscle. It is the first muscle to develop in the vertebrate embryo and is the only muscle that arises from the de-epithelialization of MuSCs from the edges of the dermomyotome without long range migration (Gros et al., 2004; Venters et al., 1999). In amniote embryos, the myotome is a striking muscle in that it is a transient muscle which segregates and transforms into epaxial and axial hypaxial musculatures before getting innervated (Deries et al., 2008, 2010). The present study shows that in *Myf5*$^{nlacZ/nlacZ}$ embryos, the epaxial myotome as described above does not form, i.e. this transient muscle stage is

skipped. It also shows that when the epaxial myotome is missing, three out of the four epaxial muscles fail to form.

The epaxial myotome is required to maintain the central dermomyotome-derived MuSCs

Due to the absence of a myotome in *Myf5*$^{nlacZ/nlacZ}$ embryos, when the central dermomyotome-derived MuSCs (the majority of which are Pax7-positive cells) undergo the EMT transition to invade the myotomal space (Kassar-Duchossoy et al., 2005; Relaix et al., 2005), they drop into a non-myogenic environment. Embryos that lack Myf5 and Mrf4, do not form the myotomal basement membrane which normally separates the myotome from the sclerotome (Bajanca et al., 2006; Tajbakhsh et al., 1996) and they display sclerotomal *Pax1* expression all the way to the dermomyotome (Grass et al., 1996), indicating that their de-epithelializing MuSCs enter a sclerotomal environment. Our data show that after central dermomyotome dissociation in *Myf5*$^{nlacZ/nlacZ}$ embryos, the area where the myotome should have been does not contain any Pax7-positive cells. Since there is no indication of an increase in apoptosis, we hypothesise that dissociating dermomyotomal cells cease to maintain the expression of Pax7 and consequently lose their muscle identity. Dermomyotomal cells have the potential to acquire several fates other than that of skeletal muscle (Deries and Thorsteinsdóttir, 2016; Kalcheim, 2015; Tajbakhsh, 2009). β-gal-positive cells in *Myf5*$^{nlacZ/nlacZ}$ embryos which fail to differentiate into myogenic cells were found to differentiate into sclerotomal and dermal cells (Tajbakhsh et al., 1996). It is thus tempting to hypothesise that in *Myf5*$^{nlacZ/nlacZ}$ embryos, de-epithelizing Pax7-positive cells from the central dermomyotome enter a sclerotomal environment, where they downregulate Pax7 and become re-committed into sclerotomal cells. Lineage-tracing of Pax7-GFP cells in *Myf5*$^{nlacZ/nlacZ}$ embryos will have to be performed to test this hypothesis.

As discussed above, our results indicate that the differentiated myotome is crucial to maintain the identity of MuSCs when they de-epithelialize from the dermomyotome. Interestingly, in *Myf5*$^{nlacZ/nlacZ}$ embryos, Pax7 is expressed again at E12.0 around the forming transversospinalis muscle fibres as well as in the hypaxial domain, suggesting that Pax7 expression may be dependent on differentiated muscle cells. In agreement with this hypothesis, it was shown that the expression of Pax7 is reduced in ACTA$^{Cre/DTA}$ mouse embryos where

differentiated muscle cells are ablated (Wood et al., 2013). Fgfs are known to be secreted by the myotome (Brent et al., 2005; de Lapeyrière et al., 1993; Han and Martin, 1993; also see Fig. 3.4) and several studies have shown the importance of Fgf signalling through Fgfr1 or Fgfr4 in regulating myogenesis (Lagha et al., 2008; Marics et al., 2002; Yablonka-Reuveni et al., 2015). Here we demonstrate that when the Fgf signalling pathway is blocked through Fgfr1 (and to a lesser extent through Fgfr4) in normal embryos, the number of Pax3 and Pax7-positive MuSCs is significantly reduced. This indicates that Fgfs from the myotome contribute significantly towards the maintenance of the identity of MuSCs as they de-epithelialize and enter the myotomal space. In contrast, blocking Pdgf (also secreted by the myotome; Tallquist et al., 2000) signalling does not significantly alter the number of Pax7- or Pax3-positive cells suggesting that Pdgfs do not contribute to maintain MuSCs and are more important for the development of the sclerotome (Tallquist et al., 2000).

The observation that only Pax7 and not Pax3 is downregulated in *Myf5*$^{nlacZ/lacZ}$ embryos, while the numbers of both Pax3- and Pax7-positive cells are reduced when Fgf signalling is blocked is puzzling. However, it might be explained by the differential distribution of Pax3- and Pax7-positive cells. At E11.0, when the central dermomyotome starts dissociating, Pax3 is mostly expressed in the lips of the dermomyotome (Goulding et al 1994; Tajbakhsh and Buckingham, 2000; see Fig. 3.3C, I) whereas Pax7 is mostly expressed in its central part as well as by cells that have entered the myotome (Galli et al., 2008; Jostes et al., 1990; also see Fig. 3.3O, U). Moreover, the predominantly Pax3-expressing epaxial and hypaxial lips stay epithelial another 12h (Relaix et al., 2005; Tajbakhsh and Buckingham 2000) which may maintain their Pax3-expression longer, or until its normal downregulation at E12.0. In contrast, cells in the central dermomyotome are predominantly Pax7-positive cells, meaning that when they de-epithelialize in *Myf5*$^{nlacZ/lacZ}$ embryos, they enter an area without the myotomal factors to sustain their Pax7 expression. Interestingly, we find that the re-appearance of Pax7-positive cells in the developing transversospinalis muscle in the *Myf5*$^{nlacZ/lacZ}$ mutant coincides with the expression of *Fgf6* by the differentiated cells in that muscle. Thus, we hypothesise that in the mutants, muscle differentiation occurs on time to maintain the MuSCs that de-epithelialized into the developing transversospinalis.

As mentioned earlier, the myotome is known to be a secreting tissue crucial for the development of the sclerotome (Tallquist et al 2000), including the ribs (Vinagre et al., 2010), and the syndetome (Brent and Tabin, 2004; Brent et al., 2005). In this study we identify one more crucial signalling role for the epaxial myotome: the maintenance of the identity of central

dermomyotome-derived MuSCs as they de-epithelialize and invade the myotomal space. Moreover, our data implicate Fgf signalling as a major contributor to this effect.

The difference between the development of the transversospinalis muscle group and the other epaxial muscle groups

Here, we show that *Myf5*$^{nlacZ/nlacZ}$ embryos only form one out of four groups of epaxial muscles. Therefore, MyoD is able to rescue the development of the transversospinalis muscle group but not of the other epaxial muscle groups. This result raises the question of the singularity of the transversospinalis group. In mammals, these muscles have a different morphology compared to the other epaxial groups (Cornwall et al., 2011; Rosatelli et al., 2008; Winckler, 1948) which can argue for potential differences in their developmental process. Our results indicate that while longissimus, iliocostalis and levatores costarum muscles can only form through a pathway initiated by the expression of Myf5, transversospinalis group can develop through the direct activation of MyoD similarly to the hypaxial muscles in *Myf5*$^{nlacZ/nlacZ}$ embryos. Thus, it is tempting to hypothesise that under normal conditions, MyoD is also an important factor for these muscles as it is for the hypaxial muscles. It is interesting to note that when MyoD cells are ablated as in *MyoD*^{iCre}*; R26*^{DTA} mutants, it seems that the epaxial-most part of the myotome is missing at E11.5 (Wood et al., 2013) which corroborates our hypothesis.

Interestingly, it has been proposed that the epaxial region of the segment contains two distinct regions: (1) the adaxial or intercalated region which undergoes myogenic differentiation in response to signals coming from the axial structures (notochord and neural tube) which corresponds to the early epaxial myotome and (2) an epaxial-most region that develops from the dorsally expanding epaxial lip and which responds to signals from mature dorsal structures to enter myogenesis and which may resemble the signals inducing myogenesis in the hypaxial region of the segment (Spörle, 2001). Our data on *Myf5*$^{nlacZ/nlacZ}$ embryos are fully compatible with such a scenario. The hypothesis that can be put forward is that the early adaxial/intercalated myotome differentiates by turning on Myf5 and/or Mrf4 in response to axial signals, forms an Fgf-expressing epaxial myotome which when the central dermomyotome dissociates and releases proliferating MuSCs into the myotome, develops into the iliocostalis, longissimus and levatores costarum muscles. The transversospinalis, on the

other hand, would according to this hypothesis develop from the later stage, epaxial-most portion of the segment, which does not require Myf5/Mrf4 expression to enter myogenesis, but can activate MyoD directly, possibly in a similar way as occurs hypaxially.

Acknowledgements

We thank Shahragim Tajbakhsh for generously sharing the *Myf5*^{nlacZ} mouse line and for his support and input throughout this study. We also thank Patrícia Ybot-Gonzalez for her precious advice on inhibitors in embryo culture. We thank Eric Olson, Ruth Diez del Corral and Moisés Mallo for generously providing us with plasmids for *in situ* hybridisation probes. The MF20, Pax3 and Pax7 antibodies were developed by DA Fischman, CP Ordahl, and A Kawakami, respectively, and were obtained from the Developmental Studies Hybridoma Bank, developed under the auspices of the NICHD and maintained by the University of Iowa, Department of Biology, Iowa City, IA 52242, USA. This work was supported by Fundação para a Ciência e a Tecnologia (FCT, Portugal) project PTDC/SAU-BID/120130/2010 and FCT scholarships SFRH/BD/90827/2012 (ABG) and SFRH/BPD/65370/2009 (MD). We also thank all members of our laboratory for helpful discussions.

References

Bajanca, F., Luz, M., Duxson, M. J. and Thorsteinsdóttir, S. (2004). Integrins in the mouse myotome: Developmental changes and differences between the epaxial and hypaxial lineage. *Dev. Dyn.* **231**, 402-415.

Bajanca, F., Luz, M., Raymond, K., Martins, G. G., Sonnenberg, A., Tajbakhsh, S., Buckingham, M. and Thorsteinsdóttir, S. (2006). Integrin α6β1-laminin interactions regulate early myotome formation in the mouse embryo. *Development* **133**, 1635-1644.

Ben-Yair, R. and Kalcheim, C. (2005). Lineage analysis of the avian dermomyotome sheet reveals the existence of single cells with both dermal and muscle progenitor fates. *Development* **132**, 689-701.

Bober, E., Franz, T., Arnold, H. H., Gruss, P. and Tremblay, P. (1994). Pax-3 is required for the development of limb muscles: a possible role for the migration of dermomyotomal muscle progenitor cells. *Development* **120**, 603-612.

Braun, T. and Arnold, H. H. (1995). Inactivation of Myf-6 and Myf-5 genes in mice leads to alterations in skeletal muscle development. *EMBO J.* **14**, 1176-1186.

Brent, A. E. and Tabin, C. J. (2004). FGF acts directly on the somitic tendon progenitors through the Ets transcription factors Pea3 and Erm to regulate scleraxis expression. *Development* **131**, 3885-3896.

Brent, A. E., Braun, T. and Tabin, C. J. (2005). Genetic analysis of interactions between the somitic muscle, cartilage and tendon cell lineages during mouse development. *Development* **132**, 515-528.

Buckingham, M. (2006). Myogenic progenitor cells and skeletal myogenesis in vertebrates. *Curr. Opin. Genet. Dev.* **16**, 525-532.

Buckingham, M. and Rigby, P. W. J. (2014). Gene regulatory networks and transcriptional mechanisms that control myogenesis. *Dev. Cell* **28**, 225-238.

Buckingham, M., Bajard, L., Chang, T., Daubas, P., Hadchouel, J., Meilhac, S., Montarras, D., Rocancourt, D. and Relaix, F. (2003). The formation of skeletal muscle: from somite to limb. *J. Anat.* **202**, 59-68.

Christ, B., Huang, R. and Scall, M. (2007). Amniote somite derivatives. *Dev. Dyn.* **236**, 2382-2396.

Cinnamon, Y., Kahane, N. and Kalcheim, C. (1999). Characterization of the early development of specific hypaxial muscles from the ventrolateral myotome. *Development* **126**, 4305-4315.

de Lapeyrière, O., Ollendorff, V., Planche, J., Ott, M. O., Pizette, S., Coulier, F. and Birnbaum, D. (1993). Expression of the Fgf6 gene is restricted to developing skeletal muscle in the mouse embryo. *Development* **118**, 601-611.

Delfini, M. C., De La Celle, M., Gros, J., Serralbo, O., Marics, I., Seux, M., Scaal, M. and Marcelle, C. (2009). The timing of emergence of muscle progenitors is controlled by an FGF/ERK/SNAIL1 pathway. *Dev. Biol.* **333**, 229-237.

Denetclaw, W. F., Christ, B. and Ordahl, C. P. (1997). Location and growth of epaxial myotome precursor cells. *Development* **124**, 1601-1610.

Deries, M. and Thorsteinsdóttir, S. (2016). Axial and limb muscle development: dialogue with the neighbourhood. *Cell. Mol. Life Sci.* **73**, 4415-4431.

Deries, M., Collins, J. J. P. and Duxson, M. J. (2008). The mammalian myotome: A muscle with no innervation. *Evol. Dev.* **10**, 746-755.

Deries, M., Gonçalves, A. B., Vaz, R., Martins, G. G., Rodrigues, G. and Thorsteinsdóttir, S. (2012). Extracellular matrix remodeling accompanies axial muscle development and morphogenesis in the mouse. *Dev. Dyn.* **241**, 350-364.

Deries, M., Schweitzer, R. and Duxson, M. J. (2010). Developmental fate of the mammalian myotome. *Dev. Dyn.* **239**, 2898-2910.

Devoto, S. H., Stoiber, W., Hammond, C. L., Steinbacher, P., Haslett, J. R., Barresi, M. J. F., Patterson, S. E., Adiarte, E. G. and Hughes, S. M. (2006). Generality of vertebrate developmental patterns: evidence for a dermomyotome in fish. *Evol. Dev.* **8**, 101-110.

Galli, L. M., Knight, S. R., Barnes, T. L., Doak, A. K., Kadzik, R. S. and Burrus, L. W. (2008). Identification and characterization of subpopulations of Pax3 and Pax7 expressing cells in developing chick somites and limb buds. *Dev. Dyn.* **237**, 1862-1874.

Gomes de Almeida, P., Pinheiro, G. G., Nunes, A. M., Gonçalves, A. B. and Thorsteinsdóttir, S. (2016). Fibronectin assembly during early embryo development: A versatile communication system between cells and tissues. *Dev. Dyn.* **245**, 520-535.

Gonçalves, A. B., Thorsteinsdóttir, S. and Deries, M. (2016). Rapid and simple method for in vivo ex utero development of mouse embryo explants. *Differentiation* **91**, 57-67.

Goulding, M., Lumsden, A. and Paquette, A. J. (1994). Regulation of Pax-3 expression in the dermomyotome and its role in muscle development. *Development* **120**, 957-971.

Gozgit, J. M., Wong, M. J., Wardwell, S., Tyner, J. W., Loriaux, M. M., Mohemmad, Q. K., Narasimhan, N. I., Shakespeare, W. C., Wang, F., Druker, B. J., et al. (2011). Potent activity of ponatinib (AP24534) in models of FLT3-driven acute myeloid leukemia and other hematologic malignancies. *Mol. Cancer Ther.* **10**, 1028-1035.

Grass, S., Arnold, H. H. and Braun, T. (1996). Alterations in somite patterning of Myf-5-deficient mice: a possible role for FGF-4 and FGF-6. *Development* **122**, 141-50.

Gros, J., Manceau, M., Thomé, V. and Marcelle, C. (2005). A common somitic origin for embryonic muscle progenitors and satellite cells. *Nature* **435**, 954-958.

Gros, J., Scaal, M. and Marcelle, C. (2004). A two-Step mechanism for myotome formation in chick. *Dev. Cell* **6**, 875-882.

Hagel, M., Miduturu, C., Sheets, M., Rubin, N., Weng, W., Stransky, N., Bifulco, N., Kim, J. L., Hodous, B., Brooijmans, N., et al. (2015). First selective small molecule inhibitor of FGFR4 for the treatment of hepatocellular carcinomas with an activated FGFR4 signaling pathway. *Cancer Discov.* **5**, 424-437.

Han, J. K. and Martin, G. R. (1993) Embryonic expression of Fgf-6 is restricted to the skeletal muscle lineage. *Dev. Biol.* **158**, 549-554.

Hasty, P., Bradley, A., Morris, J. H., Edmondson, D. G., Venuti, J. M., Olson, E. N. and Klein, W. H. (1993). Muscle deficiency and neonatal death in mice with a targeted mutation in the myogenin gene. *Nature* **364**, 501-506.

Heinrich, M. C., Griffith, D., McKinley, A., Patterson, J., Presnell, A., Ramachandran, A. and Debiec-Rychter, M. (2012). Crenolanib inhibits the drug-resistant PDGFRα D842V mutattion associated with Imatinib-resistent gastrointestinal stromal tumors. *Clin. Cancer Res.* **18**, 4375-4384.

Hogan, B., Beddington, R., Costantini, F. and Lacy, E. (1986). Manipulating the mouse embryo. A laboratory manual. 332 pp. New York: Cold Spring Harbor Laboratory Press.

Ikeda, A., Abbott, R. L. and Langman, J. (1968). Muscle proteins in the chick myotome examined by the immunofluorescent method. *J. Embryol. Exp. Morphol.* **19**, 193-202.

Jostes, B., Walther, C. and Gruss, P. (1990). The murine paired box gene, Pax-7, is expressed specificially during the development of the nervous and muscle system. *Mech. Dev.* **33**, 27-38.

Kablar, B., Krastel, K., Ying, C., Asakura, a, Tapscott, S. J. and Rudnicki, M. a (1997). MyoD and Myf-5 differentially regulate the development of limb versus trunk skeletal muscle. *Development* **124**, 4729–4738.

Kahane, N., Cinnamon, Y. and Kalcheim, C. (1998). The origin and fate of pioneer myotomal cells in the avian embryo. *Mech. Dev.* **74**, 59-73.

Kahane, N., Cinnamon, Y., Bachelet, I. and Kalcheim, C. (2001). The third wave of myotome colonization by mitotically competent progenitors: regulating the balance between differentiation and proliferation during muscle development. *Development* **128**, 2187-2198.

Kalcheim, C. (2015). Epithelial-mesenchymal transitions during neural crest and somite development. *J. Clin. Med.* **5**, E1.

Kassar-duchossoy, L., Giacone, E., Gayraud-morel, B., Jory, A., Gomès, D. and Tajbakhsh, S. (2005). Pax3/Pax7 mark a novel population of primitive myogenic cells during development. *Genes Dev.* **19**, 1426-1431.

Kassar-Duchossoy, L., Gayraud-Morel, B., Gomès, D., Rocancourt, D., Buckingham, M., Shinin, V. and Tajbakhsh, S. (2004). Mrf4 determines skeletal muscle identity in Myf5:Myod double-mutant mice. *Nature* **431**, 466-471.

Kaufman, S. J. (1982). Membrane events during myogenesis. In "Muscle development: molecular and cellular control". Pearson, M. L. and Epstein, H. F. (Eds), 1st ed. pp271-280. Cold Spring Harbor Laboratory, Cold Spring Harbor, New York.

Kaul, A., Köster, M., Neuhaus, H. and Braun, T. (2000). Myf-5 Revisited. *Cell* **102**, 17–19.

Lacosta, A. M., Muniesa, P., Ruberte, J., Sarasa, M. and Domínguez, L. (2005). Novel expression patterns of Pax3/Pax7 in early trunk neural crest and its melanocyte and non-melanocyte lineages in amniote embryos. *Pigment Cell Res.* **18**, 243-251.

Lagha, M., Kormish, J. D., Rocancourt, D., Manceau, M., Epstein, J. A., Zaret, K. S., Relaix, F. and Buckingham, M. E. (2008). Pax3 regulation of FGF signaling affects the progression of embryonic progenitor cells into the myogenic program. *Genes Dev.* **22**, 1828-1837.

Marics, I., Padilla, F., Guillemot, J., Scaal, M. and Marcelle, C. (2002). FGFR4 signaling is a necessary step in limb muscle differentiation. *Development* **129**, 4559-4569.

Martins, G. G., Rifes, P., Amaândio, R., Rodrigues, G., Palmeirim, I. and Thorsteinsdóttir, S. (2009). Dynamic 3D cell rearrangements guided by a fibronectin matrix underlie somitogenesis. *PLoS One* **4**, e7429.

Mercola, M., Wang, C. Y., Kelly, J., Brownlee, C., Jackson-Grusby, L., Stiles, C. and Bowen-Pope, D. (1990). Selective expression of PDGF A and its receptor during early mouse embryogenesis. *Dev. Biol.* **138**, 114-122.

Mohammadi, M., McMahon, G., Sun, L., Tang, C., Hirth, P., Yeh, B. K., Hubbard, S. R. and Schlessinger, J. (1997). Structures of the tyrosine kinase domain of fibroblast growth factor receptor in complex with inhibitors. *Science* **276**, 955-960.

Mohammadi, M., Froum, S., Hamby, J. M., Schroeder, M. C., Panek, R. L., Lu, G. H., Eliseenkova, A. V, Green, D., Schlessinger, J. and Hubbard, S. R. (1998). Crystal structure of an angiogenesis inhibitor bound to the FGF receptor tyrosine kinase domain. *Embo J* **17**, 5896-5904.

Murdoch, B., DelConte, C. and García-Castro, M. I. (2012). Pax7 lineage contributions to the mammalian neural crest. *PLoS One* **7**, e41089.

Nabeshima, Y., Hanaoka, K., Hayasaka, M., Esumi, E., Li, S., Nonaka, I. and Nabeshima, Y. (1993). Myogenin gene disruption results in perinatal lethality because of severe muscle defect. *Nature* **364**, 532-534.

Niswander, L. and Martin, G. R. (1992). Fgf-4 expression during gastrulation, myogenesis, limb and tooth development in the mouse. *Development* **114**, 755-768.

Orr-Urtreger, A. and Lonai, P. (1992). Platelet-derived growth factor-A and its receptor are expressed in separate, but adjacent cell layers of the mouse embryo. *Development* **115**, 1045-1058.

Orr-Urtreger, A., Bedford, M. T., Do, M. S., Eisenbach, L. and Lonai, P. (1992). Developmental expression of the alpha receptor for platelet-derived growth factor, which is deleted in the embryonic lethal Patch mutation. *Development* **115**, 289-303.

Ott, M. O., Bober, E., Lyons, G., Arnold, H. and Buckingham, M. (1991). Early expression of the myogenic regulatory gene, myf-5, in precursor cells of skeletal muscle in the mouse embryo. *Development* **111**, 1097-1107.

Patapoutian, A., Yoon, J. K., Miner, J. H., Wang, S., Stark, K. and Wold, B. (1995). Disruption of the mouse MRF4 gene identifies multiple waves of myogenesis in the myotome. *Development* **121**, 3347-58.

Patton, B. L., Miner, J. H., Chiu, A. Y. and Sanes, J. R. (1997). Distribution and function of laminin in the neuromuscular system of developing, adult and mutant mice. *J. Cell Biol.* **139**, 1507-1521.

Pourquié, O. (2001). Vertebrate somitogenesis. *Annu. Rev. Cell Dev. Biol.* **17**, 311-350.

Pownall, M. E., Gustafsson, M. K. and Emerson, C. P. (2002). Myogenic Regulatory Factors and the Specification of Muscle Progenitors in Vertebrate Embryos. *Annu. Rev. Cell Dev. Biol.* **18**, 747-783.

Preibisch, S., Saalfeld, S. and Tomancak, P. (2009). Globally optimal stitching of tiled 3D microscopic image acquisitions. *Bioinformatics* **25**, 1463-1465.

Relaix, F., Rocancourt, D., Mansouri, A. and Buckingham, M. (2005). A Pax3/Pax7-dependent population of skeletal muscle progenitor cells. *Nature* **435**, 948-953.

Rescan, P.-Y. (2008). New insights into skeletal muscle development and growth in teleost fishes. *J. Exp. Zool. B. Mol. Dev. Evol.* **310**, 541-548.

Rodríguez-Burford, C, Oelschlager, D. K., Talley, L. I., Barnes, M, N., Partridge, E. E. and Grizzle, W. E. (2003). The use of dimethylsulfoxide as a vehicle in cell culture experiments using ovarian carcinoma cell lines. *Biotech. Histochem.* **78**, 17-21.

Rosatelli, A. L., Ravichandiran, K. and Agur, A. M. (2008). Three-dimensional study of the musculotendinous architecture of lumbar multifidus and its functional implications. *Clin. Anat.* **21**, 539-546.

Rudnicki, M. A., Schnegelsberg, P. N. J., Stead, R. H., Braun, T., Arnold, H. H. and Jaenisch, R. (1993). MyoD or Myf-5 is required for the formation of skeletal muscle. *Cell* **75**, 1351-1359.

Sassoon, D., Lyons, G., Wright, W. E., Lin, V., Lassar, A., Weintraub, H. and Buckingham, M. (1989). Expression of two myogenic regulatory factors myogenin and MyoD1 during mouse embryogenesis. *Nature* **341**, 303-307.

Sato, T. (1973). Innervation and morphology of the musculi levatores costarum longi. *Proc. Japan Acad.* **49**, 555-558.

Sato, T., Rocancourt, D., Marques, L., Thorsteinsdóttir, S. and Buckingham, M. (2010). A Pax3/Dmrt2/Myf5 regulatory cascade functions at the onset of myogenesis. *PLoS Genet.* **6**, e1000897.

Scaal, M. and Christ, B. (2004). Formation and differentiation of the avian dermomyotome. *Anat. Embryol. (Berl).* **208**, 411-424.

Scaal, M. and Wiegreffe, C. (2006). Somite compartments in anamniotes. *Anat. Embryol. (Berl).* **211**, 9-19.

Sieiro-Mosti, D., De La Celle, M., Pele, M. and Marcelle, C. (2014). A dynamic analysis of muscle fusion in the chick embryo. *Development* **141**, 3605-3611.

Smith, C. L. and Hollyday, M. (1983). The development and postnatal organization of motor nuclei in the rat thoracic spinal cord. *J. Comp. Neurol.* **220**, 16-28.

Smith, T. H., Kachinsky, A. M. and Miller, J. B. (1994). Somite subdomains, muscle cell origins, and the four muscle regulatory factor proteins. *J. Cell Biol.* **127**, 95-105.

Spörle, R. (2001). Epaxial-adaxial-hypaxial regionalisation of the vertebrate somite: Evidence for a somitic organiser and a mirror-image duplication. *Dev. Genes Evol.* **211**, 198-217.

Stark, K. L., McMahon, J. a and McMahon, a P. (1991). FGFR-4, a new member of the fibroblast growth factor receptor family, expressed in the definitive endoderm and skeletal muscle lineages of the mouse. *Development* **113**, 641-51.

Stickney, H. L., Barresi, M. J. and Devoto, S. H. (2000). Somite development in zebrafish. *Dev. Dyn.* **219**, 287-303.

Summerbell, D., Halai, C. and Rigby, P. W. J. (2002). Expression of the myogenic regulatory factor Mrf4 precedes or is contemporaneous with that of Myf5 in the somitic bud. *Mech. Dev.* **117**, 331-335.

Tajbakhsh, S. (2009). Skeletal muscle stem cells in developmental versus regenerative myogenesis. *J. Intern. Med.* **266**, 372-389.

Tajbakhsh, S. and Buckingham, M. E. (1994). Mouse limb muscle is determined in the absence of the earliest myogenic factor myf-5. *Proc. Natl. Acad. Sci. U. S. A.* **91**, 747-51.

Tajbakhsh, S. and Buckingham, M. (2000). The birth of muscle progenitor cells in the mouse: spatiotemporal considerations. *Curr. Top. Dev. Biol.* **48**, 225-268.

Tajbakhsh, S., Rocancourt, D. and Buckingham, M. (1996). Muscle progenitor cells failing to respond to positional cues adopt non- myogenic fates in myf-5 null mice. *Nature* **384**, 266-270.

Tajbakhsh, S., Rocancourt, D., Cossu, G. and Buckingham, M. (1997). Redefining the genetic hierarchies controlling skeletal myogenesis: Pax- 3 and Myf-5 act upstream of MyoD. *Cell* **89**, 127–138.

Tallquist, M. D., Weismann, K. E., Hellstrom, M. and Soriano, P. (2000). Early myotome specification regulates PDGFA expression and axial skeleton development. *Development* **127**, 5059-5070.

Teboul, L., Hadchouel, J., Daubas, P., Summerbell, D., Buckingham, M. and Rigby, P. W. J. (2002). The early epaxial enhancer is essential for the initial expression of the skeletal muscle determination gene Myf5 but not for subsequent, multiple phases of somitic myogenesis. *Development* **129**, 4571-4580.

Venters, S. J., Thorsteinsdóttir, S. and Duxson, M. J. (1999). Early development of the myotome in the mouse. *Dev. Dyn.* **216**, 219-232.

Vinagre, T., Moncaut, N., Carapuço, M., Nóvoa, A., Bom, J. and Mallo, M. (2010). Evidence for a Myotomal Hox/Myf Cascade Governing Nonautonomous Control of Rib Specification within Global Vertebral Domains. *Dev. Cell* **18**, 655-661.

Williams, L. W. (1910). The somites of the chick. *Am. J. Anat.* **11**, 55-100.

Winckler, G. (1948). Les muscles profonds du dos chez de l´homme. Etude analytique de leur structure et de leur innervation. *Arch. Anat. Histol. Embryol.* **31**, 3-57.

Wood, W. M., Etemad, S., Yamamoto, M. and Goldhamer, D. J. (2013). MyoD-expressing progenitors are essential for skeletal myogenesis and satellite cell development. *Dev. Biol.* **384**, 114-127.

Yablonka-Reuveni, Z., Danoviz, M. E., Phelps, M. and Stuelsatz, P. (2015). Myogenic-specific ablation of Fgfr1 impairs FGF2-mediated proliferation of satellite cells at the myofiber niche but does not abolish the capacity for muscle regeneration. *Front. Aging Neurosci.* **7**, 1-16.

Yamaguchi, T. P., Conlon, R. a and Rossant, J. (1992). Expression of the fibroblast growth factor receptor FGFR-1/flg during gastrulation and segmentation in the mouse embryo. *Dev. Biol.* **152**, 75-88.

Supplementary Figures

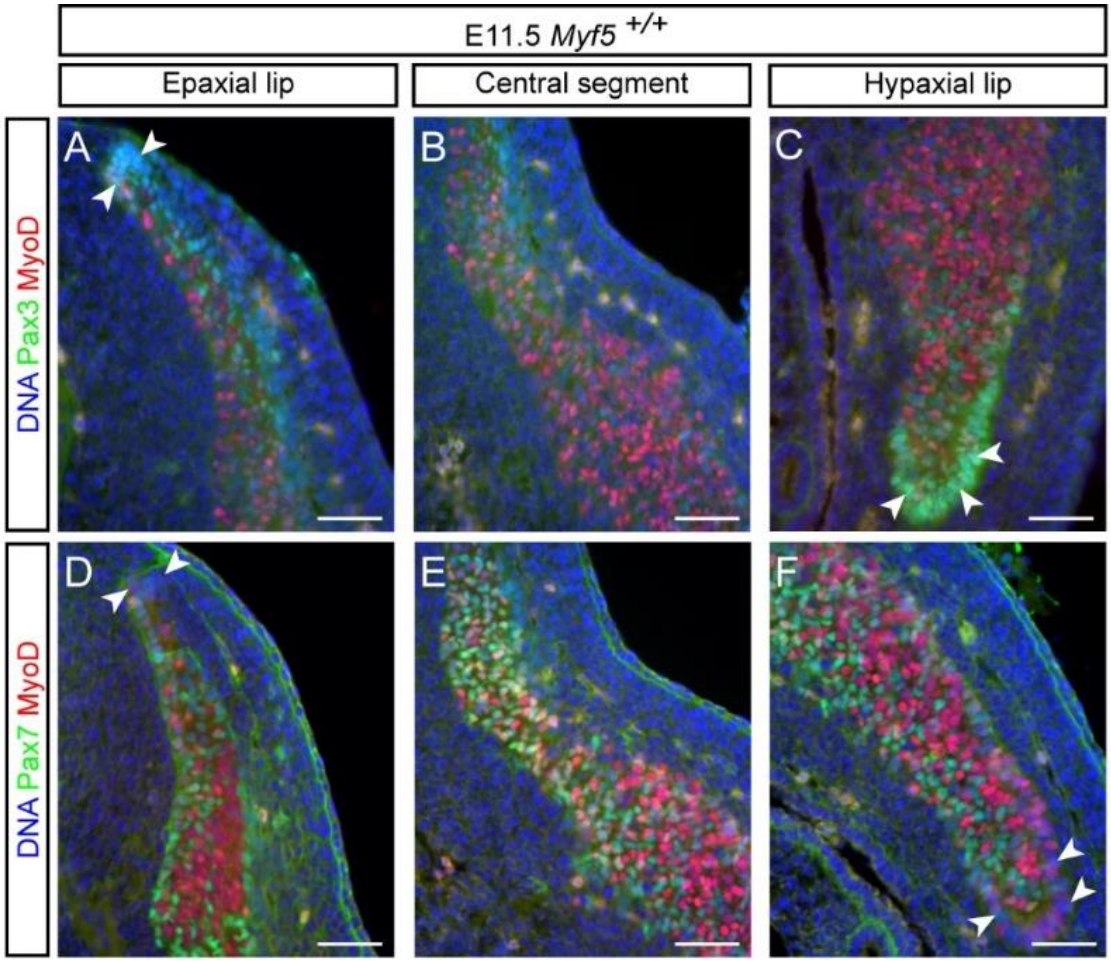

Supplementary Figure 3.1: Differential distribution of Pax3- and Pax7-positive MuSCs in E11.5 wild type embryos. Cryosectioned interlimb segments (DMM 4) of E11.5 *Myf5*$^{+/+}$ embryos showing their epaxial (A, D), central (B, E) and hypaxial regions (C, F) immunolabelled with antibodies against Pax3 (green in A, B, C), Pax7 (green in D, E, F) and MyoD (red in A-F), with DAPI staining (DNA; blue in A-F). **A-C:** After the dissociation of the central dermomyotome only a few Pax3-positive MuSCs are detected in the myotome (B), while a big proportion remain epithelial in both the epaxial and hypaxial dermomyotomal lips (arrowheads in A, C). **D-F:** In contrast, the majority of Pax7-positive MuSCs are dispersed within the myotome, among the MyoD-positive myoblasts, throughout the segment (D-F). Pax7-positive cells are relatively rare in the dermomyotomal lips (arrowheads in D, F). Dorsal is up and medial on the left. ep: epaxial; hyp: hypaxial; nt: neural tube. Scale bars: 50 µm.

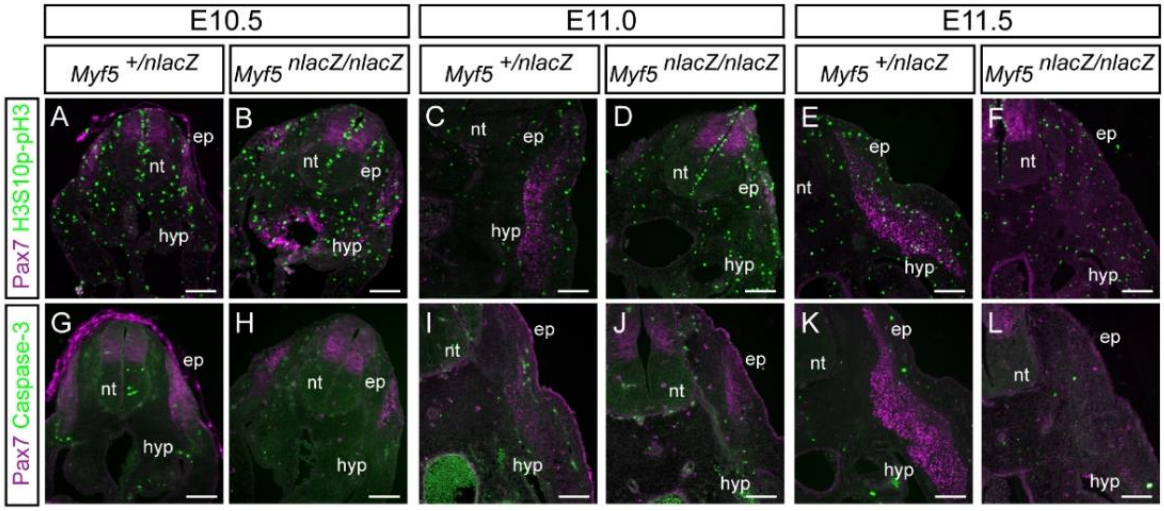

Supplementary Figure 3.2: Proliferation and apoptosis assays in *Myf5*$^{+/nlacZ}$ and *Myf5*$^{nlacZ/nlacZ}$ embryos.
Transverse interlimb cryosections of *Myf5*$^{+/nlacZ}$ (A, C, E, G, I, K) and *Myf5*$^{nlacZ/nlacZ}$ embryos (B, D, F, H, J, L) at E10.5 (A, B, G, H), E11.0 (C, D, I, J) and E11.5 (E, F, K, L). Embryos were immunolabelled with antibodies against Pax7 (magenta; A-L), H3S10p-pH3 (green; A-F) and cleaved caspase-3 (green; G-L). No difference in cell proliferation or apoptosis can be detected in the dermomyotome/myotome area of *Myf5*$^{+/nlacZ}$ and *Myf5*$^{nlacZ/nlacZ}$ embryos. Dorsal is up and medial on the left. ep: epaxial; hyp: hypaxial; nt: neural tube. Scale bars: 100 µm.

Chapter 4

Extracellular matrix dynamics during axial muscle development: distinct roles for laminins, fibronectin and tenascin-C?

Extracellular matrix dynamics during axial muscle development: distinct roles for laminins, fibronectin and tenascin-C?

André B. Gonçalves[a,b], Marianne Deries[a] and SólveigThorsteinsdóttir[a,b].

[a] Centro de Ecologia, Evolução e Alterações Ambientais, Departamento de Biologia Animal, Faculdade de Ciências, Universidade de Lisboa, 1749-016 Lisboa, Portugal.

[b] Instituto Gulbenkian de Ciência, 2781-901 Oeiras, Portugal

Contribution for the publication:

	Experimental work depicted in Fig.					Manuscript writing
	4.1	4.2	4.3	4.4	4.5	
Design and concept	II	III	III	III	III	III
Execution	II	III	III	III	III	
Analysis and interpretation	III	III	III	III	III	

Legend:

- ..... non-applicable
O ..... no intervention
I ..... minor contribution
II ..... moderate contribution
III .... major contribution/full execution

Note: this contribution does not exclude other contributions, similar or not, from the remaining authors

Abstract

Developing and adult skeletal muscle is surrounded by an extracellular matrix (ECM) including that of its connective tissue such as tendons. However, little is known about how the ECM affects the behaviour and maintenance of muscle stem cells (MuSCs) during development. Thus, we studied the spatial relationship between laminin, fibronectin and tenascin-C matrices and MuSCs, from their origin in the dermomyotome until they invade the first embryonic skeletal muscle, the epaxial myotome. For this we used 3D analysis of images obtained from whole mount immunohistochemistry of wild type mouse embryos. We demonstrate that each type of ECM exhibits a distinct distribution pattern which suggests they may have specific roles in MuSC delamination and colonisation of the myotome. Our data set the stage for studying how MuSC-ECM interactions contribute towards proper muscle development.

Keywords: Extracellular matrix; Muscle stem cells; Myotome; Laminin, Fibronectin, Tenascin-C; Mouse embryo.

Introduction

The extracellular matrix (ECM) is a non-cellular three-dimensional (3D) macromolecular network composed of proteoglycans and fibrous proteins that can bind to each other (Järveläinen et al., 2009; Schaefer and Schaefer, 2010). Fibrous proteins are predominantly glycoproteins, including laminins, fibronectin, collagens, elastins and tenascins (Alberts et al., 2007), which provide physical adhesive scaffolds for cells. Cell-ECM communications via cell surface receptors can trigger a variety of intracellular signal transduction pathways and cytoskeletal reorganisation (Harburger and Calderwood, 2009; Humphries et al., 2006). ECMs have been shown to affect not only differentiated cells in a variety of tissues, but also provide an environment regulating stem cell behaviour (Gattazzo et al., 2014). In this study, we focus on determining the distribution patterns of laminin, fibronectin and tenascin matrices during epaxial (deep back) muscle development and in particular their relationship with skeletal muscle progenitor cells, also called muscle stem cells (MuSCs).

All muscles of the body derive from the epithelial somites of the paraxial mesoderm which mature into several compartments originating different tissues. Ventrally, each somite forms the mesenchymal sclerotome, which gives rise to the axial skeleton, while the dorsal part of the somite stays epithelial and forms the dermomyotome (Christ et al., 2007). The dermomyotome contains progenitors for several mesodermal cell types, including embryonic muscle stem cells (MuSCs) (Ben-Yair and Kalcheim, 2005; Seale et al., 2008). Dermomyotomal MuSCs are the progenitor pool of trunk and limb skeletal muscles and are characterised by the expression of the transcription factors Pax3 and/or Pax7 (Buckingham, 2006). During early stages of myogenesis in the somites, MuSCs delaminate from the dermomyotome in synchronous waves to form the myotome, the third somitic compartment and first muscle to develop in the embryo. The last compartment to differentiate is the syndetome, the anlagen of axial tendon. This compartment is localised between the myotome and the sclerotome and its development depends on specific signals produced by the myotomal myocytes (Brent et al., 2003).

In the mouse embryo, myogenesis is first triggered in the epaxial lip (the dorso-medial lip or DML) of the dermomyotome by signals from axial tissues (Buckingham, 2006; Deries and Thorsteinsdóttir, 2016; Tajbakhsh, 2009). MuSCs in the epaxial lip upregulate *Myf5* at E8.0 (Ott et al., 1991), de-epithelialize and colonise the epaxial (dorsal) myotome (Venters et al.,

1999). Subsequently, a second migratory wave from the hypaxial lip (the ventro-lateral lip or VLL) of the dermomyotome colonises the hypaxial (ventral) myotome and soon after, a third wave originating from the rostral and the caudal lips forms myocytes that increase the thickness of the myotome (Gros et al., 2004; Venters et al., 1999). In the myotome, MuSCs express the myogenic regulatory factors, Myf5, Mrf4, MyoD and Myogenin to differentiate into mononucleated, postmitotic myocytes that express muscle structural proteins such as desmin and myosin heavy chain (MHC). Near the end of myotome development (E11.0), myocytes start to fuse with each other and with myoblasts to form multinucleated myotubes (Ben-Yair and Kalcheim, 2005; Hollway and Currie, 2005). Between E10.5 and E11.5, the central portion of the dermomyotome de-epithelializes releasing a fourth wave of MuSCs into the myotome. These MuSCs can either proceed to myogenic differentiation or remain undifferentiated and proliferative, forming a muscle stem cell reservoir for embryonic, foetal and postnatal growth and which gives rise to the satellite cells of the adult (Ben-Yair and Kalcheim, 2005; Gros et al., 2005; Kassar-Duchossoy et al., 2005; Relaix et al., 2005). Between E11.5 and E12.5, the epaxial (dorsal) myotome transforms into four epaxial (deep back) muscle groups including the most dorsal, the transversospinalis muscle group (Deries et al., 2010), whereas the hypaxial myotome forms hypaxial (abdominal and intercoastal) muscles (Christ et al., 1983; Kalcheim et al., 1999). All these events are accompanied by dynamic changes in the surrounding ECM. Indeed, ECM containing laminin, fibronectin and tenascin-C exhibit specific dynamic distribution patterns during mouse epaxial myogenesis (Bajanca et al., 2006; Cachaço et al., 2005; Deries et al., 2012; Nunes et al., 2017) and some of these matrices have been shown to play specific roles during myogenesis in the somites (Bajanca et al., 2006).

Basement membranes of all tissues contain laminin matrices (Durbeej, 2010). The epithelial dermomyotome is surrounded dorsally by its laminin-containing basement membrane and ventrally the myotome assembles its own basement membrane which makes a physical border with the sclerotome (Anderson et al., 2009; Bajanca et al., 2006; Tajbakhsh et al.,1996). Then, from E11.5, dermomyotomal and myotomal laminin matrices are disassembled and are not assembled again before the end of primary myogenesis (E14.5) after which each myotube is progressively wrapped with a laminin basement membrane (Cachaço et al., 2005; Deries et al., 2012; Nunes et al., 2017).

Fibronectin, which can form both pericellular and interstitial matrices, is the most abundant ECM glycoprotein in the early embryo. It supports cell adhesion, migration and growth and interacts with collagens, tenascins and other molecules of the ECM (Hynes, 1992;

Rozario and DeSimone, 2010; Zollinger and Smith, 2017). Fibronectin surrounds the somites and as somites mature, it is present at somitic boundaries and forms thick cables within the myotome (Deries et al., 2012).

Tenascins are modular hexadimeric proteins of the interstitial matrix that can associate with fibronectin (Hsia and Schwarzenbauer, 2005). Tenascin-C, the most abundant and well-studied tenascin isoform during development, has a restricted and often transient distribution pattern in the embryo (Jones and Jones, 2000; Riou et al., 1992). It is particularly enriched at intersegmental borders from which cables of tenascin-C matrix extend into the myotome, lying parallel to the myotomal myocytes (Deries et al., 2012). Later in development it becomes confined to tissues bearing tensile and mechanical stress, specifically in tendons, ligaments and smooth muscles (Chiquet-Ehrismann et al., 2014).

Although an increase knowledge exists underlying the importance of the ECM during skeletal muscle differentiation, little is known about its effect on the identity and behaviour of MuSCs. In this work, we carefully describe the spatial relationship between Pax3/Pax7-positive MuSCs and laminin, fibronectin and tenascin-C ECMs using wild type embryos during development of the epaxial myotome/muscles in the mouse embryo. We found that each of the studied ECM is in a position compatible with playing a role in the regulation of MuSCs.

Materials and Methods

Mice and embryo collection

Outbred Hsd:ICR wild type adult mice (CD-1; Charles River Laboratories International, Inc.) were crossed to produce wild type mouse embryos (E10.5-E11.5). Dated pregnancies were obtained with the day of the vaginal plug designated embryonic day 0.5 (E0.5). Pregnant females were sacrificed by cervical dislocation after isoflurane anaesthesia. To define the different stages of dermomyotome and myotome development in our study we used a recently described dermomyotome/myotome (DMM) stage system (Deries et al., 2012).

All experiments and manipulations conducted on animals including housing, husbandry and welfare were performed according to the recommended guidelines provided by Direção

Geral de Alimentação e Veterinária (DGAV) and approved through protocol 3/2016 from the Animal Welfare Body (ORBEA) of the Faculty of Sciences of the University of Lisbon.

Immunohistochemistry

Immunohistochemistry experiments were carried out in whole embryos and were performed as described in Gonçalves et al. (2016). The diaphanization of the tissues was performed according to Martins et al. (2009).

Primary and secondary antibodies used in this work are listed in Table 4.1. The polyclonal antibody raised against laminin-111, which we designate pan-muscle laminin antibody, recognises all laminin isoforms containing α1-, β1- or γ1 chains (Paulsson, 1994). Since all laminin isoforms present in the dermomyotome and/or myotome basement membranes contain at least one of these chains (Bajanca et al., 2006; Borycki, 2013), this antibody was used to study the global laminin ECM pattern during the stages under study.

Image acquisition and analysis

Whole mount immunolabelled embryos were imaged using a Leica TCS SPE confocal microscope, producing stacks of images with a 0.5 mm z-step. To show the spatial distribution of the ECM components in a single somite/segment, confocal z-stacks were analysed and three-dimensionally reconstructed and rendered using the Amira v5.3.3 software (Visage Inc.). For a better appreciation of the relationship between the ECM and the MuSCs, snapshots were taken of each 3D reconstructed somite or epaxial segment from a dorsal, ventral, transversal and frontal view. Figure 4.1 shows an illustrative scheme depicting the orientation of samples in each view as well as the observer´s point of view. Digital close-ups of the same 3D reconstructed somite are displayed next to the overviews of each whole-mount immunostaining. One individual segment and its associated matrix was then isolated by digital manual segmentation of the confocal z-stacks (i.e. “digitally erasing” the rest of the photograph).

Table 4.1: Primary and secondary antibodies used for immunohistochemistry.
DSHB: Developmental Studies Hybridoma Bank.

Antibody type	Name	Clone/Catalog	Company	Dilution
Primary antibodies	Pax3	Pax3	DSHB	Supernatant 1:20
	Pax7	Pax7	DSHB	1:50
	Laminin	L-9393	Sigma-Aldrich	1:400
	Tenascin-C	LAT-2	Gift from Arnoud Sonnenberg	1:25
	Human plasma fibronectin	F-3648	Sigma-Aldrich	1:400
Secondary antibodies	Alexa Fluor 488-conjugated goat anti mouse IgG F(ab´)2 fragments	A-11017	Life Technologies	1:500
	Alexa Fluor 568-conjugated goat anti rat IgG F(ab´)2 fragments	A-11077	Life Technologies	1:500
	Alexa Fluor 633-conjugated goat anti rabbit IgG F(ab´)2 fragments	A-21070	Life Technologies	1:500

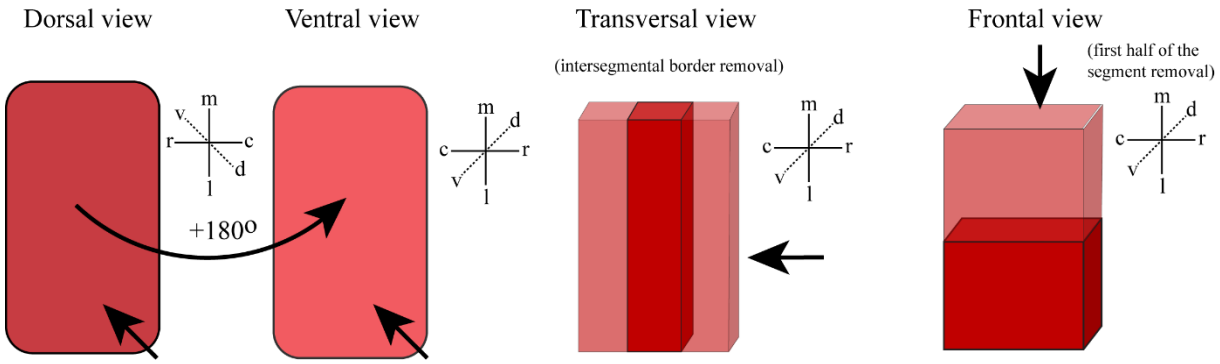

Figure 4.1: Different views of 3D reconstruction of one segment.
Scheme showing the observation points (arrows) and the orientation of the 3D reconstructed somite for each view. For a better visualisation of the distribution of the ECM inside the somite, the intersegmental borders and the first half of the segment (pink 3D boxes) were digitally removed in transverse and frontal planes, respectively. m-medial; l-lateral; v-ventral; d-dorsal; r-rostral; c-caudal.

Results and Discussion

Extracellular matrix 3D organisation in the somite and its relationship with the dermomyotomal MuSCs

To address how dermomyotomal MuSCs interact with the ECM we analysed the 3D spatial organisation of MuSCs in relation to laminin, fibronectin and tenascin-C matrices. We first analysed these interactions at E10.5 (DMM3; see Materials and Methods), a stage at which the central dermomyotome is still epithelial, but a few individual MuSCs have started to drop into epaxial myotome from the central dermomyotome (Relaix et al 2005). E10.5 wild type mouse embryos were immunolabelled with antibodies against Pax3 and Pax7, to mark the embryonic MuSCs, combined with antibodies against laminin, fibronectin and tenascin-C. The embryos were processed as whole mounts and then analysed at forelimb level. The results are displayed in Figs. 4.2 and 4.3.

At E10.5, dermomyotomal Pax3/Pax7 positive cells are contained by a discontinuous laminin basement membrane which lines their basal side (Fig. 4.2A, Aii, C, Cii, D, Dii, E, Eii; also see Deries et al., 2012). Small laminin patches extend from the dermomyotome basement membrane wrapping closely the lateral side of the MuSCs (Fig. 4.2G, Gii, Giii). Remarkably, tenascin-C immunostaining is also prominent near the basement membrane of the dermomyotome lining the epithelial MuSCs (Fig. 4.2A, Ai, C, Ci, D, Di, E, Ei, Eiii). The laminin basement membrane is discontinuous, thus permitting signals such as Wnt and Shh coming from the neural tube and notochord to trigger myogenesis (Borello et al. 2006; Borycki et al., 1999).

A thin fibronectin matrix fills the area between the dermomyotome and the ectoderm while fibronectin cables can be seen extending from the ectoderm, cross the dermomyotome and sometimes even reach the myotomal region (Fig. 4.3F, Fii, Fiii). It has been shown that cells in the ventral region of the epithelial somite (i.e. future sclerotomal cells) form filopodia which are supported by thick bundles of fibronectin ECM, called fibronectin pillars, and extend ventrally towards the notochord and the endoderm (Sato et al., 2017). Although the role of fibronectin in contact with the MuSCs of the dermomyotome is not known, it is possible that fibronectin cables observed in the dermomyotome also have a role in supporting the filopodia

of the dermomyotomal cells (Sagar et al., 2015). In fact, it is known that the dermomyotome is a very dynamic epithelium (Rios et al., 2011; Sagar et al., 2015).

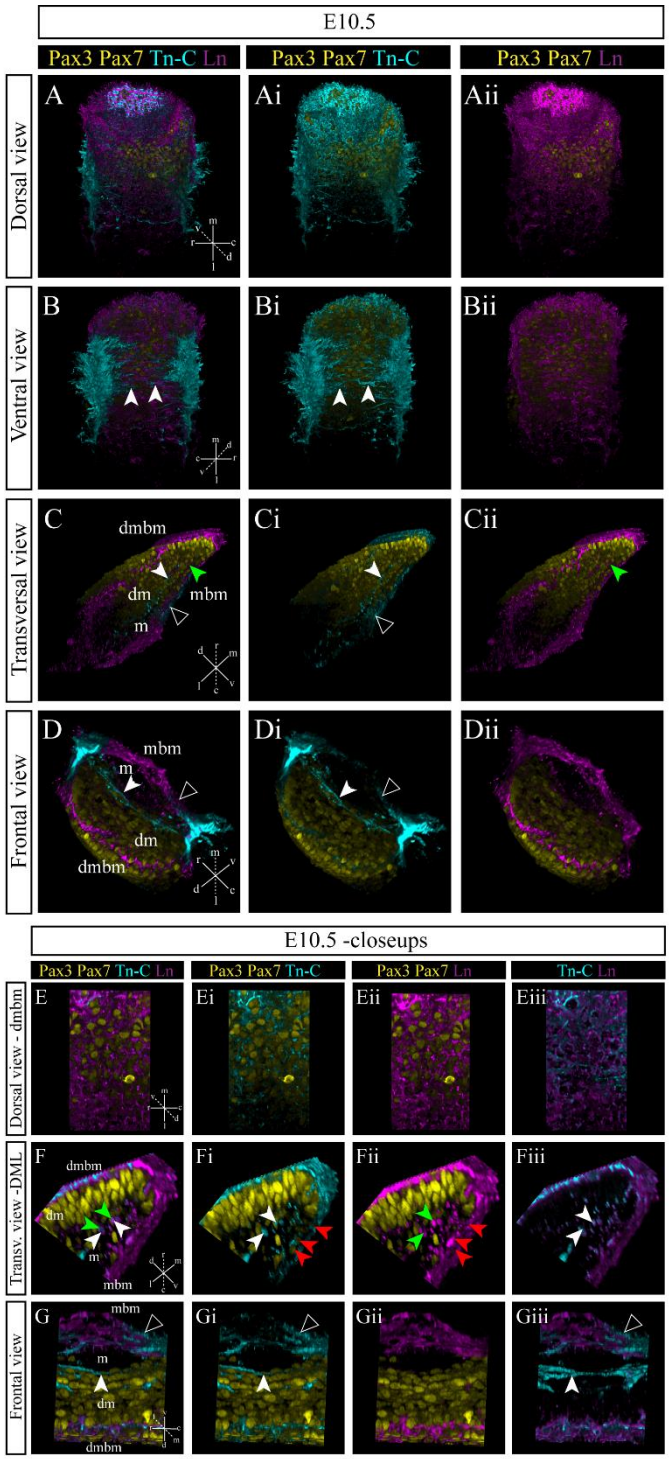

Figure 4.2: Tenascin-C appears to co-localise with laminin in the dermomyotomal and myotomal basement membranes during early myogenesis.
3D reconstruction and the respective close-ups of a E10.5 forelimb somite (DMM3), stained by whole mount immunofluorescence with antibodies against Pax3 and Pax7 (yellow), tenascin-C (Tn-C; cyan) and laminin (Ln; magenta). (**Continues next page**).

The apical side of epithelial Pax3/Pax7-positive dermomyotomal cells (i.e. the ventral part of the dermomyotome) are close to fibronectin (white arrowheads; Fig.4.3C, D, E, Eii) and tenascin matrices (arrowheads; Figs. 4.2C, Ci, D, Di; G, Gi, Giii; 4.3E, Ei, Eiii, F, Fi, Fiii) because these matrices extend cables that run in a rostro-caudal direction between the dermomyotome and the myotome (Deries et al., 2012). Even if at E10.5, MuSCs mostly enter the myotome through the lips of the dermomyotome (Venters et al., 1999), there are a few individual MuSCs that drop into the myotome from the central dermomyotomal sheet at this stage (Delfini et al; 2009; Relaix et al., 2005) which are in a position to use fibronectin and tenascin as adhesive substrates for this process. These cells will be more numerous as development proceeds until the central dermomyotome is completely dissociated. Fibronectin is known to be involved in the migration of a variety of cell types, including that of Pax3-positive cells into the limb buds in the chick (Brand-Saberi et al., 1993), that of mesenchymal stem cells to enhance vascular remodelling in combination with platelet-derived growth factors (Pdgfs) (Veevers-Lowe et al., 2011) and that of primordial germ cells (Fujimoto et al 1985; Huss et al., 2019), to name a few. Moreover, tenascin-C has been implicated in epithelial-to-mesenchymal transitions (EMTs) during development (Chiquet-Ehrismann et al., 2014; Giblin and Midwood, 2015; Yoshida et al., 2015). It is therefore tempting to suggest that these matrices may play a role in the movement of these MuSCs from the dermomyotome into the myotome.

Pax3/Pax7-positive MuSCs that have entered the myotome (Ben-Yair and Kalcheim, 2005; Gros et al., 2005; Kassar-Duchossoy et al., 2005; Relaix et al., 2005) become surrounded by laminin clusters (Fig. 4.2C, Cii, F, Fii). It is interesting to note that some other globular laminin clusters are localised in the area between the dermomyotome and myotome (green arrowheads; Fig.4.2 C, Cii, F, Fii), however, it is not known whether these laminins are produ-

---

(**Continued from previous page**). The segments are seen from a dorsal (A-Aii, E-Eiii), a ventral (B-Bii), a transversal (C-Cii, F-Fiii) or a frontal view (D-Dii, G-Giii). **A-Giii:** A thick laminin ECM surrounds the entire somite in a discontinuous pattern, forming the dermomyotomal basement membrane, (A, Aii, C, Cii, D, Dii, E, Eii, Eiii) and the myotomal basement membrane (B, Bii, C, Cii, D, Dii, F, Fii, Fiii G, Gii, Giii). Small patches of laminin are detected between the dermomyotome and the myotome and these are mostly concentrated in the epaxial domain intermingling with the MuSCs (green arrowheads in C, Cii, F, Fii). Tenascin-C is localised in two major places: 1) it is very abundant at the intersegmental borders, from where threads of tenascin extend in a the rostro-caudal direction, along the whole span of the somite (arrowheads in B, Bi; G, Gi, Giii) and 2) it surrounds the entire somite, being enriched in or near the dermomyotomal and myotomal basement membrane (A, Ai, B, Bi, C, Ci, E, Ei, Eiii, F, Fi, Fiii, G, Gi, Giii). The tenascin matrix threads that extend from the intersegmental borders are located close to the myotomal basement membrane (open arrowheads in C, Ci, D, Di, G, Gi, Giii), as well as within the area between the dermomyotome and the myotome (white arrowheads in C, Ci, D, Di, F, Fi, Fiii, G, Gi, Giii). MuSCs that are entering the myotome are surrounded by small patches of tenascin-C and fibronectin (red arrowheads in Fi, Fii). d: dorsal; v: ventral; m: medial; l: lateral; r: rostral; c: caudal; d: dermomyotome; m: myotome; dmbm: dermomyotome basement membrane; mbm: myotome basement membrane. Spatial scales are not shown because they do not account for perspective visualisation. Average medio-lateral length of a E10.5 forelimb somite: 150-180 µm (Tam, 1981).

---

ced by the dermomyotomal or myotomal cells. Laminin fragments have been studied *in vitro* in embryonic stem cells and in cancer cells and in both these systems it has been shown that they have functional roles (Horejs et al., 2014; Kikkawa et al., 2013) including a role in promoting EMTs. It would be interesting to address whether the clusters of laminin that are present in the segments are in fact fragments with functional roles.

The basement membrane of the myotome, which is on the ventral side of the myotome, is made of a discontinuous laminin matrix (Deries et al., 2012) and the MuSCs within the myotome are close to this basement membrane (Fig. 4.2F, Fii, G, Gii). Interestingly, delaminating MuSCs from the epaxial lip of the dermomyotome seem to use this myotomal basement membrane to slide-through the central myotome associated with the myotomal basement membrane (red arrowheads; Fig. 4.2Fi, Fii), suggesting that the myotomal basement membrane might be important for the maintenance of MuSCs. A similar pattern was seen for committed cells coming from the rostral and caudal lips; these cells, which have just upregulated Myf5, are the ones closest to the basement membrane, while Myogenin-positive cells were further from the basement membrane (Bajanca et al., 2006).

Both fibronectin and tenascin matrices are abundant at the segmental borders (Figs.4.2 A, Ai, B, Bi, D, Di, G, Gi, Giii; 4.3A, B, D; Deries et al., 2012). Apart from extending between the dermomyotome and myotome, they also extend cables that line the ventral side of the myotome (arrowheads; Figs 4.2B, Bi; 4.3B). Moreover, as observed for the dermomyotomal basement membrane, tenascin-C is also observed in association with the myotomal basement membrane (open arrowheads; Fig. 4.2C, Ci, D, Di), and it is most predominant at the rostral and caudal edges of the myotome (open arrowheads; Fig. 4.2G, Gi, Giii), where fibronectin is also detected (Fig. 4.3E, Eii, Eiii). According to the model proposed by Venters et al. (1999) the mammalian myotome grows in a dorso-medial to a ventro-lateral direction. Therefore, differentiated myocytes located in the central myotome (i.e. in the middle of the segment in the dorso-ventral direction) are older than those of the dorsal-most domain. Thus, the differences in the complexity of the myotomal basement membrane as well as whether it associates with fibronectin and tenascin-C matrices might provide distinct environments for the MuSCs. However, exactly what role these different matrices play within the myotome remains to be elucidated.

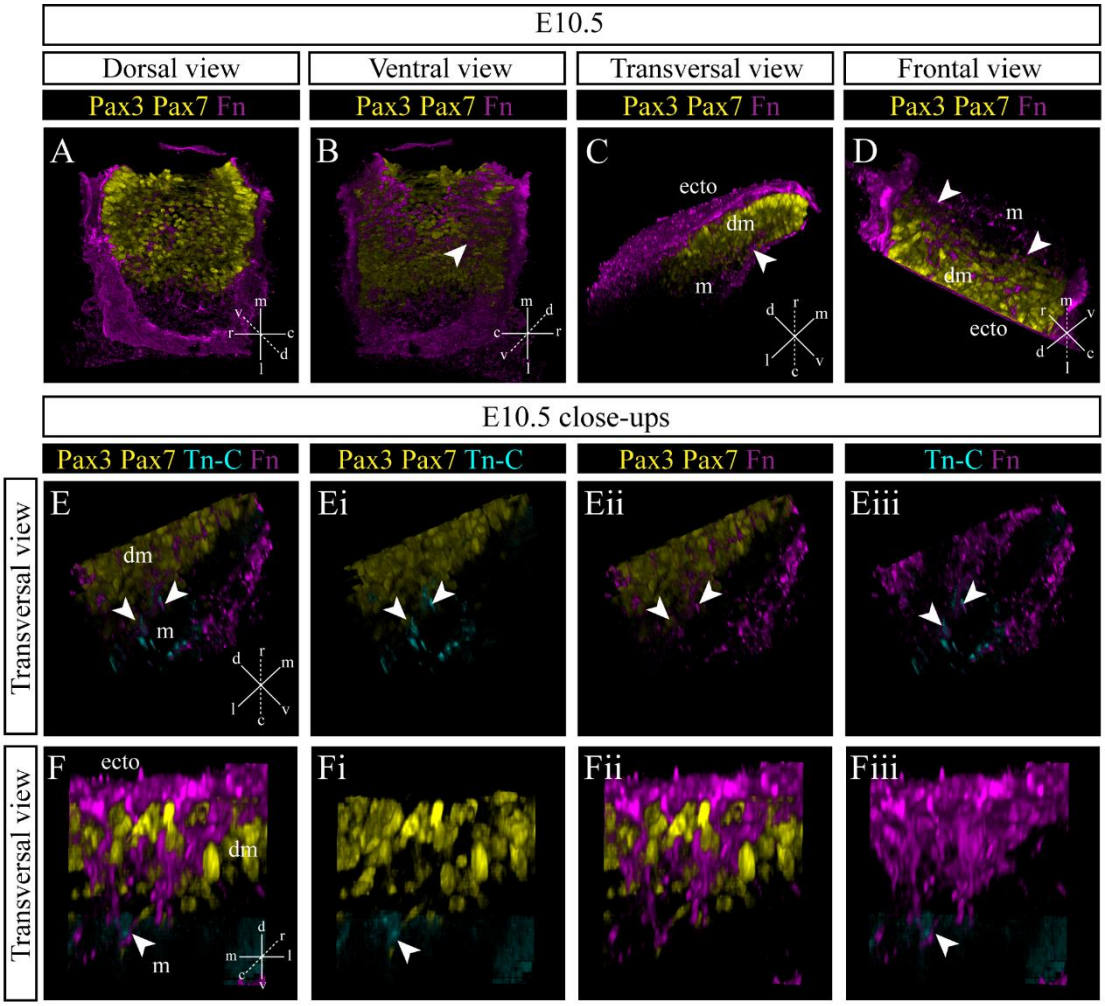

Figure 4.3: Fibronectin accumulates between the dermomyotome and the myotome before the delamination of the dermomyotomal MuSCs.
3D reconstruction of a E10.5 forelimb somite (DMM3), stained by whole mount immunofluorescence with antibodies against Pax3 and Pax7 (yellow), fibronectin (Fn; magenta) and tenascin-C (Tn-C; cyan). To visualise the somite, the fibronectin ECM lining the ectoderm was removed in the dorsal (A), ventral (B), transversal (C, E-Eiii) and frontal views (D). **A-D:** Fibronectin is abundant in the intersegmental borders (A, B). Fibronectin fibrils extend from these borders in a rostro-caudal direction along the ventral side of the somite (arrowhead in B) and at the dermomyotome/myotome interface (arrowheads in C, D). **E-Fiii:** Close-ups of the same 3D reconstructed forelimb somite. Fibronectin patches at the dermomyotome/myotome interface also extend along the medio-lateral axis of the dermomyotome (arrowheads in E, Eii). Some of these patches also contain tenascin-C and appear to surround the dermomyotomal MuSCs that are close to the myotome (arrowheads in E, Ei, Eiii). Dorsally, fibronectin matrix forms thick cables which connect to the ectoderm, penetrate the dermomyotome basement membrane and come to be in close contact with the MuSCs inside the dermomyotome (aarowheads in F, Fii, Fiii). Tenascin-C is deposited between the dermomyotome and the myotome region but does not protrude in the medio-lateral direction into the dermomyotome or myotome (F, Fi). Also, tenascin-C is close to the apical side of epithelial Pax3/Pax7-positive dermomyotomal cells (arrowheads in F, Fi, Fiii). d: dorsal; v: ventral; m: medial; l: lateral; r: rostral; c: caudal; ecto: ectoderm; dm: dermomyotome; m: myotome. Spatial scales are not shown because the 3D visualisation of Amira Software is incompatible with precise and correct scales. Average medio-lateral length of a E10.5 forelimb somite: 150-180 µm (Tam, 1981).

Relationship of myotomal MuSCs with the extracellular matrix

At E11.5 (DMM4), the central dermomyotome has de-epithelialized completely and all its MuSCs have entered the myotome and are intermingled among the myotomal myocytes (Ben-Yair and Kalcheim, 2005; Gros et al., 2005; Kassar-Duchossoy et al., 2005; Relaix et al., 2005). We analysed the relationship between these Pax3- and/or Pax7-positive MuSCs and laminin, fibronectin and tenascin-C matrices in whole epaxial interlimb segments at E11.5 (Figs. 4.4, 4.5). As in the previous stage, images of immunolabelled whole mounts were reconstructed and displayed in different views (Fig. 4.1) and at different digital magnifications.

The laminin matrix which lined the central part of the dermomyotome at E10.5 has now been disassembled and only the epaxial and hypaxial lips of the dermomyotome remain epithelial with their laminin basement membrane intact (Fig. 4.4.A, Aii, B, Bii, C, Cii; Deries et al., 2012; Tajbakhsh and Buckingham, 2000). The laminin matrix around the epaxial lip forms a sort of pouch that encloses the last epaxial reservoir of undifferentiated dermomyotomal MuSCs (Fig. 4.4 D, Dii, E, Eii; Deries et al., 2012). It has been shown that the relationship between laminin and MuSCs is important to maintain their stemness. In fact, when the laminin receptor integrin α6β1 is blocked, there is a precocious myogenic differentiation in the dermomyotome (Bajanca et al., 2006). Therefore, the close contact of laminin with cells of the dermomyotome is not only to physically contain the epithelial state of the MuSCs but also to prevent them to differentiate. Interestingly, tenascin-C is detected around the epaxial pouch (Fig. 4.4 A, Ai, B, Bi, C, Ci, E, Ei) and remains close to the laminin matrix (Fig. 4.4Eiii) as it was a day earlier. It is thus tempting to speculate that it may give support to this remnant of an epithelium.

At this stage, the laminin matrix separating the myotome from the sclerotome is also mostly disassembled (Deries et al., 2012), but some small patches of laminin immunoreactivity remain inside the myotome (arrowheads; Fig. 4.4F, Fii). This disassembly of laminin ECM could possibly be important for the segregation and morphogenesis of the epaxial musculatures because it releases the myotomal myocytes from the constraints of the segment (Deries et al., 2012; Nunes et al., 2017). Although overall the fibronectin matrix seems to be more abundant dorsally while tenascin-C is more enriched ventrally (Fig. 4.5 C-Cii), both matrices form thick fibrils in the dorsal aspect of the myotome (Fig. 4.5A-Bii).

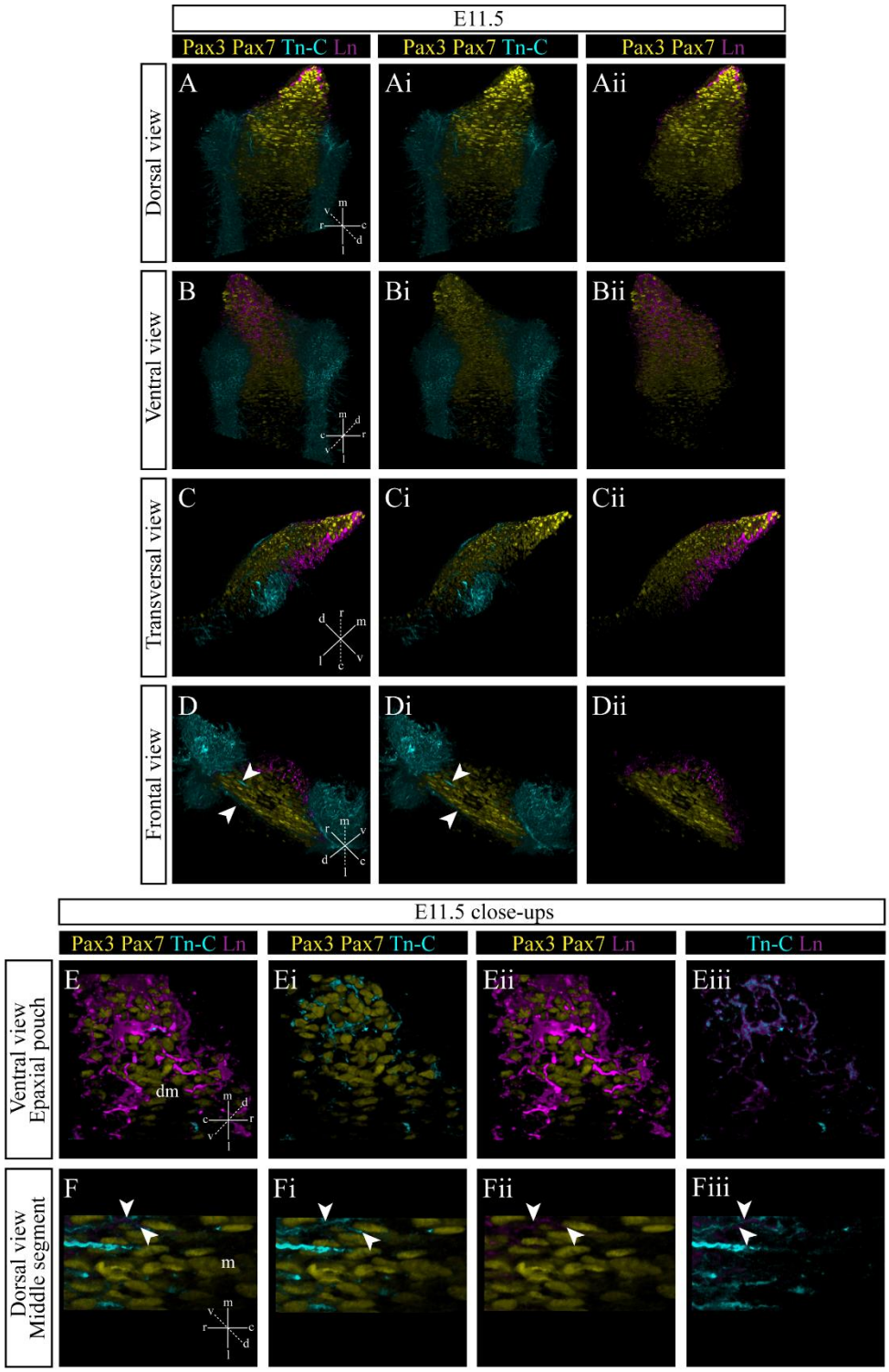

Figure 4.4: Laminin and tenascin matrices define the epaxial pouch that contains the MuSCs in the epaxial lip of the dermomyotome.
3D reconstructions overviews and close-ups of an interlimb epaxial segment from an E11.5 embryo (DMM4), stained in whole mount immunofluorescence with antibodies against Pax3 and Pax7 (yellow), tenascin-C (Tn-C; cyan) and laminin (Ln; magenta). The segment is displayed in a dorsal (A-Aii, F-Fiii), ventral (B-Bii, E-Eiii) transverse (C-Cii) or frontal view (D-Dii). **A-Fiii:** As the dermomyotome de-epithelializes, laminin is progressively disassembled and only remains the basement membrane lining the epaxial lip of the dermomyotome (A, Aii). (**Continues next page**).

Interestingly, tenascin-C is localised in the centre of the intersegmental border, while the fibronectin prevails closer to the myocytes (Fig. 4.5G-Giii). Fibronectin also appears to penetrate more deeply into the muscle segment (Fig. 4.5G-Giii).

Within the myotome, MuSCs appear to contact fibronectin and tenascin fibrils (arrowheads; Figs. 4.4 D, Di, F, Fi, Fiii, 4.5E-Eiii, F-Fiii). Fibronectin and tenascin-C interact with MuSCs during foetal development and aid their symmetric expansion (Tierney et al., 2016) and fibronectin plays a role in promoting the proliferation of activated satellite cells in the adult (Bentzinger et a., 2013). Whether the fibronectin and tenascin-C fibrils in the myotome play a similar role to regulate MuSCs fate inside the myotome is not known. To properly address this question, it would be interesting to inhibit fibronectin and tenascin-C fibrillogenesis in the myotome to investigate the effect on the proliferation, stemness or differentiation of its Pax3 and Pax7-positive MuSCs.

(**Continued from previous page**). Laminin ECM is predominantly enriched in the dorso-medial region of the segment, forming an epaxial pouch, containing the last reservoir of undifferentiated epithelial MuSCs (B, Bii, C, Cii, D, Dii, E, Eii, Eiii). Inside the myotome, laminin is practically absent, although rare laminin patches can be observed in the proximities of MuSCs (arrowheads in F, Fii, Fiii). Tenascin- C exhibits two distinct distribution patterns: 1) it continues to be highly enriched at the intersegmental borders (A, Ai, B, Bi, D, Di), from where thick cables run along the whole myotome length (A, Ai, B, Bi; arrowheads in D, Di) and 2), it is also, together with laminin matrix, localised in the epaxial pouch (A, Ai, B, Bi, C, Ci, E, Ei, Eiii). In the myotome, few patches of tenascin-C are also detected in close proximity with the MuSCs (arrowheads in F, Fi, Fiii). d: dorsal; v: ventral; m: medial; l: lateral; r: rostral; c: caudal; dm: dermomyotome; m: myotome. Oblique slices provided by the Amira software were manually oriented in the reconstructed 3D volumes as to be orthogonal to the embryo axes. For this reason, spatial scales are not shown, since they do not account for perspective visualisation. Average medio-lateral length of a E11.5 interlimb epaxial segment: 300-350 µm (Deries et al., 2010; Deries et al., 2012).

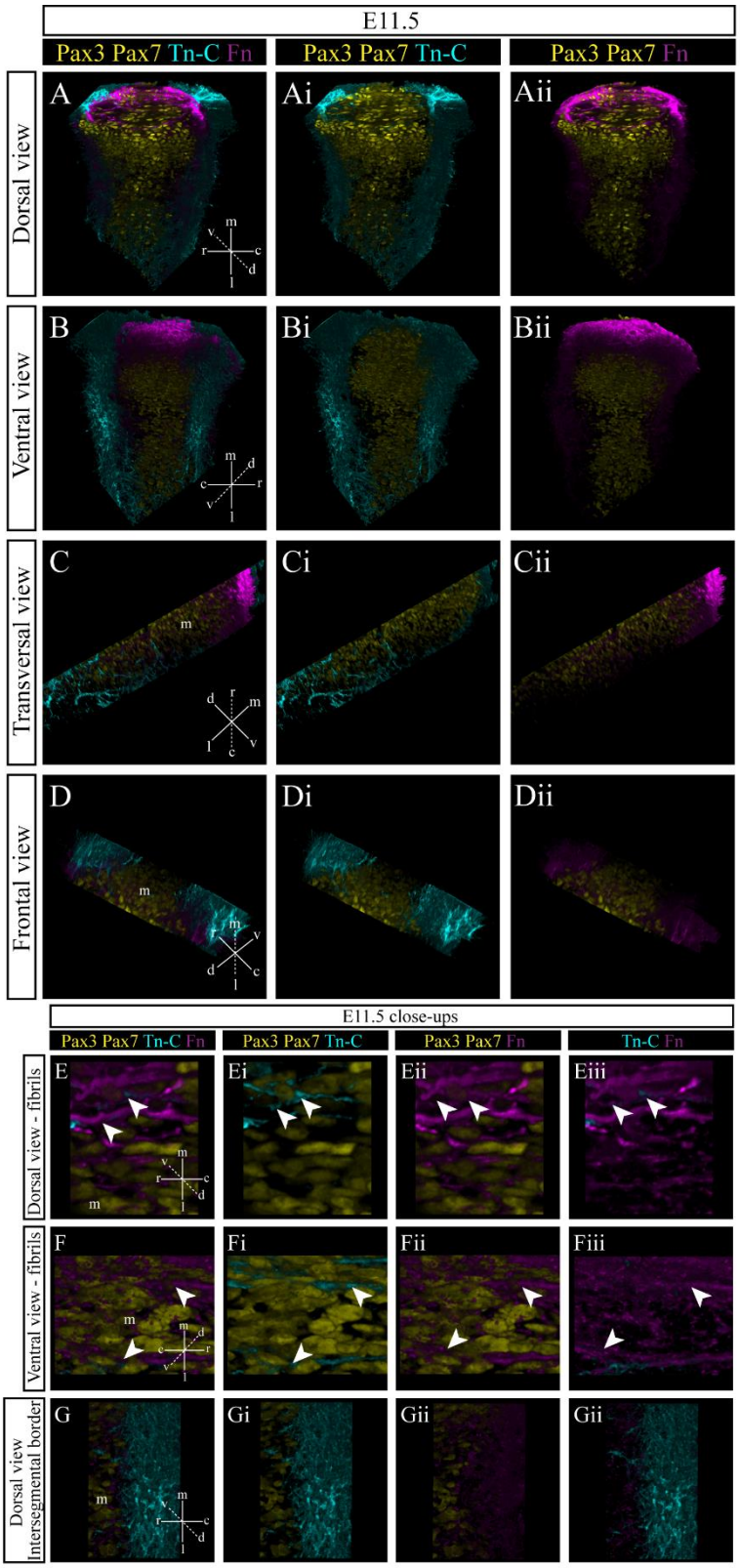

Figure 4.5 Fibronectin and tenascin-C are located in the proximity of myotomal MuSCs.
3D reconstruction and close-ups of an interlimb epaxial segment from an E11.5 embryo (DMM4), stained by whole mount immunofluorescence with antibodies against Pax3 and Pax7 (yellow), tenascin-C (Tn-C; cyan) and fibronectin (Fn; magenta). The segment is displayed in a dorsal (A-Aii, E-Eiii, G-Giii), a ventral (B-Bii, F-Fiii) transversal (C-Cii) or a frontal view (D-Dii). (**Continues next page**).

Conclusions

In this study, we highlight the distribution pattern of laminin, fibronectin and tenascin-C matrices during early stage of myogenesis and their relationship with MuSCs. Both the dermomyotomal and myotomal laminin basement membranes remain in close association with the delaminating MuSCs during their colonisation of the myotome. The spatial distribution of the fibronectin and tenascin-C matrices suggest a possible role in guiding dermomyotomal MuSCs towards the myotome before and during central dermomyotome dissociation. Finally, we unveil a previously undescribed pattern of tenascin-C distribution in the somites finding that it is located in close association with the basement membrane of both the dermomyotome and myotome. After the central dermomyotome dissociates, both laminin and tenascin-C form a pouch-like ECM around the epaxial dermomyotomal lip. This ECM might possibly contribute towards MuSCs maintenance in the dermomyotome.

(**Continued from previous page**). **A-Giii:** Both fibronectin and tenascin-C are accumulated at the intersegmental borders, from where thick fibrils elongate through the whole width of the segment (A-Aii, B-Bii). These thick fibrillar fibronectin and tenascin cables localise to the dorsal and ventral aspect of the myotome (A-Bii). While fibronectin accumulates more in the dorso-medial aspect of the segment, tenascin is enriched in the ventro-lateral region of the epaxial domain (C-Cii). Inside the myotome, tenascin fibrils are essentially localised to the dermomyotome/myotome interface (D-Dii). In opposition, fibronectin fibrils are widespread within the myotome and are close to the myotomal MuSCs (D-Dii). Interestingly, some fibrils appear to stain for both fibronectin and tenascin-C and are near some MuSCs (arrowheads in E-Fiii). A close examination of the tenascin-C and fibronectin matrices at the intersegmental borders shows that tenascin-C is enriched in the middle of the intersegmental borders, while fibronectin is localised closer to the myotome (G-Giii). d: dorsal; v: ventral; m: medial; l: lateral; r: rostral; c: caudal; dm: dermomyotome; m: myotome. Spatial scales are not shown, since they do not account for perspective visualisation. Average medio-lateral length size of a E11.5 interlimb epaxial segment: 300-350 µm (Deries et al., 2010; Deries et al., 2012).

Acknowledgments

We thank Luís Marques for his precious help in image analysis and 3D reconstructions and Arnoud Sonnenberg for giving us his LAT-2 antibody. The Pax3 antibody was developed by C. P. Ordahl and the Pax7 antibody was developed by A. Kawakami and were obtained from the Developmental Studies Hybridoma Bank, developed under the auspices of the NICHD and maintained by the University of Iowa, Department of Biology, Iowa City, IA52242, USA. This work was supported by Fundação para a Ciência e Tecnologia (FCT, Portugal) project PTDC/SAU-BID/120130/2010 and FCT scholarships SFRH/BD/90827/2012 (A.B.G) and SFRH/BDP/65370/2009 (M.D.).

References

Alberts, B., Johnson, A., Lewis, J., Raff, M., Roberts, K. and Walter, P. (2007). Molecular biology of the cell. London: Garland Science

Anderson, C., Thorsteinsdottir, S. and Borycki, A.-G. (2009). Sonic hedgehog-dependent synthesis of laminin 1 controls basement membrane assembly in the myotome. *Development* **136**, 3495-3504.

Bajanca, F., Luz, M., Raymond, K., Martins, G. G., Sonnenberg, A., Tajbakhsh, S., Buckingham, M. and Thorsteinsdóttir, S. (2006). Integrin α6β1-laminin interactions regulate early myotome formation in the mouse embryo. *Development* **133**, 1635-1644.

Ben-Yair, R. and Kalcheim, C. (2005). Lineage analysis of the avian dermomyotome sheet reveals the existence of single cells with both dermal and muscle progenitor fates. *Development* **132**, 689-701.

Bentzinger, C. F., Wang, Y. X., Von Maltzahn, J., Soleimani, V. D., Yin, H. and Rudnicki, M. A. (2013). Fibronectin regulates Wnt7a signaling and satellite cell expansion. *Cell Stem Cell* **12**, 75-87.

Borello, U., Berarducci, B., Murphy, P., Bajard, L., Buffa, V., Piccolo, S., Buckingham, M. and Cossu, G. (2006). The Wnt/beta-catenin pathway regulates Gli-mediated Myf5 expression during somitogenesis. *Development* **133**, 3723-3732.

Borycki, A. G. (2013). The myotomal basement membrane: Insight into laminin-111 function and its control by Sonic hedgehog signaling. *Cell Adhes. Migr.* **7**, 72-81.

Borycki, A. G., Brunk, B., Tajbakhsh, S., Buckingham, M., Chiang, C. and Emerson, C. P. (1999). Sonic hedgehog controls epaxial muscle determination through Myf5 activation. *Development* **126**, 4053-4063.

Brand-Saberi, B., Krenn, V., Grim, M. and Christ, B. (1993). Differences in the fibronectin-dependence of migrating cell populations. *Anat. Embryol. (Berl).* **187**, 17-26.

Brent, A. E., Schweitzer, R. and Tabin, C. J. (2003). A somitic compartment of tendon progenitors. *Cell* **113**, 235-248.

Buckingham, M. (2006). Myogenic progenitor cells and skeletal myogenesis in vertebrates. *Curr. Opin. Genet. Dev.* **16**, 525-532.

Cachaço, A. S., Pereira, C. S., Pardal, R. G., Bajanca, F. and Thorsteinsdóttir, S. (2005). Integrin repertoire on myogenic cells changes during the course of primary myogenesis in the mouse. *Dev. Dyn.* **232**, 1069-1078.

Chiquet-Ehrismann, R., Orend, G., Chiquet, M., Tucker, R. P. and Midwood, K. S. (2014). Tenascins in stem cell niches. *Matrix Biol.* **37**, 112-123.

Christ, B., Huang, R. and Scaal, M. (2007). Amniote somite derivatives. *Dev. Dyn.* **236**, 2382-2396.

Christ, B., Jacob, M. and Jacob, H. J. (1983). On the origin and development of the ventrolateral abdominal muscles in the avian embryo. An experimental and ultrastructural study. *Anat. Embryol. (Berl).* **166**, 87-101.

Delfini, M. C., De La Celle, M., Gros, J., Serralbo, O., Marics, I., Seux, M., Scaal, M. and Marcelle, C. (2009). The timing of emergence of muscle progenitors is controlled by an FGF/ERK/SNAIL1 pathway. *Dev. Biol.* **333**, 229-237.

Deries, M. and Thorsteinsdóttir, S. (2016). Axial and limb muscle development: dialogue with the neighbourhood. *Cell. Mol. Life Sci.* **73**, 4415-4431.

Deries, M., Gonçalves, A. B., Vaz, R., Martins, G. G., Rodrigues, G. and Thorsteinsdóttir, S. (2012). Extracellular matrix remodeling accompanies axial muscle development and morphogenesis in the mouse. *Dev. Dyn.* **241**, 350-364.

Deries, M., Schweitzer, R. and Duxson, M. J. (2010). Developmental fate of the mammalian myotome. *Dev. Dyn.* **239**, 2898-2910.

Durbeej, M. (2010). Laminins. *Cell Tissue Res.* **339**, 259-68.

Fujimoto, T., Yoshinaga, K. and Kono, I. (1985). Distribution of fibronectin on the migratory pathway of primordial germ cells in mice. *Anat. Rec.* **211**, 271-8.

Gattazzo, F., Urciuolo, A. and Bonaldo, P. (2014). Extracellular matrix: a dynamic microenvironment for stem cell niche. *Biochim. Biophys. Acta* **1840**, 2506-2519.

Giblin, S. P. and Midwood, K. S. (2015). Tenascin-C: Form versus function. *Cell Adh. Migr.* **9**, 48–82.

Gonçalves, A. B., Thorsteinsdóttir, S. and Deries, M. (2016). Rapid and simple method for in vivo ex utero development of mouse embryo explants. *Differentiation.* **91**, 57-67.

Gros, J., Scaal, M. and Marcelle, C. (2004). A two-Step mechanism for myotome formation in chick. *Dev. Cell* **6**, 875-882.

Gros, J., Manceau, M., Thomé, V. and Marcelle, C. (2005). A common somitic origin for embryonic muscle progenitors and satellite cells. *Nature* **435**, 954-958.

Harburger, D. S. and Calderwood, D. A. (2009). Integrin signalling at a glance. *J. Cell Sci.* **122**, 159-163.

Hollway, G. and Currie, P. (2005). Vertebrate myotome development. *Birth Defects Res. Part C - Embryo Today Rev.* **75**, 172-179.

Horejs, C.-M., Serio, A., Purvis, A., Gormley, A. J., Bertazzo, S., Poliniewicz, A., Wang, A. J., DiMaggio, P., Hohenester, E. and Stevens, M. M. (2014). Biologically-active laminin-111 fragment that modulates the epithelial-to-mesenchymal transition in embryonic stem cells. *Proc. Natl. Acad. Sci. U. S. A.* **111**, 5908-5913.

Hsia, H. C. and Schwarzbauer, J. E. (2005). Meet the tenascins: multifunctional and mysterious. *J. Biol. Chem.* **280**, 26641-26644.

Humphries, J. D., Byron, A. and Humphries, M. J. (2006). Integrin ligands at a glance. *J. Cell Sci.* **119**, 3901-3903.

Huss, D. J., Saias, S., Hamamah, S., Singh, J. M., Wang, J., Dave, M., Kim, J., Eberwine, J. and Lansford, R. (2019). Avian Primordial Germ Cells Contribute to and Interact With the Extracellular Matrix During Early Migration. *Front. Cell Dev. Biol.* **7**, 1-20.

Hynes, R. O. (1992). Integrins: versatility, modulation, and signaling in cell adhesion. *Cell* **69**, 11-25.

Järveläinen, H., Sainio, A., Koulu, M., Wight, T. N. and Penttinen, R. (2009). Extracellular matrix molecules: potential targets in pharmacotherapy. *Pharmacol. Rev.* **61**, 198-223.

Jones, P. L. and Jones, F. S. (2000). Tenascin-C in development and disease: Gene regulation and cell function. *Matrix Biol.* **19**, 581-596.

Kalcheim, C., Cinnamon, Y. and Kahane, N. (1999). Myotome formation: a multistage process. *Cell Tissue Res.* **296**, 161-173.

Kassar-Duchossoy, L., Giacone, E., Gayraud-Morel, B., Jory, A., Gomès, D. and Tajbakhsh, S. (2005). Pax3/Pax7 mark a novel population of primitive myogenic cells during development. *Genes Dev.* **19**, 1426-1431.

Kikkawa, Y., Hozumi, K., Katagiri, F., Nomizu, M., Kleinman, H. K. and Koblinski, J. E. (2012). Laminin-111-derived peptides and cancer. *Cell Adh. Migr.* **7**, 150-256.

Martins, G. G., Rifes, P., Amaândio, R., Rodrigues, G., Palmeirim, I. and Thorsteinsdóttir, S. (2009). Dynamic 3D cell rearrangements guided by a fibronectin matrix underlie somitogenesis. *PLoS One* **4**, e7429.

Nunes, A. M., Wuebbles, R. D., Sarathy, A., Fontelonga, T. M., Deries, M., Burkin, D. J. and Thorsteinsdóttir, S. (2017). Impaired fetal muscle development and JAK-STAT activation mark disease onset and progression in a mouse model for merosin-deficient congenital muscular dystrophy. *Hum. Mol. Genet.* **26**, 2018-2033.

Ott, M. O., Bober, E., Lyons, G., Arnold, H. and Buckingham, M. (1991). Early expression of the myogenic regulatory gene, myf-5, in precursor cells of skeletal muscle in the mouse embryo. *Development* **111**, 1097-1107.

Paulsson, M. (1994). Biosynthesis, tissue distribution and isolation of laminins. In Ekblom, P. and Timpl, R. (Eds), The Laminins. Hardwood Academic Publishers, Amsterdam, pp. 1-26.

Relaix, F., Rocancourt, D., Mansouri, A. and Buckingham, M. (2005). A Pax3/Pax7-dependent population of skeletal muscle progenitor cells. *Nature* **435**, 948-953.

Rios, A. C., Serralbo, O., Salgado, D. and Marcelle, C. (2011). Neural crest regulates myogenesis through the transient activation of NOTCH. *Nature* **473**, 532-535.

Riou, J. F., Umbhauer, M., Shi, D. L. and Boucaut, J. C. (1992). Tenascin: a potential modulator of cell-extracellular matrix interactions during vertebrate embryogenesis. *Biol. Cell* **75**, 1-9.

Rozario, T. and DeSimone, D. W. (2010). The extracellular matrix in development and morphogenesis: A dynamic view. *Dev. Biol.* **341**, 126-140.

Sagar, Prols, F., Wiegreffe, C. and Scaal, M. (2015). Communication between distant epithelial cells by filopodia-like protrusions during embryonic development. *Development* **142**, 665-671.

Sato, Y., Nagatoshi, K., Hamano, A., Imamura, Y., Huss, D., Uchida, S. and Lansford, R. (2017). Basal filopodia and vascular mechanical stress organize fibronectin into pillars bridging the mesoderm-endoderm gap. *Development* **144**,

281-291.

Schaefer, L. and Schaefer, R. M. (2010). Proteoglycans: From structural compounds to signaling molecules. *Cell Tissue Res.* **339**, 237-246.

Seale, P., Bjork, B., Yang, W., Kajimura, S., Chin, S., Kuang, S., Scimè, A., Devarakonda, S., Conroe, H. M., Erdjument-Bromage, H., et al. (2008). PRDM16 controls a brown fat/skeletal muscle switch. *Nature* **454**, 961-967.

Tajbakhsh, S. (2009). Skeletal muscle stem cells in developmental versus regenerative myogenesis. *J. Intern. Med.* **266**, 372-389.

Tajbakhsh, S. and Buckingham, M. (2000). The birth of muscle progenitor cells in the mouse: spatiotemporal considerations. *Curr. Top. Dev. Biol.* **48**, 225-68.

Tajbakhsh, S., Rocancourt, D. and Buckingham, M. (1996). Muscle progenitor cells failing to respond to positional cues adopt non- myogenic fates in myf-5 null mice. *Nature* **384**, 266-270.

Tierney, M. T., Gromova, A., Sesillo, F. B., Sala, D., Spenlé, C., Orend, G. and Sacco, A. (2016). Autonomous extracellular matrix remodeling controls a progressive adaptation in muscle stem cell regenerative capacity during development. *Cell Rep.* **14**, 1940-1952.

Veevers-Lowe, J., Ball, S. G., Shuttleworth, A. and Kielty, C. M. (2011). Mesenchymal stem cell migration is regulated by fibronectin through 5 1-integrin-mediated activation of PDGFR- and potentiation of growth factor signals. *J. Cell Sci.* **124**, 1288-1300.

Venters, S. J., Thorsteinsdóttir, S. and Duxson, M. J. (1999). Early development of the myotome in the mouse. *Dev. Dyn.* **216**, 219-232.

Yoshida, T., Akatsuka, T. and Imanaka-Yoshida, K. (2015). Tenascin-C and integrins in cancer. *Cell Adhes. Migr.* **9**, 96-104.

Zollinger, A. J. and Smith, M. L. (2017). Fibronectin, the extracellular glue. *Matrix Biol.* **60**–**61**, 27-37.

Chapter 5

The myotomal extracellular matrix is not required for transversospinalis and hypaxial muscle morphogenesis

The myotomal extracellular matrix is not required for transversospinalis and hypaxial muscle morphogenesis

André B. Gonçalves[a,b], Andreia M. Nunes[c], SólveigThorsteinsdóttir[a,b] and Marianne Deries[a]

[a] Centro de Ecologia, Evolução e Alterações Ambientais, Departamento de Biologia Animal, Faculdade de Ciências, Universidade de Lisboa, 1749-016 Lisboa, Portugal.

[b] Instituto Gulbenkian de Ciência, 2781-901 Oeiras, Portugal

[c] Center for Molecular Medicine, University of Nevada, Reno School of Medicine, Reno, NV 89557, USA.

Contribution for the publication:

	Experimental work depicted in Fig.			Manuscript writing
	5.1	5.2	5.3	
Design and concept	III	III	III	III
Execution	III	III	III	
Analysis and interpretation	III	III	III	

Legend:

- ..... non-applicable
O ..... no intervention
I ..... minor contribution
II ..... moderate contribution
III .... major contribution/full execution

Note: this contribution does not exclude other contributions, similar or not, from the remaining authors

Abstract

The development of muscles is accompanied by the dynamic deposition of extracellular matrix (ECM) and is synchronised with the development of the associated connective tissues including their tendons. Here we studied the role of the myotome in the organisation of these ECMs during the development of epaxial (deep back) muscles. We show that the myotome initially receives some of its ECM molecules from neighbouring tissues and its cells are essential for the organisation of these myotome-specific ECMs. Later on, during development, the muscle cells produce and assemble their own appropriate ECM. Hence, the epaxial myotome is required for the assembly of its own ECM, but the muscles that form independently of the epaxial myotome, are not dependent on the myotomal ECM.

Key words: Extracellular matrix; Muscle stem cells; Myotome; Tendon differentiation; Scleraxis, Laminin, Fibronectin, Tenascin-C; Mouse embryo.

Introduction

In amniotes, the metameric somites along the neural tube differentiate into four compartments which are all transient embryonic structures, and which mainly give rise to axial tissues. From dorsal to ventral, they are: the epithelial dermomyotome - reservoir of progenitor cells, the myotome - the first muscle to develop in the embryo, the syndetome – the source of axial tendons and the sclerotome – which develops into vertebrae and ribs (Christ et al., 2007). All the skeletal muscles of the body derive from the epithelial dermomyotome. However, in the body, there are two different ways of making a muscle (Evans et al., 2006). Either the muscle stem cells (MuSCs) delaminate from the hypaxial lip (ventro-lateral lip) of the dermomyotome and undergo a long-range migration to differentiate at their target sites (e.g. limb muscles or diaphragm; Buckingham et al., 2003; Sefton et al., 2018) or MuSCs drop from all lips of the dermomyotome to the area just beneath the dermomyotome and differentiate into the transient myotome (Deries and Thorsteinsdóttir, 2016). After a maturation of more than three days in the mouse embryo (E8.0-E11.5), the dermomyotome dissociates and releases MuSCs into the myotome (Kassar-Duchossoy et al. 2005; Relaix et al., 2005). Concomitantly with this entry of MuSCs, the myotome splits into different muscle masses and the differentiated cells translocate to acquire a new orientation to form the axial muscles (Christ et al., 1983; Deries et al. 2010). Considering the epaxial (dorsal myotome) which transforms into epaxial (deep back) muscles, the extracellular matrix (ECM) including laminins, fibronectin and tenascin, specific to the epaxial myotome accompanies its transformation (Deries et al 2012). The syndetome, which is characterised by the expression of the transcription factor Scleraxis (Scx), (Brent et al., 2003) also goes along the transformation of the myotome to form the associated tendons of the deep back muscles (Deries et al., 2010).

Here we asked whether the myotome produces and assembles laminin-111, -211, -511 and fibronectin and also what happens to the specification of axial tendons as muscles differentiate in embryos that do not form a myotome. To this end, we used the *Myf5*$^{nlacZ/nlacZ}$ mouse embryos, which are double mutants for Myf5 and Mrf4 and consequently do no form a myotome (Kassar-Duchossoy et al., 2004; Tajbakhsh et al., 1996; Chapter 3). We showed that the myotome is necessary to assemble its own ECM but later, when the epaxial transversospinalis muscles develop, these muscles can develop normal muscle ECMs and tendons. It is also interesting to note that laminins-111 and -511 and fibronectin assembly

occurs in a paracrine fashion in the developing myotome (and also later in developing muscles for fibronectin), as it is produced by neighbouring tissues rather than by the muscle tissue itself.

Results and Discussion

Myf5$^{nlacZ/nlacZ}$ embryos form a normal dermomyotomal membrane containing both laminins-111 and -511, but fail to produce laminin-211 and to assemble a myotomal basement membrane

Laminins are trimeric proteins composed of a combination of three chains α, β and γ, and they are the major components of basement membranes (Durbeej, 2010). There are five different α chains, three β and three γ chains, forming a total of sixteen different laminin trimers which are named according to the numbers of their α, β and γ chains (Aumailley et al., 2005). The dermomyotomal and myotomal basement membranes contain different laminin isoforms: the dermomyotomal basement membrane contains laminin-111 and -511, while the myotomal basement membrane, apart from these two isoforms, also contains laminin-211 (Anderson et al., 2009; Bajanca et al., 2006; Cachaço et al., 2005; Patton et al., 1997; Nunes et al., 2017). We sought to determine the importance of the myotome for the organisation and dynamics of the laminin ECMs at early myotomal stages by analysing *Myf5$^{nlacZ/nlacZ}$* mutant embryos, which do not develop a myotome (Tajbakhsh et al., 1996; also see Chapter 3). First, the expression of the different laminin α subunits (*Lama1*, *Lama2* and *Lama5*) was analysed by *in situ* hybridisation in wild type embryos to determine which embryonic tissues express these laminin subunits at E10.5 and E11.5 (Fig. 5.1). We then used immunohistochemistry to localise the laminin α1, α2 and α5 chains in *Myf5$^{+/nlacZ}$* controls compared with *Myf5$^{nlacZ/nlacZ}$* embryos.

At E10.5, *Lama1* and *Lama5* transcripts are expressed by the dermomyotome, with *Lama5* transcripts being enriched in the epaxial domain (Fig. 5.1A, D). The proteins of both of these laminin α-subunits are localised in the dermomyotome basement membrane in *Myf5$^{+/nlacZ}$* embryos (white arrowheads; Fig. 5.1B, E; also see B´, E´; Anderson et al., 2007; Bajanca et al., 2006; Patton et al., 1997). Laminin α1 and α5 proteins are present in the dermomyotome basement membrane of *Myf5$^{nlacZ/nlacZ}$* embryos, (white arrowheads; Fig. 5.1C, F; also see C´,

F´). Thus *Myf5*$^{nlacZ/nlacZ}$ embryos do not differ from *Myf5*$^{+/nlacZ}$ embryos in terms of which laminin isoforms they have in the dermomyotomal basement membrane.

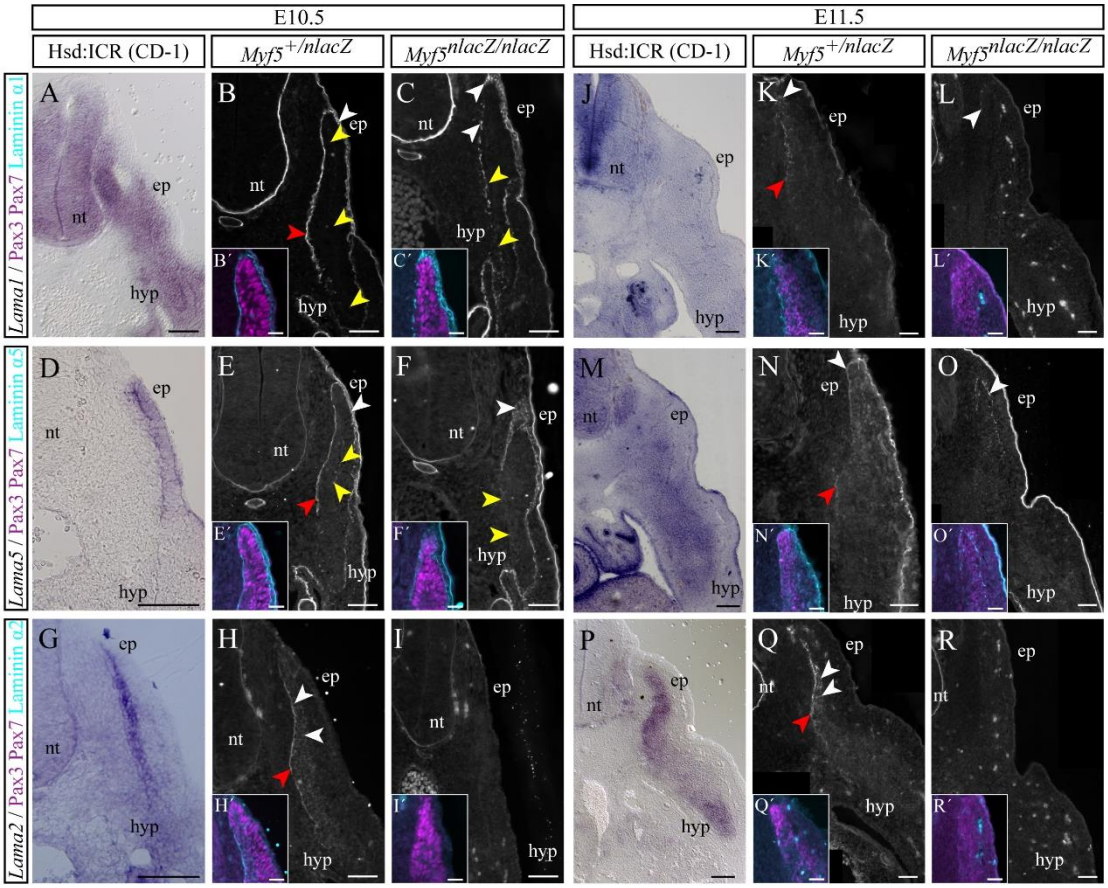

Figure 5.1: Deposition of laminins in the dermomyotomal basement membrane is normal, but the myotomal basement membrane does not form in *Myf5*$^{nlacZ/nlacZ}$ embryos.
In situ hybridisation analysis of *Lama1* (A, J), *Lama5* (D,M) and *Lama2* expression (G, P) in E10.5 (DMM3) and E11.5 (DMM4) CD-1 mouse embryos and immunolocalisation of laminin α1 (B, C, K, L; cyan in B´, C´, K´, L´), laminin α5 (E, F, N, O; cyan in E´, F´, N´, O´), laminin α2 (H, I, Q, R; cyan in H´, I´, Q´, R´) and Pax3/Pax7 proteins (magenta in B´, C´, E´, F´, H´, I´, K´, L´, N´, O´, Q´, R´) of E10.5 and E11.5 *Myf5*$^{+/nlacZ}$ and *Myf5*$^{nlacZ/nlacZ}$ interlimb segments. **A-I´:** Dermomyotomal cells express *Lama1* and *Lama5* transcripts (A, D) and both laminin α1 and α5 subunits localise in the dermomyotomal (white arrowheads in B, E; also see B´, E´) and the myotomal basement membranes (red arrowheads in B, E; also see B´, E´) in control embryos. Moreover, a few patches of laminin α1 and α5 subunits immunoreactivity can be detected between the dermomyotome and the myotome (yellow arrowheads in B, E). *Lama2* transcripts are produced by the myotome (G) and laminin α2 protein immunoreactivity forms a patchy pattern in the myotome (white arrowheads in H) and localises to the myotomal basement membrane (red arrowhead in H; also see H´). In *Myf5*$^{nlacZ/nlacZ}$ embryos, laminin α1 and α5 subunits are localised in the dermomyotomal basement membrane, including that of the epaxial lip, in a pattern identical to the one observed in control embryos (white arrowheads in C, F; also see C´, F´). However, although these laminins, are not assembled into a myotomal basement membrane (C, F), there is a patchy pattern for laminin α1 and laminin α5 subunits, medial to the dermomyotome (yellow arrowheads in C, F). As expected, no laminin α2 is observed (I, I´). **J-R´:** At E11.5, when the myotome is fully developed and the central dermomyotome has dissociated, *Lama1* transcripts become downregulated (J), *Lama5* mRNA is now detected in the myotome (M) and *Lama2* transcripts continue to be abundantly expressed through the whole myotome (P). In control embryos, the dermomyotomal basement membrane is almost completely disassembled except for the dermomyotomal lip (white arrowheads in K, N; also see K´, N´) and the myotomal basement membrane is less continuous than observed at E10.5 (red arrowheads in K, N). Laminin α2 still exhibits a patchy pattern inside the myotome (white arrowheads in Q) and is present in what is left of the myotome basement membrane (red arrowhead in Q) but this expression was not registered in the epaxial-most region of the segment (Q´). In *Myf5*$^{nlacZ/nlacZ}$ embryos, some laminin α1 and α5 immunoreactivity is present in the epaxial lip (arrowheads in L, O; also see L´, O´). Laminin α2 remains absent from *Myf5*$^{nlacZ/nlacZ}$ segments (R, R´). nt: neural tube; ep: epaxial; hyp: hypaxial. Scale bars: 100 µm in A, D, G, J, M, P, 50 µm in B, C, E, F, H, I, K, L, N, O, Q, R and 25 µm in B´, C´, E´ F´, H´, I´, K´, L´, N´, O´, Q´ R´.

In normal E10.5 embryos, *Lama1* and *Lama5* transcripts are not expressed in the myotome (Fig. 5.1A, D) but both laminin α1 and α5 proteins localise in the myotomal basement membrane (red arrowheads; Fig. 5.1B, E) suggesting that either dermomyotomal cells that enter the myotome to start differentiation bring these laminins with them or laminins produced by dermomyotomal cells are released into the myotome. In support of the latter hypothesis, a few patches of laminin α5 can be observed between the dermomyotome and the myotome (yellow arrowheads; Fig. 5.1E), but these two hypotheses are not mutually exclusive. Normal embryos at E10.5 express *Lama2* mRNA in the myotome (Fig. 5.1G) and consistent with this observation, laminin α2 protein is detected inside the myotome (white arrowheads; Fig. 5.1H) as well as in the myotomal basement membrane (red arrowhead; Fig. 5.1H; also see H´; Nunes et al., 2017). In *Myf5*$^{nlacZ/nlacZ}$ embryos, the myotome is absent, and consequently laminin α2 protein is not detected in the segments (Fig. 5.1I, I´). Moreover, a myotomal basement membrane composed of laminin α1 and α5 does not form (Bajanca et al., 2006; Tajbakhsh et al., 1996; also see Fig. 5.1C, F, I). Some positive staining was detected for both of these laminin α-units in the presumptive zone of the myotome, but no organised basement membrane comparable with that of control embryos is detected (yellow arrowheads; Fig. 5.1C; Fig. 5.1F), indicating that although these proteins are produced, the cells of the myotome are required to organise them into a basement membrane.

Later in development (E11.5), when the central dermomyotome has dissociated and MuSCs have invaded the myotomal area in normal embryos, *Lama1* mRNA has been downregulated in the segment (Fig. 5.1J) while *Lama5* transcripts are now detected within the myotome (Fig. 5.1M). Laminin α1 and α5 proteins continue lining the remaining epaxial dermomyotomal lip (white arrowheads; Fig. 5.1K, N) and the myotome medially (red arrowheads; Fig. 5.1K, N). Moreover, a few patches of laminin α1 (Fig. 5.1K, K´) and what appears to be more patches of laminin α5 are intermingled with MuSCs inside the myotome (Fig. 5.1N, N´). Indeed, when MuSCs de-epithelialize from the central dermomyotome and colonise the myotome, they can bring their gene expression profile with them into the myotome. Our results indicate that while MuSCs retain *Lama5* expression in the myotome, they apparently downregulate *Lama1*. This may explain why there appears to be more laminin α5 than α1 protein inside the myotome (compare Fig. 5.1N, K). This result raises the possibility that *Lama1* expression is not sustained after de-epithelialization of the dermomyotomal MuSCs. Indeed laminin-111 expression is characteristic of immature epithelia and is known to go down as development proceeds (Ekblom et al., 2003). *Lama2* transcripts continue to be strongly

expressed in the myotome of control embryos (Fig. 5.1P) and laminin α2 protein is detected in a patchy pattern inside the myotome (white arrowheads; Fig. 5.1Q) and is abundantly deposited in the myotomal basement membrane (red arrowhead; Fig. 5.1Q). However, expression of laminin α2 is not observed along the full extension of the epaxial basement membrane of the myotome, as this laminin sub-unit was not observed in the epaxial-most territory (Fig. 5.1Q, Q´). In *Myf5*$^{nlacZ/nlacZ}$ embryos, the central dermomyotome also de-epithelializes and the dermomyotomal basement membrane is disassembled, while, like in control embryos, laminin α1 and α5 proteins remain, lining the epaxial dermomyotomal lip (white arrowheads; Fig. 5.1L, O; also see L´, O´). As at E10.5, at E11.5 *Myf5*$^{nlacZ/nlacZ}$ embryos continue not having a myotomal basement membrane (Fig. 5.1L, O, R; also see L´, O´, R´).

Together our results demonstrate that both *Lama1* and *Lama5* are expressed in the dermomyotome and that the dermomyotomal basement membrane, containing laminins-111 and -511, forms normally in *Myf5*$^{nlacZ/nlacZ}$ embryos. Our results also show that the myotomal basement membrane is normally composed of laminins 111, 511 and 211 and confirm that this myotomal matrix does not assemble in *Myf5*$^{nlacZ/nlacZ}$ embryos (Bajanca et al., 2006; Tajbakhsh et al., 1996). Moreover, our data suggest that myotomal cells use laminin 111 and 511 produced by the dermomyotome to assemble this matrix. As expected, *Myf5*$^{nlacZ/nlacZ}$ embryos do not produce any laminin -211, which is normally expressed by differentiated muscle cells (Fig. 5.1G, P; Cachaço et al., 2005; Nunes et al., 2017). Although laminin molecules can self-assemble and form a sheet-like ECM in the absence of cells (Yurchenco, 2011) our results show that laminins-111 and -511 produced by the dermomyotome in *Myf5*$^{nlacZ/nlacZ}$ embryos only assemble in the dermomyotome and do not form a continuous matrix where the myotome should have been. This is consistent with previous studies that have shown that differentiating cells in the myotome strongly express the α6β1 integrin and dystroglycan, both laminin receptors, which may be required for the assembly of laminins into a myotomal basement membrane (Anderson et al., 2007; Bajanca et al., 2006).

Fibronectin ECM of muscles is assembled in a paracrine fashion in wild type embryos and the myotome is not necessary for normal assembly of fibronectin in transversospinalis muscle

Fibronectin is the most abundant ECM glycoprotein in the early embryo, where it mediates cell adhesion, migration and growth (Hynes, 1990; Rozario and DeSimone, 2010; Zollinger and Smith, 2017). Fibronectin is necessary for normal somitogenesis and neural tube formation (Duband et al., 1987; Martins et al., 2009; Ostrovsky et al., 1998; Rifes et al., 2007). Fibronectin is known to be present during all of the early stages of epaxial muscle morphogenesis (Deries et al., 2012; also see Chapter 4), and remains present both around and within the definitive muscle masses (Cachaço et al., 2005). Furthermore, mRNA and protein of the integrin α5 subunit (*Itga5*), part of the α5β1 integrin, the major fibronectin assembly receptor, is expressed in the myotome (Bajanca et al., 2004; Cachaço et al., 2005; Gomes de Almeida et al., 2016), suggesting that the myotome is capable of fibronectin matrix assembly.

Therefore, our next goal was to understand if the absence of the myotome directly affects the organisation and deposition of the fibronectin matrix during myotome formation and epaxial muscle morphogenesis. We analysed the expression pattern of *Fn1* in wild type embryos and studied the localisation of the fibronectin protein in $Myf5^{+/nlacZ}$ and $Myf5^{nlacZ/nlacZ}$ embryos ranging from E10.5 to E14.5 (Fig. 5.2). To mark the myotome or the epaxial muscle masses we co-immunolabelled the sections with an antibody against myosin heavy chain (MHC) (Fig. 5.2).

In E10.5 wild type embryos, *Fn1* transcripts are expressed by the central dermomyotome, the syndetome and the sclerotome, but not by the myotome (Fig. 5.2A). At E11.5, when the central dermomyotome has dissociated, *Fn1* expression is observed in the dermis, the syndetome and the sclerotome (Fig. 5.2D). Remarkably, also later in development (E12.5 and E14.5), while *Fn1* transcripts are detected in the developing cartilage (yellow arrowheads; Fig 5.2G, J) and tendons (red arrowheads; Fig 5.2G, J), *Fn1* is not expressed in skeletal muscle cells (asterisks; Fig. 5.2G).

At E10.5, an extensive fibronectin matrix fills the area of the sclerotome and fibronectin is enriched near the dermomyotomal and myotomal basement membranes (Fig. 5.2B, B´). Cables of fibronectin can also be observed between the dermomyotome and the myotome as well as within the myotome (Fig. 5.2B, B´; also see Chapter 4). In $Myf5^{nlacZ/nlacZ}$ embryos, the

fibronectin matrix of the sclerotome is indistinguishable from that of normal embryos and fibronectin is enriched near the dermomyotomal basement membrane (Fig. 5.2C, C´). However, the organisation of fibronectin into cables, normally seen in the myotome, is absent (white arrowheads; Fig. 5.2B, B´; Fig. 5.2C, C´). At E11.5, *Myf5*$^{+/nlacZ}$ embryos display thick cables of fibronectin penetrating the myotome (Fig. 5.2E, E´; also see Chapter 4). In contrast, no such cables are seen in same stage *Myf5*$^{nlacZ/nlacZ}$ embryos (Fig. 5.2F, F´).

When the transversospinalis and hypaxial muscle masses have started to differentiate in *Myf5*$^{nlacZ/nlacZ}$ embryos (see Chapter 3), a fibronectin ECM has been assembled around these muscle masses and penetrates into them (Fig. 5.2I, I´) in a similar pattern as observed for control embryos (Fig. 5.2H, H´). This pattern remains the same at E14.5 where the muscles that form in *Myf5*$^{nlacZ/nlacZ}$ embryos appear to have a normal muscle matrix (Fig. 5.2; compare K, K´ with L, L´). During the stages of myogenesis under study, cells other than muscle cells produce fibronectin. However, our data show that muscle cells are capable of binding and assembling fibronectin provided by neighbouring tissues (also see Gomes de Almeida et al., 2016) and they construct a fibronectin matrix with a muscle-specific pattern. This muscle-specific pattern is particularly evident at myotomal stages, where thick cables of fibronectin penetrate the myotome from the intersegmental borders and lie parallel to the myotomal myocytes (see Chapter 4). Thus, the muscle cells of the myotome organise their fibronectin matrix differently from that of e.g. the mesenchymal sclerotome. Why the myotome forms thicker fibronectin fibrils than for example the sclerotome is not clear. It is possible that the myotome is a comparatively denser tissue than the surrounding sclerotome and, because the myotomal myocytes attach to the ECM at the intersegmental borders (Bajanca et al., 2004; Snow et al., 2008), possibly under tension. Tension is important for fibronectin matrix assembly (Mao and Schwarzbauer, 2005) and thus may explain the thickness of the fibrils in the myotome. Interestingly, mechanical force from the pulsating aorta has been shown to be required for the formation of thick fibronectin cables, called fibronectin pillars, linking the ventral somite with the endoderm in the chick embryo (Sato et al., 2017). Culture of embryo explants in the presence of tension inhibitors (e.g. Blebbstatin or Rho kinase inhibitors) during the stages of fibronectin assembly in the myotome may be able to address whether tension is important for the formation of the myotomal fibronectin cables. Later during epaxial muscle development, fibronectin cables also penetrate the forming muscle masses. When muscles finally differentiate in the *Myf5*$^{nlacZ/nlacZ}$ mutant embryos, their fibronectin matrix is indistinguishable from that of the muscles of control embryos.

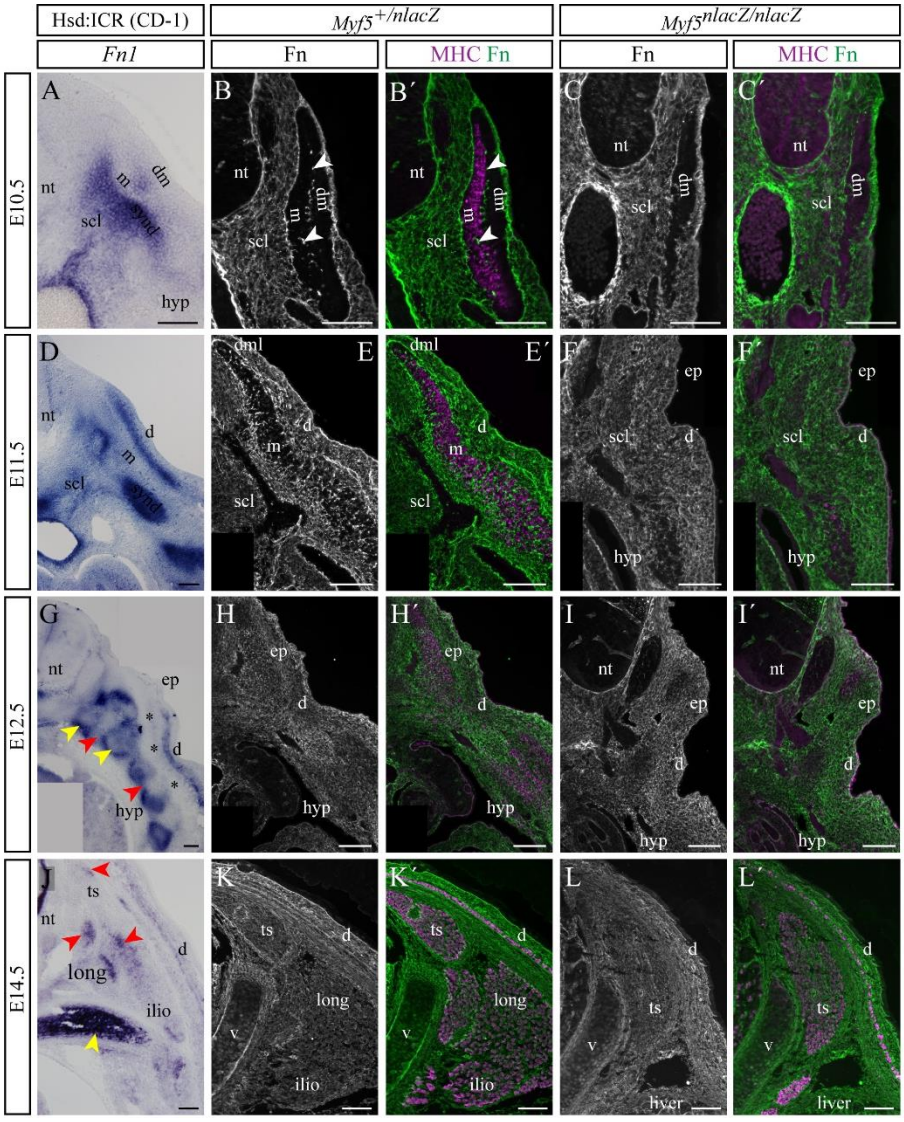

Figure 5.2: Normal *Fn1* expression in *Myf5*$^{+/nlacZ}$ and *Myf5*$^{nlacZ/nlacZ}$ embryos but the myotomal fibronectin ECM does not form in *Myf5*$^{nlacZ/nlacZ}$ embryos.

Analysis of *Fn1* transcripts by *in situ* hybridisation of interlimb cryosections of CD-1 embryos (A, D, G, J) and immunodetection of fibronectin ECM (B, C, E, F, H, I, K, L; green in B´, C´, E´, F´, H´, I´, K´, L´) and MHC (magenta in B´, C´, E´, F´, H´, I´, K´, L´) of interlimb cryosections of *Myf5*$^{+/nlacZ}$ and *Myf5*$^{nlacZ/nlacZ}$ embryos. **A-F´:** During the development and maturation of the embryonic myotome, *Fn1* transcripts are expressed by neighbouring tissues, adjacent to the myotome: the sclerotome, syndetome and the central dermomyotome at E10.5 (A) and the sclerotome, syndetome and dorsal dermis at E11.5 (D). A specific fibronectin ECM is assembled in the myotome of *Myf5*$^{+/nlacZ}$ embryos, where patches of fibronectin are detected between the dermomyotome and myotome (arrowheads in B, B´) and thick fibrils become abundant within the myotome (E, Ei). The sclerotomal fibronectin matrix in E10.5 and E11.5 *Myf5*$^{nlacZ/nlacZ}$ embryos (C, C´, F, F´) is indistinguishable from the one of *Myf5*$^{+/nlacZ.}$ embryos but, since the myotome is absent, this matrix reaches the dermomyotome at E10.5 (C, C´) and becomes continuous with the fibronectin matrix of the dermis at E11.5 (F, Fi). In contrast, the myotomal fibronectin matrix is not formed (C, C´, F, F´). **G-L´:** At E12.5, *Fn1* transcripts remain absent from the segregating definitive muscle masses but are detected in developing cartilage (yellow arrowheads in G, J) and in areas with tendinogenic cells (red arrowheads in G, J). Nevertheless, a fibronectin matrix can be detected around, as well as within, the developing epaxial and hypaxial muscle masses in *Myf5*$^{+/nlacZ.}$ embryos (H, H´, K, K´). *Myf5*$^{nlacZ/nlacZ}$ embryos have formed the transversospinalis and hypaxial muscles at this stage (I, I´, L, L´) and the fibronectin matrix seems to be normal around and within these muscle masses when compared to control embryos (H-L´). nt: neural tube; ep: epaxial; hyp: hypaxial; ts: transversospinalis; long: longissimus; ilio: iliocostalis; v: vertebra Scale bars: 100 µm in A, D, G, P and 50 µm in B-C´, E-F´, H-I´, K-L´.

The role of the myotome in the tendinogenic differentiation programme of Myf5$^{nlacZ/nlacZ}$ embryos

Tenascin-C is a marker of osteotendino- (Järvinen et al., 1999) and myotendinous junctions, and of tendons in the adult (Chiquet and Fambrough, 1984). However, it is also present early in the developing cartilage, tendons and ligaments in the embryo (Deries et al., 2012; Kardon, 1998). During embryonic development, axial tendon differentiation is activated in the syndetome which lies between the myotome and the sclerotome (Brent et al., 2003). The syndetome is characterised by the expression of the transcription factor Scleraxis (*Scx*), a marker of developing tendons and ligaments (Schweitzer et al., 2001), in response to myotomal fibroblast growth factors (Fgfs) expressed by myoblasts and myocytes (Brent et al., 2005). We therefore asked whether the tendinogenic differentiation programme, which is delayed in *Myf5$^{nlacZ/nlacZ}$* embryos due to the absence of the myotome, is rescued during the development of the only epaxial muscles able to form in these embryos, the transversospinalis muscles (Fig.3.1). To do so, we analysed the expression of *Scx* transcripts in *Myf5$^{+/nlacZ}$* embryos by *in situ* hybridisation at stages between E11.5-E14.5 and compared with that of *Myf5$^{nlacZ/nlacZ}$* embryos. This analysis was complemented by the study of the localisation of tenascin-C at the same developmental stages, through double-immunohistochemistry using antibodies against tenascin-C and MHC (Fig. 5.3).

Syndetome development starts at E10.5 in somites of wild type embryos (Brent et al., 2003; Brent et al., 2005). *Scx* upregulation is delayed in mouse embryos which do not form a myotome (Brent et al., 2005), whose expression is first detected at E11.5, but only in the hypaxial segment (Fig. 5.3; compare A with C) and tenascin-C localisation reflects *Scx* expression in both control and mutant embryos (Fig. 5.3, compare B, B´ with D, D´). At E12.5, *Scx* mRNA is detected in the newly segregated epaxial and hypaxial muscle masses in control embryos (Fig. 5.3E). In *Myf5$^{nlacZ/nlacZ}$* embryos, on the other hand, although *Scx* is upregulated throughout the hypaxial muscles, epaxially, its expression is only detected in the epaxial-most region (red arrowhead; Fig. 5.3G) which corresponds to the developing transversospinalis muscles. Thus, the areas where the missing epaxial musculatures should develop in embryos are devoid of *Scx* expression (black arrowhead; Fig. 5.3G). Concomitantly, tenascin-C ECM is present adjacent to the transversospinalis muscles of both types of embryos (arrowheads; Fig. 5.3, compare F, F´ with H, H´), but the tenascin which is normally associated with the more

ventral epaxial muscles is not present in *Myf5*$^{nlacZ/nlacZ}$ embryos (data not shown). At E14.5, *Scx* expression and tenascin-C ECM remain associated with developing muscles in control (Fig. 5.3I, J, J´) and *Myf5*$^{nlacZ/nlacZ}$ foetuses (Fig. 5.3K, L, L´). Interestingly, in E14.5 *Myf5*$^{+/nlacZ}$ embryos, two regions of strong and localised *Scx* expression can be identified, one ventral to the transversospinalis and one ventral to the longissimus (Fig. 5.3I). In contrast, *Myf5*$^{nlacZ/nlacZ}$ embryos only display one such region, namely ventral to the transversospinalis (Fig. 5.3K), which is consistent with the notion that in the trunk, signals from muscles are required to induce *Scx*.

Thus, the epaxial tendon differentiation programme is delayed until E11.5 in *Myf5*$^{nlacZ/nlacZ}$ embryos, confirming that the myotome has a major role is triggering the tendinogenic programme (Brent et al., 2005). When the first MHC- positive cells are detected in the mutant embryos, *Scx* expression is upregulated, and from this point onward, our data show that epaxial tendon formation of the transversospinalis muscles is rescued but remains lacking where muscles are missing. The fact that the tendons are able to form without the proper development of the syndetome raises the question of the necessity of a syndetome. In fact, transversospinalis is able to develop without the myotome while the three remaining epaxial muscle masses are not (Chapter 3). It would be interesting to investigate whether the tendons of longissimus, iliocostalis and levatores costarum (the epaxial muscles missing when the myotome is not there; see Chapter 3) are exclusively syndetome-derived and thus to understand whether the syndetome is necessary for the development of their tendons. If so, the development of the Myf5/Mrf4-dependent myotome would be essential for the formation of longissimus, iliocostalis and levatores costarum muscles as well as their tendons, pointing out an additional difference between these three epaxial muscles and the transversospinalis. In limbs, tendons are specified within the mesenchyme (Kardon, 1998) and the development of tendons is regulated by muscles, for example with muscle secreting Fgfs (Edom-Vovard et al., 2002). It is possible that the transversospinalis muscle cells, which do secrete Fgfs when they become MHC-positive (Chapter 3), are able to regulate the development of tendons in a similar way as occurs in the limbs.

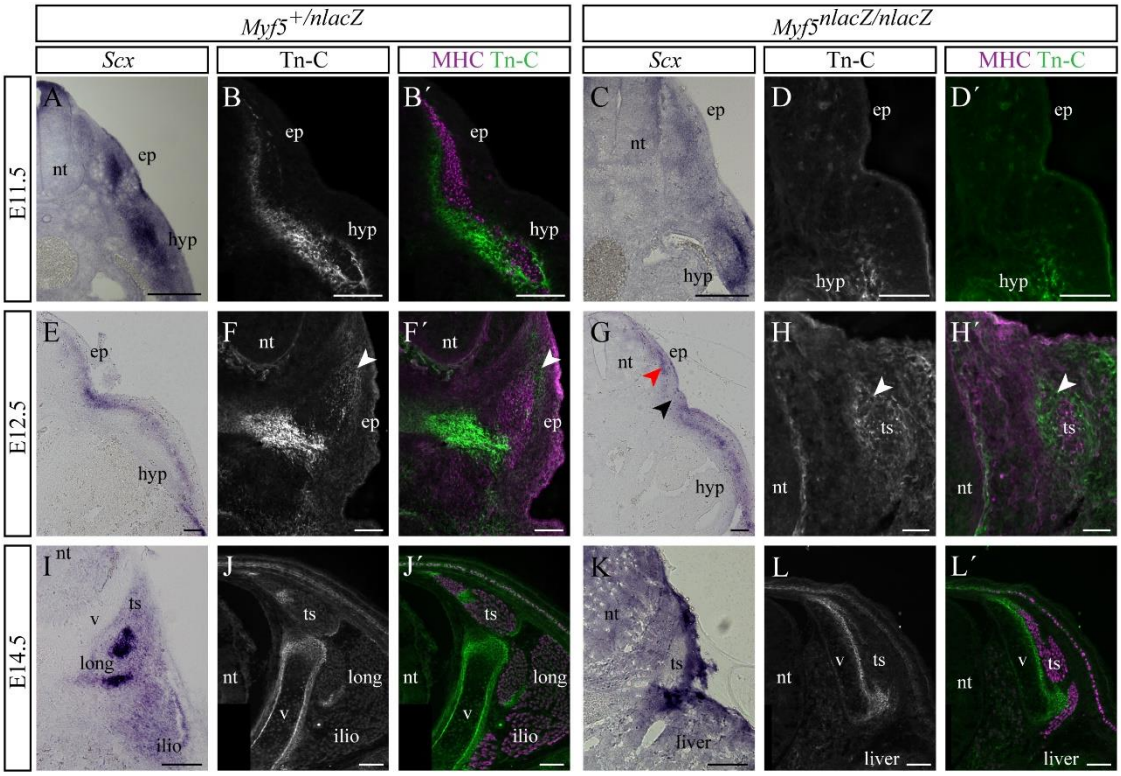

Figure 5.3: Epaxial tendinogenesis is delayed in *Myf5*$^{nlacZ/nlacZ}$ embryos and only the tendons of transversospinalis and hypaxial muscles develop.
Interlimb cryosections of *Myf5*$^{+/nlacZ}$ (A-B´, E-F´, I-J´) and *Myf5*$^{nlacZ/nlacZ}$ embryos (C-D´ G-H´, K-L´) processed for *in situ* hybridisation to analyse *Scx* expression (A, C, E, G, I, K) or immunolabeled with antibodies against tenascin-C (Tn-C; B, D, F, H, J, L; green in B´, D´, F´, H´, J´, L´) and MHC (magenta in B´, D´, F´, H´, J´, L´). **A-D´:** In *Myf5*$^{+/nlacZ}$ embryos, *Scx* transcripts are detected along the whole segment (A), but in *Myf5*$^{nlacZ/nlacZ}$ embryos, it is only detected in the hypaxial domain (C). Tenascin-C is secreted in the same areas as *Scx* transcripts in both types of embryos (compare B, B´ with D, D´). **E-H´:** At E12.5, after the translocation of the myotome, *Scx* mRNA expression is detected along the developing epaxial and hypaxial muscle masses in control embryos (E). In *Myf5*^{nlacZ} mutant embryos *Scx* expression is present along the hypaxial muscle masses and the epaxial transversospinalis muscle masses (red arrowhead in G) but is not expressed in the areas of missing epaxial muscles (black arrowhead in G). Tenascin-C is assembled around developing muscle masses both in *Myf5*$^{+/nlacZ}$ and in *Myf5*$^{nlacZ/nlacZ}$ embryos (arrowheads in F, F´, H, H´). **I-L´:** During foetal development, *Scx* transcripts of control embryos are found enriched in two stripes: one ventral to the transversospinalis muscle and another ventral of the longissimus muscles (I). Interestingly, only the stripe associated with transversospinalis muscle is present in *Myf5*$^{nlacZ/nlacZ}$ embryos (K). Weak *Scx* expression can also be detected within the muscle masses (I). Tenascin-C lines the transversospinalis muscles in both types of embryos (compare J, J´ with L, L´). nt: neural tube; ep: epaxial; hyp: hypaxial; ts: transversospinalis; long: longissimus; ilio: iliocostalis; sc: spinal cord; v: vertebra. Scale bars: 100 µm in A, C, E, G, I, K, and 50 µm in B, B´, D, D´, F, F´, H, H´, J, J´, L, L´.

Conclusions

We conclude that the myotome is required for the normal organisation of laminins, fibronectin and tenascin-C within and around it and for early tendon development. However, at later stages, when the epaxial transversospinalis and hypaxial muscle groups form in a myotome-independent manner (see Chapter 3), they are able to produce and assemble their own and apparently normal ECMs and tendons.

Materials and Methods

Mice, embryo collection and phenotyping

Outbred Hsd:ICR wild-type adult mice (CD-1; Charles River Laboratories International, Inc.) were crossed to produce wild-type mouse embryos (E10.5-E12.5) or foetuses (E14.5). *Myf5*^{nlacZ} (C57BL/6J) mice (Tajbakhsh et al., 1996) possess a *nlacZ-neo* cassette insertion replacing the coding region of the endogenous *Myf5* locus (Tajbakhsh and Buckingham, 1994). Due to its proximity to the *Myf5* locus, *Mrf4* expression is directly affected in *Myf5*$^{nlacZ/nlacZ}$ embryos. Therefore, *Myf5*$^{nlacZ/nlacZ}$ embryos are functional double-knockouts for both *Myf5* and *Mrf4* genes (Kassar-Duchossoy et al., 2004). *Myf5*$^{nlacZ/nlacZ}$ and heterozygous *Myf5*$^{+/nlacZ}$ embryos were produced by crossing adult *Myf5*$^{+/nlacZ}$ mice. Dated pregnancies were obtained with the day of the vaginal plug defined as embryonic day 0.5 (E0.5). Pregnant females were sacrificed by cervical dislocation after isoflurane anaesthesia.

Embryos derived from heterozygous *Myf5*$^{+/nlacZ}$ crossings were phenotyped using the β-galactosidase activity detection method of Hogan et al. (1986), with minor modifications. Briefly, all embryos were collected in phosphate buffer saline (PBS) and decapitated. The neck region encompassing cervical somites and a portion of the tail of each embryo/foetus, were incubated overnight (O/N) in a 0.5 mg/ml X-Gal (5-bromo-4-chloro-3-indolyl-β-D-galactopyranoside), 5 mM potassium ferricyanide, and 5 mM potassium ferrocyanide staining solution at 37°C. Wild type embryos remained unstained, while the presence of β-galactosidase

in *Myf5*$^{+/nlacZ}$ and *Myf5*$^{nlacZ/nlacZ}$ embryos was revealed by the blue colour of the transformed substrate. The cervical somites of embryos ranging from E10.5-E12.5 and a portion of the tail in E14.5 foetuses were stained to discriminate *Myf5*$^{+/nlacZ}$ from *Myf5*$^{nlacZ/nlacZ}$ embryos. At stages E10.5-E12.5, somites from *Myf5*$^{nlacZ/nlacZ}$ embryos are clearly distinguishable from those of *Myf5*$^{+/nlacZ}$ embryos in that β-Galactosidase positive cells are blocked in the dermomyotomal lips and do not form a myotome (Tajbakhsh and Buckingham, 2000), while *Myf5*$^{nlacZ/nlacZ}$ foetuses exhibit a lack of tail muscles.

To define the different stages of dermomyotome and myotome development in our study after immunostaining or *in situ* hybridisation, we used a recently described dermomyotome/myotome (DMM) stage system (Deries et al., 2012).

All experiments and manipulations conducted on animals including housing, husbandry and welfare were performed according to the guidelines provided of Direção Geral de Alimentação e Veterinária (DGAV) and approved through protocol 3/2016 from the Animal Welfare Body (ORBEA) of the Faculty of Sciences of the University of Lisbon.

In situ hybridisation

In situ hybridisation experiments were conducted in whole mount embryos/foetuses or on cryosections.

Whole mount *in situ* hybridisation was used to detect the expression pattern of the mouse *Scx* (Schweitzer et al., 2001) of E11.5-E14.5 CD-1 embryos/foetuses. Embryos/foetuses were collected from dissected uteri in PBS containing 0.05% of diethyl pyrocarbonate (PBS-DEPC) and fixed in 4% paraformaldehyde (PFA) in PBS-DEPC O/N at 4°C. After PFA fixation, all samples were washed in PBT-DEPC (PBS-DEPC with 1% Tween 20), dehydrated in a gradient of methanol and stored at -20°C until use. Whole mount *in situ* hybridisation was performed as described in Bajanca et al. (2004). Digestion treatment with proteinase K (Roche; 10 µg/ml PBS) was 45 min for E11.5 embryos, 75 min for E12.5 embryos and 100 min for E14.5 foetuses. The detection of the DIG-labelled *Scx* riboprobe was performed with 4-Nitro blue tetrazolium chloride (NBT, Roche; 450 µg/ml PBT) and 5-bromo-4-chloro-3-indolyl-phosphate, 4-toluidine salt (BCIP, Roche; 175 µg/ml PBT). After detection, the samples were washed in PBS and immediately processed for cryoembedding by incubating first in 4% sucrose in PBS, then

15% sucrose in PBS and finally in 15% sucrose and 7.5% gelatine in PBS (Bajanca et al., 2004) and stored at -80°C until sectioning (30 µm sections) in a Leica CM1860 UV cryostat.

In situ hybridisation on sections was performed to detect the expression pattern of the mouse *Lama1* (Copp et al., 2011), *Lama2* (Copp et al., 2011), *Lama5* (Copp et al., 2011), *Fn1* (Gomes de Almeida et al., 2016) and *Scx* transcripts (Schweitzer et al., 2001) of E10.5-E14.5 embryos/foetuses. Each sample was freshly collected in PBS-DEPC and immediately fixed in 4% PFA in PBS-DEPC O/N at 4°C. After fixation, the samples were washed in PBS-DEPC and processed for cryoembedding as described above. The *in situ* hybridisation was then performed as described in Gomes de Almeida et al. (2016). After staining, slides were mounted in Aquatex (Merck Millipore).

Immunohistochemistry

Immunohistochemistry experiments were carried out on cryosections as in Bajanca et al. (2004) with minor modifications. Embryos or foetuses were collected in fresh PBS and fixed with 0.2% PFA in PBS O/N at 4°C. Samples were washed in PBS and then processed for cryoembedding as described above (Bajanca et al. (2004). Cryosections (12 µm thick) were obtained in a Leica CM1860 UV cryostat and processed for immunohistochemistry. Briefly, after cryosections had dried for 45-60 min at room temperature (RT), they were washed in PBS and blocked for 20 min in 1% or 5% bovine serum albumin (for embryos and foetuses, respectively) in PBS at RT followed by the application of the primary antibodies. Primary antibodies, diluted in the blocking solutions, were incubated O/N at 4°C and secondary antibodies for 2 hours at RT. Cryosections were then placed in 4`,6-diamidine-2-phenylidole-dihydrochloride (DAPI, 5 µg/ml in PBS, 0.1% Triton X-100) for 30 seconds and mounted in 5 mg/ml propyl gallate in glycerol/PBS (9:1) with 0.01% azide. Primary and secondary antibodies used in this work are listed in Table 5.1.

Image acquisition and analysis

Cryosectioned embryos and foetuses processed for *in situ* hybridisation were photographed with a DFK 23U274 camera (The Imaging Source) coupled to an Olympus BX51 microscope. Images of cryosections processed for immunolabeling (including the ones also processed for in situ hybridisation) were acquired using a Hamamatsu Orca R2 camera coupled to an Olympus BX60 microscope with epifluorescence. Images were opened in Fiji version 1.52i and the levels of brightness and contrast were adjusted. When applicable, the pairwise stitching Fiji plugin was used to combine multiple images of one sample and generate one single image of the whole segment/muscle masses (Preibisch et al., 2009).

Table 5.1: Primary and secondary antibodies used for immunohistochemistry on sections.
DSHB: Developmental Studies Hybridoma Bank.

Antibody type	Name	Clone / Catalog	Company	Dilution
Primary antibodies	Myosin heavy chain (MHC)	MF20	DSHB	1:200
	Pax3	Pax3	DSHB	Supernatant 1:20
	Pax7	Pax7	DSHB	1:100
	Laminin α1	Mab200	Gift from Madelaine Durbeej	Supernatant (used pure)
	Laminin α2	4H8-2 / L-0663	Sigma-Aldrich	1:100
	Laminin α5	8948	Gift from Jeff Miner	1:400
	Human plasma fibronectin	F-3648	Sigma-Aldrich	1:800
	Tenascin-C	LAT-2	Gift from Arnoud Sonnenberg	Supernatant 1:50

(**Continues next page**)

(**Continued from previous page**)

Antibody type	Name	Clone / Catalog	Company	Dilution
Secondary antibodies	Alexa Fluor 568-conjugated goat anti mouse IgG F(ab´)2 fragments	A-11019	Life Technologies	1:1000
	Alexa Fluor 488-conjugated goat anti rat IgG F(ab´)2 fragments	A-11006	Life Technologies	1:1000
	Alexa Fluor 488-conjugated goat anti rabbit IgG F(ab´)2 fragments	A-11070	Life Technologies	1:1000

Acknowledgments

We thank Patricia Ybot-Gonzalez for the *Lama1*, *Lama2* and *Lama5* riboprobes, Raquel Andrade for the *Fn1* probe riboprobes and Ronen Schweitzer for providing us with the *Scx* riboprobe. We also thank Madelaine Durbeej and Jeff Miner for sharing their anti-α1 laminin and anti-α5 laminin antibodies, respectively and Arnoud Sonnenberg for giving us his LAT-2 antibody. The MF20 antibody was developed by D. A Fischman, the Pax3 antibody was developed by C. P. Ordahl and the Pax7 antibody was developed by A. Kawakami. These three antibodies were obtained from the Developmental Studies of the Hybridoma Bank, developed under the auspices of the NICHD and maintained by the University of Iowa, Department of Biology, Iowa City, IA52242, USA. This work was supported by Fundação para a Ciência e Tecnologia (FCT, Portugal) project PTDC/SAU-BID/120130/2010 and FCT scholarships SFRH/BD/90827/2012 (A.B.G), SFRH/BD/86985/2012 (A.M.N) and SFRH/BDP/65370/2009 (M.D.).

References

Anderson, C., Thorsteinsdottir, S. and Borycki, A.-G. (2009). Sonic hedgehog-dependent synthesis of laminin 1 controls basement membrane assembly in the myotome. *Development* **136**, 3495-3504.

Anderson, C., Winder, S. J. and Borycki, A. G. (2007). Dystroglycan protein distribution coincides with basement membranes and muscle differentiation during mouse embryogenesis. *Dev. Dyn.* **236**, 2627-2635.

Aumailley, M., Bruckner-Tuderman, L., Carter, W. G., Deutzmann, R., Edgar, D., Ekblom, P., Engel, J., Engvall, E., Hohenester, E., Jones, J. C. R., et al. (2005). A simplified laminin nomenclature. *Matrix Biol.* **24**, 326-332.

Bajanca, F., Luz, M., Duxson, M. J. and Thorsteinsdóttir, S. (2004). Integrins in the mouse myotome: Developmental changes and differences between the epaxial and hypaxial lineage. *Dev. Dyn.* **231**, 402-415.

Bajanca, F., Luz, M., Raymond, K., Martins, G. G., Sonnenberg, A., Tajbakhsh, S., Buckingham, M. and Thorsteinsdóttir, S. (2006). Integrin alpha6beta1-laminin interactions regulate early myotome formation in the mouse embryo. *Development* **133**, 1635-1644.

Brent, A. E., Braun, T. and Tabin, C. J. (2005). Genetic analysis of interactions between the somitic muscle, cartilage and tendon cell lineages during mouse development. *Development* **132**, 515-528.

Brent, A. E., Schweitzer, R. and Tabin, C. J. (2003). A somitic compartment of tendon progenitors. *Cell* **113**, 235-248.

Buckingham, M., Bajard, L., Chang, T., Daubas, P., Hadchouel, J., Meilhac, S., Montarras, D., Rocancourt, D. and Relaix, F. (2003). The formation of skeletal muscle: from somite to limb. *J. Anat.* **202**, 59-68.

Cachaço, A. S., Pereira, C. S., Pardal, R. G., Bajanca, F. and Thorsteinsdóttir, S. (2005). Integrin repertoire on myogenic cells changes during the course of primary myogenesis in the mouse. *Dev. Dyn.* **232**, 1069-1078.

Chiquet, M. and Fambrough, D. M. (1984). Chick myotendinous antigen. II. A novel extracellular glycoprotein complex consisting of large disulfide-linked subunits. *J. Cell Biol.* **98**, 1937-1946.

Christ, B., Jacob, M. and Jacob, H. J. (1983). On the origin and development of the ventrolateral abdominal muscles in the avian embryo. An experimental and ultrastructural study. *Anat. Embryol. (Berl).* **166**, 87-101.

Christ, B., Huang, R. and Scaal, M. (2007). Amniote somite derivatives. *Dev. Dyn.* **236**, 2382-2396.

Copp, A. J., Carvalho, R., Wallace, A., Sorokin, L., Sasaki, T., Greene, N. D. E. and Ybot-Gonzalez, P. (2011). Regional differences in the expression of laminin isoforms during mouse neural tube development. *Matrix Biol.* **30**, 301-309.

Deries, M. and Thorsteinsdóttir, S. (2016). Axial and limb muscle development: dialogue with the neighbourhood. *Cell. Mol. Life Sci.* **73**, 4415-4431.

Deries, M., Gonçalves, A. B., Vaz, R., Martins, G. G., Rodrigues, G. and Thorsteinsdóttir, S. (2012). Extracellular matrix remodeling accompanies axial muscle development and morphogenesis in the mouse. *Dev. Dyn.* **241**, 350-364.

Deries, M., Schweitzer, R. and Duxson, M. J. (2010). Developmental fate of the mammalian myotome. *Dev. Dyn.* **239**, 2898-2910.

Duband, J. L., Dufour, S., Hatta, K., Takeichi, M., Edelman, G. M. and Thiery, J. P. (1987). Adhesion molecules during somitogenesis in the avian embryo. *J. Cell Biol.* **104**, 1361-1374.

Durbeej, M. (2010). Laminins. *Cell Tissue Res.* **339**, 259-268.

Edom-Vovard, F., Schuler, B., Bonnin, M. A., Teillet, M. A. and Duprez, D. (2002). Fgf4 positively regulates scleraxis and tenascin expression in chick limb tendons. *Dev. Biol.* **247**, 351-366.

Ekblom, P., Lonai, P. and Talts, J. F. (2003). Expression and biological role of laminin-1. *Matrix Biol.* **22**, 35-47.

Evans, D. J. R., Valasek, P., Schmidt, C. and Patel, K. (2006). Skeletal muscle translocation in vertebrates. *Anat. Embryol. (Berl).* **211**, 43-50.

Gomes de Almeida, P. G., Pinheiro, G. G., Nunes, A. M., Gonçalves, A. B. and Thorsteinsdóttir, S. (2016). Fibronectin assembly during early embryo development: A versatile communication system between cells and tissues. *Dev. Dyn.* **245**, 520-535.

Hogan, B., Constantini, F. and Lacy, E. (1986). Manipulating the mouse embryo: laboratory manual. Cold Spring Harbor Laboratory Press, Cold Spring Harbor, New York, NY.

Hynes, O. R. (1990). Fibronectins and the cytoskeleton. In Fibronectins. Springer Series in Molecular Biology. Springer, New York, NY.

Järvinen, T. a L., Jozsa, L., Kannus, P., Kvist, M., Hurme, T., Isola, J., Kalimo, H. and Järvinen, M. (1999). Mechanical loading regulates tenascin-C expression in the osteotendinous junction. *J. Cell Sci.* **112 Pt 18**, 3157-3166.

Kardon, G. (1998). 4802 Muscle and tendon morphogenesis in the avian hind limb. *Development* **125**, 4019-4032.

Kassar-Duchossoy, L., Gayraud-Morel, B., Gomès, D., Rocancourt, D., Buckingham, M., Shinin, V. and Tajbakhsh, S. (2004). Mrf4 determines skeletal muscle identity in Myf5:Myod double-mutant mice. *Nature* **431**, 466-471.

Mao, Y. and Schwarzbauer, J. E. (2005). Fibronectin fibrillogenesis, a cell-mediated matrix assembly process. *Matrix Biol.* **24**, 389-399.

Martins, G. G., Rifes, P., Amaândio, R., Rodrigues, G., Palmeirim, I. and Thorsteinsdóttir, S. (2009). Dynamic 3D cell rearrangements guided by a fibronectin matrix underlie somitogenesis. *PLoS One* **4**, e7429.

Nunes, A. M., Wuebbles, R. D., Sarathy, A., Fontelonga, T. M., Deries, M., Burkin, D. J. and Thorsteinsdóttir, S. (2017). Impaired fetal muscle development and JAK-STAT activation mark disease onset and progression in a mouse model for merosin-deficient congenital muscular dystrophy. *Hum. Mol. Genet.* **26**, 2018-2033.

Ostrovsky, D., Sanger, J. W. and Lash, J. W. (1988). Somitogenesis in the mouse embryo. *Cell Differ.* **23**, 17-25.

Patton, B. L., Miner, J. H., Chiu, A. Y. and Sanes, J. R. (1997). Distribution and function of laminin in the neuromuscular system of developing, adult and mutant mice. *J. Cell Biol.* **139**, 1507-1521.

Preibisch, S., Saalfeld, S. and Tomancak, P. (2009). Globally optimal stitching of tiled 3D microscopic image acquisitions. *Bioinformatics* **25**, 1463-1465.

Rifes, P., Carvalho, L., Lopes, C., Andrade, R. P., Rodrigues, G., Palmeirim, I. and Thorsteinsdóttir, S. (2007). Redefining the role of ectoderm in somitogenesis: a player in the formation of the fibronectin matrix of presomitic mesoderm. *Development* **134**, 3155-3165.

Rozario, T. and DeSimone, D. W. (2010). The extracellular matrix in development and morphogenesis: A dynamic view. *Dev. Biol.* **341**, 126-140.

Sato, Y., Nagatoshi, K., Hamano, A., Imamura, Y., Huss, D., Uchida, S. and Lansford, R. (2017). Basal filopodia and vascular mechanical stress organize fibronectin into pillars bridging the mesoderm-endoderm gap. *Development* **144**, 281-291.

Schweitzer, R., Chyung, J. H., Murtaugh, L. C., Brent, E., Rosen, V., Olson, E. N., Lassar, A. and Tabin, C. J. (2001). Analysis of the tendon cell fate using Scleraxis, a specific marker for tendons and ligaments. *Development* **128**, 3855-3866.

Sefton, E. M., Gallardo, M. and Kardon, G. (2018). Developmental origin and morphogenesis of the diaphragm, an essential mammalian muscle. *Dev. Biol.* **440**, 64-73.

Snow, C. J., Peterson, M. T., Khalil, A. and Henry, C. A. (2008). Muscle development is disrupted in zebrafish embryos deficient for fibronectin. *Dev. Dyn.* **237**, 2542-2553.

Tajbakhsh, S. and Buckingham, M. E. (1994). Mouse limb muscle is determined in the absence of the earliest myogenic factor myf-5. *Proc. Natl. Acad. Sci. U. S. A.* **91**, 747-751.

Tajbakhsh, S. and Buckingham, M. (2000). The birth of muscle progenitor cells in the mouse: spatiotemporal considerations. *Curr. Top. Dev. Biol.* **48**, 225-268.

Tajbakhsh, S., Rocancourt, D. and Buckingham, M. (1996). Muscle progenitor cells failing to respond to positional cues adopt non-myogenic fates in myf-5 null mice. *Nature* **384**, 266-270.

Yurchenco, P. D. (2011). Basement membranes: cell scaffoldings and signaling platforms. *Cold Spring Harb. Perspect. Biol.* **3**, a004911.

Zollinger, A. J. and Smith, M. L. (2017). Fibronectin, the extracellular glue. *Matrix Biol.* **60-61**, 27-37.

Chapter 6

Discussion

I. Discussion

This thesis provides new insights into how the epaxial muscles of mammals are defined and what the mechanisms underlying their development are. It demonstrates that the myotome is crucial for the maintenance of the identity of MuSCs when they de-epithelialize from the dermomyotome into the myotome and for the development of specific epaxial muscle masses and their tendon primordia. Our results further show that fibroblast growth factors (Fgfs) which are produced by the differentiated myotomal myocytes are important for the maintenance of the Pax3- and Pax7-positive MuSC populations. Finally, the embryonic myotome assembles its own extracellular matrices (ECMs) including laminins, fibronectin and tenascin-C which each have a specific spatial relationship with dermomyotomal and myotomal MuSCs. However, these specific myotomal matrices are not necessary for the development of the transversospinalis muscles, the only epaxial muscles developing in the absence of a myotome, or the organisation of their matrices.

In this chapter, we will discuss the relevance of the major results presented along this dissertation. First, we will discuss the role of the myotome and the potential role of its matrices in the embryo. Then we discuss the possibility of the existence of three spatially and/or temporally different myogenic pathways for the development of epaxial muscles and finally, we touch on the singularity of the development of the transversospinalis muscles.

1. Role of the myotome during embryonic development

Amniotes form a transient myotome which later transforms into the definitive axial muscles (Cinnamon et al., 1999; Deries et al., 2010). The amniote myotome has many similarities to the myotomes of fish and tadpoles (Rescan, 2008; Scaal and Wiegreffe, 2006; Spörle, 2001). However, it is unique, at least in rodents, because, since it never gets innervated, it never functions as a muscle (Deries et al., 2008). Its development, independent of innervation, lasts for three days in rodents, during which the myotome grows in size and complexity, but stays segmented. This is a long time and raises the question of what the role of the myotome is, if it is not to function as a muscle.

So what does the myotome do during these three days? Neural crest cells use its basement membrane as a substrate for migration (Tosney, 1994), Fgfs from the myotomal myocytes induce the syndetome in the area of the sclerotome closest to the myotome (Brent et al., 2003, 2005), Fgfs and Pdgfs from the hypaxial myotome promote rib formation in interlimb segments (Tallquist et al., 2000; Vinagre et al., 2010) and in the chick, Fgfs from the myotome act on cells in the central dermomyotome and induce their de-epithelialization (Delfini et al., 2009). In this thesis, we discovered new functions for the myotome which are to maintain the identity of de-epithelializing MuSCs as they enter the myotomal space and to be required for the development of longissimus, iliocostalis and levatores costarum epaxial muscles. Moreover, when we block Fgfr1 and/or Fgfr4, there is a decrease in the number of Pax3- and Pax7-positive cells in the segments, strongly implicating myotomal Fgfs in this process. In contrast to the data in the chick, we did not find evidence for a failure in central dermomyotome dissociation in the absence of the myotome. The reason for this is unclear, but it is interesting to note that, unlike chick myotomal myocytes, mouse myocytes do not express Fgf8 (Brent et al., 2005), raising the possibility that Fgf8 has this specific role in the chick embryo.

2. The myotome and its matrices

In chapter 4 we addressed the distribution and organisation of the laminin, fibronectin and tenascin-C matrices during the development of the myotome as well as during and after the dissociation of the central dermomyotome. We find that the myotome assembles its own matrix, but this matrix is not necessary for the later development of the transversospinalis or its ECMs. It is possible that, like the myotome, the myotomal matrix is necessary for the development of longissimus, iliocostalis and levatores costarum. Our results show that the ECMs of the myotome are highly dynamic and thus we can ask what role these myotomal ECMs play. We identified specific spatial relationships between MuSCs and the three ECMs under study. However, our analysis is limited by the fact that we can only see the MuSC nuclei and not the cells themselves. Nevertheless, we see that the nuclei are close to certain matrices.

The laminin basement membrane of the myotome is thought to serve as a barrier between the sclerotome and the myotome (Anderson et al., 2009; Bajanca et al., 2006), and thus it is tempting to speculate that it may protect the cells in the myotome from the sclerotomal environment. It has also been shown that the laminin matrix of the dermomyotome is important

to block precocious myogenesis in these cells (Bajanca et al., 2006). Here we observed that MuSCs which de-epithelialized and invaded the myotome were often situated in proximity with the myotomal basement membrane. This raises the possibility that this basement membrane provides them with cues that maintain their undifferentiated state as it does for dermomyotomal cells.

Thick cables of fibronectin and tenascin-C matrices are assembled in the space between the myotome and the dermomyotome. The presence of these conspicuous cables is consistent with a specific role of the matrices in this area. They may give support to the elongated myocytes, which express the appropriate integrin receptors (α4β1, α5β1 and αv-integrins; Bajanca et al., 2004; Deries et al., 2012) for binding to these two matrix components. Interestingly, the α9β1 integrin, which can bind to tenascin-C (Staniszewska et al., 2008), is detected on both the apical and basal surface of dermomyotomal cells (Deries et al., 2012). Therefore, dermomyotomal cells can interact with tenascin-C matrices as they enter the myotome either by dropping into the myotomal space at E10.5 or during dermomyotome dissociation (Relaix et al., 2005). Consistent with this hypothesis, tenascin-C has been implicated in EMTs during development (Chiquet-Ehrismann et al., 2014; Giblin and Midwood, 2015; Yoshida et al., 2015).

Taking together our results shows that the three ECMs under study can potentially play several roles during myotome development.

3. The myogenic pathways

Myogenesis in the trunk is commonly thought to proceed through two major transcriptional pathways, the epaxial and the hypaxial pathways (see Fig. 1.18; Fig. 6.1A; Buckingham, 2017; Buckingham and Rigby, 2014). Our results in this thesis enable us to propose the existence of three distinct transcriptional pathways during epaxial myogenesis, which differ in terms of where they occur in space and/or time within the segments (Fig. 6.1B). First, epaxial myogenesis is triggered in the epaxial lip (DML) of the dermomyotome, where β-catenin and Gli transcription factors, activated through signalling from the neighbouring tissues, synergise and act directly on the Myf5 early epaxial enhancer, triggering the myogenic differentiation programme (Borello et al., 2006; Teboul et al., 2002). At this time and location, the activation of Myf5 is sufficient to turn on Myogenin expression (Fig. 6.1B, first box) which

leads to terminal muscle differentiation and the formation of the first myotomal myocytes. In this same location, Pax3/Dmrt2 can also activate Myf5 which turns on Myogenin (Sato et al., 2010; Fig. 6.1B, first box). A second pathway is observed in the rostral and caudal lips of the dermomyotome, where delaminating MuSCs express Myf5 and then, after entering the myotome, turn on MyoD followed by Myogenin (Fig. 6.1B; second box; Venters et al., 1999). Finally, our data unveiled the possibility of a third epaxial myogenic pathway where MyoD is activated directly in Pax3-positive cells. This activation of MyoD is independent of Myf5/Mrf4 expression and the formation of a myotome. This late epaxial myogenesis pathway is the one we hypothesise gives rise to the transversospinalis muscles (Fig. 6.1B; third box). In summary, these three pathways are thus contained within the classical schemes of the epaxial myogenesis pathway (Fig. 6.1A). However, what we propose is that they occur in three spatially and/or temporally separated MuSC populations within the dermomyotome: 1) early epaxial myogenesis (in MuSCs of the early DML), 2) early epaxial myogenesis (in MuSCs of the rostral and caudal lips of the dermomyotome) and 3) late epaxial myogenesis (in MuSCs of a developmentally "older" DML which give rise to the transversospinalis; Fig. 6.1B).

The next question to arise is how MyoD is upregulated independently of Myf5/Mrf4 in the late epaxial myogenesis pathway? Several transcription factors are known to be able to control MyoD activation directly. One of these factors is Pitx2 which is activated in the Pax3-positive MuSCs in the hypaxial myotome and plays a role in MyoD activation (L´Honoré et al., 2007). Interestingly, faint Pitx2 expression can be observed in the epaxial lip of the E10.5 dermomyotome and a robust *Pitx2* expression is detected in the E11.5 epaxial myotome (L´Honoré et al., 2007), but whether Pitx2 activates MyoD in the epaxial dermomyotome remains to be elucidated. Wnt7a from the surface ectoderm is known to be able to induce MyoD activation in the hypaxial dermomyotome (Tajbakhsh et al., 1998). Curiously, Wnt7a is also expressed in the neural tube (Parr et al., 1993). It would be interesting to test whether Wnt7a from the neural tube is involved in MyoD activation in the proposed late epaxial myogenesis pathway. Indeed, it has been postulated that the epaxial-most lip (corresponding to our proposed pathway in Fig. 6.1B, third box) and the hypaxial lip share many similarities including that of their environment and may in fact be regarded as mirror-images of each other (Spörle et al., 2001). Our data are compatible with such a scenario.

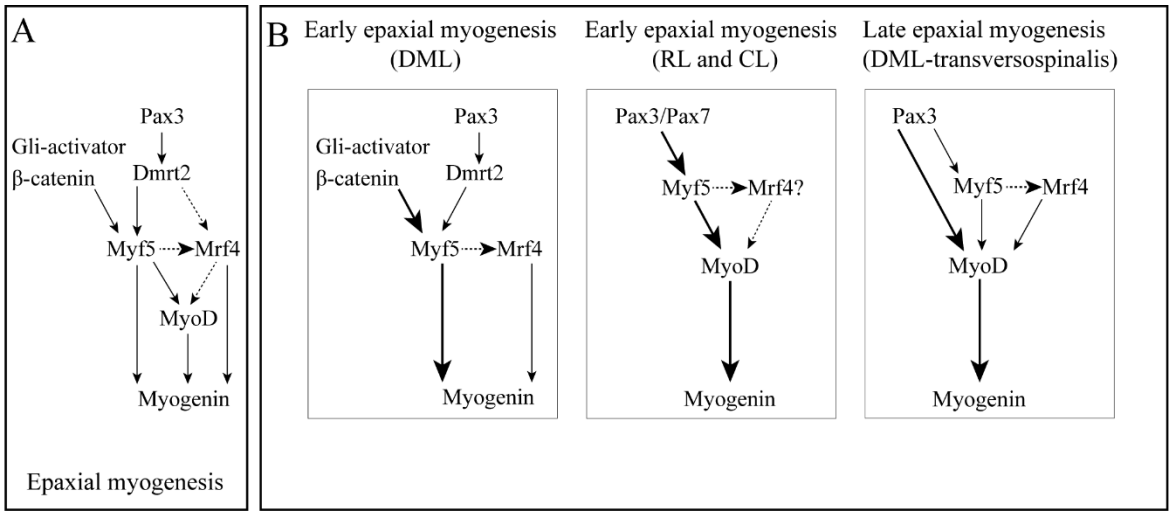

Figure 6.1: Model proposing the existence of three different myogenic transcriptional networks regulating epaxial myogenesis.
A: Overview of the whole transcriptional network regulating epaxial myogenesis (also see Fig. 1.18). **B:** Our proposed subdivision of the epaxial transcriptional network into three different spatial or temporal phases. Bold arrows in B mark proposed core genetic networks. DML: dorso-medial (i.e. epaxial) lip of the dermomyotome; RL: rostral lip of the dermomyotome; CL: caudal lip of the dermomyotome.

4. The mechanisms of development of transversospinalis muscles share similarities with that of the hypaxial muscles

Epaxial and hypaxial muscle development has for several decades been considered as being different in terms of lineage and of mechanisms of development (Ordahl and Le Douarin 1992; Kablar et al., 2003). In this thesis, we show that the mechanisms of development of transversospinalis muscles might be more similar to that of hypaxial muscles than to that of the other epaxial muscles. First of all, these muscles seem to arise from the upregulation of MyoD independently of Myf5 and Mrf4 expression which is the case for all hypaxial muscles including the limb muscles (Tajbakhsh and Buckingham, 1994). Moreover, the periodicity of myotube differentiation seems to be similar in transversospinalis muscles and limb muscles. In the trunk, myocytes stay mononucleated until E11.0 (Venters et al., 1999). Then myoblasts fuse with elongated mononucleated myocytes to form bi-and then multi-nucleated myotubes through successive fusions of more myonuclei from other myoblast and/or myocytes (Biressi et al., 2007) and while muscle fusion occurs, the length of myotubes barely changes (Siero-Mosti et al., 2014). In contrast, limb muscle multinucleation is ensured through two steps: a first step

involving fusion between myoblasts forming short-elongated myocytes that form bi-nucleated short length myotubes and a second phase where these myotubes fuse with more differentiated myoblasts (Biressi et al., 2007; Christ and Saberi, 2002; Lee et al., 2013; Siero-Mosti et al., 2014). Therefore, each myonuclear addition is accompanied by the increase of myofibre length culminating in higher fusion rates and multinucleation is achieved in a short period of time (Siero-Mosti et al., 2014). Our results demonstrate that when the first skeletal muscle cells of the transversospinalis muscle masses arise in *Myf5*$^{nlacZ/nlacZ}$ embryos, they do not go through a phase of being elongated mononucleated myocytes and instead they become multinucleated very quickly forming short myotubes that progressively grow in length as new myoblasts fuse with them. Importantly, transversospinalis muscles develop with their definitive orientation as occurs in the limb (Deries et al., 2010).

Finally, we show that in *Myf5*$^{nlacZ/nlacZ}$ embryos, transversospinalis muscles are able to develop independently of the myotome and we suggest that under normal conditions, it is possible that transversospinalis muscles do not develop through the myotomal stage. Rather they would develop through the differentiation of new MuSCs which rapidly fuse with each other, contrarily to that of the other epaxial muscles which develop through the scaffold of the myotome. Therefore, it seems that these muscles, similarly to that of limb, tongue and diaphragm muscles, do not depend on a transient myotome (Buckingham, 2017).

The mechanisms involved in the development of appendicular muscles appeared later in evolution than the axial muscle mechanisms (Neyt et al., 2000). Thus, we propose that the *modus operandi* underlying transversospinalis formation in the trunk resembles a more evolutionary recent way of skeletal muscle formation in the trunk and it is tempting to speculate that transversospinalis muscle may have evolved as a relatively recent adaption to life on land.

II. Final considerations

This thesis provides new insights into the functions of the myotome during embryonic development. We highlight how remarkable the development of the epaxial musculature is in mice by unveiling a third transcriptional pathway underlying epaxial muscle formation that characterises the development of the transversospinalis muscles. This pathway is different from that of the other epaxial muscles.

Skeletal muscle development, or for that matter any other embryonic developmental aspect of the human body, is important to understand specific congenital diseases such as muscle dystrophies and spinal diseases. More specifically, the study and the understanding of the development of transversospinalis muscles such as the multifidus muscle, which is the origin of many lumbar pains, are of interest to better comprehend the anatomy and physiology of these muscles and therefore better care for these pains.

In an anatomical perspective, transversospinalis muscles are the ones that resemble the most the adult myotomes of the fish as some of them are unisegmented, spanning only the length between two vertebrae. Because of these features, it would be tempting to claim that these muscles are the most ancient in terms of evolution. However, by analysing their mechanisms of development, we hypothesise here that these muscles arose later in evolution than the other epaxial muscles. It might be that these muscles emerged during evolution as an adaptation to support the vertebral column in a terrestrial environment.

III. References

Anderson, C., Thorsteinsdottir, S. and Borycki, A.-G. (2009). Sonic hedgehog-dependent synthesis of laminin 1 controls basement membrane assembly in the myotome. *Development* **136**, 3495-3504.

Bajanca, F., Luz, M., Duxson, M. J. and Thorsteinsdóttir, S. (2004). Integrins in the mouse myotome: Developmental changes and differences between the epaxial and hypaxial lineage. *Dev. Dyn.* **231**, 402-415.

Bajanca, F., Luz, M., Raymond, K., Martins, G. G., Sonnenberg, A., Tajbakhsh, S., Buckingham, M. and Thorsteinsdóttir, S. (2006). Integrin alpha6beta1-laminin interactions regulate early myotome formation in the mouse embryo. *Development* **133**, 1635-1644.

Biressi, S., Molinaro, M. and Cossu, G. (2007). Cellular heterogeneity during vertebrate skeletal muscle development. *Dev. Biol.* **308**, 281-293.

Borello, U., Berarducci, B.,, Murphy, P., Bajard, L., Buffa, V., Piccolo, S., Buckingham. M. and Cossu G. (2006). The Wnt/β-catenin pathway regulates Gli-mediated Myf5 expression during somitogenesis. *Development* **133**, 3723-3732.

Brent, A. E., Schweitzer, R. and Tabin, C. J. (2003). A somitic compartment of tendon progenitors. *Cell* **113**, 235–48.

Brent, A. E., Braun, T. and Tabin, C. J. (2005). Genetic analysis of interactions between the somitic muscle, cartilage and tendon cell lineages during mouse development. *Development* **132**, 515-528.

Buckingham, M. (2017). Gene regulatory networks and cell lineages that underlie the formation of skeletal muscle. *Proc. Natl. Acad. Sci.* **114**, 5830-5837.

Buckingham, M. and Rigby, P. W. J. (2014). Gene regulatory networks and transcriptional mechanisms that control myogenesis. *Dev. Cell* **28**, 225-238.

Chiquet-Ehrismann, R., Orend, G., Chiquet, M., Tucker, R. P. and Midwood, K. S. (2014). Tenascins in stem cell niches. *Matrix Biol.* **37**, 112-123.

Christ, B. and Brand-Saberi, B. (2002). Limb muscle development. *Int. J. Dev. Biol.* **46**, 905-914.

Cinnamon, Y., Kahane, N. and Kalcheim, C. (1999). Characterization of the early development of specific hypaxial muscles from the ventrolateral myotome. *Development* **126**, 4305-4315.

Delfini, M. C., De La Celle, M., Gros, J., Serralbo, O., Marics, I., Seux, M., Scaal, M. and Marcelle, C. (2009). The timing of emergence of muscle progenitors is controlled by an FGF/ERK/SNAIL1 pathway. *Dev. Biol.* **333**, 229-237.

Deries, M., Collins, J. J. P. and Duxson, M. J. (2008). The mammalian myotome: A muscle with no innervation. *Evol. Dev.* **10**, 746-755.

Deries, M., Schweitzer, R. and Duxson, M. J. (2010). Developmental fate of the mammalian myotome. *Dev. Dyn.* **239**, 2898-2910.

Deries, M., Gonçalves, A. B., Vaz, R., Martins, G. G., Rodrigues, G. and Thorsteinsdóttir, S. (2012). Extracellular matrix remodeling accompanies axial muscle development and morphogenesis in the mouse. *Dev. Dyn.* **241**, 350-364.

Giblin, S. P. and Midwood, K. S. (2015). Tenascin-C: Form versus function. *Cell Adh. Migr.* **9**, 48-82.

Kablar, B., Krastel, K., Tajbakhsh, S. and Rudnicki, M. A. (2003). Myf5 and MyoD activation define independent myogenic compartments during embryonic development. *Dev. Biol.* **258**, 307-318.

L'Honoré, A., Coulon, V., Marcil, A., Lebel, M., Lafrance-Vanasse, J., Gage, P., Camper, S. and Drouin, J. (2007). Sequential expression and redundancy of Pitx2 and Pitx3 genes during muscle development. *Dev. Biol.* **307**, 421-433.

Neyt, C., Jagla, K., Thisse, C., Thisse, B., Haines, L. and Currie, P. D. (2000). Evolutionary origins of vertebrate appendicular muscle. *Nature* **408**, 82-86.

Ordahl, C. P. and Le Douarin, N. M. (1992). Two myogenic lineages within the developing somite. *Development* **114**, 339-353.

Parr, B. A., Shea, M. J., Vassileva, G. and McMahon, A. P. (1993). Mouse Wnt genes exhibit discrete domains of expression in the early embryonic CNS and limb buds. *Development* **119**, 247-261.

Relaix, F., Rocancourt, D., Mansouri, A. and Buckingham, M. (2005). A Pax3/Pax7-dependent population of skeletal muscle progenitor cells. *Nature* **435**, 948-953.

Rescan, P.-Y. (2008). New insights into skeletal muscle development and growth in teleost fishes. *J. Exp. Zool. B. Mol. Dev. Evol.* **310**, 541-548.

Sato, T., Rocancourt, D., Marques, L., Thorsteinsdóttir, S. and Buckingham, M. (2010). A Pax3/Dmrt2/Myf5 regulatory cascade functions at the onset of myogenesis. *PLoS Genet.* **6**, e1000897.

Scaal, M. and Wiegreffe, C. (2006). Somite compartments in anamniotes. *Anat. Embryol. (Berl).* **211**, 9-19.

Sieiro-Mosti, D., De La Celle, M., Pelé, M. and Marcelle, C. (2014). A dynamic analysis of muscle fusion in the chick embryo. *Development* **141**, 3605-11.

Spörle, R. (2001). Epaxial-adaxial-hypaxial regionalisation of the vertebrate somite: Evidence for a somitic organiser and a mirror-image duplication. *Dev. Genes Evol.* **211**, 198-217.

Staniszewska, I., Sariyer, I. K., Lecht, S., Brown, M. C., Walsh, E. M., Tuszynski, G. P., Safak, M., Lazarovici, P. and Marcinkiewicz, C. (2008). Integrin alpha9 beta1 is a receptor for nerve growth factor and other neurotrophins. *J. Cell Sci.* **121**, 504-513.

Tajbakhsh, S. and Buckingham, M. E. (1994). Mouse limb muscle is determined in the absence of the earliest myogenic factor myf-5. *Proc. Natl. Acad. Sci. U. S. A.* **91**, 747-751.

Tajbakhsh, S., Borello, U., Vivarelli, E., Kelly, R., Papkoff, J., Duprez, D., Buckingham, M. E. and Cossu, G. (1998). Differential activation of Myf5 and MyoD by different Wnts in explants of mouse paraxial mesoderm and the later activation of myogenesis in the absence of Myf5. *Development* **125**, 4155-4162.

Tallquist, M. D., Weismann, K. E., Hellstrom, M. and Soriano, P. (2000). Early myotome specification regulates PDGFA expression and axial skeleton development. *Development* **127**, 5059-5070.

Teboul, L., Hadchouel, J., Daubas, P., Summerbell, D., Buckingham, M. and Rigby, P. W. J. (2002). The early epaxial enhancer is essential for the initial expression of the skeletal muscle determination gene Myf5 but not for subsequent, multiple phases of somitic myogenesis. *Development* **129**, 4571-4580.

Tosney, K. W., Dehnbostel, D. B. and Erickson, C. A. (1994). Neural crest cells prefer the myotome's basal lamina over the sclerotome as a substratum. *Dev. Biol.* **163**, 389-406.

Venters, S. J., Thorsteinsdóttir, S. and Duxson, M. J. (1999). Early development of the myotome in the mouse. *Dev. Dyn.* **216**, 219-232.

Vinagre, T., Nóvoa, A., Bom, J., Moncaut, N., Mallo, M. and Carapuço, M. (2010). Evidence for a Myotomal Hox/Myf Cascade Governing Nonautonomous Control of Rib Specification within Global Vertebral Domains. *Dev. Cell* **18**, 655-661.

Yoshida, T., Akatsuka, T. and Imanaka-Yoshida, K. (2015). Tenascin-C and integrins in cancer. *Cell Adhes. Migr.* **9**, 96-104.